Tracing Microplastics at the Wastewater Treatment Plant: Development of Methods for Recovery, Enumeration, and Identification

By

Anggelia Essi Christian
Master of Nanotechnology

Thesis
Submitted to Flinders University
for the degree of

Doctor of Philosophy
College of Science and Engineering
27 November 2024

TABLE OF CONTENTS

SUMMARY

This thesis addresses the growing concern surrounding microplastics contamination in wastewater treatment plants, focusing on techniques for their recovery, enumeration, and identification within these systems. Collaborative efforts with South Australia (SA) Water aim to contribute for monitoring and mitigating microplastic pollution, recognising wastewater treatment plants as significant pathways for their entry into the environment.

Extensive research has highlighted ecological concerns linked to microplastics, emphasizing the need for experimental testing to understand their impacts fully. Reviewing available analytical tools reveals a lack of standardized methods, suggesting tailored approaches based on specific data requirements are necessary for practical applications.

Introducing semi-automatic mapping using FTIR Microspectroscopy for particles above 25 µm and Flow Cytometry for those below 25 µm offers efficient solutions for microplastics analysis in wastewater and sludge samples. Recommendations for further refinement and validation of these methods underscore collaboration with experts for continued improvement.

Investigation into seasonal and treatment effects on plastic loads within wastewater treatment plants reveals significant variations in microplastic concentrations and compositions. Understanding these dynamics is essential for optimizing treatment processes and accurately assessing microplastic pollution levels.

Future research directions may include exploring the effects of treatment processes on microplastic morphology, standardizing analytical methods for routine analysis, and investigating alternative sources of microplastics. These endeavours will advance out understanding of microplastic contamination dynamics and inform effective mitigation strategies.

In conclusion, this thesis contributes to our understanding of microplastics contamination in wastewater treatment plants, offering insights into analytical techniques and mitigation approaches. Continued research efforts are crucial for addressing this pressing environmental issue and protecting ecosystems and human health.

ACKNOWLEDGEMENTS

Completing this thesis would not have been possible without the support, guidance, and encouragement of numerous individuals who have contributed in various ways. I would like to express my deepest gratitude to all those who have helped me along this journey.

First, I am immensely grateful to my thesis advisor, Associate Professor Ingo Köper, for his unwavering support, invaluable guidance, and insightful feedback throughout every stage of this research. His expertise, patience, and encouragement have been instrumental in shaping this work and pushing me to strive for excellence.

I extend my heartfelt appreciation to my co-supervisor, Professor Paul Kirkbride, for his invaluable suggestions, specifically for sharing his expertise in analytical chemistry on FTIR Microspectroscopy and interpretation of the infrared spectra. His advice has significantly enriched the quality of this research.

The South Australia Water (SA Water) Corporation gratefully supports this project, with special acknowledgements to the SA Water team at the wastewater treatment plant in [redacted] including Adam James, Chloe Downes, Jamie, and Phil, as well as the headquarters office team, Alex Keegan, Ilda Clos, Milena Fernandes, and Melody Lau.

I am grateful to have received Flinders University Research Scholarship (FURS) and the university tuition fee waive, that financially supports me on this research endeavour.

I am deeply thankful to Shima Ziajahromi from the Australian Rivers Institute, Griffith University, for her valuable guidance on the pretreatment procedure and microplastics analysis expertise. Additionally, to Professor Jim Mitchell and James Patterson for their invaluable advice on Flow Cytometry technique, which was informed by their prior study in laser lines and threshold settings for microplastics analysis, and for generously providing the FTIC green beads, as well as to Giles Best from Flinders Medical Centre played a pivotal role by assisting with instrument training and booking.

To Jason Gascooke, thank you for your assistance and guidance in Raman microspectroscopy, your expertise is greatly appreciated. To Russel fuller, thank you for your support and sharing your expertise for using Pyrolysis-GC/MS. To Anthony, Darren, and Chris, thank you for your assistance in modifying the mesh holder, oven exhaust, and laser cutting the mesh.

My sincere thanks go to the Köper group past and present who worked alongside me – Alex, Mayisha, Ashley, Brodie, and Braden, whose intellectual contributions, friendship, and moral support have made this academic

journey more fulfilling and enjoyable. To Mikaela and Paris, whose had helped me with some side projects related to this microplastics research.

I owe a debt of gratitude to my mother, Esther and my brother, Nathan for their unconditional love, unwavering support, and sacrifices they have made to enable me to pursue my academic aspirations. Their encouragement and belief in my abilities have been a constant source of strength and motivation.

I want to express my heartfelt appreciation to all my friends who have stood by me, provided encouragement, and offered words of wisdom during moments of doubt and difficulty.

To everyone who has played a part, no matter how big or small, in the completion of this thesis, I extend my sincere thanks. Your contributions have been invaluable, and I am deeply grateful for your support and encouragement.

Last, I just wanted to quote these wise words from a scientist I do respect, John C. Lennox – mathematician, bioethicist, and Christian apologist.

"The more we get to know about our universe, the more the hypothesis that there is a Creator God, who designed the universe for a purpose, gains in credibility as the best explanation of why we are here"

"God to me is a mystery but is the explanation for the miracle of existence – why there is something rather than nothing"

LIST OF FIGURES

LIST OF TABLES

ABBREVIATIONS

d.w.	dry weight
ABS	acrylonitrile butadiene styrene
AUC	Analytical Ultracentrifugation
BOD5	The 5-day biochemical oxygen demand
COD	Chemical Oxygen Demand
DOC	Dissolved Organic Carbon
NH3-N	Ammonia Nitrogen
DN	Dissolved Nitrogen
EPS	Extracellular Polymeric Substances
FITC	Fluorescein isothiocyanate
FTIR	Fourier transform infrared
Py-GC/MS	Pyrolysis Gas Chromatography/Mass Spectrometry
PET	poly(ethylene terephthalate)
PEs	polyester
PUR	polyurethane
EVA	ethyl vinyl acetate
EA	ethyl acrylate
PAN	polyacrylonitrile
LDPE	low density polyethylene
HDPE	high density polyethylene
PP	polypropylene

PE	polyethylene
PS	polystyrene
PMMA	poly(methyl methacrylate)
PVC	poly(vinyl chloride)
PVA	poly(vinyl alcohol)
PVS	poly(vinyl stearate)
PA	polyamide
PBT	polybutylene terephthalate
PLA	Polylactic acid
Tm	Melting Point temperature
Tg	Glass Transition temperature
WPC	wood plastics composite

PUBLICATIONS AND RESEARCH COMMUNICATIONS

Publications:

1. Christian, A. E.; Köper, I., Microplastics in biosolids: A review of ecological implications and methods for identification, enumeration, and characterization. Science of The Total Environment 2023, 864, 161083. https://doi.org/10.1016/j.scitotenv.2022.161083

Oral Presentation:

1. **Anggelia Essi Christian**, Paul Kirkbride, Ingo Köper, "Tracing Microplastics at Wastewater Treatment Plant: Development of Methods for Recovery, Enumeration, and Identification", Annual Molecular Science & Technology Conference, Flinders University, Adelaide, South Australia, 2023.

Poster Presentation:

1. **Anggelia Essi Christian**, Melody Lau, Milena Fernandes, Paul Kirkbride, Ingo Köper, "Tracking Microplastics at Wastewater Treatment Plants: Method Development", Annual Molecular Science & Technology Conference, Flinders University, Adelaide, South Australia, 2021.
2. **Anggelia Essi Christian**, Melody Lau, Milena Fernandes, Paul Kirkbride, Ingo Köper, "Tracking Microplastics at Wastewater Treatment Plants: Method Development", Annual Institute of Nanoscale Science & Technology Conference, Flinders University, Adelaide, South Australia, 2022.
3. **Anggelia Essi Christian**, Melody Lau, Milena Fernandes, Shima Ziajahromi, Paul Kirkbride, Ingo Köper, "Tracing Microplastics at the wastewater treatment plant – solid waste stream", Clean Up International Conference", Adelaide Convention Centre, Adelaide, South Australia, 2022.
4. **Anggelia Essi Christian**, Melody Lau, Milene Fernandes, Shima Ziajahromi, Paul Kirkbride, Ingo Köper, "Microplastics load at wastewater treatment plant: Seasonal Trend", Institute of Nanoscale Science & Technology" Flinders University, Adelaide, South Australia, 2023

Other Research Communications:

1. An interview-based article on "Standardising analysis of microplastics in biosolids", the Australian Water Association (AWA), June 2023. https://www.awa.asn.au/resources/latest-news/standardising-analysis-of-microplastics-in-biosolids.
2. A radio interview with Radio Adelaide (101.5FM) for Slice of Science session, on-air in April 2024. https://radioadelaide.org.au/program/slice-of-science/2024-04-11

DECLARATION

I, Anggelia Essi Christian, declare that this thesis titled “Tracing Microplastics at the Wastewater Treatment Plant: Development of Methods for Recovery, Enumeration, and Identification” is my original work, except where indicated otherwise. I have acknowledged all sources used and received assistance in the acknowledgement section. This thesis has not been submitted for any other degree. I affirm the authenticity of the research and understand the consequences of academic misconduct.

Anggelia Essi Christian

1st April 2024

CHAPTER 1: INTRODUCTION

1 Background

The presence of microplastics, small plastic particles size between 1 µm and 5 mm, in the soil environment is a major concern, as it is likely to influence the overall ecosystem. One of the possible sources for microplastics is from the application of biosolids for landfill or agricultural purposes. Biosolids or treated sludges are a by-product of wastewater treatment processes and are rich in nutrients, minerals, as well as microbes that are beneficial for soils.[1-3]

In response to other countries' reports on the amount of microplastics discharged into the environment through sludge and biosolids from Wastewater Treatment Plants (WWTPs) and because of the possibility of their adverse impact on soils and organisms, there is an urgent need to obtain field data for Australia. Estimated microplastics abundance in the Australian context based on other countries' data is not reliable for various reasons, mainly, geographical differences. For instance, storm water runoff from roofs, pavements, and roads is handled separately from wastewater in Australian utilities.[1]

There is no single procedure for the analysis of micro- and nanoplastics that covers all the possible parameters such as size, type, sample environment, etc. Each sample matrix requires a specific and customized set of techniques. A defined research question, which reflects the information that wants to be obtained such as size, geometry, and chemical composition of the sample, will be the first step in designing a framework. Then, a set of appropriate techniques can be chosen covering all analysis steps including sample collection, preconcentration, separation, and characterization methods.[4]

2 Research Scope and Aims

This research project was conducted in collaboration with SA Water, and focused on the waste solid stream, mainly sludges at WWTPs in South Australia. The goal was to better understand the transport, fate, and

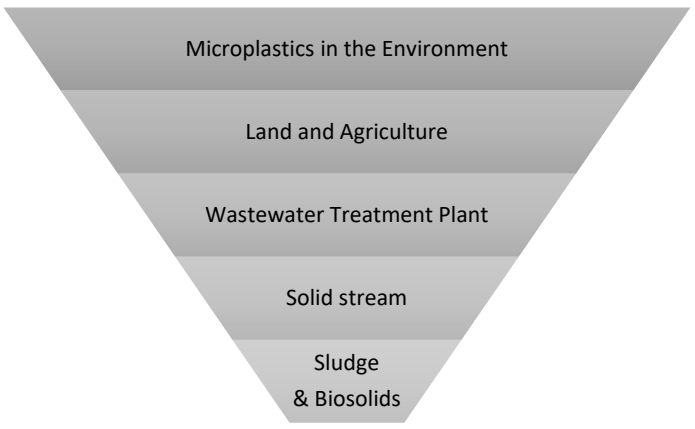

Figure 1-1. Area of Research

impact of solid waste, specifically sludge and biosolids, within the solid stream of a wastewater treatment plant, and their potential role as source of microplastics in the environment (Figure 1-1).

The sample used were sludges collected from different sampling points in the solid waste stream at a wastewater treatment plant in South Australia, as illustrated in Figure 1-2 below. Sampling points included Influent, effluent of primary sedimentation, secondary sedimentation, sludge treatment (digestion), and dewatering.

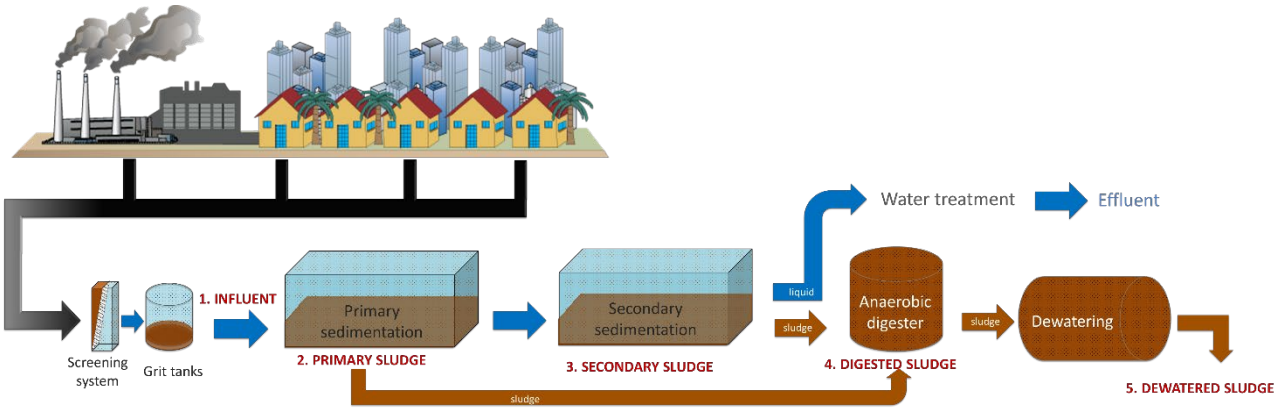

Figure 1-2. Sampling points scheme at the wastewater treatment plant

The sampling time depended on the sub-project goal. For the seasonal trend study, samples were collected by grab sample at the same day, and for the treatment study, samples were collected following the timeframe of the treatment processes in the wastewater treatment plant. For example, the primary sludge is at day-0, the secondary sludge at day-1 (following the flow of the wastewater). If the wastewater is settled for 3 days, then the sample will be collected on day 3.

The typical solid waste treatment process at a wastewater treatment plant takes approximately 36 to 48 days, or five to seven weeks. This process includes about two hours for primary sedimentation, around ten days for secondary sedimentation, 18 to 30 days in a digester, seven days for settling in a silo, followed by continuous dewatering process, and approximately one week in a silo before the solid waste is designated as biosolids for further use. These treatment stages, with varying flow rates and residence time, can influence the number of microplastics present throughout the process.

Two main themes for this research project were a) method development and b) plastic load recovery. In the method development, validated and verified techniques for identification, quantification, and characterization of plastic particles in the solid waste matrix were explored. The goal was to construct a quality assurance system including a standard operational procedure, reporting, calibration, and traceability guidelines of such a sample analysis. Then, the method developed was used to study the plastic loads recovery. The goal was to gain data on the treatment efficacy, and the effects of seasons (i.e. wet/cold and

dry/hot), as well as sources (industries, residential area, population, and urbanization) for the plastic loads e.g. types and amount.

3 Research Approach

To achieve the above-mentioned aims, a literature review was conducted to gain more understanding on the microplastics impacts on the ecosystem, and to what extent the importance of microplastics analysis at the wastewater treatment plant as one of microplastics' pathway into the environment. Some analytical techniques for microplastics' analysis were also compared and discussed in this review article. This section is presented in Chapter 2 of this thesis.

As currently no standard technique available, the second part of the research was to develop a validated and verified analytical method specifically for sludge samples. The following criteria were considered during the method development:

1. For the validation, a positive-control sample or spiked recovery measurement was conducted for each method used. This step is undertaken to reduce the risk of false-negative or underestimation and false-positive or overestimation during the analysis. Such validation is recommended for microplastics analysis.[5]
2. For verification, the limit of detection (LOD) and limit of quantification (LOQ) for each technique used were measured using blank samples. This verification step is suggested as part of the Quality Assurance/Quality Control system for microplastics analysis. [6] The measurement followed the available standard guideline by the Environment Protection Authority (EPA) Australia.[7-9]

In this thesis, two main techniques have been developed: semi-automated mapping mode of FTIR Microspectroscopy (Chapter 3), and Flow Cytometry (Chapter 4). Both methods were chosen because of the industrial purposes in which cost and time need to be seriously considered. Moreover, these methods can be used for different size fraction of plastic particles identification and characterization.

Technique optimization and proof-of-concept development were conducted and reported as appendices in this thesis, including the following sections:

1. For the FTIR microspectroscopy technique, in addition to the instrument spectrum library, some polymer standard spectra were collected. The polymers used vary from the original or pure plastics to the commercial and weathered plastics occurring in the sludge or environment. A manufactured or commercial plastic, which possibly has additives and chemical modifications by industries were used. This included plastics fragmented from yarn, textiles, dishwashing sponge, toothbrush brittle, artificial grass, shoes' sole, car rubber mat, etc.
2. Optimization for the instrument setting of the Py-GC/MS method was conducted during preliminary experiments, including solvent used and temperature setting. Due to instrument difficulties and limitations, this technique was not used as the main analytical method.

3. Another technique that was developed but still at early stage was using Flow Cytometry and Raman Microspectroscopy instruments in a simultaneous mode.

The third part of this study was the application of the developed techniques for microplastics enumeration and identification in sludge samples from a wastewater treatment plant. The techniques that have been validated in the second part of this project were used to gain data on microplastics loads for two different sub-projects i.e., seasonal trend (Chapter 6), and treatment study (Chapter 7).

4 Structure of the thesis

This thesis is presented in seven main chapters as illustrated in Figure 1-3. There are three main parts of this thesis: 1) background research, 2) techniques development, and 3) applications. Chapter 2 reviews the impact of microplastics on the environment and its analytical methods, while chapter 3 summaries the type of microplastics present in the environment as well as their isolation techniques. Chapter 4 and 5 introduce the two developed techniques, semi-automated mapping mode FTIR Microspectroscopy and Flow Cytometry, for microplastics quantification and characterization. Chapter 6 and 7 utilize the developed analytical techniques to study microplastics load in different seasons and treatment effect respectively. Chapter 8 concludes the research and outlines recommendations for further studies.

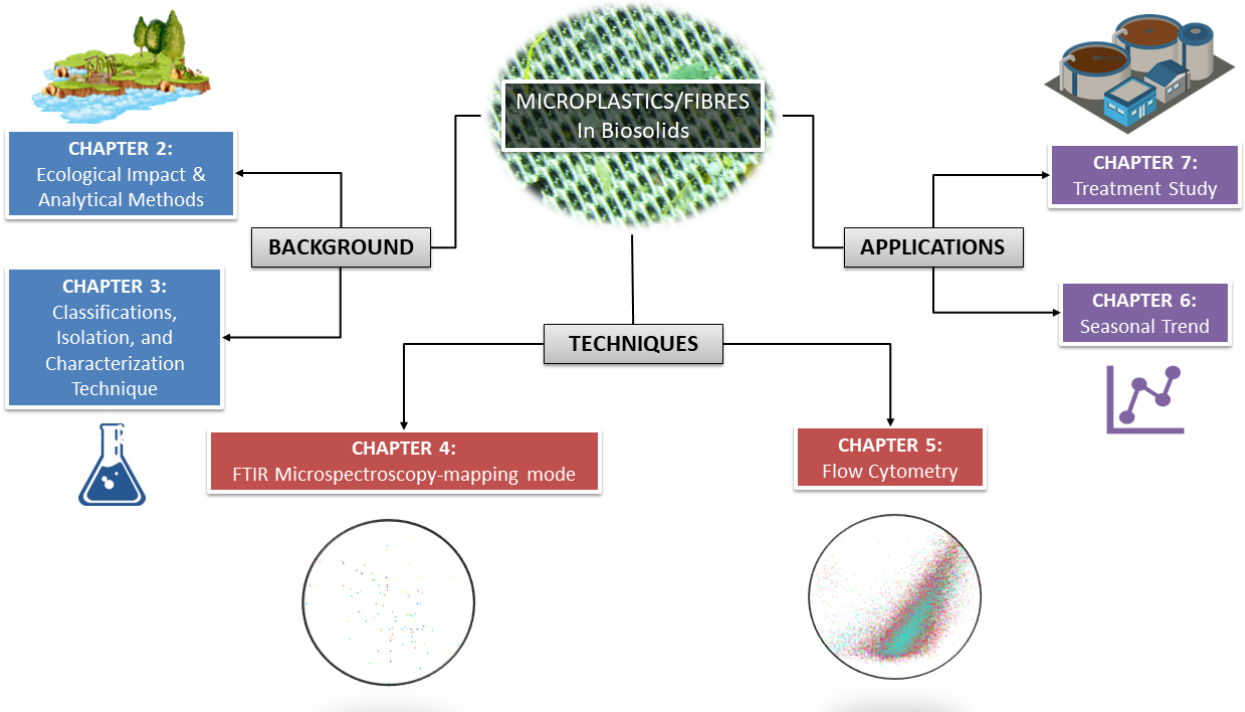

Figure 1-3. Graphical Abstract of this thesis

The preliminary experiments data were presented in Appendix B of this thesis. Some complement experiments including verification of the digestion method effect on the microplastics identification,

microscope stage modification for optimizing the FTIR microspectroscopy technique, and additional in-house library of IR spectrum of some commercial and weathered microplastics were given in Appendix C, G, and H, respectively. A standard operational procedure for a semi-automated mapping technique of FTIR Microspectroscopy was detailed in Appendix L. As part of the further studies recommendations, a preliminary data on the development of a simultaneous method of Flow Cytometry and Raman microspectroscopy was discussed in Appendix K.

References

1. Hopewell, K.; Batstone, D.; Dale, G.; Keegan, A.; Lee, E.; Randall, L.; Tao, E. *ANZBP Preliminary Report on Microplastics Risk for the Australian and New Zealand Biosolids Industry July 2020*; 2020.
2. Toffey, W.; Brown, S., Biosolids and ecosystem services: Making the connection explicit. *Current Opinion in Environmental Science & Health* **2020,** *14*, 51-55.
3. Hartmann, N. B.; Hüffer, T.; Thompson, R. C.; Hassellöv, M.; Verschoor, A.; Daugaard, A. E.; Rist, S.; Karlsson, T.; Brennholt, N.; Cole, M.; Herrling, M. P.; Hess, M. C.; Ivleva, N. P.; Lusher, A. L.; Wagner, M., Are We Speaking the Same Language? Recommendations for a Definition and Categorization Framework for Plastic Debris. *Environmental Science & Technology* **2019,** *53* (3), 1039-1047.
4. Schwaferts, C.; Niessner, R.; Elsner, M.; Ivleva, N. P., Methods for the analysis of submicrometer- and nanoplastic particles in the environment. *TrAC Trends in Analytical Chemistry* **2019,** *112*, 52-65.
5. Ball H, C. R., Grove E, Horton A, Johnson A, Jürgens M, Read D, Svendsen C, Sink To River - River To Tap. A Review of Potential Risks From Nanoparticles and Microplastics. *UK Water Industry Research Limited* **2019,** *EQ 01 A 231*.
6. Dawson, A. L.; Santana, M. F. M.; Nelis, J. L. D.; Motti, C. A., Taking control of microplastics data: A comparison of control and blank data correction methods. *Journal of Hazardous Materials* **2023,** *443*, 130218.
7. Environment Protection Authority, Sampling and Analysis of Waters, Wastewaters, Soils, and Wastes. Australia, 2009.
8. National Association of Testing Authorities, Guidelines for the validation and verification of chemical test methods. Australia, 2006.
9. National Association of Testing Authorities, General Accreditation Gudance-Validation and verification of quantitative and qualitative test methods. Australia, 2018.

CHAPTER 2: MICROPLASTICS IN BIOSOLIDS - A REVIEW OF ECOLOGICAL IMPLICATIONS AND METHODS FOR IDENTIFICATION, ENUMERATION, AND CHARACTERIZATION

This chapter has been published in the journal Science of the Total Environment with the title “Microplastics in Biosolids: A review of ecological implications and methods for identification, enumeration, and characterization”. It is a literature review addressing the occurrence of microplastics at wastewater treatment plants, specifically in the solid waste stream, and their impact on the soil ecosystem. It also highlights current methods for microplastics analysis. the manuscript was authored by **Anggelia Essi Christian** and Ingo Köper (https://doi.org/10.1016/j.scitotenv.2022.161083)

Abstract

Biosolids, or treated sludge, are by-products of the wastewater treatment processes and are commonly used in agricultural applications to enrich soil nutrients. However, it contains microplastics, plastic particles with a diameter below 1 mm. Microplastics exist and accumulate in the environment, which can have major impacts on the ecosystem. Despite their abundance in the environment, there are to date no standardized methods for their enumeration and characterization.

A literature review was conducted focusing on the occurrence of microplastics at wastewater treatment plants, particularly in the solid waste stream, and their influence on the soil ecosystem where biosolids is applied. We found a conflicting evidence to which extent microplastics negatively impact the ecosystem. Some reported either a direct negative impact of microplastics or because of microplastic interaction with other soil contaminants. Meanwhile, other studies showed no effect or at certain amount of microplastics on the ecosystem.

We also found that microplastics size, shape, type, concentration, and exposure time play a critical role in their ecological impacts. However, currently, there is no unified approach for microplastics identification and characterization in solid waste resulting in a various and incomparable data. Therefore, utilizing standardized methods for microplastics analysis must be considered as the initial step to better understand the impact of microplastics onto the environment. We suggest a method's scaling comparison as a practical approach to select and develop techniques based on cost, time, data obtained, accuracy, and sensitivity criteria. Further research into the ecotoxicity of microplastics and continuous monitoring of biosolid applications are also necessary.

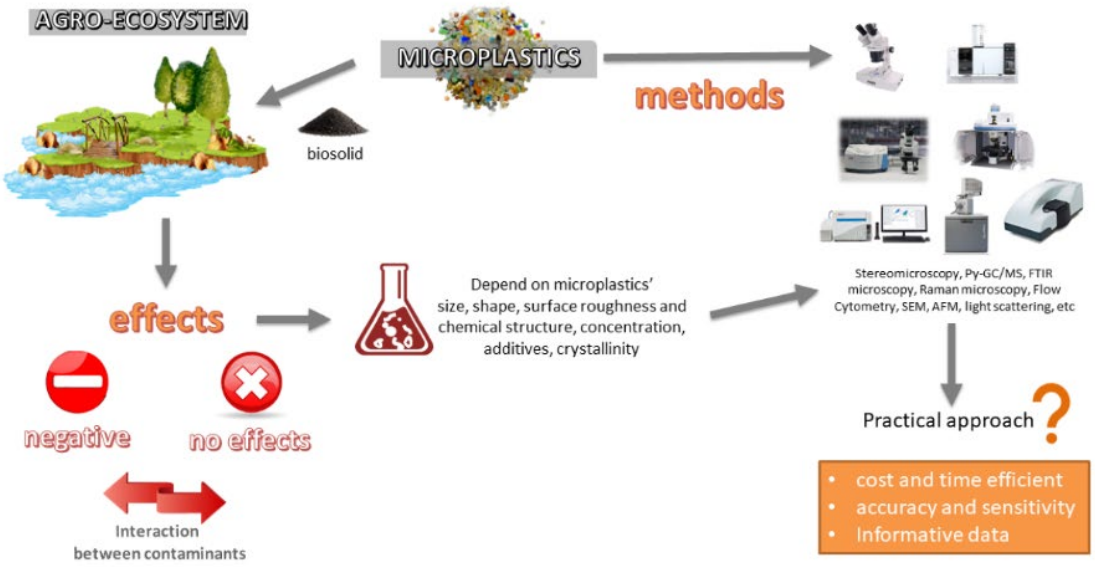

Figure 2-4. Graphical Abstract of the published paper "Microplastics in Biosolids: A Review of Ecological Implications and Methods for Enumeration, Identification, and Characterization"

1 Introduction

Microplastics (we will use the term microplastics when we talk about microplastic particles), are commonly defined as plastic particles with a size between 1 µm and 5 mm; they have become an emerging environmental issue over the past decade. [1-3]

Microplastics are considered an environmental contaminant because they can harm organisms in the ecosystems, and eventually disrupt the food chain.[4-7] They can enter the ecosystem through various pathways, one of them is through biosolid application for agricultural purposes. Although biosolid are rich in nutrients and minerals,[8, 9] they are known as a sink for plastic particles from household and industrial activities.[10] Current wastewater treatments aim to remove plastic particles from the wastewater flow, but most of these particles (around 99 %) are transferred and retained in the sewage sludge, which then through some treatments, such as drying and lime stabilization, is converted into biosolids.[10-13]

Once biosolids are applied to the soil, the contained plastic particles tend to persist in the soil ecosystem.[11, 14-18] Consequently, the amount of microplastics in the soil increases over time. For example, Corradini et al. investigated agricultural fields in Chile that underwent sludge application for a period of ten years and observed an 800 % increase in the microplastics load in the soil.[19, 20]

The amount of microplastics reported in sludge varies between countries and regions. For example, Mahon et al. found 4196 to 15,385 particles kg^{-1} (dry weight) in sludge from seven different WWTPs in Ireland[21],

whereas Li et al. [22] reported 1600 to 56,400 particles kg^{-1} of dry sludge in 28 different wastewater treatments plants across 11 Chinese provinces.

There are several studies on microplastics analysis in the solid waste stream at the wastewater treatment plant, yet no standardized methods have been established. It leads to a highly variable in microplastics data. There are some challenges in developing the techniques for analyzing and tracing microplastics at the wastewater treatment plant. This including the ununified definition and classification of microplastics[1], the various possible pathways and sources of microplastics entering the wastewater treatment plant and into the ecosystem[23-25], and the numerous yet discrete studies reported on the implications of microplastics on the agroecosystems linked to solid waste i.e., sludge and biosolids.[26-32] As microplastics are mostly invisible by the naked eye, physical and chemical analysis is required in combination with some analytical instruments in order for accurate characterization and enumeration.

This article reviews the emerging issue of microplastics in sludge as a contaminant for land or agricultural applications. This includes the implications of plastic particles on the agroecosystem, the available analytical techniques and guidelines of plastics identification, enumeration, and characterization, as well as recommended approaches in selecting and developing the methods of analysis. This paper aims to show how the characteristics of plastic particles such as size, shape, and type are critical to discern their impacts on the ecosystem. For enumeration, a consistent measure, for example number of microplastics per unit mass is also important. Accurate and validated methods used for microplastics identification and enumeration are essential, yet largely missing.

2 Definition of microplastics

There is ambiguity in the definition of microplastics. When the term was introduced in 2004, Thompson et al. reported plastics fragments they found in the ocean around the UK of about 20 µm in size.[33] Since then, there is an increased interest to study microplastics in the environment, and the need for a standardized definition and category for plastic debris has been identified. In 2008, the first International Microplastics Workshop in Washington was hosted by the National Oceanic and Atmospheric Administration; it defined microplastics as plastic particles with a size <5 mm.[3, 34] The European Commission adopted the same definition in 2011 in their guideline for Monitoring of Marine Litter in European Sea.[35] In 2017, Ivelva et al., introduced a new submicrometer category for any plastic particle with a size between 100 nm and 1 µm.[36]

In 2019, Nana B. Hartmann et al. recommended a framework for the definition and classification of plastic debris.[1] They suggested four categories: (i) nanoplastics (1 to <1000 nm), with subdivisions for nanoplastics (1 to <100 nm) and submicron-plastics (100 to <1000 nm); (ii) microplastics (1 to <1000 µm); (iii) mesoplastics (1 to 10 mm) and (iv) macroplastics (1 cm and larger). However, these categories leave plastic fragments sized 11 mm to 999 mm with no group. In 2020, the International Organization for Standardization released

ISO/TR 21960:2020, which defines any solid plastic particles insoluble in water with any dimensions ranging from 1 µm to 1000 µm (=1 mm) as microplastics, from 1 mm to 5 mm as large microplastics, and above 5 mm as macroplastics.[37]

In this paper, and for comparison of literature data, we will adopt the definition as shown in Figure 2-5, which classifies plastic particles in six size-depending subcategories.

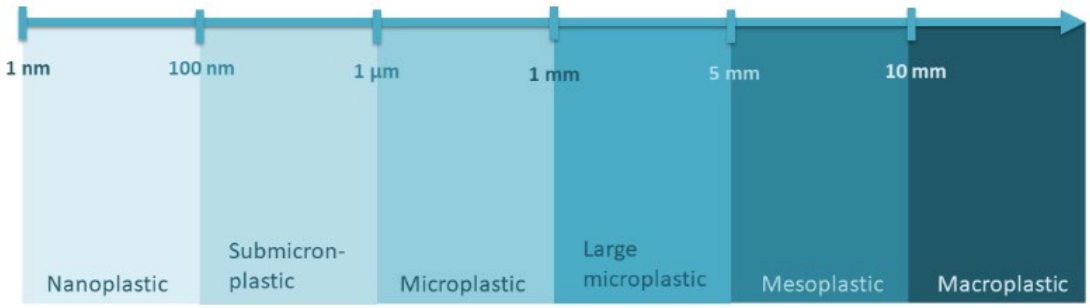

Figure 2-5. Suggested definition and classification of plastic particles adopted in this manuscript

3 Pathways of microplastics into the agroecosystem

There are various pathways how microplastics enter the wastewater treatment plant and a detailed knowledge can inform effective removal treatments and control strategies.[1, 2, 34, 35, 38] Microplastics reach the wastewater from a wide range of sources including households (e.g. laundry washing, toilet, showering or bathing) and industries such as textile, food and beverage, and cosmetic and personal care (Figure 2-6).[39]

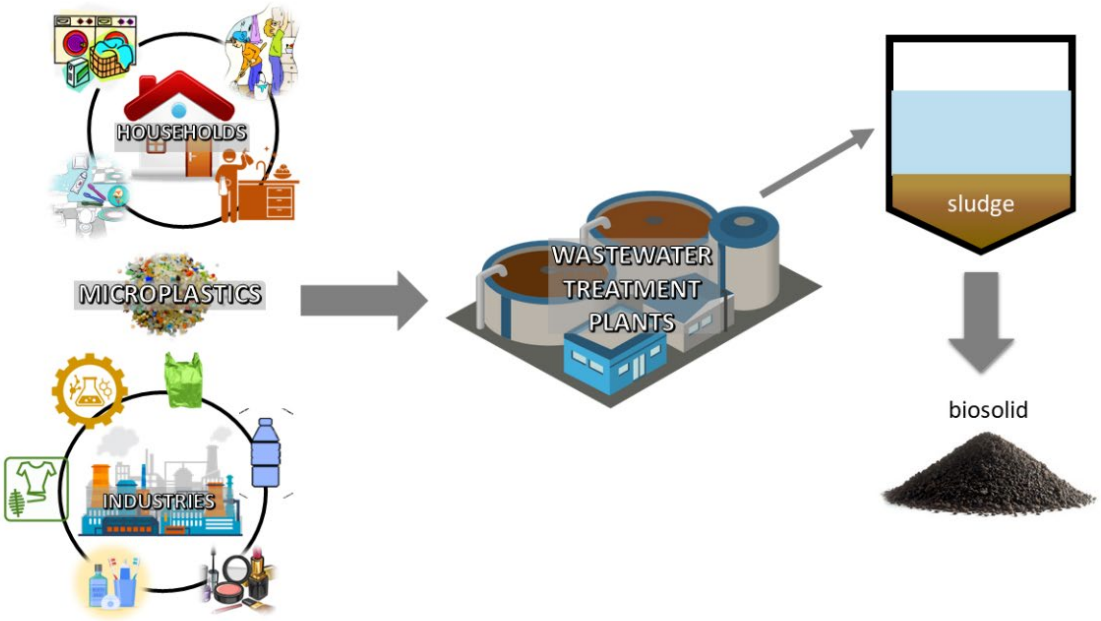

Figure 2-6. Illustration on the pathways of microplastics from sources to biosolids

During the treatment processes in the wastewater treatment plant, sewage sludges are generated in sedimentation and settling tanks after the aeration or floatation process. Ninety-nine percent of the plastic material in the wastewater is retained in the sludge.[40-43] The sewage sludges undergo additional treatments such as digestion, lime stabilization, composting, and heat treatment with the aim of pathogen inactivation, dewatering, nutrient management, and stabilization.[40]

The removal efficacy of microplastics during wastewater treatments depends on the treatment techniques used, and there is currently no approach that can remove all plastic materials in sewage sludge.[20, 40, 44] For example, a study by Mahon et al. analysed sludge that had been treated with different processes i.e. thermal drying, anaerobic digestion, and lime stabilization and found 4196 to 15,385 microplastics particles per kg (d.w.) of sludge (Mahon et al., 2016). Despite the plastic content, the resulting biosolids are typically used for applications such as landfilling, landscaping, composting, or disposal through incineration (Figure 2-7). Such applications transfer microplastics into the environment; the incineration process can also produce harmful contaminants such as dioxins and polychlorinated biphenyls emitted to the air.[5]

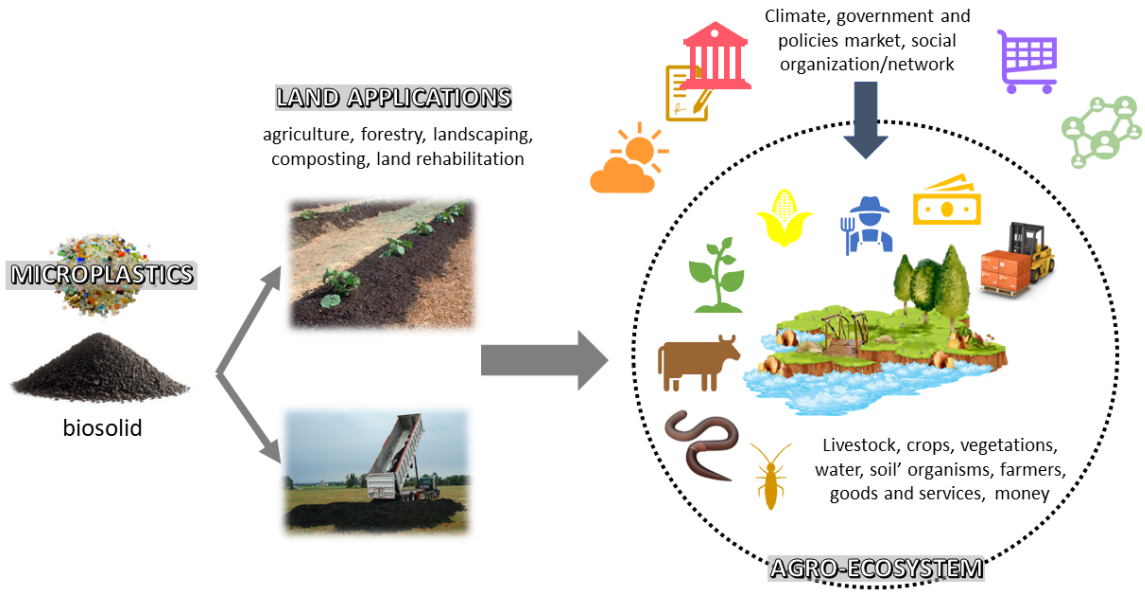

Figure 2-7. Illustration on microplastics pathways from biosolids to agroecosystem

Biosolids from wastewater treatment plants are not the only source for microplastics entering the environment, especially the land ecosystem. Agricultural practices, such as plastic mulching, compost from bio-wastes, irrigation pipes, and cleaned sewage or groundwater for irrigation, are other sources of plastic debris in the soils. It is also likely that external inputs from street littering, road and urban areas runoff, flooding in the riparian zone, and wind which could blow out the debris from other surface areas, are potential suppliers of microplastics.[8, 15, 45] Biosolids for landfill applications are also a source of microplastics in the ocean due to leaching and transport through surface run-off.[38]

4 Impact of microplastics on the ecosystem

There is an emerging debate about the impact of microplastics on the ecosystems and human health. This includes the role of microplastics in bio- solids, either as plastic material, or as a transporter of other contaminants. Concentration, size, and shape of microplastics as well as exposure time are factors that influence potentially negative effects on the ecosystem. In terms of type, pristine, weathered, and commercial microplastics shown different impact on the ecosystem.[46, 47] Table 2-1 summaries recent studies about the impact of microplastics and it seems that there is contradicting evidence. Some studies found direct adverse effect of microplastics, while other studies reported no effects. Additionally, there are studies showing the effect of microplastics only at certain concentration. Variation in parameters used in the reported studies making it incomparable and difficult to isolate the impact of the microplastics alone.

Table 2-1. Various effects of different type, size, concentration, and exposure time of microplastics on organisms and ecosystem.

Effect	Affected organisms or ecosystem	Type of plastics [b]	Size	Amount	Exposure Duration	Impacts	Reference
Negative	Earthworms	Polystyrene [a]	58 µm	1-2%	30 days	Growth slowed, mortality increased	[48]
	Soil	Polyacrylic fibres [c]	1540 – 6300 µm	Up to 2%	35 days	Microbial activity decreased, Water holding capacity, structure, and function changed	[30]
		Polyamide beads [a]	>10 µm				
		Polyester fibres [c]	>10 µm				
		Polyethylene fragments [a]	160 – 1200 µm				
	Soil	HDPE [a]	102.6 µm	0.1%	30 days	pH, water-stable aggregate profile, macro-aggregates altered significantly	[26]
		PLA [a]	65.6 µm	0.1%			
		Synthetic fibres [a]	<2mm; 2-7 mm; >7mm	0.0001%			
	Lolium perenne	HDPE [a]	102.6 µm	0.1%	30 days	Germinated grass seeds decreased; the shoot height reduced	[26]
		PLA [a]	65.6 µm	0.1%			
		Synthetic fibres [a]	<2mm; 2-7 mm; >7mm	0.0001%			
	Collembola	PVC [c]	80-250 µm	0.1%	56 days	Growth and reproduction inhibited	[49]
	Spring onions	PA [a]	15-20 µm	2%	60 days	Change in plant biomass, tissue elemental composition, and root traits; effects depended on plastic types	[29]
		HDPE [a]	643 µm	2%			
		PES [c]	5000 µm	2%			
		PET [a]	222-258 µm	2%			
		PP [a]	647-754 µm	2%			
		PS [a]	555-647 µm	0.2%			
	Wheat	Degraded plastic mulch [c] (LDPE and starch-based)	50 µm – 1 mm	1%	120 days	Vegetative and reproductive growth disturbed	[50]

Effect	Affected organisms or ecosystem	Type of plastics [b]	Size	Amount	Exposure Duration	Impacts	Reference
No Effect	Isopods	Plastic bag films [c]	183 nm	0.4%	14 days	Did not show any change in body mass, food ingestion rate, food assimilation rate, defecation rate, mortality, and energy reserve	[51]
		Beads from facial cleanser [c]	137 nm				
	Earthworms	Polyethylene [a]	250-1000 µm	0-0.1%	28 days	No significant changes in survival, number of juvenile, and final weight of adult earthworms	[52]
	Wheat and mixed-waste organic output	HDPE [c]	<2 mm	0.01-1%	270 days	No significant effect, and no clear trend observed on microbial community growth and diversity	[53]
		PET [c]					
		PVC [c]					
At certain level	Earthworms	Polystyrene [a]	58 µm	1-2%	30 days	Little effects on the fitness at lower concentration (<0.5%), while it was significantly increased at higher concentration (>1%)	[48]
	Earthworms	Polyethylene [a]	<150 µm	7-60%	60 days	Growth rate and weight decreased at higher concentration (28-60%), but no effect was observed on reproduction even though at higher concentration	[54]
	Garden cress	Polystyrene [a]	50-4800 nm	103-107 particles/mL	24 hours	Reduction in germination rate after 8 hours, but no effect at 24 hours; no difference in germination rate regardless the microplastics size, yet different in the root growth	[27]

[a] Pristine plastics.

[b] Weathered plastics. This type of plastics was not used among the above studies.

[c] Commercial plastics.

Microplastics can significantly affect the structure of soil and microorganisms within the soil.[6] One example showed that after intentionally exposing earthworms with polystyrene microplastics, their growth slowed and their mortality increased.[48] A different study exposed soil to different types of microplastics, and a decrease in soil bulk density and microbial activity was observed. Changes in the water retention capacity, soil structure and function were observed as well. Especially the internal soil structure in terms of macroaggregates was significantly modified.[26, 30]

Similar results were obtained by Zhu et al. in their study using springtails (Collembola, *Folsomia candida*), organism that contribute to the fragmentation of organic materials and the control of soil microbial communities. After exposing Collembola to PVC microplastics, changes in the collembolan gut structure were observed as well as an inhibition in organ- ism growth and reproduction.[49]

The effect of microplastics on plants was reported by Boots et al.[26] They showed that microplastics (HDPE, PLA, and synthetic fibres) decreased the number of germinated grass seeds and reduced the shoot height (*Lolium perenne*). de Souza Machado et al.[29] reported a significant change in plant biomass, tissue elemental composition, and root traits of *Allium fistulosum* (spring onion) after they were exposed to six different microplastics types (PA, HDPE, PES, PET, PP, and PS). However, the degree of impacts was varied depending on the type of plastic. Degraded plastic mulch (LDPE and starch-based) also showed negative effects on vegetative and reproductive growth of wheat (*Triticum aestivum*).[50]

Not all studies of microplastics have shown a negative impact on organisms. Kolkalj et al. reported that microplastics did not affect the feeding behavior and energy reserve of terrestrial isopods, *Porcellio scaber*, which play an important role in breaking down organic mate- rials. After intentionally exposing the isopods for 14 days with derived microplastics from plastic bags and facial cleanser, the isopods did not show any significant change in body mass, food ingestion rate, food assimilation rate, defecation rate, mortality, and energy reserve.[51]

A similar result was seen by Rodriguez et al. in their study of microplastics effects on earthworms, *Eisenia Andrei*. After exposing the earthworms for 28 days to polyethylene microplastics, no significant changes were seen in the earthworms' survival, number of juveniles, and final weight of adult earthworms.[52]

Another study investigating plants and soil biota also reported no significant effect of HDPE, PET, and PVC microplastics on wheat seedling growth and biomass production, as well as on earthworm mortality, growth, or avoidance behavior after nine months. Microplastics were intentionally added into compost-like output and no clear trends on microbial community growth and diversity were observed.[53]

Most studies reporting negative effects of microplastics on invertebrates used concentrations well above any realistic values that might result from the application of biosolid to land or soil.[8] Additionally, concentrations used often vary in number and units, resulting in inconclusive and incomparable results.

There are few studies that investigated the concentration and particle-size dependence on the observed effects. For example, earthworm fitness was hardly affected at lower concentrations of polystyrene microplastics (≤0.5 % w/w), while the effect was significantly increased at higher concentrations (>1% w/w).[48]

Similarly, 7 % w/w of polyethylene microplastics (size <150 µm) after 60 days did not affect the fitness of earthworms *Lumbricus terrestris*, whereas higher concentrations (28–60 %) led to a decrease in the earthworms' growth and weight. However, no effect was observed on their reproduction.[54]

In addition to the concentration of microplastics, other parameters such as size, shape, type, surface character, and exposure time also can play in important role, however relevant studies are still very limited.[5] For example, PE particles with sizes <150 µm (0–60 % for 60 days) led to a decreased growth rate and weight in earthworms, while larger particles (250–1000 µm, 0–0.1 % for 28 days) showed no significant effects.[52, 54] In a study investigating different exposure times, a short exposure (8 h) of garden cress (*Lepidium sativum*) to polystyrene microplastics (size 50–4800 nm; concentration 103–107 particles/mL) showed a reduction in germination rate. For longer exposure times (24 h), the germination rate was not affected, however a decrease root growth rate has been observed.[27]

Further implications of microplastics on a higher level of the ecosystem, particularly on humans, are still unknown. Such investigations are challenging as factors such as diversity in food intake, soil condition, animal activities and metabolisms have to be taken into account.[6, 55]

5 Microplastics analysis

Microplastics analysis is significantly impeded by the lack of standardized methods. In the following we review current guidelines and methods to then discuss a systematic approach to analyzing microplastics. Most of the current work is focused on marine samples such as seawater and sediment. Techniques used include Fourier-transform Infrared (FTIR) and Raman microspectroscopy, Py-GC/MS, and Flow Cytometry.

To date, three guidelines have been published about microplastics analysis for solid samples (Table 2-2). Two of them, the guidelines from the European Commission in 2013 and from the National Oceanographic and Atmospheric Agency in 2015, are for sediments in the marine environments, and only the guideline from the UK Water Industry Research refers to solid waste, i.e. sludge and biosolids.[10, 56, 57]

Table 2-2. Published guidelines of microplastics analysis for solid samples

Guideline/by/year	Samples	Sampling tools / Methods	Identification methods	Reports
Guidance on Monitoring of Marine Litter in European Seas / Joint Research Center of the European Commission, Marine Strategy Framework Directive (MSDF)/ 2013 [56]	Beach Intertidal and Subtidal Sediments	Veen grab, multi corer, or box cores / Samples are fractioned into two classes (20 µm – 1 mm and 1 – 5 mm) using metal sieves, followed by the density separation with concentrated saline NaCl solution	Binocular microscope (50x magnifying), and FTIR or Raman spectroscopy	items/ml of sediment in size bins of 100 µm i.e., 20-100 µm, 101-200 µm and so on. The characters of plastic particles are reported based on the main colors, shapes, and polymer types
Laboratory Methods for the Analysis of Microplastics in the Marine Environment: Recommendations for quantifying synthetic particles in waters and sediments / National Oceanic and Atmospheric Administration, Marine Debris Division, US Department of Commerce/2015 [57]	Beach and Bed Sediments	Shovel, spade, corer, or grab sampler e.g., Ponar sampler / Samples are dried overnight, and potassium metaphosphate is added, followed by lithium metatungstate for density separation. Fenton's reagent is used to remove organic matters, then NaCl solution is added for further isolate microplastics particles.	Dissecting microscope (40X magnification) and gravimetric analysis	mass of all microplastics in the size range of 0.3 – 5 mm
Sink to River – River to Tap: A Review of Potential Risks from Nanoparticles and Microplastics / UK Water Industry Research/2019 [10]	Sludges	Trowel / Samples are dried at 50^{o}C for around one week prior to analysis. Sub-sampling is recommended i.e., 1 g dry mass sludge sampled from the sieved material (1 mm size pore mesh), followed by Fenton's reaction to remove organic materials, flotation using $ZnCl_2$ solution for density separation, and cellulase enzyme digestion. Plastic particles then are separated into "coarse" (>178 µm) and "fine" (<178 µm) fractions	FTIR spectrometer analysis combined with MPhunter software for data analysis.	number of particles with size >25 µm complemented by their polymer type

Additionally, the three guidelines lead to very different outcomes, mainly focusing on the enumeration of plastic particles, and much less on their identification.

5.1 Analytical Technique

Microplastics analysis is basically divided into three stages: (1) sample collection, (2) sample processing or pre-treatment, and (3) sample analysis that includes identification, characterization, and quantification. Among the techniques that can be used for sample analysis, the following methods are the most common ones.

5.1.1 Light or optical microscopy

This is a visual identification method usually combined with dyes such as Nile Red and Rose Bengal to differentiate between synthetic and natural polymer or other organic and inorganic particles. Image processing software, e.g. ImageJ or MP-VAT, can be used for automatic particles counting, size estimation, and shape characterization.[19, 58-62]

5.1.2 FTIR and Raman spectroscopy

FTIR and Raman are the most used spectroscopic techniques for microplastics analysis[63], however they are limited by the particles size that can be analysed. The FTIR or micro-FTIR technique is able to detect microplastics down to a size of 20 µm, while Raman or micro-Raman can be used for plastic particles down to 1 µm.[2, 64, 65] Software such as ParticleFinder and siMPle is commonly applied to assist in particles counting, size measurement, and shape characterization.[66, 67] Although the sample analysis can be time consuming (several hours or even days could be needed to obtain final data), these methods are still recommended for microplastics analysis due to their accuracy and sensitivity. Some adjustments may be necessary depending on the type of sample. For example, in Raman spectroscopy, because of its sensitivity to fluorescent particles, choosing a suitable substrate or filter material of membrane filter is recommended to avoid background interference.[68]

5.1.3 Py-GC.MS or TED-GC/MS

Pyrolysis (Py) and Thermal Extraction Desorption (TED) in combination with gas chromatography and mass spectrometry (GC/MS) is a thermo- analytical approach that is more time-efficient compared with spectro-scopic methods. The techniques can give insights into polymer concentra- tion and type. Particle count, size, and shape characteristics cannot be generated, due to the destructive nature of the method where particles are intentionally thermo-degraded.[69, 70]

5.1.4 Others: Flow Cytometry, Dynamic Light Scattering, Nanoparticle Tracking Analysis

Less common methods used for microplastics analysis are Scanning Electron Microscopy (SEM) and Atomic Force Microscopy (AFM). They can give access to detailed information on size, shape, and surface characteristics of the plastic particles. Flow cytometry/imaging, Dynamic Light Scattering (DLS), and Nanoparticle Tracking Analysis (NTA) are mainly utilized to characterize size distribution, particle count, and surface charge.[67, 71-73]

5.2 Selection and development of methods

There is no single technique, that will provide a complete analysis of a microplastics sample. The large number of different analytic techniques, each with different requirements and outcomes, makes it difficult to identify a preferred one. We rather recommend a purpose-fit approach to design an appropriate analytical approach: (1) determine the desired approach, e.g. routine monitoring, mapping, treatment efficacy

monitoring; (2) choose the evidence or parameters required, e.g. size, type, shape, amount (3) select the methods that generate the required data.

5.2.1 Strategy and criteria

Method selection and development are study dependent. While there are some commonly used techniques for microplastics analysis in sludge and biosolid samples, often a combination of methods is necessary, depending on the research goal. For examples, in order to understand the morphology of plastic particles such as surface roughness and size, electron microscopy is the suitable method, yet will not yield the chemical nature of the particles. On the other hand, the combination between light microscopy and FTIR spectroscopy is the most common technique to gain data on the amount, size, shape, and type of the plastic particles.[64, 65] Further exploration on the possible novel insight in the microplastics analysis could be done by enabling the online or direct analysis of some available techniques which could reduce the risks of cross contamination.[74] Also, the synthesis of nanoparticles is a recent approach to trace or tag the nanoplastics in the environment matrices.[75, 76]

When selecting a method, additional parameters such as costs, working time, data obtained, accuracy, and sensitivity have to be taken into account. These factors are considered as the critical ones in determining the method for commercial or industrial purposes.

5.2.2 Scaling comparison

A scaling approach is using a number or scale to compare available analytical techniques. The approach should help choosing a specific (or combination of) technique(s) depending on circumstances of the study and desired outcomes. This approach is more practical for industrial purposes than listing the benefits and limitations of each technique or instrument, which are endless as their development is still ongoing.

The following tables are the scaling comparison of different analytical methods for microplastics evaluated based on some referred resources. The higher of the scale number represents the preferable methods that implied less working time and costs as well as more accurate and sensitive method (Table 2-3). This scale comparison can be adjusted depending on the aims of the research and type of samples.

Table 2-3. The scale number for method comparison

Scale	Time	Cost	Accuracy	Sensitivity	Data-types
1	Most time-consuming (weeks)	Most expensive	Least accurate	Least sensitive	One
2	Days	Expensive	Low accuracy	Low	Two
3	1 day	Average	Average	Average	Three
4	Hours (less than 1 day)	Cheap	Less accurate	Less sensitive	Four

5	Fastest (minutes)	Cheapest	High accuracy	High sensitivity	Five	

For pre-treatment and separation methods, Fenton reagent and Floatation using salt share the same total scale number. They are considered as the best as it is the fastest with average costs, and a quite high accuracy as well as sensitivity. Both techniques are commonly used subsequently to gain higher organic matter removal efficiency of the matrices.[45, 61, 62, 77-79] Although Field Flow Fractionation (FFF) has high accuracy, the cost is more expensive and may require a trained analyst (Table 2-4).

Table 2-4. Scaling of commonly used methods for pre-treatment and separation

Method	Time	Cost [a]	Accuracy [b]	Sensitivity [c]	SUM	Average
Field Flow Fractionation [64, 74]	4	2	3	5	14	3.5
Fenton reagent [10, 45, 77]	5	4	4	4	17	4.25
Trichlorobenzene (TCB)[78]	5	4	3	3	15	3.75
Floatation with salt e.g. NaI, $ZnCl_2$ [10, 45]	4	5	4	4	17	4.25
Flocculation with $KAl(SO_4)_2$ [78]	5	4	3	3	15	3.75

[a] Cost is in USD, estimated based on commercial prices and/or [67]
[b] Validation by Recovery/Spike rates = false positive and blanks/controls = false negative tested or potential used for soil, sediment, sludge, or biosolid samples
[c] Verification and Calibration with LOD (Limit of Detection) and LOQ (Limit of Quantification)

For identification, quantification, and characterization methods, Py- GC/MS is preferred because of its high accuracy and sensitivity for mass quantification. This method is not limited to certain size and shape of the plastic particles but depends on the purpose of the study because the generated data are limited to total mass and type of polymers. Therefore, Py-GC/ MS is recommended to be employed in complement of FTIR or Raman microspectroscopy as these techniques produce information on size and shape of the particles. As an alternative, DLS or NTA are suggested as their working time is the fastest although they are not as accurate and sensitive compared with FTIR, Raman, and Py-GC/MS (Table 2-5). However, there is a possibility to modify the DLS or NTA method by combination with Py-GC/MS as explained in the following paragraph.

Table 2-5. Scaling of commonly used methods for identification, quantification, and characterization

Method	Time	Cost [a]	Accuracy [b]	Sensitivity [c]	Data obtained	SUM	Average
Light microscopy [58]	3	5	1	1	4 size, shape, type, counts	14	2.8
FTIR microspectroscopy [63]	3	2	5	3	4 size, shape, type, mass	17	3.4
Raman microspectroscopy [63]	3	1	5	4	4 size, shape, type, mass	17	3.4
Py-GC/MS [70]	4	2	5	5	2 type, mass	18	3.6

DLS/NTA [d] [72, 73]	4	3	3	4	3	size, shape, counts	17	3.4
Flow cytometry/imaging [67, 71]	3	2	3	4	4	size, shape, counts, type	16	3.2

[a] Cost (in USD): Light microscopy $2-3k; FTIR/μFTIR $200-250k; Raman/μRaman $200-400k; Py-GC/MS $>$215k; DLS/NTA $60-120k; Flow Cytometry/imaging $>130k. It is estimated based on commercial prices and/or Primpke, Christiansen, et al. (2020).

[b] Validation by Recovery/Spike rates = false positive and blanks/controls = false negative tested or potential used for soil, sediment, sludge, or biosolid samples

[c] Verification and Calibration with LOD (Limit of Detection) and LOQ (Limit of Quantification)

[d] DLS: Dynamic Light Scattering; NTA: Nanoparticle Tracking Analysis

Combination of Pressurized Liquid Extraction (PLE) and Py-GC/MS (combination D), and ultrafiltration, DLS, and Py-GC/MS (combination F) placed the highest scale number because their time, cost, and sensitivity are outnumbered the others. However, combination D is limited to total mass and type of polymer (Table 2-6). Such downsides can be covered by either FTIR or Raman spectroscopy techniques or using combination F. However, combination F method has not been validated for sludge or biosolid sample as well as other solid environmental samples.

Table 2-6. Scaling of combination methods for microplastics analysis in solid environmental matrices

Method	Time	Cost [a]	Accuracy [b]	Sensitivity [c]	Data obtained		SUM	Average
A (FFF-UV-MALS-RT [d]) [74]	3	1	3	5	4	size, shape, type, mass	16	3.2
B (Fenton-Density-Visual-FTIR) [79]	3	2	4	4	4	size, shape, type, mass	17	3.4
C (Nile Red + automated software MP-VAT) [61]	3	4	4	3	3	size, shape, counts	17	3.4
D (Pressurized Liquid Extraction + Py-GC/MS) [70]	3	3	5	5	2	type, mass	18	3.6
E (micro-Raman + software "Particle Finder") [68]	3	2	4	4	4	size, shape, type, mass	17	3.4
F (ultrafiltration + DLS + Py-GC/MS) [73]	3	3	3	5	4	size, type, counts, mass	18	3.6
G (Fenton + $KAl(SO_4)_2$ + TCB + Py-GC/MS) [78]	4	1	4	4	2	type, mass	15	3
H (Metal-doped nanoplastics) [75, 76]	2	3	5	5	2	counts, mass	17	3.4

[a] Cost is in USD, estimated based on commercial prices and/or [67].

[b] Validation by Recovery/Spike rates = false positive and blanks/controls = false negative tested or potential used for soil, sediment, sludge, or biosolid samples

[c] Verification and Calibration with LOD (Limit of Detection) and LOQ (Limit of Quantification)

[d] FFF: Field Flow Fractionation; MALS: Multi Angle Light Scattering; RT: Raman Tweezers

6 Final thoughts and future studies

6.1 How many microplastics to be considered as contaminants

Browne et al. suggested using hypothetical links to assess the likely impacts of plastic debris for the unknown ecological linkages. Using the known toxicological consequences for the individual organism, the identified variables can be utilized to develop a guideline for risk assessment and management. Such guidelines, then, can provide early warning for ecological impacts and assist to monitor the contaminated systems toward recovery. The authors also pointed out on considering the population impacts instead of individuals because responses to debris vary among individuals. Nevertheless, experimentally testing relevant hypotheses impacts is necessary to demonstrate causalities and direct effects.[80, 81]

Developing the hypothetical links for impacts of sludge and biosolid containing microplastics on the ecosystem needs a systematic literature review, which is not the aim of this study. However, the research reports, so far, on microplastics effect on the ecosystems, have shown that concentration, size, type of microplastics, and time exposed significantly influence the degree of effects. In fact, all these factors vary widely for each research report. In terms of concentration, it is difficult to determine the lethal limit of microplastics presence in the ecosystem because its effects vary for each organism's behavior and soil biophysical composition.

Since microplastics are contaminants, they have poisonous impacts on the ecosystem. Evidence proves that microplastics cause disruption and death of the organisms, but it does at a certain level, size, type, and is varied for each organism. Then, the problem is on determining the limits of microplastics' amount, which needs a long-term study and monitoring. At present, risk assessment and management as well as developing the guidelines for microplastics removal treatment and recovery are steps that can be taken while continuing with experiments to collect the data and assemble the ecotoxicological effects.

6.2 A field evaluation is crucial

Field evidence is a crucial factor in determining ecological linkage.[80] Using other countries' data for plastic loads estimation is unreliable due to variation in the field condition between regions and countries. Spatial and temporal conditions influence the plastic loads greatly.

Rolsky et al. [20] suggested that data coverage in geographical conditions is essential to obtain a better understanding of how microplastics are likely to occur and accumulate in the ecosystem. This includes seasonality and sociality or urbanization. For example, a study in South Korea by Lee and Kim showed that increasing precipitation positively correlated with the number of microplastics in sludge.[82] In China, increasing infra- structure and industrial activities as well as smaller areas of afforested land also showed a positive correlation with a higher concentration of microplastics in sludge.[22] These factors also reflect the population size and their behavior.

6.3 Continuous studies

Microplastics in biosolids should be considered as a contaminant for agricultural applications, yet their presence is unavoidable. To what level should they be limited or rejected for land applications?

Plastic debris disrupts the ecosystem, and more experiments are necessary to determine the magnitude of sublethal and lethal impacts from plastics exposures. This includes detailed information on plastic-type, size, shape, dimensions, volume, and mass. Thus, accurate and precise microplastics' quantification and characterization methods are urgently needed.

Incorporation with the identification techniques development, continuous monitoring of biosolids application i.e. frequency or period, and the amount of application are necessary as well. The reason is plastic debris tends to accumulate and its degradation needs days, months, even years, so does the ecosystem that is evolving. Also, the interactions of microplastics with other contaminants, such as additives and persistent organic pollutants, could worsen the effects on the ecosystem. It is arguable that the only source of microplastics in agricultural soils is from biosolids applications. There is a possibility of other sources such as plastic mulch, twine, rope, and irrigation pipe.[8]

Achieving zero plastic debris in biosolids sounds very unlikely considering the current usage of plastic materials in diverse applications from households to industries. However, if we do not start to increase our awareness of how it could vastly and unnoticedly increase for the years to come, such invisible threats could be a silent killer for the next generation.

Author contributions

Both authors contributed equally to the manuscript.

Data availability

No data used for the research described in the article.

Declaration of competing interest

The authors report no conflicts of interests. The authors alone are responsible for the content and writing of this article

Acknowledgement

This on-going project is supported by South Australia Water (SA Water) corporation. The authors acknowledge Alexandra Keegan, Milena Fernandes, Clos Ilda, and Melody Lau (SA Water) for their continuous support and advice on this project; to Professor Paul Kirkbride (Flinders University) for his assistance on analytical techniques; and Shima Ziajahromi (Griffith University) for her advice in this study.

References

1. Hartmann, N. B.; Hüffer, T.; Thompson, R. C.; Hassellöv, M.; Verschoor, A.; Daugaard, A. E.; Rist, S.; Karlsson, T.; Brennholt, N.; Cole, M.; Herrling, M. P.; Hess, M. C.; Ivleva, N. P.; Lusher, A. L.; Wagner, M., Are We Speaking the Same Language? Recommendations for a Definition and Categorization Framework for Plastic Debris. *Environmental Science & Technology* **2019,** *53* (3), 1039-1047.
2. Hidalgo-Ruz, V.; Gutow, L.; Thompson, R. C.; Thiel, M., Microplastics in the Marine Environment: A Review of the Methods Used for Identification and Quantification. *Environmental Science & Technology* **2012,** *46* (6), 3060-3075.
3. Thompson, R. C., Microplastics in the marine environment: sources, consequences and solutions. In *Marine anthropogenic litter*, Springer, Cham: 2015; pp 185-200.
4. de Sá, L. C.; Oliveira, M.; Ribeiro, F.; Rocha, T. L.; Futter, M. N., Studies of the effects of microplastics on aquatic organisms: What do we know and where should we focus our efforts in the future? *Science of The Total Environment* **2018,** *645*, 1029-1039.
5. Lambert, S.; Scherer, C.; Wagner, M., Ecotoxicity testing of microplastics: Considering the heterogeneity of physicochemical properties. *Integrated Environmental Assessment and Management* **2017,** *13* (3), 470-475.
6. Ng, E.-L.; Huerta Lwanga, E.; Eldridge, S. M.; Johnston, P.; Hu, H.-W.; Geissen, V.; Chen, D., An overview of microplastic and nanoplastic pollution in agroecosystems. *Science of The Total Environment* **2018,** *627*, 1377-1388.
7. Oehlmann, J.; Schulte-Oehlmann, U.; Kloas, W.; Jagnytsch, O.; Lutz, I.; Kusk, K. O.; Wollenberger, L.; Santos, E. M.; Paull, G. C.; Van Look, K. J. W.; Tyler, C. R., A Critical Analysis of the Biological Impacts of Plasticizers on Wildlife. *Philosophical Transactions: Biological Sciences* **2009,** *364* (1526), 2047-2062.
8. Hopewell, K.; Batstone, D.; Dale, G.; Keegan, A.; Lee, E.; Randall, L.; Tao, E. *ANZBP Preliminary Report on Microplastics Risk for the Australian and New Zealand Biosolids Industry July 2020*; 2020.
9. Toffey, W.; Brown, S., Biosolids and ecosystem services: Making the connection explicit. *Current Opinion in Environmental Science & Health* **2020,** *14*, 51-55.
10. Ball H, C. R., Grove E, Horton A, Johnson A, Jürgens M, Read D, Svendsen C, Sink To River - River To Tap. A Review of Potential Risks From Nanoparticles and Microplastics. *UK Water Industry Research Limited* **2019,** *EQ 01 A 231*.
11. Bayo, J.; Olmos, S.; LÓPez-Castellanos, J.; Alcolea, A., Microplastics and Microfibers in the Sludge of A Municipal Wastewater Treatment Plant. *International Journal of Sustainable Development and Planning* **2016,** *11* (5), 812-821.
12. Murphy, F.; Ewins, C.; Carbonnier, F.; Quinn, B., Wastewater Treatment Works (WwTW) as a Source of Microplastics in the Aquatic Environment. *Environmental Science & Technology* **2016,** *50* (11), 5800-5808.
13. Okoffo, E. D.; O'Brien, S.; O'Brien, J. W.; Tscharke, B. J.; Thomas, K. V., Wastewater treatment plants as a source of plastics in the environment: a review of occurrence, methods for identification, quantification and fate. *Environmental Science: Water Research & Technology* **2019,** *5* (11), 1908-1931.
14. Alexander, J.; Barregard, L.; Bignami, M.; Ceccatelli, S.; Cottrill, B.; Dinovi, M.; Edler, L.; Grasl-Kraupp, B.; Hogstrand, C.; Hoogenboom, L.; Knutsen, H. K.; Nebbia, C. S.; Oswald, I.; Petersen, A.; Rogiers, V. M.; Rose, M.; Roudot, A.-C.; Schwerdtle, T.; Vleminckx, C.; Vollmer, G.; Wallace, H.; Chain, E. P. C. F., Presence of microplastics and nanoplastics in food, with particular focus on seafood. *Efsa Journal* **2016,** *14* (6).
15. Bläsing, M.; Amelung, W., Plastics in soil: Analytical methods and possible sources. *Science of The Total Environment* **2018,** *612*, 422-435.
16. Bretas Alvim, C.; Mendoza-Roca, J. A.; Bes-Piá, A., Wastewater treatment plant as microplastics release source – Quantification and identification techniques. *Journal of Environmental Management* **2020,** *255*, 109739.
17. He, D.; Luo, Y.; Lu, S.; Liu, M.; Song, Y.; Lei, L., Microplastics in soils: Analytical methods, pollution characteristics and ecological risks. *TrAC Trends in Analytical Chemistry* **2018,** *109*, 163-172.
18. Toussaint, B.; Raffael, B.; Angers-Loustau, A.; Gilliland, D.; Kestens, V.; Petrillo, M.; Rio-Echevarria, I. M.; Van den Eede, G., Review of micro- and nanoplastic contamination in the food chain. *Food Additives & Contaminants: Part A* **2019,** *36* (5), 639-673.

19. Corradini, F.; Meza, P.; Eguiluz, R.; Casado, F.; Huerta-Lwanga, E.; Geissen, V., Evidence of microplastic accumulation in agricultural soils from sewage sludge disposal. *Science of The Total Environment* **2019,** *671*, 411-420.
20. Rolsky, C.; Kelkar, V.; Driver, E.; Halden, R. U., Municipal sewage sludge as a source of microplastics in the environment. *Current Opinion in Environmental Science & Health* **2020,** *14*, 16-22.
21. Mahon, A. M.; Connell, B.; Healy, M.; O'Connor, I.; Officer, R.; Nash, R.; Morrison, L., Microplastics in Sewage Sludge: Effects of Treatment. *Environmental Science & Technology* **2016,** *51*.
22. Li, X.; Chen, L.; Mei, Q.; Dong, B.; Dai, X.; Ding, G.; Zeng, E. Y., Microplastics in sewage sludge from the wastewater treatment plants in China. *Water Research* **2018,** *142*, 75-85.
23. Gatidou, G.; Arvaniti, O. S.; Stasinakis, A. S., Review on the occurrence and fate of microplastics in Sewage Treatment Plants. *Journal of Hazardous Materials* **2019,** *367*, 504-512.
24. Hurley, R. R.; Nizzetto, L., Fate and occurrence of micro(nano)plastics in soils: Knowledge gaps and possible risks. *Current Opinion in Environmental Science & Health* **2018,** *1*, 6-11.
25. Ziajahromi, S.; Neale, P. A.; Rintoul, L.; Leusch, F. D. L., Wastewater treatment plants as a pathway for microplastics: Development of a new approach to sample wastewater-based microplastics. *Water Research* **2017,** *112*, 93-99.
26. Boots, B.; Russell, C. W.; Green, D. S., Effects of Microplastics in Soil Ecosystems: Above and Below Ground. *Environmental Science & Technology* **2019,** *53* (19), 11496-11506.
27. Bosker, T.; Bouwman, L. J.; Brun, N. R.; Behrens, P.; Vijver, M. G., Microplastics accumulate on pores in seed capsule and delay germination and root growth of the terrestrial vascular plant Lepidium sativum. *Chemosphere* **2019,** *226*, 774-781.
28. Cartwright, C. D.; Thompson, I. P.; Burns, R. G., Degradation and impact of phthalate plasticizers on soil microbial communities. *Environmental Toxicology and Chemistry* **2000,** *19* (5), 1253-1261.
29. de Souza Machado, A. A.; Lau, C. W.; Kloas, W.; Bergmann, J.; Bachelier, J. B.; Faltin, E.; Becker, R.; Görlich, A. S.; Rillig, M. C., Microplastics Can Change Soil Properties and Affect Plant Performance. *Environmental Science & Technology* **2019,** *53* (10), 6044-6052.
30. de Souza Machado, A. A.; Lau, C. W.; Till, J.; Kloas, W.; Lehmann, A.; Becker, R.; Rillig, M. C., Impacts of Microplastics on the Soil Biophysical Environment. *Environmental Science & Technology* **2018,** *52* (17), 9656-9665.
31. Hamilton, K. A.; Ahmed, W.; Rauh, E.; Rock, C.; McLain, J.; Muenich, R. L., Comparing microbial risks from multiple sustainable waste streams applied for agricultural use: Biosolids, manure, and diverted urine. *Current Opinion in Environmental Science & Health* **2020,** *14*, 37-50.
32. Jacques, O.; Prosser, R. S., A probabilistic risk assessment of microplastics in soil ecosystems. *Science of the Total Environment* **2021,** *757*.
33. Thompson, R. C.; Olsen, Y.; Mitchell, R. P.; Davis, A.; Rowland, S. J.; John, A. W. G.; McGonigle, D.; Russell, A. E., Lost at sea: where is all the plastic? *Science (New York, N.Y.)* **2004,** *304* (5672), 838.
34. Arthur, C.; Baker, J. E.; Bamford, H. A., Proceedings of the International Research Workshop on the Occurrence, Effects, and Fate of Microplastic Marine Debris, September 9-11, 2008, University of Washington Tacoma, Tacoma, WA, USA. **2009**.
35. European Commission, Commission recommendation of 18 October 2011 on the definition of nanomaterial. *Off. J. Eur. Union* **2011,** *275*, 38.
36. Ivleva, N. P.; Wiesheu, A. C.; Niessner, R., Microplastic in Aquatic Ecosystems. *Angewandte Chemie International Edition* **2017,** *56* (7), 1720-1739.
37. The International Organization for Standardization, ISO/TR 21960:2020 Plastics - Environmental aspects - State of knowledge and methodologies. 2020.
38. He, P.; Chen, L.; Shao, L.; Zhang, H.; Lu, F., Municipal solid waste (MSW) landfill: A source of microplastics?-Evidence of microplastics in landfill leachate. *Water Research* **2019,** *159*, 38-45.
39. Environment Protection Authority, Guidelines for the safe handling and reuse of biosolids in South Australia. Adelaide, South Australia, 2020.
40. Australian & New Zealand Biosolids Partnership Biosolids. https://www.biosolids.com.au/info/what-are-biosolids/#:~:text=Sewage%20sludge%20is%20regarded%20as,15%25%20to%2090%25%20solids. (accessed 10 September).

41. Kerstin, M.; Norén, F., Screening of microplastic particles in and downstream a wastewater treatment plant. *Swedish Environmental Research Institute, Report* **2014**.
42. Liu, X.; Yuan, W.; Di, M.; Li, Z.; Wang, J., Transfer and fate of microplastics during the conventional activated sludge process in one wastewater treatment plant of China. *Chemical Engineering Journal* **2019,** *362*, 176-182.
43. Lusher, A. L.; Hurley, R.; Vogelsang, C.; Nizzetto, L.; Olsen, M. *Mapping microplastics in sludge*; 8257769509; Norwegian Institute for Water Research,: Norway, 11 December 2017, 2017; p 55.
44. Lusher, A.; Hurley, R.; Vogelsang, C., Microplastics in sewage sludge: Captured but released? *Microplastics in Water and Wastewater, Hrissi K. Karapanagioti, Ioannis K. Kalavrouziotis Download citation file: Ris (Zotero) Reference Manager EasyBib Bookends Mendeley Papers EndNote RefWorks BibTex Close Search* **2019**.
45. Hurley, R. R.; Lusher, A. L.; Olsen, M.; Nizzetto, L., Validation of a Method for Extracting Microplastics from Complex, Organic-Rich, Environmental Matrices. *Environmental Science & Technology* **2018,** *52* (13), 7409-7417.
46. Qi, R.; Jones, D. L.; Li, Z.; Liu, Q.; Yan, C., Behavior of microplastics and plastic film residues in the soil environment: A critical review. *Science of the Total Environment* **2020,** *703*.
47. Renner, G.; Schmidt, T. C.; Schram, J., Analytical methodologies for monitoring micro(nano)plastics: Which are fit for purpose? *Current Opinion in Environmental Science & Health* **2018,** *1*, 55-61.
48. Cao, D.; Wang, X.; Luo, X.; Liu, G.; Zheng, H., Effects of polystyrene microplastics on the fitness of earthworms in an agricultural soil. *IOP Conference Series: Earth and Environmental Science* **2017,** *61*, 012148.
49. Zhu, D.; Chen, Q.-L.; An, X.-L.; Yang, X.-R.; Christie, P.; Ke, X.; Wu, L.-H.; Zhu, Y.-G., Exposure of soil collembolans to microplastics perturbs their gut microbiota and alters their isotopic composition. *Soil Biology and Biochemistry* **2018,** *116*, 302-310.
50. Qi, Y.; Yang, X.; Pelaez, A. M.; Huerta Lwanga, E.; Beriot, N.; Gertsen, H.; Garbeva, P.; Geissen, V., Macro- and micro- plastics in soil-plant system: Effects of plastic mulch film residues on wheat (Triticum aestivum) growth. *Science of The Total Environment* **2018,** *645*, 1048-1056.
51. Jemec Kokalj, A.; Horvat, P.; Skalar, T.; Kržan, A., Plastic bag and facial cleanser derived microplastic do not affect feeding behaviour and energy reserves of terrestrial isopods. *Science of The Total Environment* **2018,** *615*, 761-766.
52. Rodriguez-Seijo, A.; Lourenço, J.; Rocha-Santos, T. A. P.; da Costa, J.; Duarte, A. C.; Vala, H.; Pereira, R., Histopathological and molecular effects of microplastics in Eisenia andrei Bouché. *Environmental Pollution* **2017,** *220*, 495-503.
53. Judy, J. D.; Williams, M.; Gregg, A.; Oliver, D.; Kumar, A.; Kookana, R.; Kirby, J. K., Microplastics in municipal mixed-waste organic outputs induce minimal short to long-term toxicity in key terrestrial biota. *Environmental Pollution* **2019,** *252*, 522-531.
54. Huerta Lwanga, E.; Gertsen, H.; Gooren, H.; Peters, P.; Salánki, T.; van der Ploeg, M.; Besseling, E.; Koelmans, A. A.; Geissen, V., Microplastics in the Terrestrial Ecosystem: Implications for Lumbricus terrestris (Oligochaeta, Lumbricidae). *Environmental Science & Technology* **2016,** *50* (5), 2685-2691.
55. Prata, J. C.; da Costa, J. P.; Lopes, I.; Andrady, A. L.; Duarte, A. C.; Rocha-Santos, T., A One Health perspective of the impacts of microplastics on animal, human and environmental health. *Science of the Total Environment* **2021,** *777*.
56. Galgani, F.; Hanke, G.; Werner, S.; Oosterbaan, L.; Nilsson, P.; Fleet, D.; Kinsey, S.; Thompson, R. C.; Franeker, J. v.; Vlachogianni, T.; Scoullos, M.; Viega, J. M.; Palatinus, A.; Matiddi, M.; Maes, T.; Korpinen, S.; Budziak, A.; Leslie, H.; Gago, J.; Liebezeit, G., Guidance on Monitoring of Marine Litter in European Seas. *Publication Office of the European Union* **2013**, 128.
57. Masura, J.; Baker, J. E.; Foster, G. D.; Arthur, C.; Herring, C., Laboratory methods for the analysis of microplastics in the marine environment : recommendations for quantifying synthetic particles in waters and sediments. **2015**.
58. Bayo, J.; Olmos, S.; López-Castellanos, J., Removal of Microplastics from Wastewater. *Handbook of Microplastics in the Environment* **2020**, 1-20.

59. Lv, L.; Qu, J.; Yu, Z.; Chen, D.; Zhou, C.; Hong, P.; Sun, S.; Li, C., A simple method for detecting and quantifying microplastics utilizing fluorescent dyes - Safranine T, fluorescein isophosphate, Nile red based on thermal expansion and contraction property. *Environmental Pollution* **2019,** *255*, 113283.
60. Maes, T.; Jessop, R.; Wellner, N.; Haupt, K.; Mayes, A. G., A rapid-screening approach to detect and quantify microplastics based on fluorescent tagging with Nile Red. *Scientific Reports* **2017,** *7* (1), 44501.
61. Prata, J. C.; Reis, V.; Matos, J. T. V.; da Costa, J. P.; Duarte, A. C.; Rocha-Santos, T., A new approach for routine quantification of microplastics using Nile Red and automated software (MP-VAT). *Science of The Total Environment* **2019,** *690*, 1277-1283.
62. Prata, J. C.; da Costa, J. P.; Duarte, A. C.; Rocha-Santos, T., Methods for sampling and detection of microplastics in water and sediment: A critical review. *TrAC Trends in Analytical Chemistry* **2019,** *110*, 150-159.
63. Lares, M.; Mohamed Chaker, N.; Sillanpää, M.; Sillanpää, M., Intercomparison study on commonly used methods to determine microplastics in wastewater and sludge samples. *Environmental Science and Pollution Research International* **2019,** *26* (12), 12109-12122.
64. Schwaferts, C.; Niessner, R.; Elsner, M.; Ivleva, N. P., Methods for the analysis of submicrometer- and nanoplastic particles in the environment. *TrAC Trends in Analytical Chemistry* **2019,** *112*, 52-65.
65. Sun, J.; Dai, X.; Wang, Q.; van Loosdrecht, M. C. M.; Ni, B.-J., Microplastics in wastewater treatment plants: Detection, occurrence and removal. *Water Research* **2019,** *152*, 21-37.
66. Frère L, P. P. I., Moreau J, Soudant P, Lambert C, , Huvet A, Rinnert E, A semi-automated Raman micro-spectroscopy method for morphological and chemical characterizations of microplastic litter. *Marine Pollution Bulletin* **2016,** *113* (1), 461-468.
67. Primpke, S.; Christiansen, S. H.; Cowger, W.; De Frond, H.; Deshpande, A.; Fischer, M.; Holland, E.; Meyns, M.; O'Donnell, B. A.; Ossmann, B., Critical Assessment of Analytical Methods for the Harmonized and Cost Efficient Analysis of Microplastics. *Applied Spectroscopy* **2020,** *74* (9), 1012-1047.
68. Oßmann, B. E.; Sarau, G.; Schmitt, S. W.; Holtmannspötter, H.; Christiansen, S. H.; Dicke, W., Development of an optimal filter substrate for the identification of small microplastic particles in food by micro-Raman spectroscopy. *Analytical and Bioanalytical Chemistry* **2017,** *409* (16), 4099-4109.
69. Hermabessiere, L.; Himber, C.; Boricaud, B.; Kazour, M.; Amara, R.; Cassone, A.-L.; Laurentie, M.; Paul-Pont, I.; Soudant, P.; Dehaut, A.; Duflos, G., Optimization, performance, and application of a pyrolysis-GC/MS method for the identification of microplastics. *Analytical and Bioanalytical Chemistry* **2018,** *410* (25), 6663-6676.
70. Okoffo, E. D.; Ribeiro, F.; O'Brien, J. W.; O'Brien, S.; Tscharke, B. J.; Gallen, M.; Samanipour, S.; Mueller, J. F.; Thomas, K. V., Identification and quantification of selected plastics in biosolids by pressurized liquid extraction combined with double-shot pyrolysis gas chromatography–mass spectrometry. *Science of The Total Environment* **2020,** *715*.
71. Braun, U.; Jekel, I. M.; Gerdts, G.; Ivleva, N. P.; Reiber, J. *Microplastics Analytics: Sampling, Preparation and Detection Methods*; 2018.
72. Gallego-Urrea, J.; aacute; n, A.; Tuoriniemi, J.; Pallander, T.; Hassell; ouml; v, M., Measurements of nanoparticle number concentrations and size distributions in contrasting aquatic environments using nanoparticle tracking analysis. *Environmental Chemistry* **2010,** *7* (1), 67-81.
73. Ter Halle, A.; Jeanneau, L.; Martignac, M.; Jardé, E.; Pedrono, B.; Brach, L.; Gigault, J., Nanoplastic in the North Atlantic Subtropical Gyre. *Environmental Science & Technology* **2017,** *51* (23), 13689-13697.
74. Schwaferts, C.; Sogne, V.; Welz, R.; Meier, F.; Klein, T.; Niessner, R.; Elsner, M.; Ivleva, N. P., Nanoplastic Analysis by Online Coupling of Raman Microscopy and Field-Flow Fractionation Enabled by Optical Tweezers. *Analytical Chemistry* **2020,** *92* (8), 5813-5820.
75. Frehland, S.; Kaegi, R.; Hufenus, R.; Mitrano, D. M., Long-term assessment of nanoplastic particle and microplastic fiber flux through a pilot wastewater treatment plant using metal-doped plastics. *Water research* **2020,** *182*, 115860-115860.
76. Mitrano, D. M.; Beltzung, A.; Frehland, S.; Schmiedgruber, M.; Cingolani, A.; Schmidt, F., Synthesis of metal-doped nanoplastics and their utility to investigate fate and behaviour in complex environmental systems. *Nature Nanotechnology* **2019,** *14* (4), 362-+.

77. Al-Azzawi, M. S. M.; Kefer, S.; Weißer, J.; Reichel, J.; Schwaller, C.; Glas, K.; Knoop, O.; Drewes, J. E., Validation of Sample Preparation Methods for Microplastic Analysis in Wastewater Matrices—Reproducibility and Standardization. *Water* **2020,** *12* (9), 2445.
78. Steinmetz, Z.; Kintzi, A.; Munoz, K.; Schaumann, G. E., A simple method for the selective quantification of polyethylene, polypropylene, and polystyrene plastic debris in soil by pyrolysis-gas chromatography/mass spectrometry. *Journal of Analytical and Applied Pyrolysis* **2020,** *147*.
79. Ziajahromi, S.; Neale, P. A.; Telles Silveira, I.; Chua, A.; Leusch, F. D. L., An audit of microplastic abundance throughout three Australian wastewater treatment plants. *Chemosphere* **2021,** *263*, 128294.
80. Browne, M. A.; Underwood, A. J.; Chapman, M. G.; Williams, R.; Thompson, R. C.; van Franeker, J. A., Linking effects of anthropogenic debris to ecological impacts. *Proceedings. Biological sciences* **2015,** *282* (1807), 20142929-20142929.
81. Jiang, B.; Kauffman, A. E.; Li, L.; McFee, W.; Cai, B.; Weinstein, J.; Lead, J. R.; Chatterjee, S.; Scott, G. I.; Xiao, S., Health impacts of environmental contamination of micro- and nanoplastics: a review. *Environmental Health and Preventive Medicine* **2020,** *25* (1).
82. Lee, H.; Kim, Y., Treatment characteristics of microplastics at biological sewage treatment facilities in Korea. *Marine Pollution Bulletin* **2018,** *137*, 1-8.

CHAPTER 3: MICROPLASTICS CLASSIFICATIONS, ISOLATION, AND CHARACTERIZATION TECHNIQUES

This chapter serves to delineate the categories of microplastics and provides the foundational background for the isolation techniques used on solid samples. It also elucidates the methods for quantifying and characterizing microplastics, focusing on advanced techniques such as FTIR Microspectroscopy and Flow Cytometry. These methods are essential for understanding and analyzing microplastics in various environmental contexts. The subsequent sections delve into the specific processes and results obtained through these techniques, contributing to a comprehensive understanding of microplastics' impact on ecosystems.

This chapter also discusses a standardized framework for categorizing plastic debris, which includes criteria such as size, shape, color, and chemical composition. This classification helps ensure consistency in microplastics research and provides a basis for why different size fractions and shapes are used in microplastics measurement. Additionally, it explains the isolation process for microplastics, highlighting methods like sample collection, processing, preconcentration, and physical separation. FTIR Microspectroscopy and Flow Cytometry are emphasized as key tools for polymer identification and precise particle detection, although challenges such as sample thickness and plastic additives can influence results.

While chapter 2 focuses on the implications of microplastics in biosolids and agriculture as well as explains why and how the research is conducted using available techniques, chapter 3 provides the necessary background for understanding plastics debris categorization and the methodologies used in subsequent research chapters. It offers a deeper insight into the characteristics of microplastics and why they are measured in different size bins, helping both the writer and reader grasp the complexity of microplastics analysis.

1 Categorization of Plastic Debris

Given the considerable variation in terms, definitions, and categorizations of plastic fragments or debris in the existing body of research, Hartmann and a group of scientists across Europe[3] proposed a unified framework consisting of seven criteria Figure 3-8. Criteria I – III establish the classification of a material as "plastic" and "plastic debris" based on chemical composition, solid state, and solubility. Meanwhile, criteria IV – VII further categorize these plastic materials based on size, shape and structure, color, and origin.

Criterion IV delineates plastic debris into four distinct groups: nanoplastic (1-1000 nm), microplastic (1-1000 µm), mesoplastic (1-10 mm), and macroplastic (1 cm and above), with the largest dimension serving as the classifier. The shapes of plastic debris are classified into fibers, films, irregular particles, and spheres under criterion V. Criterion VI and VII categorize plastic debris based on their color and origin (primary or

secondary), respectively. This standardized framework aims to bring coherence and consistency to the classification of plastic debris, providing a solid foundation for researchers in the field[3].

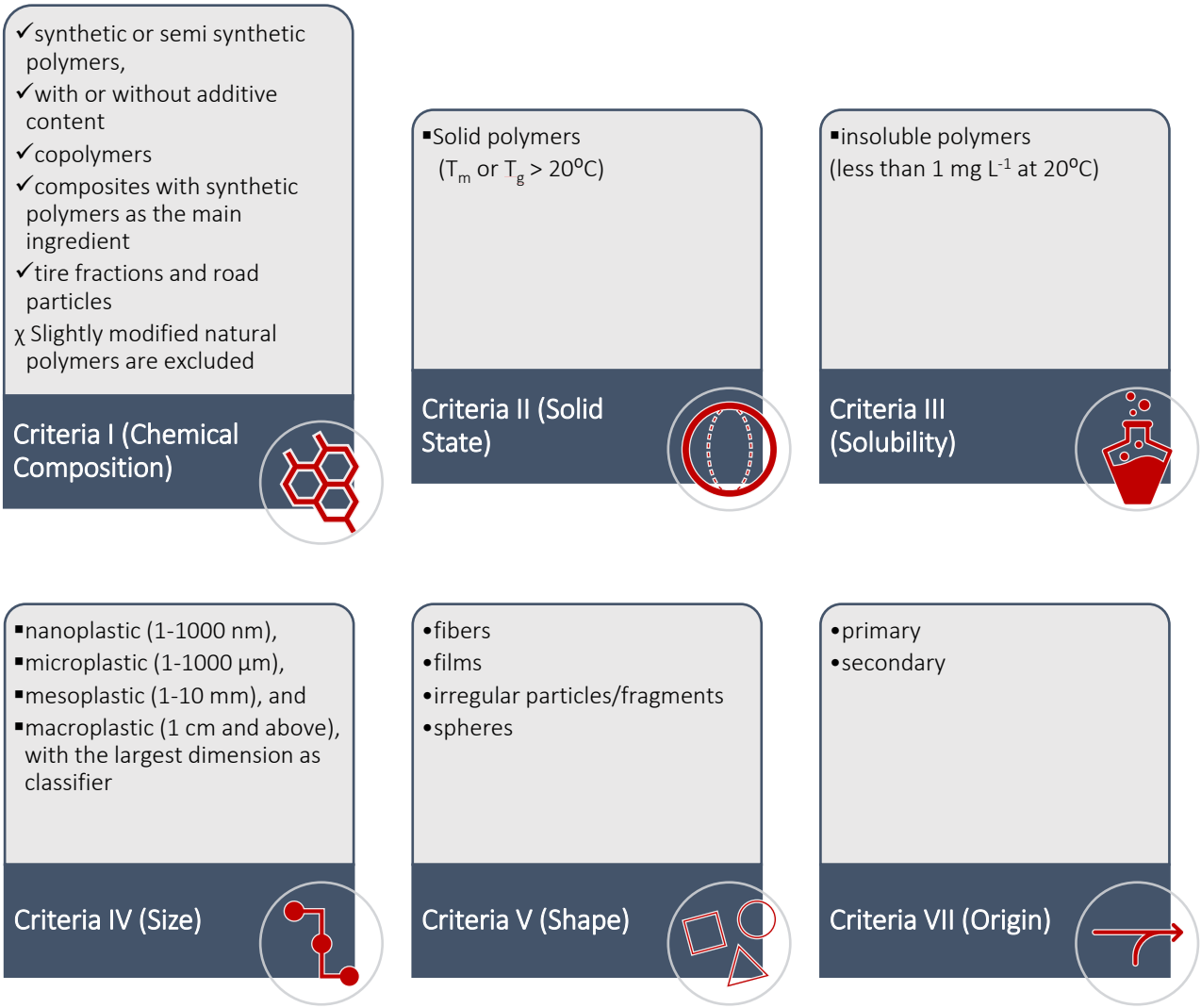

Figure 3-8. Plastic debris can be categorized according to its chemical composition, solid state, solubility, size, shape, and origin, offering a comprehensive framework for understanding its environmental impact and management strategies.

1.1 Size

Standardization of size fractions for the quantification of microplastics is imperative to ensure comparability across studies. In a review by Hidalgo-Ruz et al. (2011)[4], which analyzed 68 publications related to microplastics up to December 2011, it was suggested to use two main size fractions: (i) <500 µm with a stated lower limit, and (ii) 500 µm – 5 mm. Therefore, sample processing should involve the use of a 500 µm sieve, and the fraction passing through the sieve should be prepared by density separation and filtering.

In an Australian study conducted by Wijesekara et al. (2018)[5], microplastic in biosolids, surface soil, and sediment samples from various locations were quantified. The term "microbeads" was used to represent microplastics sized from 5 µm to 1 mm, and their quantification was reported with four different size fractions: ≤50 µm, 50-100 µm, 100-250 µm, and 250-1000 µm. In their laboratory practice, they utilized a series of stainless-steel screens sized 1000, 250-, 125, and 53 µm, as well as filter papers with a pore size of 11 µm. Despite categorizing microplastics size ≤50 µm, the use of sieves and filters left microplastics size 1 µm to <100 µm, or 5 µm to <11 µm in the case of microbeads uncounted.

Meanwhile, Ziajahromi et al. (2017)[6] reported their research on microplastics abundance in the effluent of three major wastewater treatment plants in Sydney, Australia, by the average number of microplastics per liter effluent. They employed a customized in situ fractionated sampling tool consisting of four removable stainless-steel sieves (500, 190, 100, 25 µm). The same sampling tool was used in their study on microplastics from tires in sediment at a stormwater floating treatment wetland.[7] However, the sieved meshes used left microplastics sized 1 µm to <25 µm uncollected and uncounted.

The focus is shifting to smaller plastic particles, known as nanoplastics, which are believed to have a higher negative impact on the environment due to their small size. Nanoplastics potentially absorb more toxic compounds and contaminants.[8] Although the definition of nanoplastics is still debated,[9] the European Commission defines them as plastic particles sized less than 100 nm.[10]

1.2 Shape

Plastic particles are generally categorized based on their shapes, including fragments, pellets, fibers, and spheres. These classifications are recommended for reporting the abundance of microplastics in various environmental samples.[3]

1.3 Structure

In the context of chemical composition, a material is classified as plastic if it comprises synthetic or semi-synthetic polymers with or without additive content, copolymers, composites with synthetic polymers as the main ingredients, tire fractions, and road particles. Slightly modified natural polymers, such as dyed wool and cellulose, are excluded in Criterion I. Solid polymers (T_m or T_g > 20^oC) and insoluble polymers (less than 1 mg L^{-1} at 20^oC) constitute Criteria II and III, respectively.[3]

1.4 Origin

Microplastics can either be directly manufactured, referred to as primary microplastics, commonly used in personal care and cosmetic products such as microbeads. Alternatively, they can be formed from large plastic debris that has undergone fragmentation, known as secondary microplastics, due to exposure to environmental stressors such as water, sunlight, and wind.[6, 11] Different sources are identified as contributors

to the origin of microplastics, including clothing, packaging, and rope [12]. Nanoplastics are primarily formed from the degradation or fragmentation of microplastics [13], which can be caused by natural environmental factors such as sunlight and wind, manufacturing processes, or even the use of plastic objects. [9]

1.5 Unit

The use of a convertible unit is recommended whenever possible to facilitate data comparison. Common units employed in research reported up to December 2011 include "items per m^2" for the abundance of microplastics and "grams per m^2" for the mass of microplastics in sediment and sea surface studies. For water column studies, "items per m^3" is commonly used.[4]

2 Microplastics isolation of solid samples

As for now, three essential procedures for identifying microplastics in solid samples have been established, involving the stages of collection, processing and analysis. [14] Recommended by prominent institutions such as the US National Oceanic and Atmospheric Administration (NOAA, 2015), European Commission for Marine Strategy Framework Directive (MFSD, 2013), and UK Water Industry Research (UKWIR, 2019), each procedure is elaborated upon in Chapter 2 of this thesis.

2.1 Sample Collection

Ensuring the collection of a representative sample poses a challenge in this step. The choice of sampling tools and techniques varies widely based on the sample's phase (liquid or solid) and its sources, be it the marine environment, wastewater treatment plants, or organisms. Common methods for liquid samples, such as sea floor, water column, and wastewater, include surface filtration, containers with stacked steel sieves, neuston net, epibenthic sled, zooplankton net, and pump with a glass fiber filter. For solid samples, especially sediment and sludge, techniques such as tweezers, tablespoons, handpicking, Ekman and van Veer grabs, trowels, and quadrats corer are widely recognized. [4, 11]

2.2 Sample Processing

Pretreatment is designed to isolate microplastics from their original matrices, primarily in samples like sludge, known for their high content of various organic and inorganic materials. This treatment is imperative for the chemical identification of microplastics. [11] Improper pretreatment could lead to underestimated results in microplastics quantification, particularly in matrices rich organic materials like sludge, where some plastic particles entrapped in the extracellular polymeric substances (EPS) may remain unextracted and consequently, uncounted. [15] Mechanical or stressful techniques, such as ultrasonic baths, should be avoided to prevent the degradation and further fragmentation of plastics, which could significantly impact the results of microplastics quantification. [16]

2.2.1 Physicochemical properties

Samples may need to be tested for physicochemical properties, depending on the study's objectives, such as pH, Chemical Oxygen Demand (COD), Biochemical Oxygen Demand (BOD5), Dissolved Organic Carbon (DOC), Ammonia Nitrogen (NH_3-N), and Dissolved Nitrogen (DN). [17] Considering that the microplastics collected were from environmental samples, conditions of the environment itself may influence the analysis result. For instance, sample collected from digested sludge may have been settled in the digester that may have low pH, this could influence the identification of microplastics as it may change the chemical structure of the particles. As mentioned, these physicochemical tests may be required depending on the research goal.

2.2.2 Bio (Chemical) treatment

Biochemical treatment is a crucial step before physical separation to remove organic matters and other non-plastic materials. This treatment is particularly important for samples with high organic content. The aim is to extract and purify plastic particles from the matrix. Two main categories for samples digestion are chemical and enzyme degradation. [18, 19] In chemical treatment, acid and base solutions, such as NaOH, KOH, H_2O_2, and H_2SO_4, are commonly used. Some methods involve a combination of these solutions or complement them with physical treatments such as ultrasonic bath. [20]. However, certain treatments, like acid, alkaline, and H_2O_2 solutions, have been reported to cause particle aggregation and negatively influence the fluorescence signals of labelled plastic particles. [21, 22] A recent report by Hurley et al. showed that treatment with Fenton's reagent, a mixture of 30% H_2O_2 and Fe(II) solutions with a ratio of 2:1, displayed no sign of polymers' degradation, required less reaction time, and successfully reduced a large portion of organic matters in sludge samples. [23] Similar results were reported by Al-Azzawi et al., in which H_2O_2 and Fenon reaction were the most effective digestion techniques to remove natural organic matters in wastewater matrices without affecting the microplastics. [24] Cunsolo et al. reported a 60-106% recovery rate of polystyrene (PS) and polymethyl methacrylate (PMMA) using the combination digestion method of wet peroxide oxidation (WPO) and Fenton reagent, followed by density separation with $ZnCl_2$. [25] Fenton reagent[26], a mixture of hydrogen peroxide and ferrous salts, has been widely used as an effective oxidant for organic substances. The decomposition of H_2O_2 catalysed by iron salts generate 'OH radical as an active intermediate:[27]

$$Fe^{2+} + H_2O_2 + H^+ \rightarrow Fe^{3+} + H_2O + {}^*OH$$

This may yield an organic free radical in the presence of organic substrates, depending on the relative rates of the reactions of the metal-peroxide complex and its reaction with organic substrates.[28]

For enzymatic techniques, it requires different type of enzymes depending on the type of the matrix. This could increase the cost of such a treatment and longer sample processing due to the required incubation time for each enzyme reaction. For example, an enzymatic digestion method was applied for microplastics purification in treated wastewater samples, which required 14 days incubation time in total for different type

of enzymes i.e., protease, lipase, and cellulase. So, in the same study, they decided not to use this method for their sewage sludge samples but ignoring such technique for sludge samples resulting in the insufficient purification of microplastics for micro-FTIR analysis.[18, 29]

2.2.3 Preconcentration

This critical step is recommended to address the limit of detection challenge inherent in microplastics analysis. Each instrument utilized for microplastics analysis, such as FTIR and Raman spectroscopy, has its unique detection limit. These limitations pose a challenge for detecting smaller and less concentrated plastic debris, rendering them undetectable by the instrument. For instance, FTIR faces difficulty in detecting particles smaller than 5 µm, and Py-GC/MS requires a minimum sample concentration of 4 mg/L for detection. [11, 18, 21]

The preconcentration step aims to elevate the concentration of plastic particles in a sample, especially when collected environmental samples may be too dilute for a specific microplastic analysis. Increased concentrations of microplastics in a sample have the potential to enhance analysis sensitivity, depending on the techniques employed. [21] For instance, a technique developed by Schwaferts et al., employing a Flow Cell in simultaneous coupling analysis with Raman microscopy, necessitates sufficient concentrations of plastic particles flowing through the cell to be efficiently detected by the laser for satisfactory signal acquisition. [13] Similarly, in the case of Fischer et al., utilizing Py-GC/MS for microplastics quantification, an adequate concentration of microplastics is required for detection by the instrument. [30]

Various techniques are employed for preconcentration, including membrane filtration, ultracentrifugation, ultrafiltration, and solvent evaporation. Each method possesses its own set of advantages and limitations, with ultrafiltration emerging as superior, particularly for submicron and nanoplastics analysis. Another suggested technique is Analytical Ultracentrifugation (AUC), where the sample is analysed spectroscopically through light absorption, monitoring sedimentation during the centrifugation process. However, it is worth noting that this technique has not been tested extensively for plastic debris analysis. [21]

2.2.4 Physical separation

Instead of resorting to manual separation of plastic particles, density separation emerges as a more time-efficient method for isolating microplastics from environmental samples. Polymers inherently possess a lighter density compared to natural organic and inorganic substances, whether they are introduced during the bio(chemical) pretreatment stages or not. Consequently, plastic particles that float can be effectively isolated using the density separation technique.

Commonly employed chemicals for density separation include saturated NaCl (1.2 g/cm^3), NaI (1.8 g/cm^3), and $ZnCl_2$ (1.5 g/cm^3).[16, 31] These substances aid in creating specific density gradients that facilitate the separation of microplastics from the sample matrix, enhancing the efficiency and accuracy of the isolation

process. This approach is pivotal in ensuring a reliable and representative analysis of microplastics within environmental samples.

3 Characterization methods

3.1 Fourier Transform Infrared (FTIR) Microspectroscopy

Fourier Transform Infrared Microspectroscopy is a widely utilized technique in analytical chemistry, grounded in vibrational spectroscopy. This method captures a spectrum resulting from transitions between quantized vibrational energy states, encompassing the simple motion of the two atoms in a diatomic molecule to the intricate motion of each atom in a large polyfunctional molecule. The application of an interferometer and a Fourier-transformation mathematical process enhances the quality of infrared spectra while minimizing the time required for data acquisition. In FTIR microscope, a beam is focused onto the sample with three identical Cassegrain optics, as shown in Figure 3-9.[2, 32] Specifically in this research, FTIR Microspectroscopy Nicolet iS50 Thermo Scientific with schematic as illustrated in Figure 3-10.

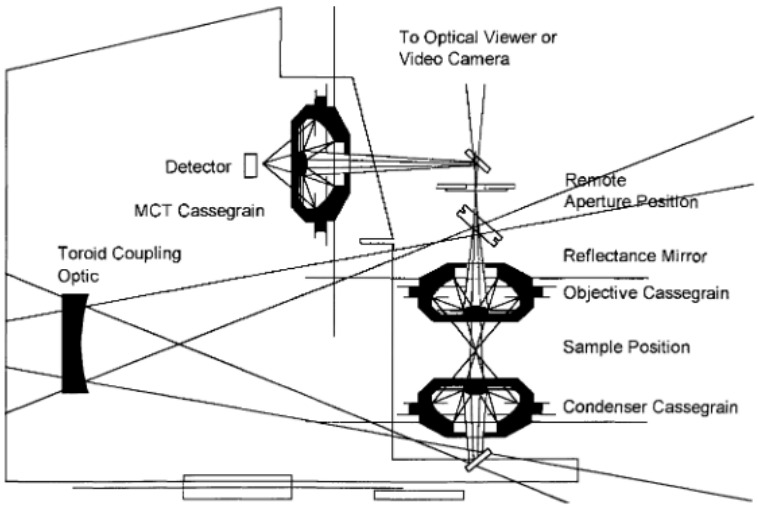

Figure 3-9. Optics of a typical microscope with a single aperture used for FT-IR microspectroscopy (Courtesy of PerkinElmer Corporation; Licence ID 1534873-2)[32]

FTIR Microspectroscopy has found extensive applications in the analysis of both organic and inorganic molecules. Its diverse uses span polymers characterization, biological applications (lipids, proteins, nucleic acids, plants, etc.), and industrial and environmental applications (pharmaceuticals, food science, agriculture). [2] Given its proficiency in polymers identification and characterization, FTIR Microspectroscopy presents a promising avenue for microplastics analysis.

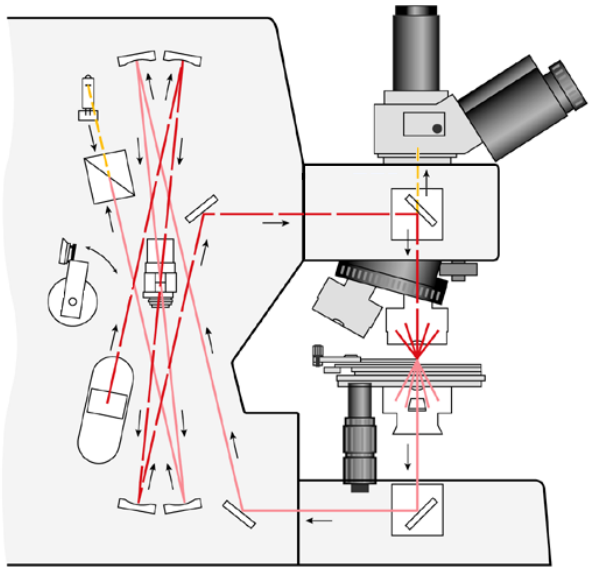

Figure 3-10. Schematic diagram of FTIR Microspectroscopy Nicolet iN50 Thermo Scientific (internal source)

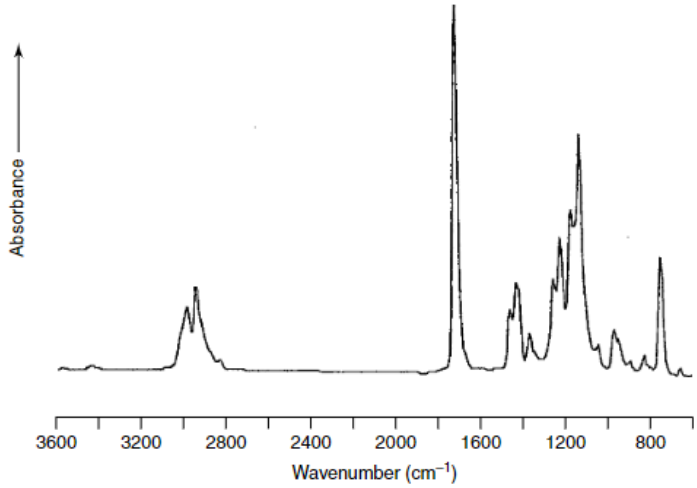

Figure 3-11. IR spectrum of PMMA (captured from Stuart, 2005; Licence ID 1534873-1).[2]

Identification of plastics types or polymers is achievable by interpreting the spectrum of each particle, as different types of plastics exhibit distinct IR spectra based on their chemical structure. For instance, poly (methyl methacrylate) or PMMA displays characteristics peaks corresponding to the C-H group (2900 cm^{-1}) in the backbone chain, the C=O (1729 cm^{-1}), and C-O units of the ester group, and the C-H units of the methyl substituent (1300 cm^{-1}, and 1400 cm^{-1}), as depicted in Figure 3-11. Polypropylene (PP), as shown in Figure 3-12, manifest distinct peaks at 970 and 1460 cm^{-1}, with variations at 840, 1000, and 1700 cm^{-1} depending on their stereoisomers (atactic, syndiotactic, or isotactic).[2]

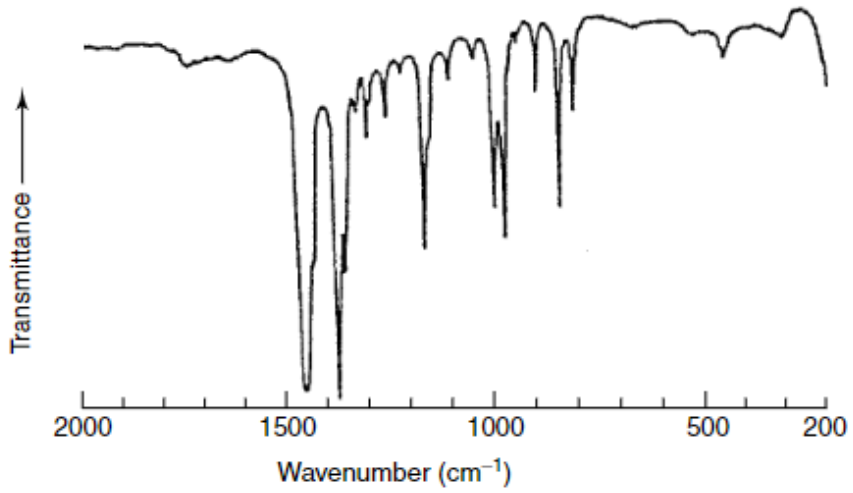

Figure 3-12. IR spectrum of PP isotactic (captured from Stuart, 2005; Licence ID 1534873-1).[2]

However, challenges exist, particularly in the context of microplastics analysis, as these particles exhibit varied shapes, including fragments, fibers, and spheres, along with differing thicknesses. These factors can influence spectral accuracy, with thicker specimens potentially introducing photometric inaccuracies and loss of peak resolution. For example, if specimen transmits radiation, it will refract and absorb some of it as well as reflect and scatter incident radiation. Also, the absorbance values for every peak are proportionally increased as the thickness increased. If the sample is too thick, there will be a high level of photometric inaccuracy, and loss of peak resolution. Furthermore, in the region of very high beam absorbance, there is very little light reaching the detector, consequently the spectrum will have a low signal-to-noise ratio; the tops of the peaks will be very noisy and exhibit splitting.[33]

Furthermore, the presence of additives in commercial plastics, such as plasticizers and fillers, as well as the spectra collection techniques i.e., reflectance, transmission and ATR, can introduce distortion in the IR spectrum. To mitigate these challenges, an open library containing IR spectra of various commercial and weathered plastic particles was employed in this research. [34] However, it is worth noting that this open library

was compiled in ATR mode, resulting in spectra that may differ from those collected in reflectance mode on the stainless-steel mesh used in this study. Hence, IR spectra of locally sourced commercial and weathered plastic particles were collected, in reflectance mode on a stainless-steel mesh, to augment the instrument library for comprehensive particle identification.

3.2 Flow Cytometry

Flow Cytometry has found extensive use in the analysis of microorganisms and cells, ranging in size from micrometers to nanometers.[35-38] In recent studies, it has emerged as a valuable tool for microplastics analysis. Offering precise particle detection through both light scattering and fluorescence, Flow Cytometry operates by assessing individual particle properties as they flow through a fluidic system consisting of a central core and enclosed by an outer sheath fluid. Utilizing the Bernoulli effect, particles are focused, creating a stream of single particles, referred to as hydrodynamic focusing.[1]

As depicted in Figure 3-13, each particle subsequently passes through one or more laser beams, where light scattering, or fluorescence emission provides information about the particle's characteristics. The lasers employed cover a range from ultraviolet to far red, with variable power levels. Forward Scatter Channer (FSC) collects light scattered in the forward direction, offering an estimation of particle size. Side Scatter (SSC), measured at a 90° angle to the excitation line, provides insights into the relative complexity or granularity of the particles. FSC and SSC, unique for each particle, are combined to differentiate particle types in a heterogenous particle population.[1]

Figure 3-13. Hydrodynamic focusing producing a stream of single particle (captured from Bio-Rad Laboratories.[1]

Figure 3-14. Schematic of a typical cytometer setup. FL, fluorescence; PMT, photomultiplier tuber; blue arrow, light path (captured from Bio-Rad Laboratories[1])

Detectors, either photomultiplier tubes (PMT) or avalanche photodiodes (APD), control the specificity of detection through optical filters that block certain wavelengths while transmitting others. Long pass filters (520 nm), short pass filters (575 nm), and band pass filters (630/20 nm) are the three major filter types. Additionally, a dichroic filter (540 nm) acts as a mirror when placed at an angle to the oncoming light, allowing specific wavelengths to pass in the forward direction and reflecting light at a 90° angle. Every time a particle passes through, it generates a signal and pulse in each detector. These pulses, plotted as a function of time, represent events, with the generation of a pulse termed an "event". As the particle enters the laser beam spot, it produces scattered light and fluorescence signals, manifesting as a stream of electrons (current), the magnitude of which is proportional to the intensity of the scatter or fluorescence signal (Figure 3-14).[1]

References

1. Bio-Rad Laboratories, I., *Flow Cytometry Basics Guide-Practical Advice to Get you Started in Flow*.
2. Stuart, B. H., *Infrared Spectroscopy: Fundamentals and Applications*. Chichester, UK: John Wiley & Sons, Ltd: Chichester, UK, 2005.
3. Hartmann, N. B.; Hüffer, T.; Thompson, R. C.; Hassellöv, M.; Verschoor, A.; Daugaard, A. E.; Rist, S.; Karlsson, T.; Brennholt, N.; Cole, M.; Herrling, M. P.; Hess, M. C.; Ivleva, N. P.; Lusher, A. L.; Wagner, M., Are We Speaking the Same Language? Recommendations for a Definition and Categorization Framework for Plastic Debris. *Environmental Science & Technology* **2019,** *53* (3), 1039-1047.

4. Hidalgo-Ruz, V.; Gutow, L.; Thompson, R. C.; Thiel, M., Microplastics in the Marine Environment: A Review of the Methods Used for Identification and Quantification. *Environmental Science & Technology* **2012,** *46* (6), 3060-3075.
5. Wijesekara, H.; Bolan, N. S.; Bradney, L.; Obadamudalige, N.; Seshadri, B.; Kunhikrishnan, A.; Dharmarajan, R.; Ok, Y. S.; Rinklebe, J.; Kirkham, M. B.; Vithanage, M., Trace element dynamics of biosolids-derived microbeads. *Chemosphere* **2018,** *199*, 331-339.
6. Ziajahromi, S.; Neale, P. A.; Rintoul, L.; Leusch, F. D. L., Wastewater treatment plants as a pathway for microplastics: Development of a new approach to sample wastewater-based microplastics. *Water Research* **2017,** *112*, 93-99.
7. Ziajahromi, S.; Drapper, D.; Hornbuckle, A.; Rintoul, L.; Leusch, F. D. L., Microplastic pollution in a stormwater floating treatment wetland: Detection of tyre particles in sediment. *Science of The Total Environment* **2020,** *713*, 136356.
8. Rios Mendoza, L. M.; Karapanagioti, H.; Álvarez, N. R., Micro(nanoplastics) in the marine environment: Current knowledge and gaps. *Current Opinion in Environmental Science & Health* **2018,** *1*, 47-51.
9. Gigault, J.; Halle, A. t.; Baudrimont, M.; Pascal, P.-Y.; Gauffre, F.; Phi, T.-L.; El Hadri, H.; Grassl, B.; Reynaud, S., Current opinion: What is a nanoplastic? *Environmental Pollution* **2018,** *235*, 1030-1034.
10. Toussaint, B.; Raffael, B.; Angers-Loustau, A.; Gilliland, D.; Kestens, V.; Petrillo, M.; Rio-Echevarria, I. M.; Van den Eede, G., Review of micro- and nanoplastic contamination in the food chain. *Food Additives & Contaminants: Part A* **2019,** *36* (5), 639-673.
11. Sun, J.; Dai, X.; Wang, Q.; van Loosdrecht, M. C. M.; Ni, B.-J., Microplastics in wastewater treatment plants: Detection, occurrence and removal. *Water Research* **2019,** *152*, 21-37.
12. Thompson, R. C.; Olsen, Y.; Mitchell, R. P.; Davis, A.; Rowland, S. J.; John, A. W. G.; McGonigle, D.; Russell, A. E., Lost at sea: where is all the plastic? *Science (New York, N.Y.)* **2004,** *304* (5672), 838.
13. Schwaferts, C.; Sogne, V.; Welz, R.; Meier, F.; Klein, T.; Niessner, R.; Elsner, M.; Ivleva, N. P., Nanoplastic Analysis by Online Coupling of Raman Microscopy and Field-Flow Fractionation Enabled by Optical Tweezers. *Analytical Chemistry* **2020,** *92* (8), 5813-5820.
14. Okoffo, E. D.; O'Brien, S.; O'Brien, J. W.; Tscharke, B. J.; Thomas, K. V., Wastewater treatment plants as a source of plastics in the environment: a review of occurrence, methods for identification, quantification and fate. *Environmental Science: Water Research & Technology* **2019,** *5* (11), 1908-1931.
15. Li, X.; Chen, L.; Ji, Y.; Li, M.; Dong, B.; Qian, G.; Zhou, J.; Dai, X., Effects of chemical pretreatments on microplastic extraction in sewage sludge and their physicochemical characteristics. *Water Research* **2020,** *171*.
16. Renner, G.; Schmidt, T. C.; Schram, J., Analytical methodologies for monitoring micro(nano)plastics: Which are fit for purpose? *Current Opinion in Environmental Science & Health* **2018,** *1*, 55-61.
17. Bolan, N. S.; Baskaran, S.; Thiagarajan, S., Methods of Measurement of Dissolved Organic Carbon of Plant Origin in Soils, Manures, Sludges and Stream Water. In *Analysis of Plant Waste Materials*, Linskens, H. F.; Jackson, J. F., Eds. Springer Berlin Heidelberg: Berlin, Heidelberg, 1999; pp 1-19.
18. Lusher, A. L.; Hurley, R.; Vogelsang, C.; Nizzetto, L.; Olsen, M. *Mapping microplastics in sludge*; 8257769509; Norwegian Institute for Water Research,: Norway, 11 December 2017, 2017; p 55.
19. Ball H, C. R., Grove E, Horton A, Johnson A, Jürgens M, Read D, Svendsen C, Sink To River - River To Tap. A Review of Potential Risks From Nanoparticles and Microplastics. *UK Water Industry Research Limited* **2019,** *EQ 01 A 231*.
20. Ivleva, N. P.; Wiesheu, A. C.; Niessner, R., Microplastic in Aquatic Ecosystems. *Angewandte Chemie International Edition* **2017,** *56* (7), 1720-1739.
21. Schwaferts, C.; Niessner, R.; Elsner, M.; Ivleva, N. P., Methods for the analysis of submicrometer- and nanoplastic particles in the environment. *TrAC Trends in Analytical Chemistry* **2019,** *112*, 52-65.
22. Rist, S.; Baun, A.; Hartmann, N. B., Ingestion of micro-and nanoplastics in Daphnia magna–Quantification of body burdens and assessment of feeding rates and reproduction. *Environmental Pollution* **2017,** *228*, 398-407.
23. Hurley, R. R.; Lusher, A. L.; Olsen, M.; Nizzetto, L., Validation of a Method for Extracting Microplastics from Complex, Organic-Rich, Environmental Matrices. *Environmental Science & Technology* **2018,** *52* (13), 7409-7417.

24. Al-Azzawi, M. S. M.; Kefer, S.; Weißer, J.; Reichel, J.; Schwaller, C.; Glas, K.; Knoop, O.; Drewes, J. E., Validation of Sample Preparation Methods for Microplastic Analysis in Wastewater Matrices—Reproducibility and Standardization. *Water* **2020,** *12* (9), 2445.
25. Cunsolo, S.; Williams, J.; Hale, M.; Read, D. S.; Couceiro, F., Optimising sample preparation for FTIR-based microplastic analysis in wastewater and sludge samples: multiple digestions. *Analytical and Bioanalytical Chemistry* **2021,** *413* (14), 3789-3799.
26. Fenton, H. J. H., LXXIII.—Oxidation of tartaric acid in presence of iron. *Journal of the Chemical Society, Transactions* **1894,** *65* (0), 899-910.
27. Haber, F.; Weiss, J., The catalytic decomposition of hydrogen peroxide by iron salts. *Proceedings of the Royal Society of London. Series A, Mathematical and physical sciences* **1934,** *147* (861), 332-351.
28. Goldstein, S.; Meyerstein, D.; Czapski, G., The Fenton reagents. *Free Radical Biology and Medicine* **1993,** *15* (4), 435-445.
29. Mintenig, S. M.; Int-Veen, I.; Löder, M. G. J.; Primpke, S.; Gerdts, G., Identification of microplastic in effluents of waste water treatment plants using focal plane array-based micro-Fourier-transform infrared imaging. *Water Research* **2017,** *108*, 365-372.
30. Fischer, M.; Scholz-Böttcher, B. M., Simultaneous Trace Identification and Quantification of Common Types of Microplastics in Environmental Samples by Pyrolysis-Gas Chromatography–Mass Spectrometry. *Environmental Science & Technology* **2017,** *51* (9), 5052-5060.
31. Li, Q.; Wu, J.; Zhao, X.; Gu, X.; Ji, R., Separation and identification of microplastics from soil and sewage sludge. *Environmental Pollution* **2019,** *254*, 113076.
32. Griffiths, P. R.; De Haseth, J. A.; Winefordner, J. D., *Fourier Transform Infrared Spectrometry*. 2 ed.; Wiley: Newark, 2007; Vol. 171.

33. Kirkbride, K. P., Infrared Microspectroscopy of Fibres. In *Forensic examination of fibres*, Third edition ed.; Boca Raton, Florida; London, England; New York: CRC Press: 2018; pp 245-288.
34. De Frond, H.; Rubinovitz, R.; Rochman, C. M., µATR-FTIR Spectral Libraries of Plastic Particles (FLOPP and FLOPP-e) for the Analysis of Microplastics. *Analytical Chemistry* **2021,** *93* (48), 15878-15885.
35. Caputo, F.; Vogel, R.; Savage, J.; Vella, G.; Law, A.; Della Camera, G.; Hannon, G.; Peacock, B.; Mehn, D.; Ponti, J.; Geiss, O.; Aubert, D.; Prina-Mello, A.; Calzolai, L., Measuring particle size distribution and mass concentration of nanoplastics and microplastics: addressing some analytical challenges in the sub-micron size range. *Journal of Colloid and Interface Science* **2021,** *588*, 401-417.
36. Elsayed, A. A.; Erfan, M.; Sabry, Y. M.; Dris, R.; Gaspéri, J.; Barbier, J. S.; Marty, F.; Bouanis, F.; Luo, S.; Nguyen, B. T. T.; Liu, A. Q.; Tassin, B.; Bourouina, T., A microfluidic chip enables fast analysis of water microplastics by optical spectroscopy. *Scientific Reports* **2021,** *11* (1).
37. Kaile, N.; Lindivat, M.; Elio, J.; Thuestad, G.; Crowley, Q. G.; Hoell, I. A., Preliminary Results From Detection of Microplastics in Liquid Samples Using Flow Cytometry. *Frontiers in Marine Science* **2020,** *7* (856).
38. Wang, X.-S.; Song, H.; Liu, Y.-L.; Pan, X.-R.; Zhang, H.-C.; Gao, Z.; Kong, D.-Z.; Wang, R.; Wang, L.; Ma, J., Quantitively Analyzing the Variation of Micrometer-Sized Microplastic during Water Treatment with the Flow Cytometry-Fluorescent Beads Method. *ACS ES&T Engineering* **2021,** *1* (12), 1668-1677.

CHAPTER 4: SEMI-AUTOMATED MAPPING TECHNIQUE OF FTIR MICROSPECTROSCOPY FOR MICROPLASTICS ANALYSIS

This chapter has been submitted as a manuscript to the Royal Society of Chemistry-Environmental Science-Process and Impact, entitled "Semi-automated mapping technique of FTIR microspectroscopy for microplastics analysis". It describes original research method into methods for microplastics/fibers analysis by modifying current time-consuming FTIR microspectroscopy techniques. It highlights the technique's accuracy and sensitivity as well as its practicality to use due to the short time required to acquire the data. It is authored by **Anggelia Essi Christian**, Ingo Köper, and Paul Kirkbride.

Abstract

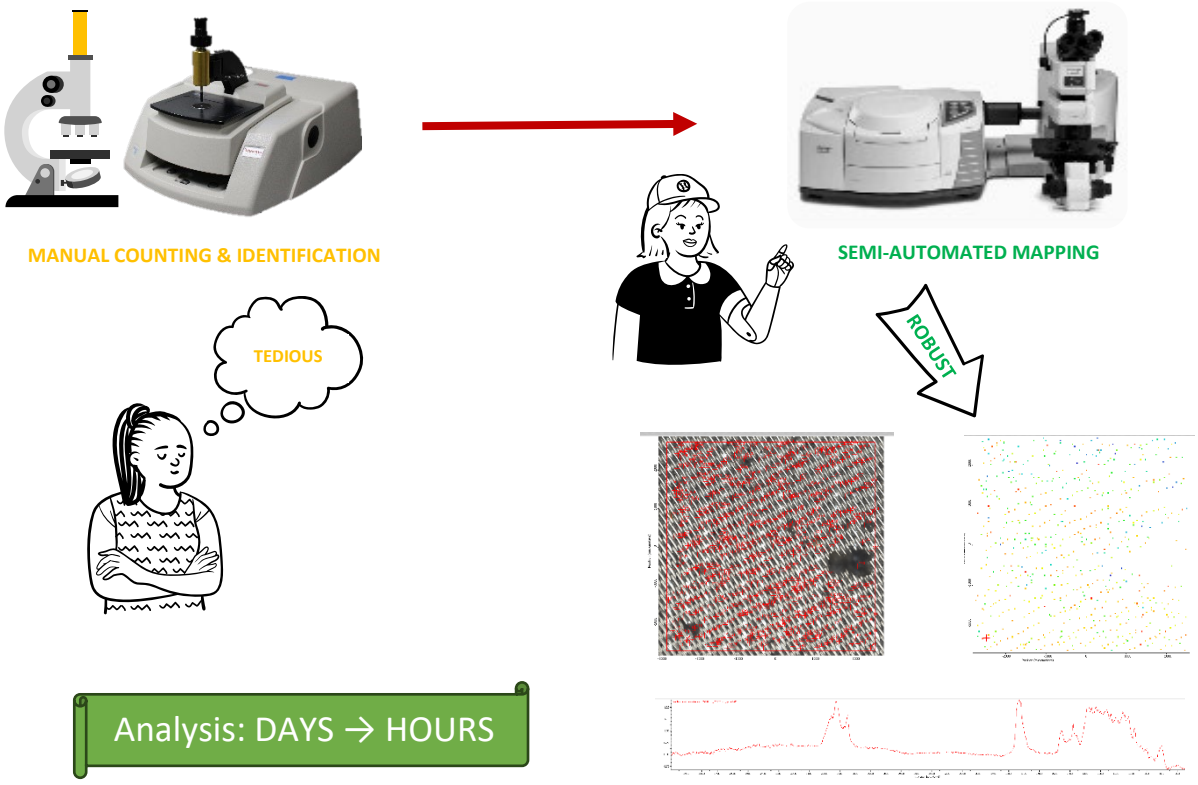

Figure 4-15. Graphical Abstract

Microplastic particles have received increasing interest in the past years, mainly for their potentially negative impact on the environment. Establishing a standardized method for the analysis of microplastics is essential to effectively mitigate and monitor their presence and environmental impact. The most commonly employed methods involve the use of an optical microscope coupled with FTIR spectroscopy, a very lengthy and time-consuming during analysis. To address this, here we describe the development of a novel mapping mode technique utilizing FTIR microspectroscopy to characterize particles of size 25 µm and above. The utilization of a validated sub-sampling mapping mode resulted in a substantial reduction in analysis time, from several

days to just a matter of hours per sample. Despite the inherent challenges posed by the nature of the samples, we achieved a reasonably accurate analysis, with an accuracy rate of 47%, while maintaining a high level of sensitivity exceeding 80%. Based on our findings, this semi-automated mapping technique offer a significant potential for microplastics analysis. However, it is important to take into consideration several key factors and conditions, including the minimum confirmed microplastics/fibers relative to the total isolated particles, the comprehensiveness of the IR spectrum library database, potential sub-sampling errors, and the distribution of particles within the samples.

1 Introduction

Microplastics are small plastic particles sized less than 5 mm, as discussed in chapter 3. They have become a growing concern due to their significant ecological impacts,[1-4] attracting the attention of environmental agencies and local authorities, and prompting them to actively pursue the establishment of a monitoring and control system.[5, 6]

However, the current methods employed for the analysis of microplastics, particularly stereomicroscopy in conjunction with FTIR-ATR or reflection mode, are notably time-consuming. The current practice entails manually counting particles under a microscope and characterizing at least 20% of the total particles by individually transfering particles for ATR mode spectrum collection and identification,[7, 8] a process that becomes increasingly problematic when dealing with a large number of samples to be analyzed.

One common strategy to mitigate the challenges associated with manual counting and individual identification involves the implementation of a mapping mode to scan particles on filters. Despite its potential efficacy, this approach demands a substantial time investment to yield conclusive results. An inherent challenge lies in determining whether the mapped area accurately represents the entirety of the residue or particles within a given sample. Subsequently, particle enumeration can be achieved through conventional mapping, followed by the recognition of particles via the detection of infrared anomalies or through the utilization of image analysis software. Regardless of the chosen method, the automated identification of particles poses a formidable challenge. The complexity arises from the need to differentiate between microplastics and non-microplastics, and further categorize microplastics into natural, synthetic, regenerated, or modified forms.

Several studies have introduced software solutions aimed at assisting with particle recognition or detection, including tools such as siMPle (Systematic Identification of MicroPLastics in the Environment), MP-VAT (Microplastics Visual Analysis Tool), and LDIR (Laser Direct Infrared) Chemical Imaging software.[8-11] However, there are notable limitations associated with these techniques. Some of them are not compatible with a wide range of analytical instruments from different brands. Additionally, adopting more advanced software may incur higher cost.

To expedite the analysis process, one effective strategy is to focus on mapping a smaller area of the filter. This mapping technique has been extensively studied, comparing various mapping patterns and total mapping areas across different sample types, including drinking water, wastewater, sludge, sediment, and soil samples.[12-14]

In a study conducted by Brandt et al., different sub-sampling methods for mapping were examined. They employed a 2x2mm box-based pattern and assessed various patterns representing different proportions of the total filter area, including a quarter (7.3%), a cross-section of both axes (7.3%), and a helical assembly (15.5%), and a randomized distribution (8.2%). Their findings indicated that no specific pattern outperformed the others. However, it is important to note that only a small percentage, ranging from 0.5% to 4.7% of the total particles were confirmed as plastics. Therefore, they recommended optimizing the sample pretreatment process to improve microplastics isolation from non-microplastics or increasing the mapping fraction.[13]

Another study by Schymanski et al., compared various mapping patterns, including cake, snail, helix, and random mapping patterns, each representing 20% of the total area. They ultimately recommended the use of the random mapping pattern as the subsampling strategy, as it proved to be less susceptible to issue related to the uneven distribution of particles on the filter or mesh.[14]

Rather than investing additional resources in developing new software that is compatible with existing instruments, an alternative approach is to modify and optimize the capabilities of the used instrument itself. Our approach involved leveraging the instrument's capability to perform automatic mapping and collect particle spectra while still requiring manual pinpointing of particles due to the absence of built-in particle-finding software. To address the time required for mapping the entire filter or mesh, which can range from hours to days, we conducted a comprehensive comparison and validation of both small and large mapping areas.

2 Materials and Methods

A brief illustration of the methods used for this study are presented in Figure 4-16. This encompasses sample processing or pretreatment, as well as data collecting utilizing FTIR Microspectroscopy.

2.1 Sample processing

Three different types of dried sludge samples, namely dewatered, primary, and secondary sludges, were obtained from a local wastewater treatment plant. We followed a series of digestion and separation procedure adapted from Ziajahromi et.al. [15] The process uses approximately 1 gram (dry weight) of sludge, mixed with 100 mL of filtered ultrapure water. This is subjected to a 50 mL 30% H_2O_2 digestion for 24 hours at 60°C. Subsequently an additional 24-hour digestion step was carried out using 20 mL of 30% H_2O_2. After

approximately 48 hours of digestion or until the water content had evaporated and no further reaction was observed, a wet peroxide oxidation phase was initiated, involving the addition of 10 mL of 0.05M $FeSO_4$ (pH 3) and 20 mL of 30% H_2O_2 for approximately 6 hours or until no further reactions were observed.

The digestion phase was followed by a density separation procedure employing filtered ultrapure water and 4.5M NaI solution. The resulting supernatant was carefully collected and filtered through a stainless-steel Hollander weave woven wire mesh (diameter 47 mm; 25 µm opening area). Finally, the filtered material was dried at 40°C for 15 minutes to obtain the sample for analysis.

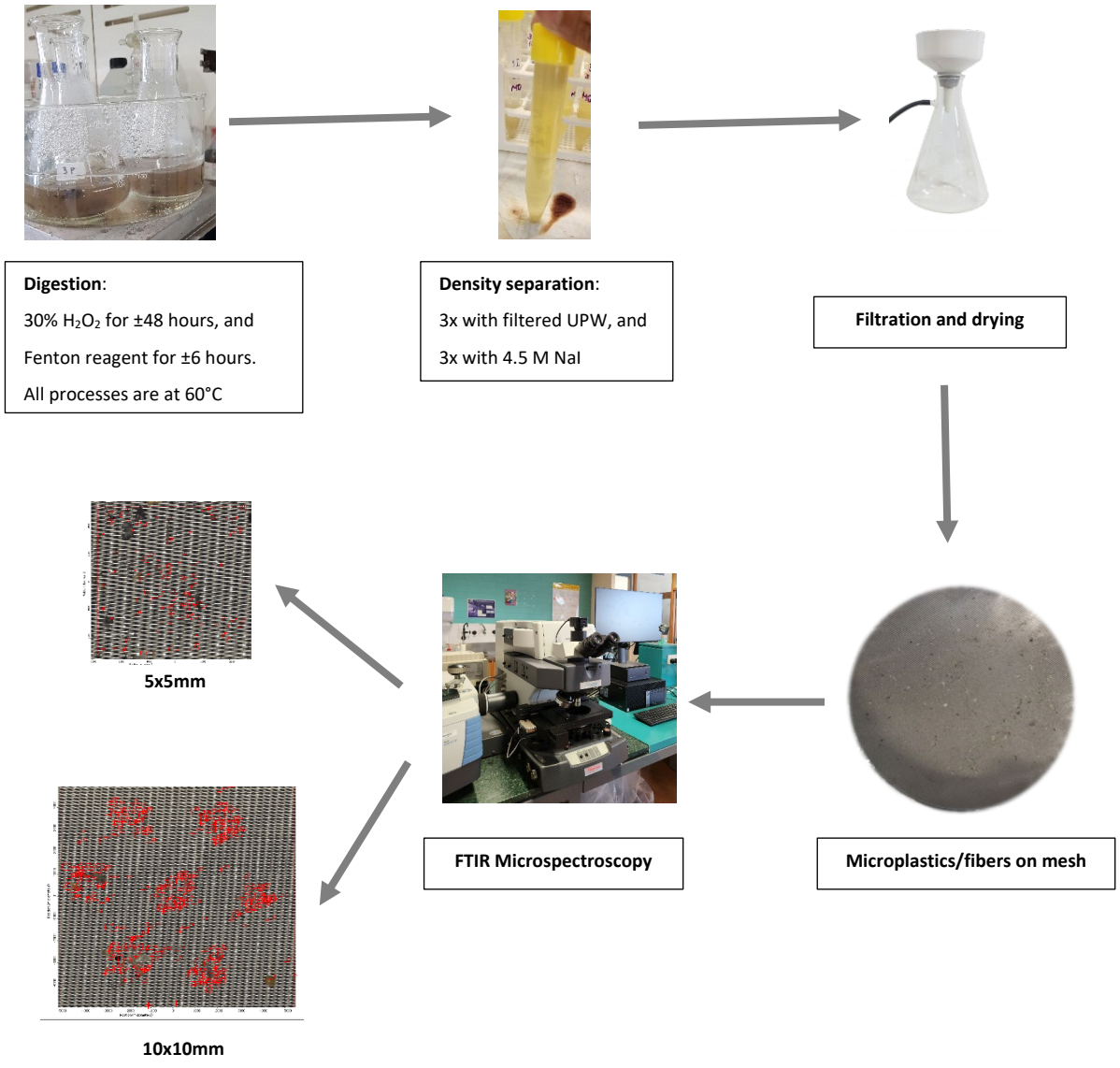

Figure 4-16. Analysis Flow Chart

2.2 Data collection

FTIR Microspectroscopy (Thermo Scientific™ Nicolet™ iS50; Thermo Scientific™ Nicolet™ Continuum microscope attachment and OMNIC software) in reflectance mode (25 scans; 8 cm^{-1} resolution) was used to collect the IR spectra of the particles on the mesh. Our approach incorporated the instrument's mapping mode capability to gather data from a specific area of the mesh. Rather than undertaking the laborious process of generating a grid map of the entire mesh and then searching for particles after collection of the map, we adopted a customized point-by-point mapping approach to capture the random distribution of microplastics/fibers on the mesh. Plastics with a length significantly greater than their width, as defined by the length-to-diameter ratio, are often interchangeably called fibers or filaments, both of which describe thread-like forms. In the field of toxicology, however, the term 'fibers' is traditionally used to describe these structures rather than 'filaments.[16] On the hand, plastic particles on other shapes, such as fragments, pellets, beads, or spheres, are generally referred to as microplastics.

Subsequently, manual selection of particles on the mesh was conducted, followed by the automatic collection of IR spectra by the instrument at only the selected locations.

For the validation process, we applied and compared two types of mapping areas as follows:

A. Small mapping area

   In this approach, we conducted mapping of a 5x5 mm area at five distinct and randomly selected spots on the mesh (Figure 4-17), each serving as a replicate. These individual spots accounted for 2% of the total mesh area. The quantification of microplastics within a gram of the sample enabled us to extrapolate and estimate the number of microplastics/fibers across the entire mesh.

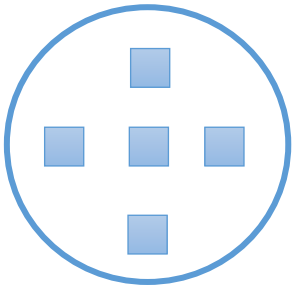

Figure 4-17. Illustration of small mapping area. Each box represents 5x5 mm area of mapping.

B. Large mapping area

   In this alternative approach, we extended our mapping to a 10x10 mm area at five different and randomly chosen spots on the mesh (Figure 4-18). As replicates, we combine results from five unique random combinations of four distinct spots, collectively representing 20-30% of the total mesh area. Similar to the small mapping area approach, the quantification of microplastics within a gram of the sample allowed us to extrapolate and ascertain the overall microplastics/fibers content across the entire mesh.

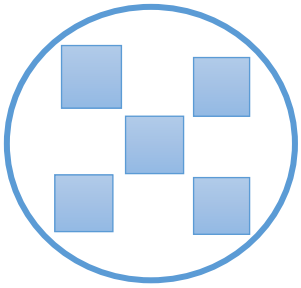

Figure 4-18. Illustration of small mapping area. Each box represents 10x10 mm area of mapping.

2.3 Data processing

2.3.1 Microplastics identification

The collected IR spectra were identified by cross-referencing them against multiple libraries. These libraries include the instrument library, an open-source IR library specially curated for microplastics research, encompassing representations of common everyday items and environmental plastic particles.[17] Additionally, we utilized an in-house library maintained by Flinders University, which comprises a diverse range of entries, encompassing local commercial plastic materials as well as weathered polymer-based substances, as detailed in Appendix H of this thesis. The spectra were obtained using the same spectrometer and microscope that was employed for particle analysis in both ATR mode and micro-reflectance mode, with the particles positioned on the stainless-steel mesh. For the identification of microplastics or fibers in environmental samples, a minimum HQI (Hit Quality Index) score of 65% was deemed requisite to confirm the specific type.[18] When multiple polymers yielded similar hit scores, human interpretation was necessary to determine the best match to the sample's spectra. Accurate identification was challenging due to chemical alterations caused by environmental factors such as weather, water, and interactions with organic and inorganic materials.

2.3.2 Statistical analysis

A paired t-test was conducted using IBM SPSS Statistics (version 28) to assess the comparative number of microplastics/fibers in each sample. The Null hypothesis posited that there is no difference in the quantity of microplastics/fibers between the small and large mapping area techniques, while the Alternative hypothesis proposed that a difference does exist in the number of microplastics/fibers between these two mapping approaches.

3 Results and Discussion

3.1 Why 5x5mm

Time efficiency constitutes a pivotal factor in the reduction of the mapping area in this technique. Given that mapping the entire mesh necessitates several days to complete, we undertook an assessment utilizing 25% of the mesh, measuring 23.5x23.5mm, which still demanded 2.5 days for completion. Mapping a 23.5x23.5

mm area of the mesh required an overnight process, followed by 8-10 hours for manual particle identification, and another overnight for spectrum collection. To optimize efficiency, we explored mapping a smaller area while maintaining data accuracy representative of the sample. The outcomes of this evaluation are presented in the Appendix E of this thesis.

In order to strike a balance between expeditious mapping and alignment with established mapping technique standards, which emphasize random location selection and the representation of at least 20% of the total area, [12-14] we conducted a validation study. The objective was to ascertain whether a smaller mesh area (5x5mm) could yield results significantly different from those obtained using larger areas (four boxes of 10x10mm, constituting 23% of the total mesh area). Mapping a smaller 5x5mm section of the mesh required 1.5 hours for analysis completion, whereas mapping the larger 10x10mm area necessitated 3.5 hours.

3.2 Distribution test

This test aimed to determine Parametric or Non-Parametric test. Parametric test for Normal distribution while non-parametric test for a non-normal distribution.

“Five” corresponds to the small mapping area technique (5x5mm - ± 2% of the total mesh area), while “Ten” designates the large mapping area technique (four boxes of 10x10mm – ± 23% of the total mesh area). The samples are labelled as follows: Sample 1 represents dewatered sludge, Sample 2 denotes primary sludge, and Sample 3 signifies secondary sludge.

Table 4-7. Skewness and Kurtosis test

Descriptive Statistics											
	N	Minimum	Maximum	Mean	Std. Deviation	Skewness			Kurtosis		
	Statistic	Statistic	Statistic	Statistic	Statistic	Statistic	Std. Error	Z-value	Statistic	Std. Error	Z-value
Five_sample_1	5	5147.00	7922.00	6438.6000	1088.23219	0.402	0.913	**0.441**	-0.927	2.000	**-0.463**
Ten_sample_1	5	6094.00	7146.00	6652.6000	386.62165	-0.375	0.913	**-0.411**	0.814	2.000	**0.407**
Five_sample_2	5	1695.00	5023.00	3206.4000	1370.06452	0.489	0.913	**0.535**	-1.760	2.000	**-0.880**
Ten_sample_2	5	2406.00	2759.00	2564.6000	156.53530	0.425	0.913	**0.465**	-2.577	2.000	**-1.289**
Five_sample_3	5	3233.00	10049.00	6334.4000	2637.64569	0.502	0.913	**0.550**	-0.499	2.000	**-0.250**
Ten_sample_3	5	5271.00	6487.00	5847.6000	480.77105	0.297	0.913	**0.325**	-1.146	2.000	**-0.573**
Valid N (listwise)	5										

As all Z-values fall between -1.96 to 1.96 (Table 4-7), it can be concluded that the data are normally distributed. So, parametric test was used for the hypothesis test. Paired t-test was fitted for this experiment because it compares same subject, or sample tested differently.

3.3 Parametric test: Paired t-test

The average number of microplastics per gram (dried) dewatered sludge is 6439 (N=5; SD=1088.23) and 6653 (N=5; SD=386.62) for small and large mapping area respectively; per gram (dried) primary sludge is 3206

(N=5; SD=1370.06) and 2564 (N=5; SD=156.54) for small and large mapping area respectively; per gram (dried) secondary sludge is 6334 (N=5; SD=2637.65) and 5847 (N=5; SD=480.77) for small and large mapping area respectively.

Table 4-8. Paired Samples Correlations

		N	Correlation	Significance	
				One-Sided p	Two-Sided p
Pair 1	Five_sample_1 & Ten_sample_1	5	**0.547**	0.170	**0.340**
Pair 2	Five_sample_2 & Ten_sample_2	5	**-0.878**	0.025	**0.050**
Pair 3	Five_sample_3 & Ten_sample_3	5	**0.307**	0.307	**0.615**

The correlation coefficient shows that there is a relationship between the small and large mapping area, r(5) = 0.547, 0.878, and 0.307 with p=0.340, 0.050, 0.615 for dewatered sludge, primary sludge, and secondary sludge respectively (Table 4-8). Both dewatered and primary sludge samples showed a large correlation between techniques, while secondary sludge sample showed a medium correlation[19].

Table 4-9. Paired Samples Test

		Paired Differences					t	df	Significance	
		Mean	Std. Deviation	Std. Error Mean	95% Confidence Interval of the Difference				One-Sided p	Two-Sided p
					Lower	Upper				
Pair 1	Five_sample_1 - Ten_sample_1	-214.00000	934.43325	417.89125	-1374.25213	946.25213	**-0.512**	4	0.318	**0.636**
Pair 2	Five_sample_2 - Ten_sample_2	641.80000	1509.42893	675.03714	-1232.40356	2516.00356	**0.951**	4	0.198	**0.396**
Pair 3	Five_sample_3 - Ten_sample_3	486.80000	2531.52231	1132.13119	-2656.50011	3630.10011	**0.430**	4	0.345	**0.689**

Table 4-10. Paired Samples Effect Sizes

			Standardizer [a]	Point Estimate	95% Confidence Interval	
					Lower	Upper
Pair 1	Five_sample_1 - Ten_sample_1	Cohen's d	934.43325	**-0.229**	-1.106	0.674
		Hedges' correction	1171.13840	**-0.183**	-0.882	0.538
Pair 2	Five_sample_2 - Ten_sample_2	Cohen's d	1509.42893	**0.425**	-0.519	1.324
		Hedges' correction	1891.78862	**0.339**	-0.414	1.056
Pair 3	Five_sample_3 - Ten_sample_3	Cohen's d	2531.52231	**0.192**	-0.705	1.067
		Hedges' correction	3172.79270	**0.153**	-0.562	0.851

a. The denominator used in estimating the effect sizes.
Cohen's d uses the sample standard deviation of the mean difference.
Hedges' correction uses the sample standard deviation of the mean difference, plus a correction factor.

To rigorously compare the number of microplastics/fibers obtained using the small and large mapping area techniques, we conducted a paired-sample t-test. This analysis was executed across three distinct sludge samples, with each sample subjected to both the small and large mapping area techniques. There was no statistically significant difference ($p>0.05$) between the number of microplastics/fibers determined using the small and large mapping techniques. Specifically, for dewatered, primary, and secondary sludges, the t-values were 0.512, 0.951, and 0.430, respectively, with corresponding p-values of 0.636, 0.396, and 0.689 (Table 4-9).

The effect size for the small and big mapping area techniques was calculated using Cohen's d and Hedges's correction, resulting in a value from 0.153 to 0.425 for all samples (Table 4-10), consistently fell within the category of a small sample size effect. This small effect implies that there is no substantial difference between the two techniques and any observed difference is negligible. Negative values indicated that the large mapping area yielded a lower total estimated count of microplastics/fibers compared to the smaller mapping area.[19-21] These results further substantiated the interpretation of the p-values, as elaborated in the previous paragraph.

3.4 Subsampling error

A subsampling error formula was adopted from Brandt et.al. [13] to assess the performance of any considered subsampling model. This formula involved dividing the estimated microplastics/fibers (MPs/Fs) count of the small mapping area by the estimated MPs/Fs count of the large mapping area, with the requirement that the latter fulfilled a minimum of 20% of the total mesh area.

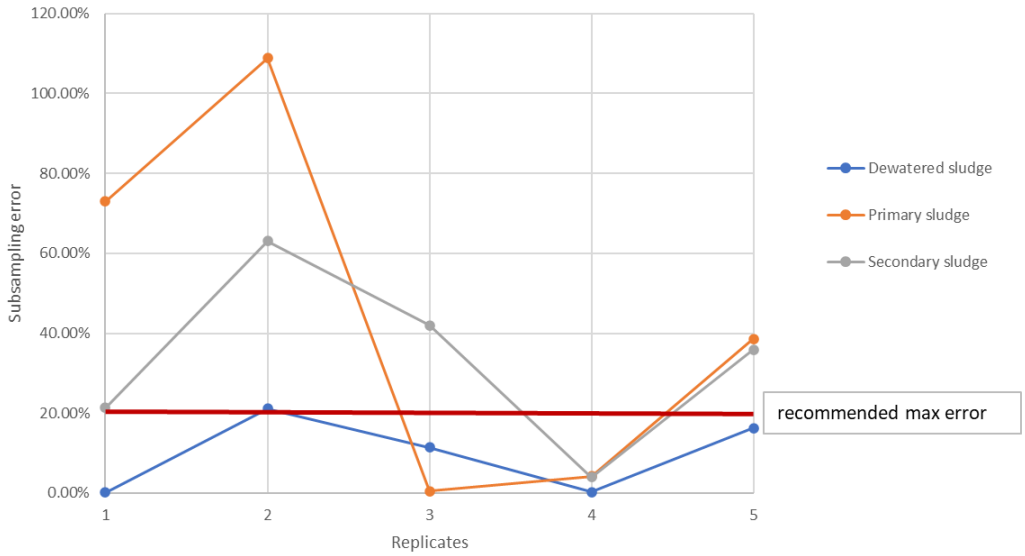

Figure 4-19. Subsampling error for each sample

As shown in Figure 4-19, out of the total 15 data points, seven (47%) met the criteria for maximum subsampling error, which is set at 20%[13]. However, examining the subsampling error percentages for dewatered sludge (3.36%), primary sludge (27.68%), and secondary sludge (7.93%), we observed that

employing replicates, each representing five random spots of the "5x5mm" mapping area, could effectively mitigate error. We recommend calculating the estimated MPs/Fs count of a sample by averaging the estimated MPs/Fs count obtained from at least five distinct "5x5mm" mapping spots within a mesh. While this approach may extend the analysis time from 1.5 hours to approximately 8 hours per sample, it offers the benefit of significantly reducing the potential for over- or underestimation of MPs/Fs counts within a sample.

Table 4-11. Number of microplastics/fibers per gram of dried dewatered sludge - sample 1

One box of 5x5mm		Four boxes of 10x10mm		
replicate	**MPs/Fs (items/g)**	**replicate**	**MPs/Fs (items/g)**	**Subsampling error (%)**
1	6083	1	6094	-0.17
2	5147	2	6527	-21.13
3	5917	3	6683	-11.45
4	7124	4	7146	-0.31
5	7922	5	6813	16.28
AVERAGE	6439		6652	-3.36

Table 4-12. Number of microplastics/fibers per gram of dried primary sludge - sample 2

One box of 5x5mm		Four boxes of 10x10mm		
replicate	**MPs/Fs (items/g)**	**replicate**	**MPs/Fs (items/g)**	**Subsampling error (%)**
1	4227	1	2444	72.95
2	5023	2	2406	108.77
3	2502	3	2515	-0.54
4	2585	4	2699	-4.21
5	1695	5	2759	-38.56
AVERAGE	3206		2565	27.68

Table 4-13. Number of microplastics/fibers per gram of dried secondary sludge - sample 3

One box of 5x5mm		Four boxes of 10x10mm		
replicate	**MPs/Fs (items/g)**	**replicate**	**MPs/Fs (items/g)**	**Subsampling error (%)**
1	5101	1	6487	-21.36
2	10049	2	6161	63.10
3	3233	3	5575	-42.00
4	5483	4	5271	4.04
5	7806	5	5744	35.90
AVERAGE	6335		5848	7.93

3.5 Distribution of microplastics/fibers in the mapped area based on type of plastics

The behaviour of particles within a suspension as they are collected on the filter is influenced by several factors, including particle size, the filter's material and matrix, and the filtration method employed.[22] Notably,

the use of a vacuum filtration setup can often result in an uneven distribution of particles on the filter.[23] To address this issue, we implemented the subsampling error calculation method, as detailed in the previous section. Despite the inherent challenges posed by the non-uniform distribution of particles, it is possible for certain types of plastics to concentrate within specific regions of the mesh due to intermolecular interactions among similar plastic types.[24] In this study, we did not observe a discernible pattern in the distribution of plastic types, indicating a random distribution across the mesh. We conducted mapping of two clusters, each covering a "4x4mm" area of the mesh, as depicted in Figure 4-20. Interestingly, several types of plastic were not detected in either of the clusters. As demonstrated in Figure 4-21, ABS, EAA, and modified cellulose were present in cluster 1, while PAN copolymer, PA, and WPC were found in cluster 2. However, EVA, PE, PEs, PET, PP PUR, PVC, and rubber were detected in both clusters. These findings remained consistent across both small and large mapping areas, as evidenced in Figure 4-22 and Figure 4-23.

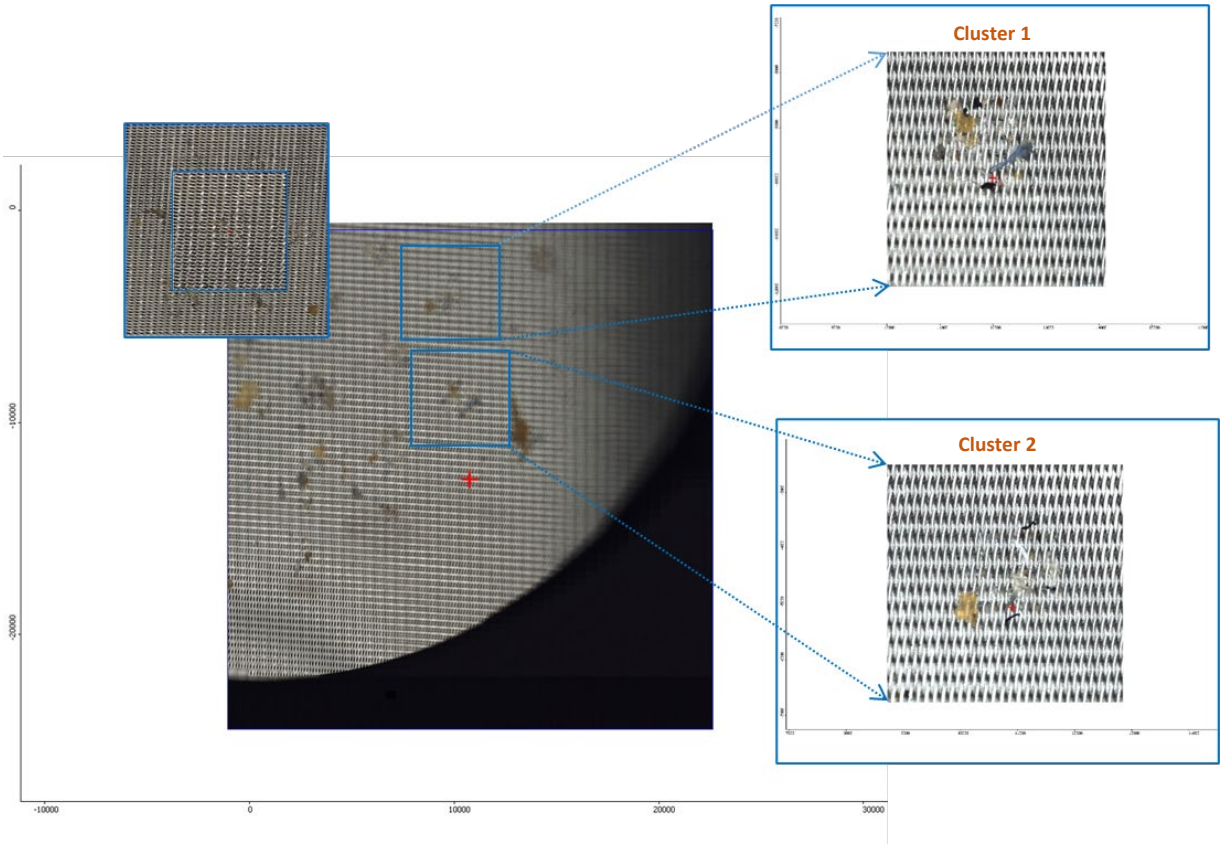

Figure 4-20. Sub-sampled area of mesh to study the plastic's type distribution

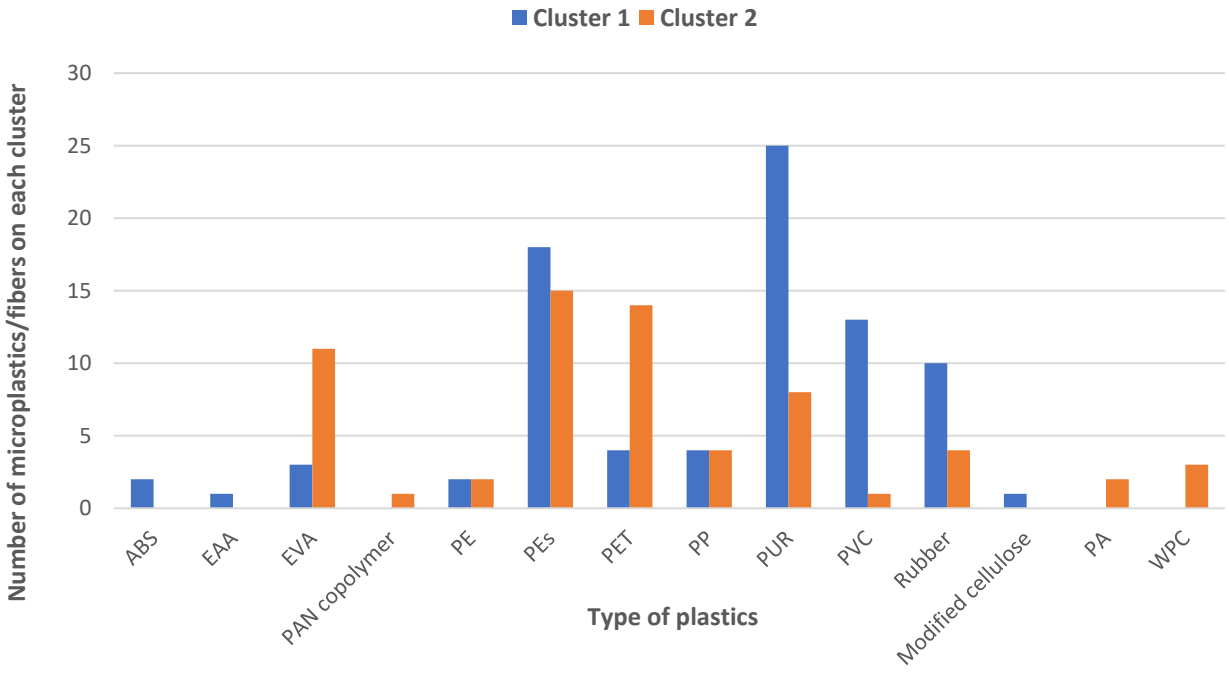

Figure 4-21. Number of microplastics proportionally for each type on two different clusters

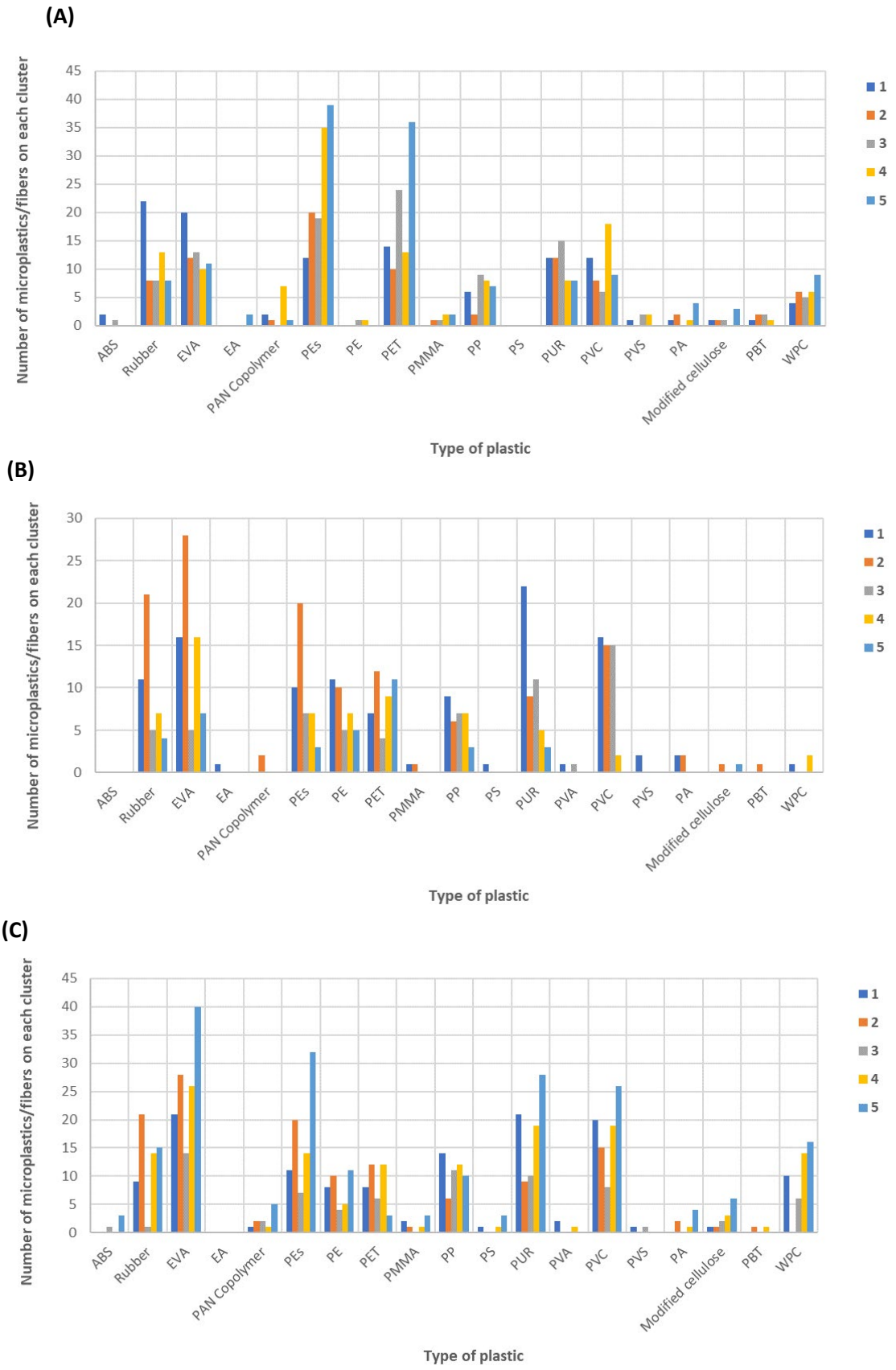

Figure 4-22. Number of microplastics proportionally for each plastic's type at five different small "5x5mm" clusters in (A) Dewatered sludge (B) Primary sludge (C) Secondary sludge

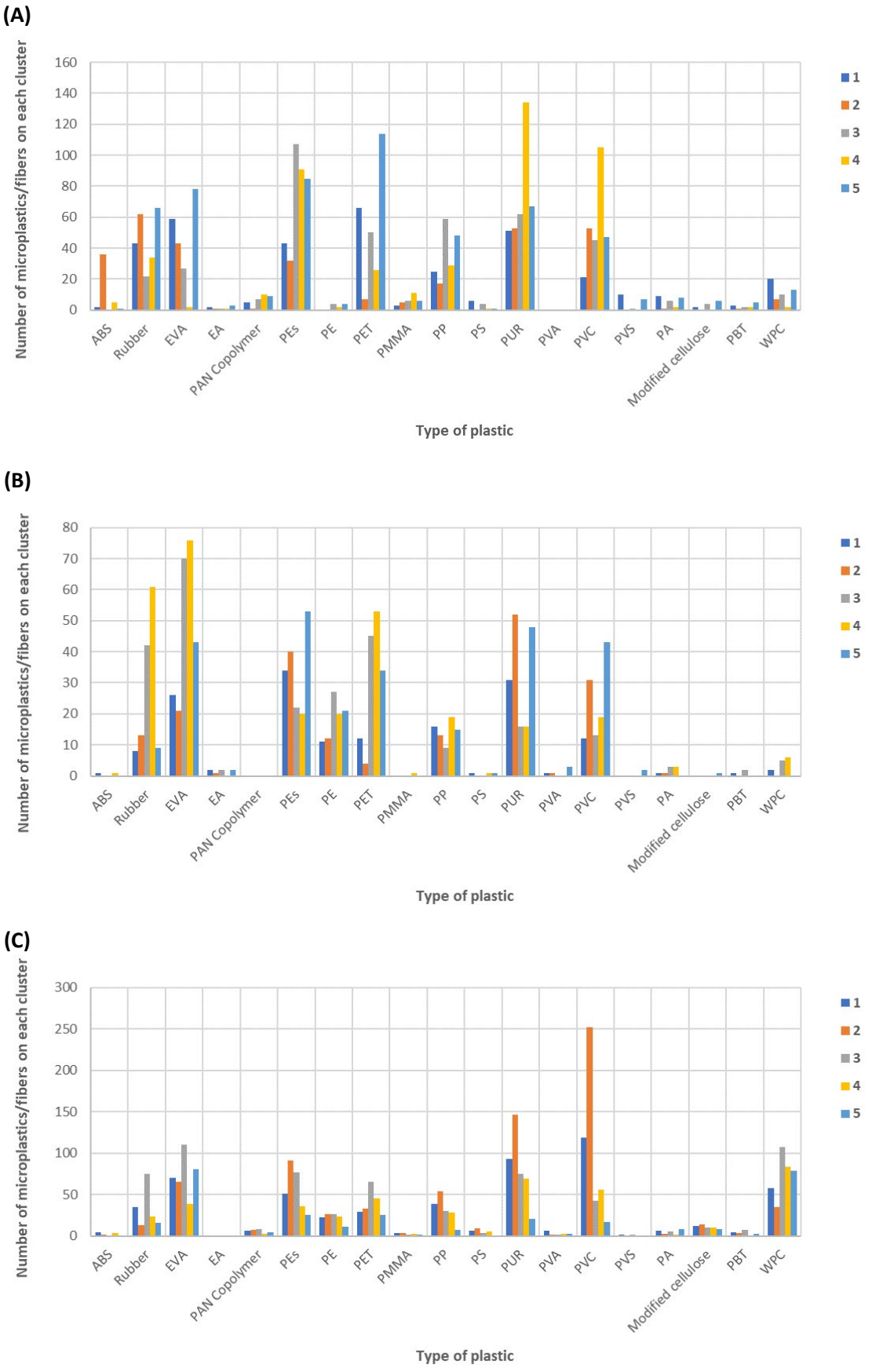

Figure 4-23. Number of microplastics proportionally for each plastic's type at five different big "10x10mm" clusters in (A) Dewatered sludge (B) Primary sludge (C) Secondary sludge

3.6 Distribution of microplastics based on number of particles of each type

We conducted a comprehensive examination of the number of each type of microplastics/fibers in both the small and large mapping areas to gain insights into the potential for error in detecting specific plastic type before and after extrapolation. This investigation aimed to address critical questions: firstly, if a particular type of plastic was absent in the small mapping area, would it be absent in the actual sample as well? Conversely, if a specific type was detected in the small mapping area, would it indeed be present in the actual sample? We defined these scenarios as instance of false negative and false positive in the analysis, respectively.

To assess these conditions, we employed a boxplot statistical analysis to reveal the median, minimum, and maximum counts of each type of microplastics/fibre. This analysis served as valuable tools for discerning which types of plastics were prone to being falsely categorized as either positive or negative. Table 4-14 summarizes the data extracted from the boxplots (Appendix F), shedding light on the presence or absence of specific plastic types in the small and large mapping areas. Notably, ABS (sample 2), and PS (sample 1) were identified as false negatives, as they were not detected in the small mapping area but were present in the larger one. Conversely, PAN copolymer (sample 2) was found in the small mapping area but not in the larger one, hence identified as false positive. However, it is noteworthy that the majority of plastics, approximately 84%, were identified in both mapping techniques, confirming the random and inhomogeneous distribution of particles on the filter.

Moreover, the data reveal an important trend: the lower the number of microplastics/fibers detected in the small mapping area, the higher the relative error in detecting and identifying them within the actual sample.

Table 4-14. Boxplot data median, minimum, and maximum for each plastic's type

Type of plastics	Sample	Small mapping area ~ ±2% of total mesh			Big mapping area ~ ± 23% of total mesh		
		Median	Minimum	Maximum	Median	Minimum	Maximum
ABS	1	0	0	2	42	8	44
	2	0	0	0	2	1	2
	3	1	0	3	7	4	8
Rubber	1	8	8	22	184	161	205
	2	7	4	21	120	72	125
	3	12	1	15	139	87	149
EVA	1	12	10	20	166	131	207
	2	16	5	28	193	160	215
	3	26	14	45	295	255	326
EA	1	0	0	2	7	5	7
	2	0	0	1	5	5	7
	3	0	0	0	0	0	0
PAN copolymer	1	1	0	7	25	22	31
	2	0	0	2	0	0	0
	3	2	1	5	21	19	25
PEs	1	20	12	39	273	251	326
	2	7	3	20	135	116	149
	3	14	7	32	229	189	255
PE	1	0	0	1	8	6	10
	2	7	5	11	71	64	80

	3	8	4	12	85	82	97
PET	1	14	10	36	213	149	256
	2	9	4	12	114	95	144
	3	8	3	14	164	132	172
PMMA	1	1	0	2	25	20	28
	2	0	0	1	1	0	1
	3	2	0	3	8	7	9
PP	1	7	2	9	149	119	161
	2	7	3	9	57	53	63
	3	12	10	19	128	104	151
PS	1	0	0	0	11	6	12
	2	0	0	1	2	2	3
	3	1	0	3	18	14	23
PUR	1	12	8	15	305	233	316
	2	9	3	22	132	111	147
	3	21	10	37	329	258	383
PVA	1	0	0	0	0	0	0
	2	0	0	1	4	2	5
	3	1	0	2	10	6	11
PVC	1	9	6	18	224	166	250
	2	15	0	16	99	75	106
	3	20	8	38	430	234	469
PVS	1	1	0	2	17	8	18
	2	0	0	2	2	0	2
	3	1	0	1	2	1	2
PA	1	1	0	4	20	17	25
	2	0	0	2	7	5	8
	3	1	0	4	17	14	21
Modified cellulose	1	1	0	3	10	6	12
	2	0	0	1	1	0	1
	3	2	1	6	44	40	46
PBT	1	1	0	2	11	8	12
	2	0	0	1	3	1	3
	3	0	0	1	13	9	16
WPC	1	6	4	9	42	32	50
	2	0	0	2	11	7	13
	3	14	6	24	283	255	327

False negative : not find in a small area, but present in big ones
False positive : find in a small area, but not present in big ones

3.7 Conditions of compliance

In order to attain higher data accuracy through the implementation of this semi-automated mapping mode, several essential conditions must be met. Firstly, this study was conducted with a minimum of 80% of the total particles present on the filter are confirmed as microplastics/fibers. The lower number of confirmed microplastics/fibers, the higher sub-sampling error value.[13] The attainment of this criterion hinges on the effectiveness of the pretreatment process in effectively isolating microplastics from samples with high organic content, such as sludge or other similar materials.

Secondly, since the identification of microplastics/fibers relies on the Hit Quality Index (%HQI), the robustness of the FTIR spectrum library database becomes paramount. It is crucial to expand this database by incorporating spectra from a diverse array of sources, including commercial, industrial, and weathered plastics using the same acquisition techniques which is reflectance mode on stainless-steel mesh. This expansion is necessary to enhance the %HQI's capacity to accurately represent the multitude of plastic

particles encountered in environmental settings. This is particularly important because commercial and environmental plastic particles often undergo modifications and may be composite materials with other substances, such as dyes, adhesives, water/fire-resistant coatings, and more. These types of plastics generate different infrared spectrum in comparison to their original or pure polymers. Additionally, factors such as UV exposure and contact with water changes the molecular structure and profoundly affect the infrared (IR) spectrum of these plastic particles, necessitating a comprehensive database to improve accuracy in their identification.[25, 26]

3.8 Reporting data and QA/QC

The data presented in this study are expressed as estimated numbers of microplastic/fibers, a result achieved through an extrapolation technique. To ensure the quality assurance and control (QA/QC) of these measurements, it is advisable to compute the subsampling error, with a recommended value maximum of 20%. This calculation serves to demonstrate the accuracy of the estimated particle counts.

Furthermore, it is essential to report the distribution of plastics on the filter according to their types, encompassing details such as median, minimum, and maximum particle counts. This reporting is indispensable for confirming the presence of a random and non-uniform distribution pattern. Such an analysis also allows for a more comprehensive examination of potential false positives and false negatives within the extrapolation technique.

3.9 Method benefits and limitations

As previously highlighted, the implementation of this semi-automated mapping technique has effectively reduced the analysis time from days down to approximately 2 hours per sample, depending on the number of particles on the filter. However, it is important to emphasize that the process of spectrum interpretation and identification continues to rely on human judgement that requires an hour for 40-50 spectra, necessitating individual scrutiny for each spectrum.

On the other hand, it is important to note that the potential for a notable subsampling error exist, and therefore, this error should be duly reported in any research employing this technique for microplastics analysis. Normalizing particle counts to the original sample can be challenging with this technique. While constructing a filtration apparatus to focus the sample on a smaller area (e.g., 10x10mm) may be an option, it risks particle overlap and complicating accurate counting. Additionally, processing less than 1 g of sample may not yield a representative sample of the wastewater treatment plant's output, potentially affecting the validity of the results. Another limitation was the data reported are counts and polymer classification, but not specifically classifying the particles based on shape and appearance.

4 Conclusions and further study

This study presents the use of a semi-automatic mapping technique utilizing FTIR Microspectroscopy for microplastics analysis, particularly in the context of high organic content samples, as exemplified by the sludge samples examined here. Remarkably, this technique yields a substantial reduction in analysis time, compressing the timeframe from hours or even days down to approximately 1-2 hours per sample. Importantly, this efficiency enhancement comes without the need for additional investments in advanced analytical instruments or dedicated built-in software.

The statistical analysis, as evidenced by the calculated p-values, reveals no significant differences between the small and large mapping modes. With 47% of the dataset conforms to the criteria of achieving a minimal 20% subsampling error, the technique demonstrates a reasonable level of accuracy in predicting the quantity of microplastics/fibers, considering the variability and inhomogeneity nature of the samples analyzed.

Regarding the distribution of particles, our investigation indicates a random and non-uniform spread on the filter, devoid of any discernible pattern related to specific plastic types. Additionally, an examination of false negative and positive data reveals that the majority of plastic types (>80%) were consistently detected in both small and large mapping modes, showing the technique's high sensitivity.

However, certain conditions must be adhered to when employing this method for microplastic analysis. It is imperative that at least 80% of the particles on the filter be confirmed as microplastics/fibers, a criterion influenced by the environmental plastics database within the instrument's IR spectrum library.

Furthermore, data are reported in terms of estimated microplastics/fibers counts for each sample, and whenever feasible, reporting the subsampling error along with the distribution of plastics is recommended. These measures serve to ensure the reliability of the analysis report.

To enhance the technique's accuracy, it is advisable to conduct additional testing on a broader range of samples, including various types of sample matrices such as water samples. Potential modifications to the sample pretreatment process, involving preconcentration, may be necessary to meet the minimum subsampling error threshold of 20% and to achieve a truly randomized plastic distribution.

The development of a compatible, built-in software for automatic spectrum identification of samples holds promise for reducing data processing time and streamlining the overall analysis process. However, this necessitates further exploration of both standard and environmental IR spectrum databases for polymer type identification, which may involve human validation and the integration of additional analytical instruments. Collaboration with data scientists and software engineers is a crucial step in realizing these advancements.

We also recommend conducting a systematic study using selected polymers to evaluate the reliability of the identification process by collecting reflectance spectra at various sizes and thicknesses across multiple replicates and analysing the variance. Additionally, different search algorithms should be considered, as they can significantly impact the hit index, with some algorithms placing more emphasis on broad peaks, which may be problematic for reflectance spectra with broad features.

Acknowledgement

This project receives support from South Australia Water (SA Water) Corporation. The authors extend their gratitude to the SA Water team stationed at the wastewater treatment plant in [redacted], South Australia, as well as the headquarters office team. Special acknowledgements go to Shima Ziajahromi from Australian Rivers Institute, Griffith University, for her valuable guidance on the pretreatment procedure and her expertise in microplastics analysis. Anggelia Essi Christian is the recipient of a Flinders University scholarship for the Ph.D. degree.

References

1. Ball H, C. R., Grove E, Horton A, Johnson A, Jürgens M, Read D, Svendsen C, Sink To River - River To Tap. A Review of Potential Risks From Nanoparticles and Microplastics. *UK Water Industry Research Limited* **2019,** *EQ 01 A 231*.
2. Ng, E.-L.; Huerta Lwanga, E.; Eldridge, S. M.; Johnston, P.; Hu, H.-W.; Geissen, V.; Chen, D., An overview of microplastic and nanoplastic pollution in agroecosystems. *Science of The Total Environment* **2018,** *627*, 1377-1388.
3. Jung, J. W.; Park, J. W.; Eo, S.; Choi, J.; Song, Y. K.; Cho, Y.; Hong, S. H.; Shim, W. J., Ecological risk assessment of microplastics in coastal, shelf, and deep sea waters with a consideration of environmentally relevant size and shape. *Environmental Pollution* **2021,** *270*.
4. Allouzi, M. M. A.; Tang, D. Y. Y.; Chew, K. W.; Rinklebe, J.; Bolan, N.; Allouzi, S. M. A.; Show, P. L., Micro (nano) plastic pollution: The ecological influence on soil-plant system and human health. *Science of the Total Environment* **2021,** *788*.
5. Hopewell, K.; Batstone, D.; Dale, G.; Keegan, A.; Lee, E.; Randall, L.; Tao, E. *ANZBP Preliminary Report on Microplastics Risk for the Australian and New Zealand Biosolids Industry July 2020*; 2020.
6. Australian & New Zealand Biosolids Partnership *ANZBP Factsheet on Microplastics*; 2020.
7. Lares, M.; Mohamed Chaker, N.; Sillanpää, M.; Sillanpää, M., Intercomparison study on commonly used methods to determine microplastics in wastewater and sludge samples. *Environmental Science and Pollution Research International* **2019,** *26* (12), 12109-12122.
8. Primpke, S.; Christiansen, S. H.; Cowger, W.; De Frond, H.; Deshpande, A.; Fischer, M.; Holland, E.; Meyns, M.; O'Donnell, B. A.; Ossmann, B., Critical Assessment of Analytical Methods for the Harmonized and Cost Efficient Analysis of Microplastics. *Applied Spectroscopy* **2020,** *74* (9), 1012-1047.
9. Prata, J. C.; Reis, V.; Matos, J. T. V.; da Costa, J. P.; Duarte, A. C.; Rocha-Santos, T., A new approach for routine quantification of microplastics using Nile Red and automated software (MP-VAT). *Science of The Total Environment* **2019,** *690*, 1277-1283.
10. Oßmann, B. E.; Sarau, G.; Schmitt, S. W.; Holtmannspötter, H.; Christiansen, S. H.; Dicke, W., Development of an optimal filter substrate for the identification of small microplastic particles in food by micro-Raman spectroscopy. *Analytical and Bioanalytical Chemistry* **2017,** *409* (16), 4099-4109.
11. Primpke, S.; Cross, R. K.; Mintenig, S. M.; Simon, M.; Vianello, A.; Gerdts, G.; Vollertsen, J., Toward the Systematic Identification of Microplastics in the Environment: Evaluation of a New Independent Software Tool (siMPle) for Spectroscopic Analysis. *Applied Spectroscopy* **2020,** *74* (9), 1127-1138.
12. Huppertsberg, S.; Knepper, T. P., Instrumental analysis of microplastics—benefits and challenges. *Analytical and Bioanalytical Chemistry* **2018,** *410* (25), 6343-6352.

13. Brandt, J.; Fischer, F.; Kanaki, E.; Enders, K.; Labrenz, M.; Fischer, D., Assessment of Subsampling Strategies in Microspectroscopy of Environmental Microplastic Samples. *Frontiers in Environmental Science* **2021,** *8*.
14. Schymanski, D.; Oßmann, B. E.; Benismail, N.; Boukerma, K.; Dallmann, G.; von der Esch, E.; Fischer, D.; Fischer, F.; Gilliland, D.; Glas, K.; Hofmann, T.; Käppler, A.; Lacorte, S.; Marco, J.; Rakwe, M. E. L.; Weisser, J.; Witzig, C.; Zumbülte, N.; Ivleva, N. P., Analysis of microplastics in drinking water and other clean water samples with micro-Raman and micro-infrared spectroscopy: minimum requirements and best practice guidelines. *Analytical and Bioanalytical Chemistry* **2021,** *413* (24), 5969-5994.
15. Ziajahromi, S.; Neale, P. A.; Telles Silveira, I.; Chua, A.; Leusch, F. D. L., An audit of microplastic abundance throughout three Australian wastewater treatment plants. *Chemosphere* **2021,** *263*, 128294.
16. Hartmann, N. B.; Hüffer, T.; Thompson, R. C.; Hassellöv, M.; Verschoor, A.; Daugaard, A. E.; Rist, S.; Karlsson, T.; Brennholt, N.; Cole, M.; Herrling, M. P.; Hess, M. C.; Ivleva, N. P.; Lusher, A. L.; Wagner, M., Are We Speaking the Same Language? Recommendations for a Definition and Categorization Framework for Plastic Debris. *Environmental Science & Technology* **2019,** *53* (3), 1039-1047.
17. De Frond, H.; Rubinovitz, R.; Rochman, C. M., µATR-FTIR Spectral Libraries of Plastic Particles (FLOPP and FLOPP-e) for the Analysis of Microplastics. *Anal Chem* **2021,** *93* (48), 15878-15885.
18. Tian, Y.; Chen, Z.; Zhang, J.; Wang, Z.; Zhu, Y.; Wang, P.; Zhang, T.; Pu, J.; Sun, H.; Wang, L., An innovative evaluation method based on polymer mass detection to evaluate the contribution of microfibers from laundry process to municipal wastewater. *Journal of Hazardous Materials* **2021,** *407*.
19. Sullivan, G. M.; Feinn, R., Using Effect Size-or Why the P Value Is Not Enough. *J Grad Med Educ* **2012,** *4* (3), 279-82.
20. Cohen, J., A Power Primer. *Psychological bulletin* **1992,** *112* (1), 155-159.
21. Ferguson, C. J., An Effect Size Primer: A Guide for Clinicians and Researchers. *Professional psychology, research and practice* **2009,** *40* (5), 532-538.
22. Merck, AD030 Air and fluid particle monitoring guide. Merck KGaA: Darstamdt, Germany, 2018.
23. Thaysen, C.; Munno, K.; Hermabessiere, L.; Rochman, C. M., Towards Raman Automation for Microplastics: Developing Strategies for Particle Adhesion and Filter Subsampling. *Appl Spectrosc* **2020,** *74* (9), 976-988.
24. Buffle, J.; Leppard, G. G., Characterization of Aquatic Colloids and Macromolecules. 2. Key Role of Physical Structures on Analytical Results. *Environmental Science & Technology* **1995,** *29* (9), 2176-2184.
25. Cheng, F.; Zhang, T.; Liu, Y.; Zhang, Y.; Qu, J., Non-Negligible Effects of UV Irradiation on Transformation and Environmental Risks of Microplastics in the Water Environment. *J Xenobiot* **2021,** *12* (1), 1-12.
26. Gewert, B.; Plassmann, M. M.; MacLeod, M., Pathways for degradation of plastic polymers floating in the marine environment. *Environmental Science: Processes & Impacts* **2015,** *17* (9), 1513-1521.

CHAPTER 5: FLOW CYTOMETRY FOR MICROPLASTICS ANALYSIS

This chapter provides the groundwork for the Chapter 6 and 7, focusing on the application of the Flow Cytometry technique. It includes the validation, advantages, and limitations of the technique. The primary objective is to evaluate its accuracy and sensitivity.

Abstract

Counting microplastics, especially with sizes smaller than 25 µm, presents a significant challenge. Both FTIR and Raman microspectroscopy are able to characterize the plastics composition, yet still rely on the manual counting or using a software for particles' image analysis. In contrast, Flow Cytometry offers the capability to enumerate particles ranging from 0.2 µm to 150 µm automatically, providing a distinct advantage for counting smaller size of microplastics. This study delineates the impacts of analytical parameters on counting accuracy, including laser lines, fluorophores, threshold acquisition, and recovery rates, established through a calibration curve utilizing Fluorescein (FITC) green beads-green labelled polystyrene. With an approximate 96% recovery rate, Flow Cytometry emerges as a viable option for initiating microplastics counts in samples, specifically demonstrated in this case with sludge samples. However, it is imperative to note that further validation is necessary to confirm the absence of non-plastic particles within the plastic's gating distribution. Additionally, assessing the recovery rate for polymers other than polystyrene will fortify the current findings.

1 Introduction

Studies have demonstrated that plastic particles undergo fragmentation over time, a phenomenon exacerbated by diverse environmental conditions, particularly when plastics accumulate in the soil. Complex biochemical reactions and physical alterations, such as varying pH, soil salinity, fluctuating temperature, gas generation (e.g., CO_2 and CH_4), physical stress, and microbial degradation, can lead not only to the fragmentation of plastic particles but also to adverse effects on environmental conditions [1-4].

To detect and enumerate small microplastics, an alternative analytical instrument is required. Current commonplace techniques like optical microscopy, FTIR microspectroscopy, and Raman microspectroscopy are limited to certain size of particles, a time-consuming technique of manual counting of particles, and an automatic particles counting using a software that still rely on the human justification and interpretation.[5-7] Optical Photothermal InfraRed (O-PTIR) microspecroscopy has been proposed to detect particles as small as 500 nm and automatically count and characterize them using software.[8 9] However, when using O-PTIR for microplastics analysis, certain factors need to be considered. For instance, the ability to focus the laser beams to detect and locate the particles on a surface, either by human or software, is crucial for gaining accurate spectra and identifying particle types. This can be achieved more easily by focusing the laser beam and identifying particle individually using conventional microspectroscopy. Despite of this condition, O-PTIR

microspectroscopy produces transmission spectra that are fit most current libraries used. Nevertheless, it is necessary to develop a user library to represent the plastics found in the local environment and to tailor it to the technique and/or filter type used. Moreover, there is a need for a rapid and portable analytical instrument for microplastic counting, especially in field applications. Flow Cytometry is an automatic technique to detect and count microplastics.

Flow Cytometry, widely employed in biology studies focusing on microorganisms and cells with sizes ranging from micrometres to nanometres[10, 11], offers a potential solution. This technique can measure individual particle properties through a fluidic system, creating hydrodynamic focusing based on the Bernoulli effect. The particles flow in a singe file, enabling single-cell analysis. As each particle passess through one or more laser beams, it undergoes light scattering or fluorescence emission, providing some information about its composition. Flow Cytometry detects particles ranging from 0.2 µm or 200 nm to 250 µm[9], making it suitable for counting microplastics. Previous studies, such as those by Kaile et al. using Nile Red to selectively dye the plastic's particles by absorption of the lipophilic dye into hydrophopic plastics [11], and Wang et al using FITC beads to mimic the particles[10], have utilized flow cytometry technique for microplastics enumeration.

In this study, we employed flow cytometry technique to count plastic particles isolated from wastewater and sludge samples, driven by its feasibility and its potential to provide insights into plastic loads in wastewater treatment. To validate the technique, we conducted a serial validation procedure, adjusting instrument settings to esablish plastic particle gate distribution, creating a calibration curve using FITC green beads suspension itself, and subsequently spiking the samples. This comprehensive approach serves as a validation technique, demonstrating the method's utility for microplastic analysis. Despite these advancements, there is currently no standard technique for data comparison in this field.

2 Materials and Methods

The instrument (CytoFLEX S Flow Cytometer; Beckman Coulter) settings were established based on a prior study to determine lasers, threshold acquisition, and fluorophore. The laser lines employed were Violet (405-407 nm) and Blue (488 nm), with the fluorophore being FITC (fluorescein isothiocyanate) present in polystyrene microspheres of diameter size of 3 µm. The threshold acquisition setting was FITC-height (primary) 850 and SSC 10000. In the cytogram, side scatter (SSC) reflected particles' granularity, while forward scatter (FSC) provided an estimate of particle's size. A cytogram provides information on the microplastics distribution based on their granularity (SSC) against FITC green beads. It also can be set against the particle's size (FSC) to observe the particle's size against FITC green beads. In this study, we were using SSC as the axis to determine the gating distribution.

Firstly, using the aforementioned lasers and acquisition setting, the gating distribution of plastic particles was determined using standard reference polymers (LDPE, HDPE, PET, PP, PS, PMMA, and PVC). These polymers

were prepared by either using a coffee bean grinder or a nail file to fragment particles, which were then suspended in ethanol, filtered through 25 µm stainless steel filters, 10 µm, and 0.2 µm polycarbonate membranes, rapidly oven-dried, and subsequently resuspended in Tris-EDTA Buffer. 500 µl of each polymer suspensions, with size ranges of 10-25 µm and 0.2-10 µm, were analyzed using Flow Cytometer and their native fluorescence, with additional 10 µl FITC green beads as the positive control.

Secondly, to construct a calibration curve for FITC green beads, a series of dilutions ranging from 23,000 to 230,000 times were prepared in filtered ultrapure water, and the bead counts (measured from 500 µl of each suspension) were analysed using the Flow Cytometer. This calibration curve was then utilized to calculate the bead counts spiked into the actual sample in the recovery rate validation step.

Thirdly, to assess the recovery rate or accuracy of the technique, samples (microplastics sized 10-25 µm and 0.2-10 µm, isolated from dried secondary sludge collected on June 8, 2022, and suspended in TE Buffer) were spiked with varying volumes of FITC green beads, then measured. Consequently, two different sets of spiked microplastics suspensions were created. The recovery rate was calculated by comparing FITC green beads detected by the Flow Cytometer with the spiked FITC green beads calculated using the Pearson correlation equation of the FITC calibration curve above. Then, a correlation curve was created to present the linear regression between the detected and spiked FITC green beads.

3 Results and Discussion

3.1 Gating distributions of green beads and plastic's particles

The gating distribution of FITC green beads was established by adding 10 µL of FITC green beads in TE Buffer, it was used to suspend samples, and in filtered ultrapure water, it was used to suspend FITC green beads, as

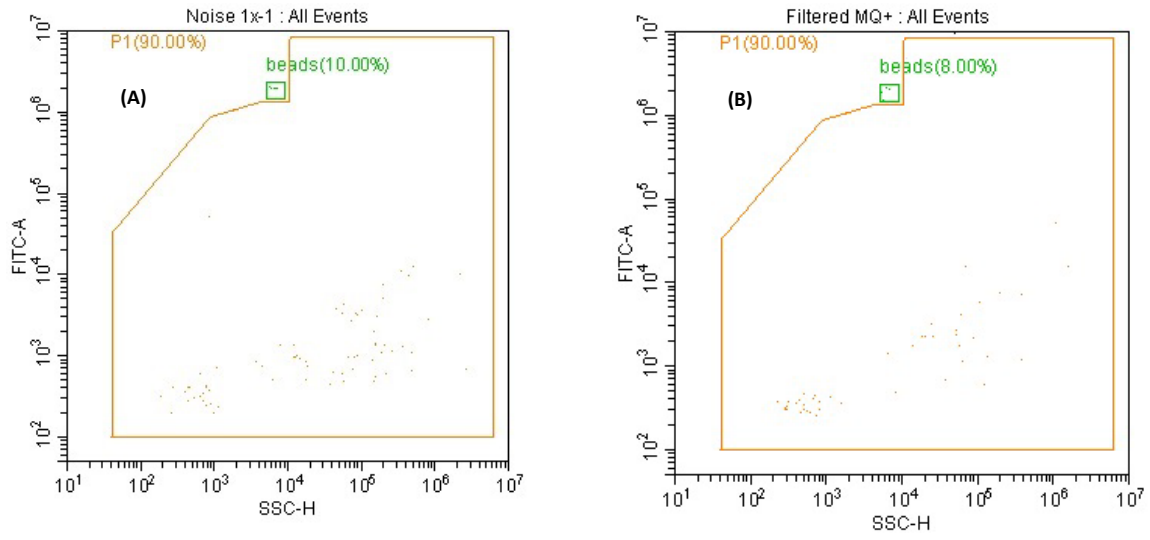

Figure 5-24. Cytograms of FITC green beads gating distibution in (A) TE Buffer, and (B) filtered ultrapure water

illustrated in Figure 5-24. No particles were detected in the area of TE Buffer and filtered ultrapure water when no FITC green beads were added, as depicted in Figure 5-25.

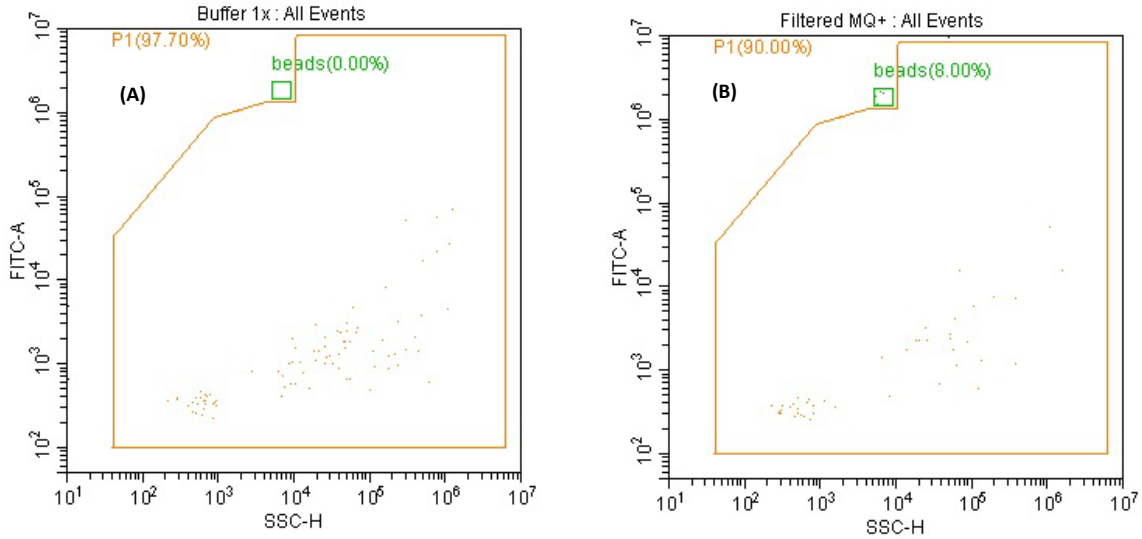

Figure 5-25. Cytograms of (A) TE Buffer and (B) Filtered ultrapure water without FITC green beads

Concurrently, the gating distribution for plastic particles was configured based on the particle distribution of seven standard polymer references for the range of 10-25 µm and five different polymers for 0.2-10 µm (Figure 5-26).

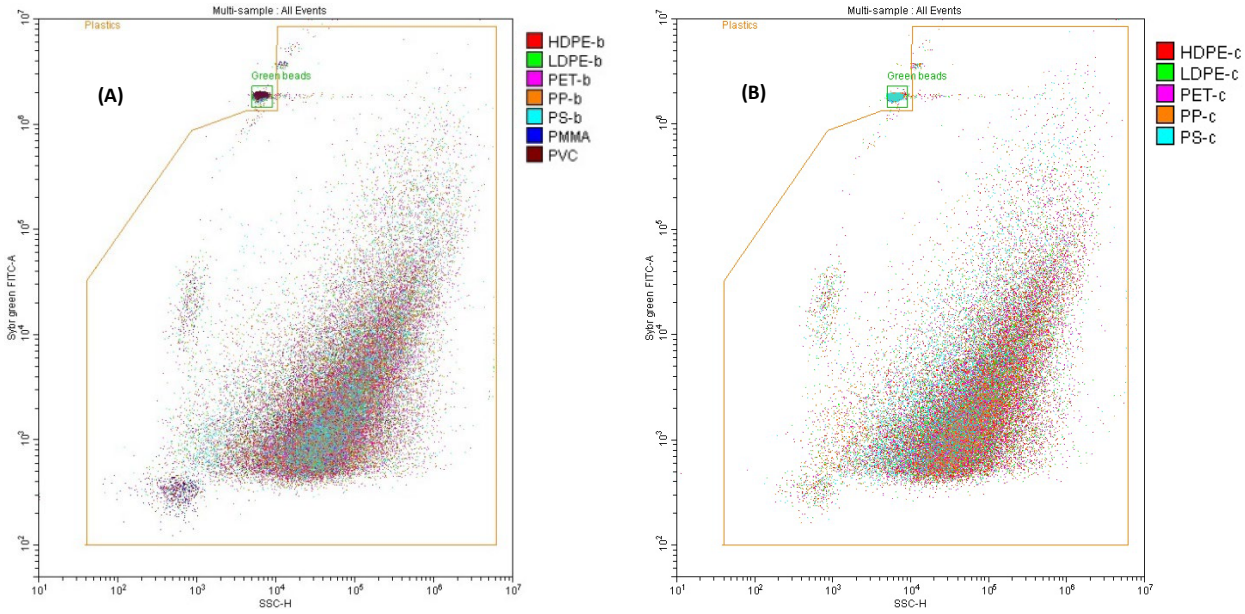

Figure 5-26. Cytogram of plastic's particles gating distribution for size (A) 10-25µm, and (B) 0.2-10µm

These predetermined gating distributions for both FITC green beads and plastic particles served as templates for determining both bead and microplastic counts, for sizes 0.2-10 µm and 10-25 µm, in the analysis. Particles detected in the plastic's gating distribution without the sample or solely in TE Buffer (Figure 5-25) were considered noise and were subtracted from the total counts of plastic particles detected with the sample.

Nevertheless, no validation test has been conducted for the distribution of non-plastic particles. Despite the microplastics isolation procedure's efficiency, where the digestion and wet peroxide oxidation procedure yield more than 80% efficiency[12, 13], it is imperative to ensure the absence of non-plastic particles in the gating distribution of plastic particles. Therefore, further experiments are warranted.

3.2 FITC green beads calibration

Utilizing the gating distribution template outlined in Section 3.1, various dilutions of FITC green beads in filtered ultrapure water were prepared and analyzed (Figure 5-28). Subsequently, a FITC green beads calibration curve was generated (Figure 5-27). The Pearson's correlation equation was applied to enumerate the beads particles spiked into the actual samples (refer to Section 3.3), termed as spiked-beads counts, and compared with the detected-beads counts.

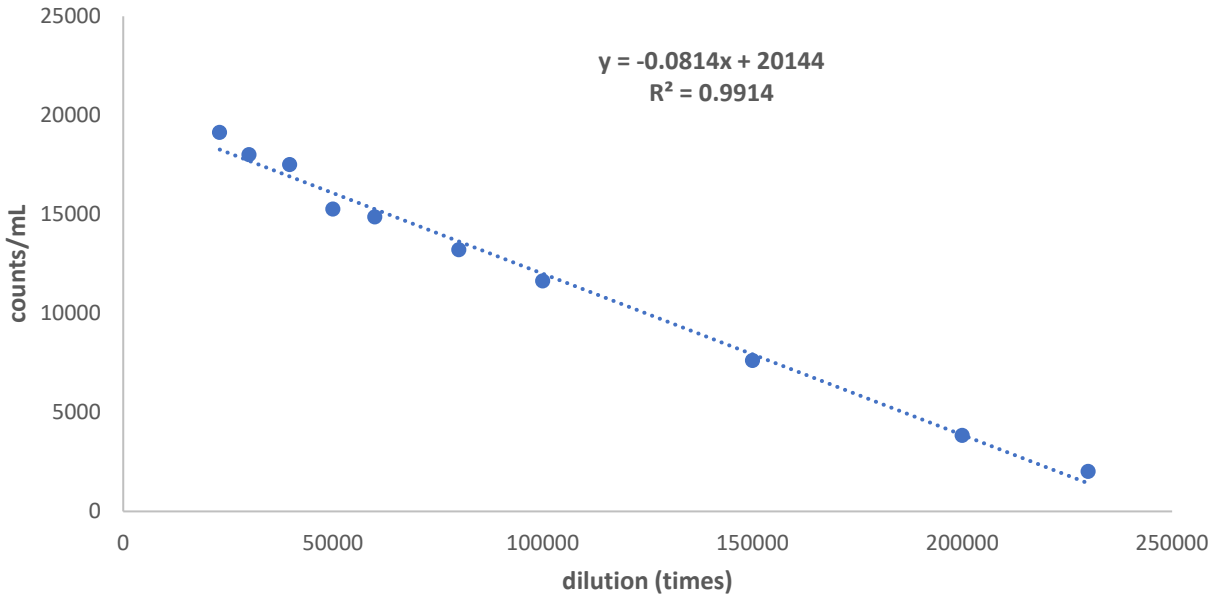

Figure 5-27. FITC green beads calibration curve

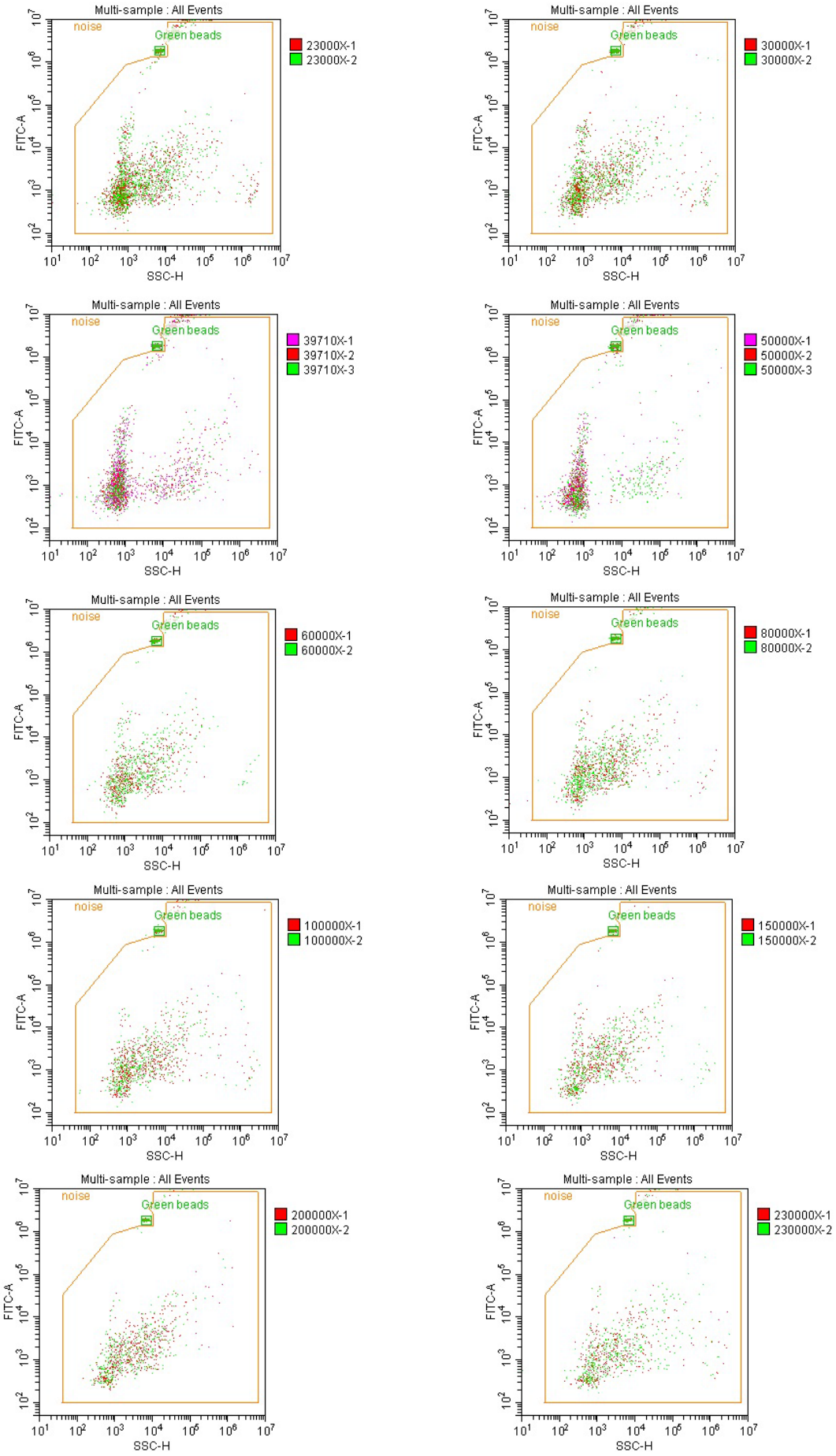

Figure 5-28. Cytograms of microplastics sized 10-25µm spiked with different concentrations of FITC green beads

3.3 Recovery rates

To validate the accuracy of this technique, microplastics isolated in sizes ranging from 10-25 µm and 0.2-10 µm were spiked with FITC green beads or green-labelled polystyrene at varying concentrations. The number of detected green beads, as depicted in Figure 5-31 and Figure 5-32, was subsequently compared to the calculated counts of beads spiked in the samples, employing the Pearson's correlation equation outlined in Section 3.2. Given the varied concentrations at which the samples were spiked, a correlation linear trendline between detected and spiked beads was achieved (Figure 5-29 and Figure 5-30).

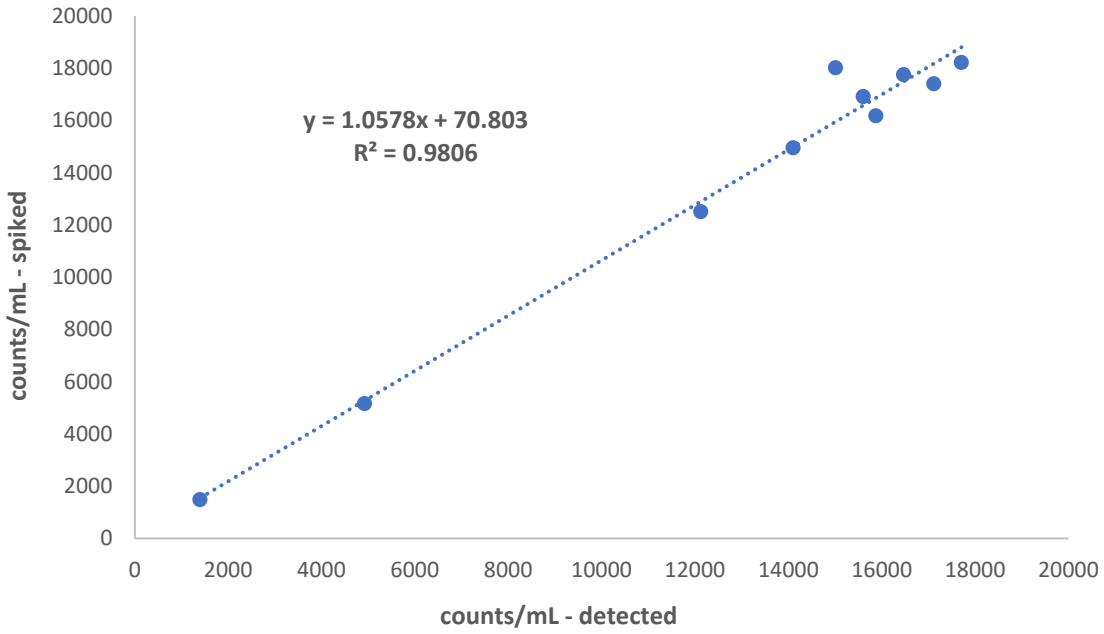

Figure 5-29. Recovery rates curve for microplastics sized 10-25µm

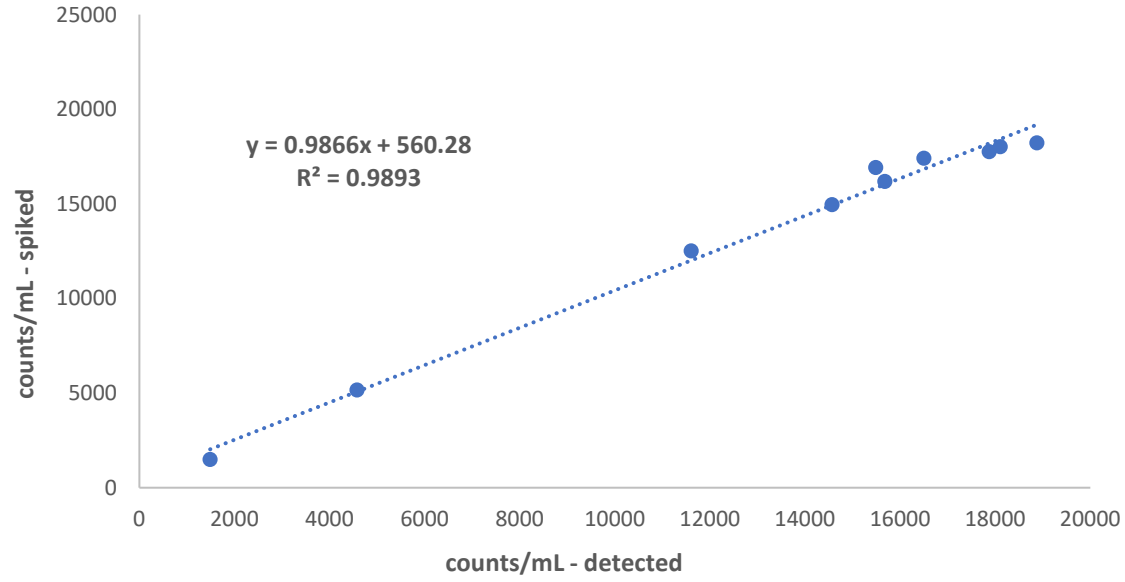

Figure 5-30. Recovery rates curve for microplastics sized 0.2-10µm

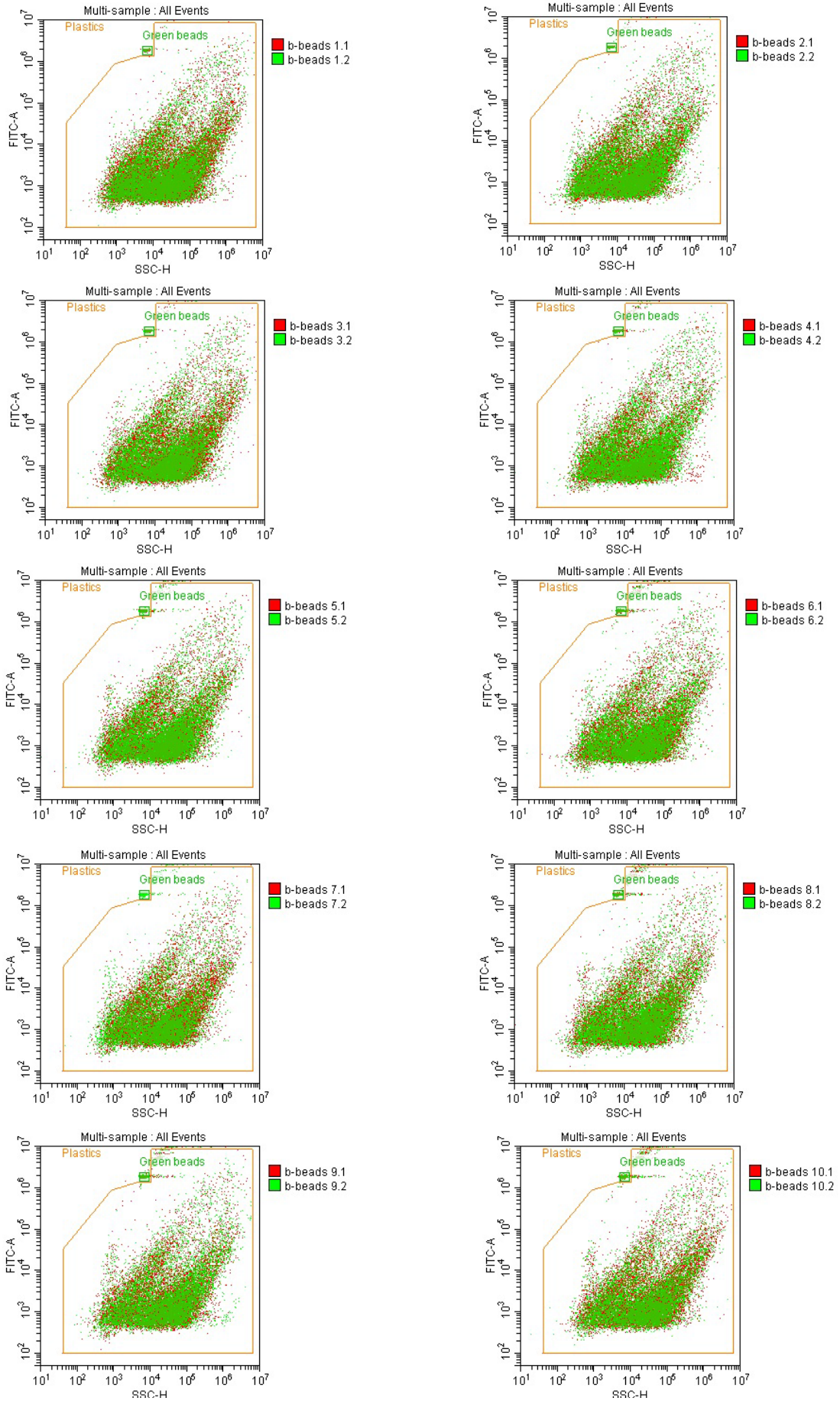

Figure 5-31. Cytograms of microplastics sized 10-25 µm spiked with different concentrations of FITC green beads

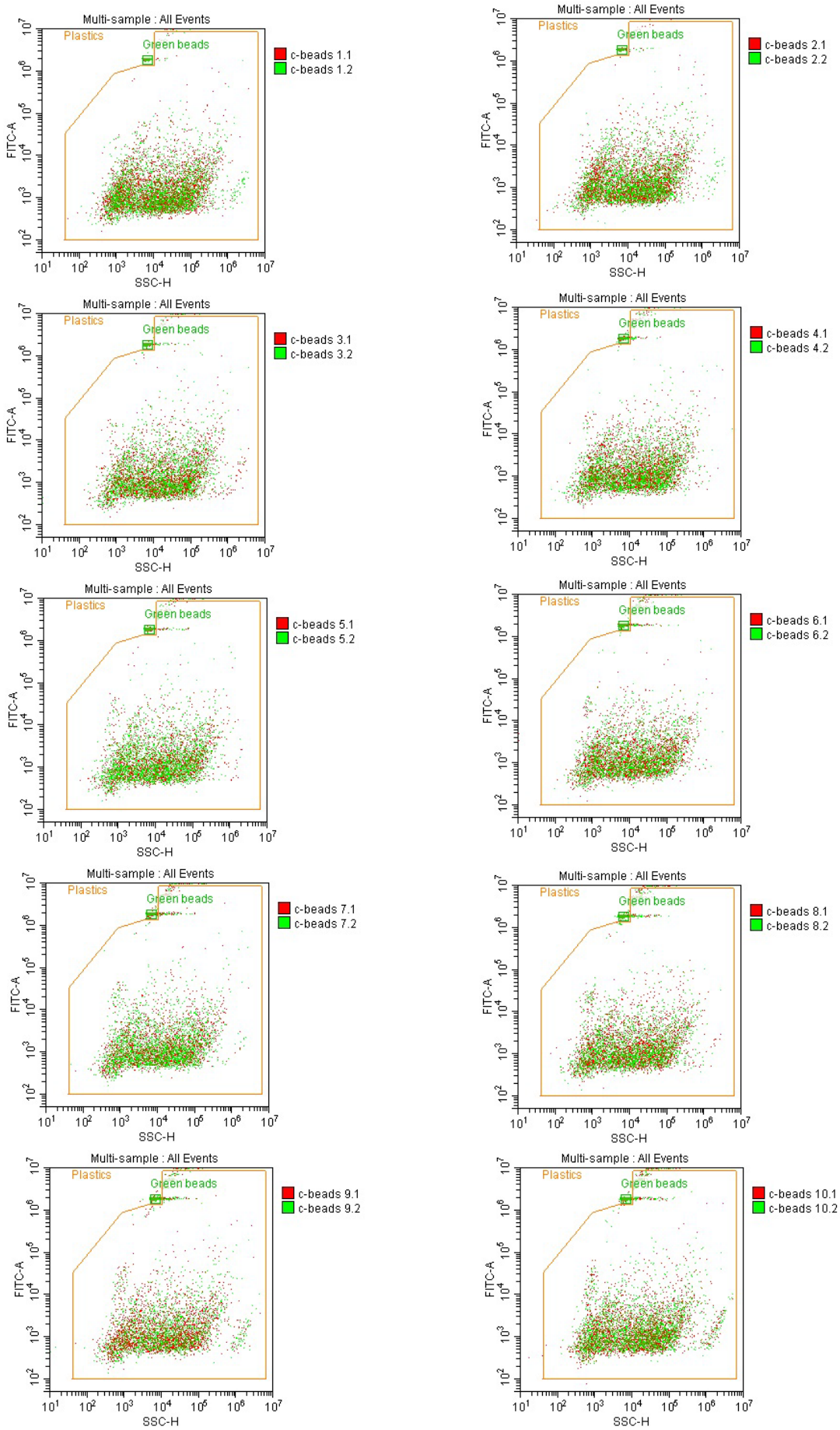

Figure 5-32. Cytograms of microplastics sized 0.2-10µm spiked with different concentrations of FITC green beads

The resulting average recovery rate was 96%, determined by the ratio of counts-detected over counts-spiked. This signifies that approximately 96% of the green beads spiked into the samples were accurately detected or recovered, representing the precision of the analysis. Nevertheless, as highlighted in Section 3.1, no validation test has been conducted for the distribution of non-plastic particles, and only polystyrene was utilized as a control positive.

3.4 Size Effect of subsampling

It is noteworthy that this analysis employed a subsampling technique, as only 200 µL in a 500 µL suspension was analyzed by the instrument. For the 0.2-10 µm size fraction of samples, considering the challenge of filtering a high number of particles and a slow filtration rate, only 10 mL of the original sample's filtrate (roughly 150-300 mL) was filtered through a 0.2 µm membrane filter. Consequently, only 3-7% of the total microplastics counts were sampled, and of those, only 2% were subjected to analysis. While extrapolation was employed in the calculations, it is important to acknowledge that this proportion of sampled material may not fully represent the actual number of microplastics in the sample. In comparison, the FTIR technique typically requires testing a minimum of 20% of the total microplastics[14-16]. Suggestions for optimizing these techniques are outlined in page 71, section 4 of this chapter giving the option to modify the filtration procedure.

3.5 Unclear effect of digestion procedure on smaller size of plastics particles

This study did not explore the extent to which the hydrogen peroxide-based digestion procedure impacts microplastics below 25 µm. As flow cytometry cannot identify polymer types, Raman spectroscopy is suggested as an option to assess the identity of particles with and without the digestion procedure, capable of identifying plastics as small as 10 µm. Beyond potential alterations to the chemical identity of microplastics, the digestion process may also lead to particle digestion, resulting in lost particles counts or fragmentation into smaller sizes than the original ones. No existing studies have explored this aspect, emphasizing the need for further testing.

4 Conclusion and Further Studies

With a recovery rate of approximately 96% and tailored gating distribution setting for microplastics detection, Flow Cytometry offers an effective method for providing microplastics counts, albeit without polymer identification. This technique provides an initial insight into plastic loads for microplastics sized below 25 µm.

Further investigations are required to confirm the absence of non-plastic particles in the gating distribution set for plastic particles. Additionally, conducting recovery rate tests using other types of polymers is advisable, followed by cross-analysis with alternative analytical instruments such as Flow Cytometry imaging

to study particle topology and Nanoparticle Tracking Analysis to further validate the technique's accuracy in detecting and counting microplastics.

Regarding the subsampling technique's impact size, it is recommended that all filtrate collected after 10 µm filtration to be filtered through 0.2 µm and analysed. However, the current filtration setting, using vacuum filtration with a PC (polycarbonate) membrane (pore 0.2 µm; diameter 19 mm), may prove time-consuming. Therefore, it is suggested to explore and modify more efficient filtration techniques. The use of a 96-well plate for Flow Cytometer analysis could be considered as an option for efficient sample analysis compared to using a flow cytometry tube, which would necessitate tube changes for each sample.

References

1. He, P.; Chen, L.; Shao, L.; Zhang, H.; Lu, F., Municipal solid waste (MSW) landfill: A source of microplastics?-Evidence of microplastics in landfill leachate. *Water Research* **2019,** *159*, 38-45.
2. Zbyszewski, M.; Corcoran, P. L., Distribution and Degradation of Fresh Water Plastic Particles Along the Beaches of Lake Huron, Canada. *Water, Air, & Soil Pollution* **2011,** *220* (1), 365-372.
3. Chen, X.; Xu, M.; Yuan, L. M.; Huang, G.; Chen, X.; Shi, W., Degradation degree analysis of environmental microplastics by micro FT-IR imaging technology. *Chemosphere* **2021,** *274*.
4. Zhang, K.; Hamidian, A. H.; Tubić, A.; Zhang, Y.; Fang, J. K. H.; Wu, C.; Lam, P. K. S., Understanding plastic degradation and microplastic formation in the environment: A review. *Environmental Pollution* **2021,** *274*.
5. Hidalgo-Ruz, V.; Gutow, L.; Thompson, R. C.; Thiel, M., Microplastics in the Marine Environment: A Review of the Methods Used for Identification and Quantification. *Environmental Science & Technology* **2012,** *46* (6), 3060-3075.
6. Schwaferts, C.; Niessner, R.; Elsner, M.; Ivleva, N. P., Methods for the analysis of submicrometer- and nanoplastic particles in the environment. *TrAC Trends in Analytical Chemistry* **2019,** *112*, 52-65.
7. Sun, J.; Dai, X.; Wang, Q.; van Loosdrecht, M. C. M.; Ni, B.-J., Microplastics in wastewater treatment plants: Detection, occurrence and removal. *Water Research* **2019,** *152*, 21-37.
8. Krafft, C., Chapter 9 - Optical photothermal infrared spectroscopic applications in microplastics—comparison with Fourier transform infrared and Raman spectroscopy. In *Molecular and Laser Spectroscopy*, Gupta, V. P., Ed. Elsevier: 2022; pp 305-336.
9. Beckman Coulter, I., *Instruction for Use CytoFlex Platform*. 2021.
10. Wang, X.-S.; Song, H.; Liu, Y.-L.; Pan, X.-R.; Zhang, H.-C.; Gao, Z.; Kong, D.-Z.; Wang, R.; Wang, L.; Ma, J., Quantitively Analyzing the Variation of Micrometer-Sized Microplastic during Water Treatment with the Flow Cytometry-Fluorescent Beads Method. *ACS ES&T Engineering* **2021,** *1* (12), 1668-1677.
11. Kaile, N.; Lindivat, M.; Elio, J.; Thuestad, G.; Crowley, Q. G.; Hoell, I. A., Preliminary Results From Detection of Microplastics in Liquid Samples Using Flow Cytometry. *Frontiers in Marine Science* **2020,** *7* (856).
12. Al-Azzawi, M. S. M.; Kefer, S.; Weißer, J.; Reichel, J.; Schwaller, C.; Glas, K.; Knoop, O.; Drewes, J. E., Validation of Sample Preparation Methods for Microplastic Analysis in Wastewater Matrices—Reproducibility and Standardization. *Water* **2020,** *12* (9), 2445.
13. Hurley, R. R.; Lusher, A. L.; Olsen, M.; Nizzetto, L., Validation of a Method for Extracting Microplastics from Complex, Organic-Rich, Environmental Matrices. *Environmental Science & Technology* **2018,** *52* (13), 7409-7417.
14. Brandt, J.; Fischer, F.; Kanaki, E.; Enders, K.; Labrenz, M.; Fischer, D., Assessment of Subsampling Strategies in Microspectroscopy of Environmental Microplastic Samples. *Frontiers in Environmental Science* **2021,** *8*.
15. Huppertsberg, S.; Knepper, T. P., Instrumental analysis of microplastics—benefits and challenges. *Analytical and Bioanalytical Chemistry* **2018,** *410* (25), 6343-6352.

16. Schymanski, D.; Oßmann, B. E.; Benismail, N.; Boukerma, K.; Dallmann, G.; von der Esch, E.; Fischer, D.; Fischer, F.; Gilliland, D.; Glas, K.; Hofmann, T.; Käppler, A.; Lacorte, S.; Marco, J.; Rakwe, M. E. L.; Weisser, J.; Witzig, C.; Zumbülte, N.; Ivleva, N. P., Analysis of microplastics in drinking water and other clean water samples with micro-Raman and micro-infrared spectroscopy: minimum requirements and best practice guidelines. *Analytical and Bioanalytical Chemistry* **2021,** *413* (24), 5969-5994.

CHAPTER 6: SEASONAL TREND OF PLASTIC LOADS AT WASTEWATER TREATMENT PLANT

This chapter delves into the application of techniques introduced in Chapter 4 (semi-automated mapping mode of FTIR microspectroscopy) and Chapter 5 (flow cytometry). The primary objective is to assess the trends in plastic loads across different seasons.

Abstract

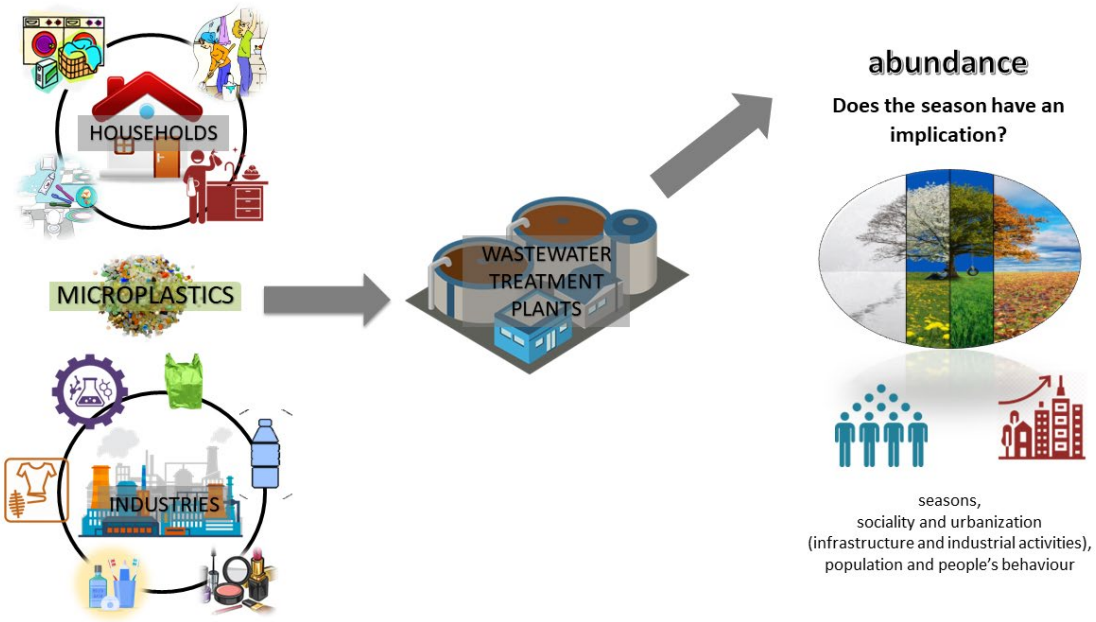

Figure 6-33. Graphical Abstract

While the presence of microplastics in wastewater treatment plants is well-known, their seasonal variations remain underexplored. This study seeked to enhance our understanding of the seasonal impact on microplastic abundance, particularly in the solid waste stream of a wastewater treatment plant. Samples, comprising influent, primary, secondary, digested, and dewatered sludges, were collected throughout 2021 and 2023, during spring, wet-winter, and dry-summer seasons. Employing digestion and density separation methods, microplastics were isolated, quantified, and identified using FTIR microspectroscopy for particles larger than 25 µm and Flow Cytometer for particles within the size ranges of 10-25 µm and 0.2-10 µm.

Results indicate that the wet-winter season (month of June with 3.6 mm average rainfall per day) exhibits the highest microplastic concentration, registering 9.06 x 10^{11} particles per kg of dried solid or 2.41 x 10^{16} particles per day. Spring (month of September with 1.4 mm rainfall) and summer (month of February with 0.6-0.7 mm rainfall) seasons follow in descending order. Approximately 84% of the microplastics over all the

seasons were within the 10-25 µm size range, particularly prevalent during the summer season. Particle identification was limited to particles larger than 25 µm because Flow Cytometry, the method used for particles smaller than 25 µm, is unable to identify polymer type. Polypropylene (PP) and polyvinyl chloride (PVC) as the most abundant plastic types across all seasons for the particle larger than 25 µm. Furthermore, polyethylene terephthalate (PET) and other polyesters (PEs) exhibited higher presence during winter, potentially linked to increased usage of winter clothes made from PEs and PET during this season.

Statistical analysis underscores a significant disparity in plastic loads among seasons at each sampling point, affirming the influence of seasons on microplastic abundance. Nevertheless, it is imperative to acknowledge the study's limitations, specifically the use of two different analytical instruments for particles larger than 25 µm and those within the range of 0.2-25 µm, potentially leading to incomparable data. Despite this, discernible trends provide valuable insights for wastewater treatment plants, aiding in the development of techniques and decision-making regarding microplastic treatment during varying seasons. Future research is recommended to explore spatial trends between different locations of wastewater treatment plant, providing a comprehensive understanding of population density and behaviour including residential, offices, and industries, in relation to microplastics abundance.

1 Introduction

Assessing seasonal changes that influence plastic loads in Wastewater Treatment Plants (WWTP) is crucial for gaining a better understanding of their drivers and sources.[1] This assessment can shed light on the density and behaviour of the population in different seasons. For instance, Browne et al (2011)[2] conducted a global study on microplastic accumulation on shorelines, revealing a higher influx of microfibers into WWTP during the winter season. These microfibers originated from winter garments such as fleece, blankets, shirts, and winter jackets, shed during laundry. Similarly, Xia et all (2021)[3] investigated microplastics in river sediments and found a slightly higher occurrence of microplastics in the size range of 50-500 µm at the end of the dry season (May) compared to the end of the rainy season (October). The rainy season facilitated the accumulation of smaller microplastics in sediment, with polyethylene constituting over 50% of the total microplastics.

Comprehensive information on seasonal variations' impact on plastic loads is essential for informing policymakers in their decision-making processes regarding regulations. For instance, the regulation around the management of stormwater. Additionally, presenting plastic load data in correlation with seasons and population can enhance the comparability of data between different locations and/or countries.[4] It is also crucial to consider precipitation rates when studying plastic loads, as they are linked to the pathways of plastic particles via atmospheric inputs, such as wind, runoff, and stormwater. Ideally, runoff and stormwater

are not treated at wastewater treatment facilities; however, during periods of significant rainfall, this practice may be modified based on operational requirements, as observed in June 2023 (internal data from SA Water).

This study specifically focusses on observing the seasonal impact on plastic loads at a local wastewater treatment plant, providing insights into population behaviour during specific seasons. Typically, the weather in South Australia consists of a hot and dry summer and a mild, wetter winter. The wastewater treatment plant serves a population of 160,185 customers, according to the latest figures for the financial year 2022/2023 (Internal SA Water data, 2023).

2 Materials and Methods

2.1 Sampling points, samples, and weather conditions

As detailed in Chapter 1 of this thesis, our study encompassed five distinct sampling points, namely influent, primary sedimentation, secondary sedimentation, digestion, and dewatering. Each sampling point was represented by a grab sample: 5 litres for influent, and 1 litre each of primary, secondary, digested, and dewatered sludges. These samples were systematically collected across three distinct seasons on four specific dates: 7th September 2021 (Spring season), 24th February 2022 (Summer season), 8th June 2022 (Winter season), and 8th February 2023 (Summer season). The corresponding weather conditions for each sampling date are presented in Table 6-15:

Table 6-15. Weather conditions during the sampling dates

Batch	Season	Sampling date	Average temperature (°C)	Rainfall (mm)	Relative humidity (%)	Wind speed (km/h)
One week weather history						
1	Spring	7th September 2021	15	1.3	67	15
2	Summer	24th February 2022	20	0.2	52	16
3	Winter	8th June 2022	13	7.2	78	15
4	Summer	8th February 2023	19	0.8	61	18
40 days weather history						
1	Spring	7th September 2021	13	1.4	70	16
2	Summer	24th February 2022	23	0.6	53	16
3	Winter	8th June 2022	15	3.6	72	13
4	Summer	8th February 2023	22	0.7	49	17

2.2 Sample processing and Data collection

The collected sludge samples underwent oven-drying, and the isolation of plastic particles followed established digestion and separation techniques adapted from Ziajahromi et.al. [5] The detailed procedure is

outlined in Chapter 4, except for influent samples. No wet peroxide oxidation step involving Fenton reaction (a mixture of 10 mL 0.05M $FeSO_4$ pH 3 and 20mL of 30% H_2O_2) was applied to the influent samples. Microplastics were isolated with a density separation procedure employing filtered ultrapure water and 4.5M NaI solution both three times. Subsequent to microplastics isolation, the process involved size fractionation. Isolated microplastics were initially filtered through a stainless-steel Hollander weave woven wire mesh (diameter 47 mm; 25 µm opening area). The filtrate then underwent further filtration through 10 µm polycarbonate (PC) membrane filters (diameter 47 mm) and subsequently through 0.2 µm ones (diameter 19 mm). The particles collected on the stainless-steel mesh dried at 40°C for 15 minutes. Meanwhile, the particles collected on the 10 µm and 0.2 µm PC membrane filters were suspended in 10 mL of TE Buffer. This resulted in three distinct microplastic size fractions: particles larger than 25 µm on the stainless-steel mesh for FTIR microspectroscopy analysis, particles in the size range of 10-25 µm and 0.2-10 µm in TE Buffer for Flow Cytometer analysis.

The data collection process using the semi-automated mapping mode of FTIR microspectroscopy was elucidated in Chapter 4 of this thesis. Regarding Flow Cytometry, 500 µL of each sample was transferred into a flow cytometry tube, with the addition of 10 µL of FITC green working bead suspension as a positive control. The instrument setting for Flow Cytometry were detailed in Chapter 5 of this thesis. The overall analysis process is illustrated in Figure 6-34.

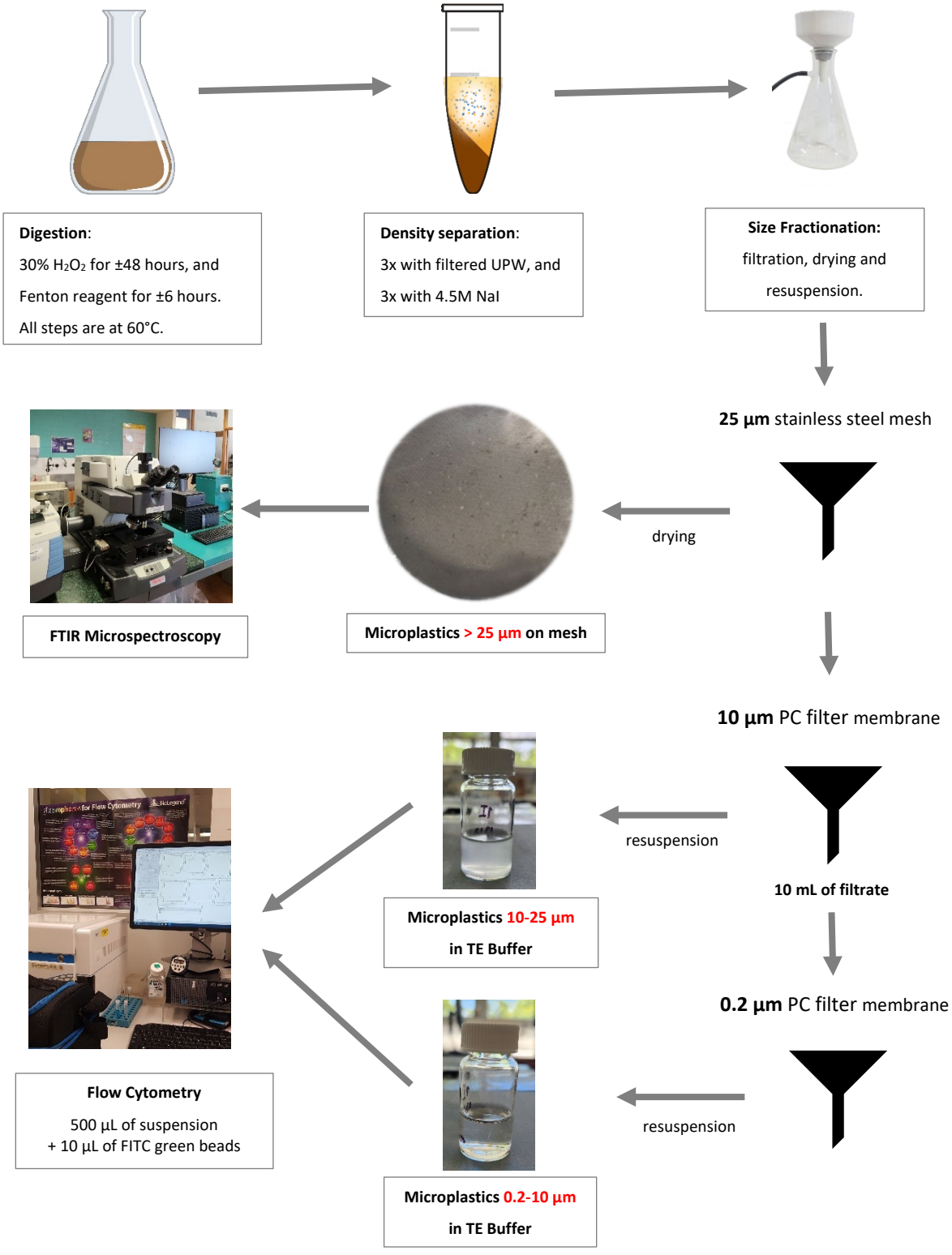

Figure 6-34. Analysis Flow Chart

2.3 Data processing

2.3.1 FTIR spectrum identification

To identify each collected IR spectrum, a thorough cross-referencing was conducted against multiple libraries, as detailed in Chapter 4 of this thesis. This identification process yielded crucial information regarding the types of plastic present, particularly for microplastics larger than 25 µm.

2.3.2 Flow Cytometry data processing

The counts of particles detected in each sample within the flow cytometry tube were extrapolated to determine the actual quantity of the analyzed sample.

2.3.3 Microplastics count

The number of particles for each sample was reported across three distinct size bins: >25 µm, 10-25 µm, and 0.2-10 µm. These counts were expressed both in number of particles per kg of dried samples and per day, calculated using the Total Solid and Flow Rate of each treatment at the respective sampling point. The approach ensures comprehensive reporting of microplastic data in relation to both the sample's mass and the daily rate, offering valuable insights into the variations across different size fractions.

Equation 1. Microplastics counts (particles/kg) in sludges

$$Microplastics\ counts\ (particles\ per\ kg) = \left(\frac{mesh\ area}{mapped\ area} \times\ particles\ on\ mapped\ area\right) \div (amount\ of\ tested\ sample\ \times 1000)$$

Equation 2. Microplastics loads (particles/day) in sludges

$$Microplastics\ loads\ (particles\ per\ day) = microplastics\ counts\ \div flow\ rate$$

The above formulas were used for sludge samples. For influent, Total Solid (%) was used for microplastics counts calculation as the following equation:

Equation 3. Microplastics counts (particles/kg) in influent

$$Microplastics\ counts\ (particles\ per\ kg) = \left(\left(\frac{mesh\ area}{mapped\ area} \times\ particles\ on\ mapped\ area\right) \div (amount\ of\ tested\ sample\ \times 1000)\right) \div Total\ Solid$$

, and for microplastics loads as follows:

Equation 4. Microplastics loads (particles/day) in influent

$$Microplastics\ loads\ (particles\ per\ day) = microplastics\ counts\ \times flow\ rate$$

The flow rate and total solid for each sampling point and sample were as follows:

Table 6-16. Flow rate and Total solid for each sampling point at different seasons

Samples	September 2021 (Spring)		February 2022 (Summer)		June 2022 (Winter)		February 2023 (Summer)	
	Total Solid (%)	Flow Rate	Total Solid (%)	Flow Rate	Total Solid (%)	Flow Rate	Total Solid (%)	Flow Rate
Sewage/Influent	0.1	34ML/d	0.1	31 ML/d	0.1	34 ML/d	0.03	31.5 ML/d
Primary Sludge/RST	2.3	238 kL/d	2.2	195 kL/d	2.2	248 kL/d	2.0	181kL/d
Secondary Sludge/DAFT	3.5	157 kL/d	3.2	140 kL/d	3.3	135 kL/d	3.27	151kL/d
Digested Sludge 1	1.5		1.5		1.5		1.49	
Digested Sludge 2	1.5	444 kL/d	1.5	360 kL/d	1.5	444 kL/d	1.48	316kL/d
Digested Sludge 3	1.5		1.5		1.5		1.36	
Dewatered/ Centrifuge Thickened Sludge	17.5	~30T/d	17.7	~30T/d	17.0	~30T/d	17.4	20.9T/d

2.3.4 Statistical analysis

A One-Way Multivariate Analysis of Variance (ANOVA) [6, 7] was conducted using IBS SPSS Statistics (version 28), employing seasons as the independent variable to compare the number of microplastics per size bin (>25 µm, 10-25 µm, 0.2-10 µm) as dependent variables. MANOVA was used because there was one independent variable (seasons) and more than one dependent variables (three size bins i.e., >25 µm, 10-25 µm, and 0.2-10 µm). This analysis was not applied within a season between sampling points due to the nature of grab samples, rendering them incomparable as they did not represent the actual timeframe of treatment processes. Consequently, a comparative analysis was performed for each type of sample across seasons.

2.4 Quality Control

Control samples, comprising both positive and negative controls, are indispensable for any analytical experiment, particularly in microplastics analysis. Positive controls, or spiked matrix samples, are essential to monitor the recovery rate of different types of polymers and sizes during isolation and identification techniques. Conversely, negative controls are crucial for detecting any background microplastics cross-contamination during samples collection and analysis. Ultrapure water was filtered through a 0.2 µm polyester filter, and stored in a glass jar, which was then left open either during sampling at the wastewater plant or during analysis in the laboratory. Plastic particles identified in negative controls were utilized to calculate the Limit of Detection (LOD=mean+3SD, the lowest concentration where detection is feasible) and

Limit of Quantification (LOQ=mean+10SD, values greater than LOQ have a higher likelihood of being true quantitative values and not random fluctuations of the blank). [8-11]

For this research, a total of five negative controls, each with three replicates (including both field and laboratory controls), were prepared and used to calculate LOD and LOQ. LOD was subtracted from microplastic count as a general baseline. It was not possible to use polymer-specific baselines due to statistical difficulties. This could be room for future studies. As for positive controls (spiked samples), seven different pure standard polymer references (PP, HDPE, LDPE, PS, PET, PMMA, and PVC) with particle size ranges between 25 µm and 1 mm were spiked into three different samples of dried sludge. Each dried sludge sample was spiked with 70, 49, and 25 total polymer particles, or 10, 7, and 5 particles of each type, respectively. All samples followed the same procedures as non-spiked samples mentioned in Section 2.2. Additionally, to minimize cross-contamination, plastic-related materials were avoided in all experimental procedures, such as using glass jars with metal lids or glass bottles with aluminium foil-covered lids for sample collection.

3 Results and Discussion

This section is organized into three sub-sections to present and discuss the plastic loads based on size, namely >25 µm and 0.2-25 µm, utilizing FTIR Microspectroscopy and Flow Cytometry, respectively. It also covers the overall size trend and the quality assurance/quality control (QA/QC) of the experiment. The overall statistics test results are presented in Appendix I of this thesis. The sampling documentation and some plastic particles images collected with stereomicroscope are given in Appendix A of this thesis.

3.1 Seasonal trend of microplastics >25 µm and 0.2-25 µm

3.1.1 Plastic counts per kg dried solid and loads per day of microplastics >25 µm.

The measurement of plastic particles > 25 µm involved the use of the semi-automated mapping mode of FTIR Microspectroscopy, with the resulting IR spectrum cross-referenced with the IR library database to determine polymer type. Figure 6-35 illustrates the microplastic counts per kg dried solid for each sample during different seasons. The influent showed the highest number ($84x10^6$ particles/kg dried solid) during winter 2022, followed by spring 2021 ($67x10^6$ particles/kg dried solid), summer 2023 ($38x10^6$ particles/kg dried solid), and summer 2022 ($6x10^6$ particles/kg dried solid). However, this trend did not align with subsequent treatments or sludge samples. The highest sludge microplastic counts were during spring 2021 for primary and digested sludges, winter 2022 for secondary sludge, and summer 2022 for dewatered sludge. Conversely, the lowest counts occurred during summer in 2022 for primary, secondary, and digested sludges and during spring 2021 and winter 2022 for dewatered sludge.

Statistical analysis, using one-way MANOVA, demonstrated a significant difference between seasons within each sampling point (F (15,3) = 10.745, p = 0.033; Wilk's λ = 0.000, partial η^2 = 0.974) (Table 6-17 and Table 6-18). Further examination via the test between-subjects effects (Table 6-19) revealed that seasons had a statistically significant effect on the number of microplastics in influent (F (3,5) = 8.658; p = 0.020; partial η^2 = 0.839), primary sludge (F (3,5) = 145.856; p <0.001; partial η^2 = 0.989), secondary sludge (F (3,5) = 13.008; p = 0.008; partial η^2 = 0.886), digested sludge (F (3,5) = 48.556; p <0.001; partial η^2 = 0.967), and dewatered sludge (F (3,5) = 13.804; p = 0.007; partial η^2 = 0.892). However, a Turkey post hoc test (Table 6-20) revealed specific instances of non-significant differences among seasons within each sampling point. For example, for the influent, there was no significant difference between spring 2021, winter 2022, summer 2022, and summer 2023. Primary sludge showed no significant difference between winter 2022 and summer 2023.

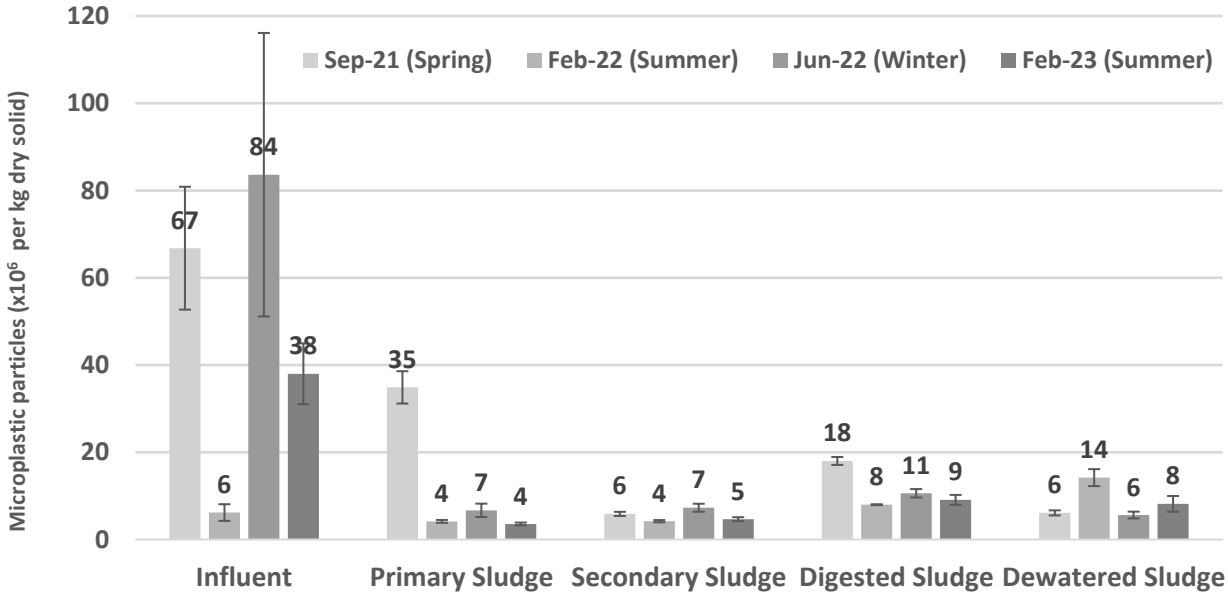

Figure 6-35. Microplastics size >25 µm per kg dried solid

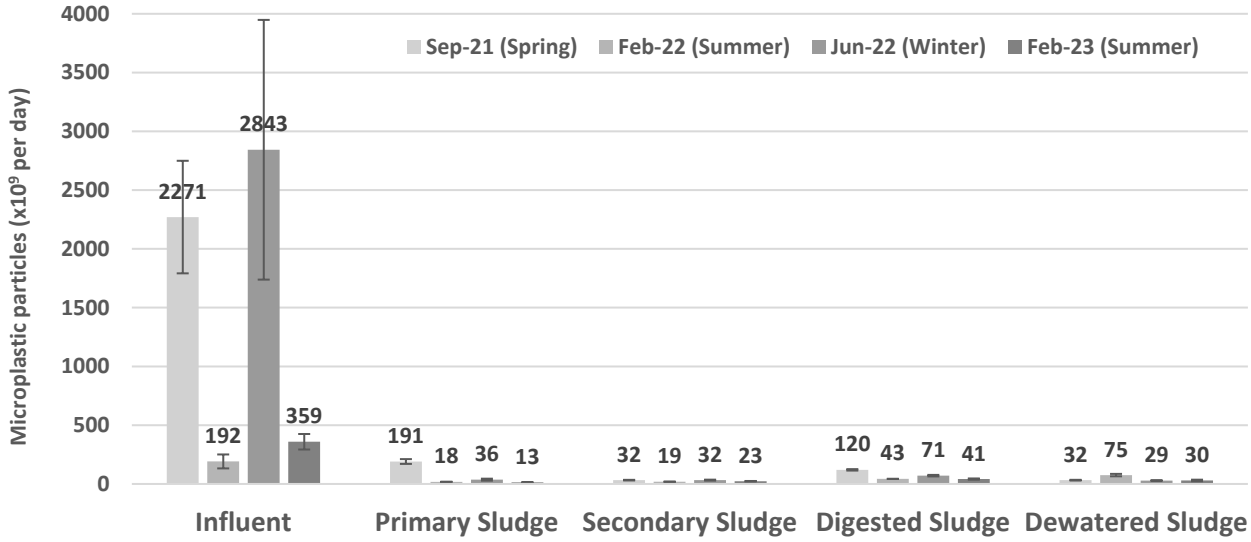

Figure 6-36. Microplastics size >25 µm load per day

Considering the flow rate during sampling, plastic loads per day per sampling point mirrored the microplastic counts per kg dried solid trend (Figure 6-36). Winter 2022 posed the highest plastic loads for influent (2.84 x 10^{12} particles per day) and secondary sludge (3.24 x 10^{10} particles per day), while spring 2021 did so for primary (1.91 x 10^{11} particles per day) and digested (1.20 x 10^{11} particles per day) sludges. Exceptionally, summer 2022 had the highest plastic loads for dewatered sludge (7.5 x 10^{10} particles per day). The lowest plastic loads were dominated by summer 2022 and summer 2023 for all sampling points, except for dewatered sludge (2.9 x 10^{10} particles per day), where winter 2022 had the lowest loads.

Statistical analysis for plastic loads per day, akin to per kg dried solid, revealed a significant difference between seasons within each sampling point ($F(15,3) = 15.271$, $p = 0.019$; Wilk's $\lambda = 0.000$, partial $\eta^2 = 0.981$) (Table 6-17 and Table 6-18). The test of between-subjects effects (Table 6-19) showed that seasons had statistically significant effect on plastic loads in influent ($F(3,5) = 13.407$; $p = 0.008$; partial $\eta^2 = 0.889$). Similarly, statistically significant effects of seasons on plastic loads were found in primary sludge ($F(3,5) = 155.774$; $p < 0.001$; partial $\eta^2 = 0.989$), secondary sludge ($F(3,5) = 13.839$; $p = 0.007$; partial $\eta^2 = 0.893$), digested sludge ($F(3,5) = 109.250$; $p < 0.001$; partial $\eta^2 = 0.985$), and dewatered sludge ($F(3,5) = 24.407$; $p = 0.002$; partial $\eta^2 = 0.936$). Subsequent multiple comparisons tests (Table 6-20) indicated specific instances of no significant differences among seasons within each sampling point. For example, primary sludges had no significant difference in plastic loads between summer 2022, winter 2022, and summer 2023. For secondary sludge, no significant difference was found between spring 2021 and winter 2022, and between summer 2022 and summer 2023. Digested sludges only between summer 2022 and summer 2023 showed no

significant difference, and dewatered sludges had no significant difference between spring 2021, winter 2022, and summer 2023.

3.1.2 Plastic counts per kg dried solid and loads per day of microplastics 0.2-25 µm.

For plastic particles sized 0.2-25 µm (Figure 6-37), influent samples during winter 2022 (667x10^9 particles/kg dried solid) exhibited the highest number, followed by spring 2021 (384x10^9 particles/kg dried solid), summer 2023 (349x10^9 particles/kg dried solid), and summer 2022 (87x10^9 particles/kg dried solid). However, the trend diverged in subsequent treatment stages. Primary sludge recorded the highest counts during summer 2022, secondary sludge during summer 2023, and digested sludge during winter 2022. Dewatered sludge displayed the highest counts during summer 2022. Similar to >25 µm plastic counts, summer 2022 and 2023 generally exhibited lower counts for all sampling points, except for digested sludge in spring 2021.

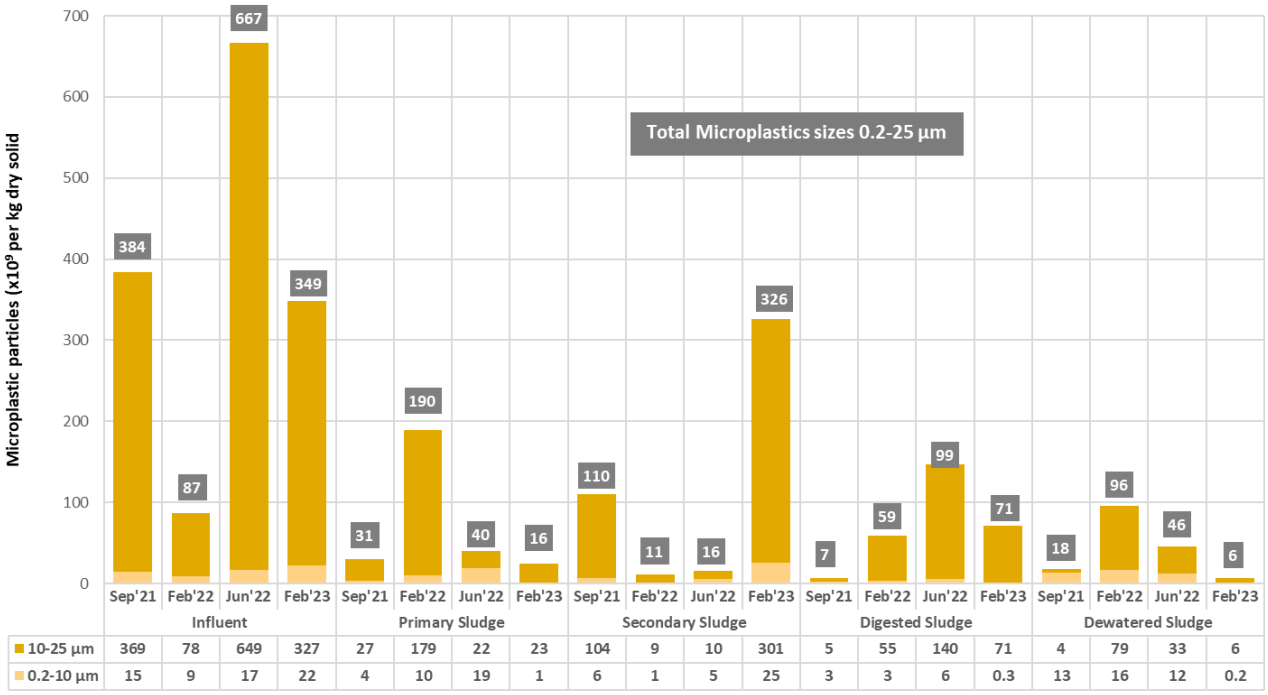

Figure 6-37. Microplastics size 0.2-25 µm per kg dried solid

Plastic loads per day mirrored the counts per kg dried solid trend (Figure 6-38). Winter 2022 showed the highest plastic loads for influent (2.27 x 10^{16} particles per day) and digested sludge (6.62 x 10^{14} particles per day), during summer 2022 for primary sludge (8.14 x 10^{14} particles per day) and dewatered sludge (5.07 x 10^{14} particles per day), and summer 2023 for secondary sludge (1.61 x 10^{15} particles per day). Slightly different for the lowest plastic loads, in which were during summer 2022 in influent (2.692 x 10^{15} particles per day), summer 2023 in primary sludge (5.9 x 10^{13} particles per day) and dewatered sludge (2.3 x 10^{13} particles per day), summer 2022 in secondary sludge (4.8 x 10^{13} particles per day), and spring 2021 in digested sludge (4.8 x 10^{13} particles per day).

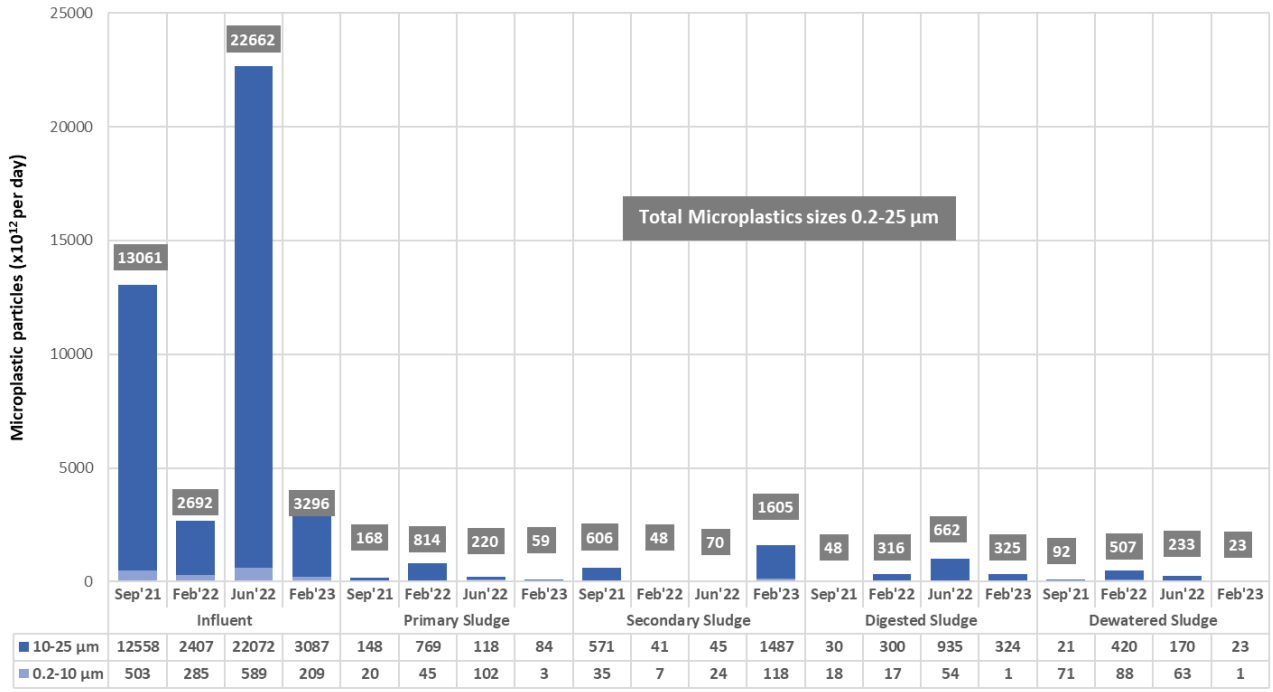

Figure 6-38. Microplastics size 0.2-25 µm load per day

For number of microplastics per kg dried solid for size bin 10-25 µm, there was a statistically significant difference between seasons (Table 6-17 and Table 6-18) within a sampling point as determined by one-way MANOVA ($F(12,3) = 16.200$, $p = 0.022$; Wilk's $\lambda = 0.000$, partial $\eta^2 = 0.976$). Similar results for plastic loads per day for the same size bin ($F(12,3) = 13.493$, $p = 0.029$; Wilk's $\lambda = 0.000$, partial $\eta^2 = 0.971$).

For number of microplastics per kg dried solid for size bin 0.2-10 µm, there was also a statistically significant difference between seasons (Table 6-17 and Table 6-18) within a sampling point as determined by one-way MANOVA ($F(12,3) = 9.309$, $p = 0.048$; Wilk's $\lambda = 0.000$, partial $\eta^2 = 0.961$). For plastic loads per day for the same size bin, it indicated that there was a significant difference between seasons ($F(12,3) = 11.028$; $p = 0.038$; Wilk's $\lambda = 0.000$) within the same sampling point. Moreover, seasons had a large influence on plastic loads within sample based on the partial eta squared (partial $\eta^2 = 0.966$) calculation.

Further test for both size bin 10-25 µm and 0.2-10 µm as shown in Table 6-19, indicating that for microplastics seasons has no significant effect on microplastic counts and plastic loads per day in influent and dewatered sludge.

Table 6-17. Multivariate ANOVA (MANOVA) test results summary

Size bin_unit	Wilks' Lambda value	F	Hypothesis df	Error df	Sig./p-value	Partial Eta Squared (η^2)
25 µm_per kg dried solid	0.000	10.745	15.000	3.162	0.033	0.974
25 µm_per day	0.000	15.271	15.000	3.162	0.019	0.981
10-25 µm_per kg dried solid	0.000	16.200	12.000	2.937	0.022	0.976
10-25 µm_per day	0.000	13.493	12.000	2.937	0.029	0.971
0.2-10 µm_per kg dried solid	0.000	9.309	12.000	2.937	0.048	0.961
0.2-10 µm_per day	0.000	11.028	12.000	2.937	0.038	0.966

Table 6-18. MANOVA test results interpretation

Size bin_unit	Wilks' Lambda *	Sig./p-value**	Partial Eta Squared (η^2)***
25 µm_per kg dried solid	Large	YES	Large
25 µm_per day	Large	YES	Large
10-25 µm_per kg dried solid	Large	YES	Large
10-25 µm_per day	Large	YES	Large
0.2-10 µm_per kg dried solid	Large	YES	Large
0.2-10 µm_per day	Large	YES	Large

*Large/Small = large/small **difference** between seasons (independent variable) within sample or sampling point (dependent variable)

** YES/NO = yes/no **significant difference** between seasons within sample or sampling point

*** Large/Small = seasons had a large/small **influence** on number of microplastics within sample or sampling point (dependent variable)

Table 6-19. MANOVA-Test of Between-Subjects Effects

Size bin_unit	Sample	F	Hypothesis df	Error df	Sig./p-value	Partial Eta Squared (η^2)
25 µm_per kg dried solid	Influent	8.658	3	5	0.020	0.839
	Primary	145.856	3	5	<0.001	0.989
	Secondary	13.008	3	5	0.008	0.886
	Digested	48.556	3	5	<0.001	0.967
	Dewatered	13.804	3	5	0.007	0.892
25 µm_per day	**Influent**	**1.304**	**3**	**5**	**0.370**	**0.439**

Size bin_unit	Sample	F	Hypothesis df	Error df	Sig./p-value	Partial Eta Squared (η^2)
	Primary	155.774	3	5	<0.001	0.989
	Secondary	13.839	3	5	0.007	0.893
	Digested	109.250	3	5	<0.001	0.985
	Dewatered	24.407	3	5	0.002	0.936
10-25 µm_per kg dried solid	**Influent**	**2.964**	**3**	**4**	**0.161**	**0.690**
	Primary	11.034	3	4	0.021	0.892
	Secondary	**6.843**	**3**	**4**	**0.047**	**0.837**
	Digested	55.684	3	4	0.001	0.977
	Dewatered	**4.037**	**3**	**4**	**0.106**	**0.752**
10-25 µm_per day	**Influent**	**4.261**	**3**	**4**	**0.098**	**0.762**
	Primary	10.533	3	4	0.023	0.888
	Secondary	**6.763**	**3**	**4**	**0.048**	**0.835**
	Digested	84.502	3	4	<0.001	0.984
	Dewatered	**4.248**	**3**	**4**	**0.098**	**0.761**
0.2-10 µm_per kg dried solid	**Influent**	**2.826**	**3**	**4**	**0.171**	**0.679**
	Primary	13.039	3	4	0.016	0.907
	Secondary	9.491	3	4	0.027	0.877
	Digested	104.626	3	4	<0.001	0.987
	Dewatered	10.939	3	4	0.021	0.891
0.2-10 µm_per day	**Influent**	**1.352**	**3**	**4**	**0.377**	**0.504**
	Primary	**6.391**	**3**	**4**	**0.053**	**0.827**
	Secondary	**5.531**	**3**	**4**	**0.066**	**0.806**
	Digested	**0.826**	**3**	**4**	**0.544**	**0.382**
	Dewatered	**1.606**	**3**	**4**	**0.321**	**0.546**

Table 6-20. MANOVA-Multiple Comparison-Turkey HSD

Size bin_unit	Overall p-value	Sample	Multiple comparison (Exceptional than overall p-value/ showed NO significant difference) seasons	p-value
25 µm_per kg dried solid	<0.001	Influent	Spring 2021 vs Winter 2022	0.945
			Spring 2021 vs Summer 2023	0.751
			Summer 2022 vs Winter 2022	0.063
			Summer 2023 vs Winter 2022	0.454
		Primary	Summer 2023 vs Winter 2022	0.375

Size bin_unit	Overall p-value	Sample	Multiple comparison (Exceptional than overall p-value/ showed NO significant difference) seasons	p-value
		Secondary	Spring 2021 vs Winter 2022	0.347
			Spring 2021 vs Summer 2023	0.387
		Digested	Winter 2022 vs Summer 2023	0.410
		Dewatered	Spring 2021 vs Winter 2022	1.000
			Spring 2021 vs Summer 2023	0.962
25 µm_per day	0.012	Influent	Spring 2021 vs Summer 2022	0.459
			Spring 2021 vs Winter 2022	0.465
			Spring 2021 vs Summer 2023	0.394
			Summer 2022 vs Winter 2022	1.000
			Summer 2022 vs Summer 2023	1.000
			Winter 2022 vs Summer 2023	1.000
		Primary	Summer 2022 vs Winter 2022	0.338
			Summer 2022 vs Summer 2023	0.944
			Summer 2023 vs Winter 2022	0.153
		Secondary	Spring 2021 vs Winter 2022	1.000
			Summer 2022 vs Summer 2023	0.396
		Digested	Summer 2022 vs Summer 2023	0.983
		Dewatered	Spring 2021 vs Winter 2022	0.951
			Spring 2021 vs Summer 2023	0.978
			Winter 2022 vs Summer 2023	0.998
10-25 µm_per kg dried solid	0.021	Influent	Spring 2021 vs Summer 2022	0.549
			Spring 2021 vs Winter 2022	0.577
			Spring 2021 vs Summer 2023	0.814
			Summer 2022 vs Winter 2022	0.151
			Summer 2022 vs Summer 2023	0.945
			Winter 2022 vs Summer 2023	0.253
		Primary	Spring 2021 vs Winter 2022	0.998
			Spring 2021 vs Summer 2023	0.993
			Winter 2022 vs Summer 2023	0.972
		Secondary	Spring 2021 vs Summer 2022	0.621
			Spring 2021 vs Winter 2022	0.627
			Spring 2021 vs Summer 2023	0.171
			Summer 2022 vs Winter 2022	1.000
			Summer 2022 vs Summer 2023	0.056
			Winter 2022 vs Summer 2023	0.057
		Digested	Summer 2022 vs Summer 2023	0.530
		Dewatered	Spring 2021 vs Summer 2022	0.120
			Spring 2021 vs Winter 2022	0.663
			Spring 2021 vs Summer 2023	1.000

Size bin_unit	Overall p-value	Sample	Multiple comparison (Exceptional than overall p-value/ showed NO significant difference) seasons	p-value
			Summer 2022 vs Winter 2022	0.371
			Summer 2022 vs Summer 2023	0.127
			Winter 2022 vs Summer 2023	0.698
10-25 µm_per day	0.026	Influent	Spring 2021 vs Summer 2022	0.495
			Spring 2021 vs Winter 2022	0.539
			Spring 2021 vs Summer 2023	0.453
			Summer 2022 vs Winter 2022	0.126
			Summer 2022 vs Summer 2023	1.000
			Winter 2022 vs Summer 2023	0.116
		Primary	Spring 2021 vs Winter 2022	0.996
			Spring 2021 vs Summer 2023	0.999
			Winter 2022 vs Summer 2023	1.000
		Secondary	Spring 2021 vs Summer 2022	0.546
			Spring 2021 vs Winter 2022	0.551
			Spring 2021 vs Summer 2023	0.204
			Summer 2022 vs Winter 2022	1.000
			Summer 2022 vs Summer 2023	0.057
			Winter 2022 vs Summer 2023	0.058
		Digested	Summer 2022 vs Summer 2023	0.973
		Dewatered	Spring 2021 vs Summer 2022	0.115
			Spring 2021 vs Winter 2022	0.681
			Spring 2021 vs Summer 2023	1.000
			Summer 2022 vs Winter 2022	0.344
			Summer 2022 vs Summer 2023	0.115
			Winter 2022 vs Summer 2023	0.680
0.2-10 µm_per kg dried solid	0.007	Influent	Spring 2021 vs Summer 2022	0.518
			Spring 2021 vs Winter 2022	0.552
			Spring 2021 vs Summer 2023	0.998
			Summer 2022 vs Winter 2022	0.136
			Summer 2022 vs Summer 2023	0.602
			Winter 2022 vs Summer 2023	0.472
		Primary	Spring 2021 vs Winter 2022	0.987
			Spring 2021 vs Summer 2023	0.998
			Winter 2022 vs Summer 2023	0.999
		Secondary	Spring 2021 vs Summer 2022	0.528
			Spring 2021 vs Winter 2022	0.562
			Spring 2021 vs Summer 2023	0.105
			Summer 2022 vs Winter 2022	1.000
		Digested	Summer 2022 vs Summer 2023	0.468

Size bin_unit	Overall p-value	Sample	Multiple comparison (Exceptional than overall p-value/ showed NO significant difference) seasons	p-value
		Dewatered	Spring 2021 vs Winter 2022	0.447
			Spring 2021 vs Summer 2023	0.902
			Summer 2022 vs Winter 2022	0.134
			Summer 2023 vs Winter 2022	0.235
0.2-10 µm_per day	0.076		All showed significant difference	

3.1.3 Overall microplastics seasonal trend and statistical analysis

The overall seasonal trend of microplastics, categorized by size bin and unit quantification, is summarized in Table 6-21. A discernible pattern emerged, indicating varying microplastic counts during specific seasons. For instance, the counts were notably higher during winter for influent and digested sludge, while reaching their lowest in summer and spring for primary, secondary, and dewatered sludges. Contrary to the general trend, an intriguing observation surfaced in the case of secondary sludges during the summer seasons spanning 2022 and 2023. While these sludges exhibited the lowest microplastic counts in summer 2022, they registered a peak in summer 2023. However, by observing the overall sampling points, this nuanced fluctuation challenges the anticipated decline in microplastics during summer. Both data for summer season were collected in 2022 and 2023, and from both years it was observed lowest number of microplastics among other seasons. It is crucial to acknowledge a temporal constraint on this research, which precluded further comparisons across seasons, specifically during winter and spring in different years. This limitation underscores the necessity for caution when extrapolating trends and underscores the potential influence of temporal and contextual factors that may vary across study years.

Table 6-21. Summary seasonal trend of microplastics per size bin and unit quantification

Size bin_unit	Influent		Primary		Secondary		Digested		Dewatered	
	↑	↓	↑	↓	↑	↓	↑	↓	↑	↓
25 um per kg	Winter 22	Summer 22	Spring 21	Summer 22 & 23	Winter 22	Summer 22	Spring 21	Summer 22	Summer 22	Winter 22
25 um per day	Winter 22	Summer 22	Spring 21	Summer 23	Winter 22	Summer 22	Spring 21	Summer 23	Summer 22	Winter 22
10 um per kg	Winter 22	Summer 22	Summer 22	Winter 22	Summer 23	Summer 22	Winter 22	Spring 21	Summer 22	Spring 21
10 um per day	Summer 22	Spring 21	Summer 22	Summer 23	Summer 23	Summer 22	Winter 22	Spring 21	Summer 22	Spring 21
0.2 um per kg	Summer 23	Summer 22	Winter 22	Summer 23	Summer 23	Summer 22	Winter 22	Spring 21	Summer 22	Spring 21
0.2 um per day	Winter 22	Summer 23	Winter 22	Summer 23	Summer 23	Summer 22	Winter 22	Summer 23	Summer 22	Summer 23

↑ : highest ↓ : lowest

The results pertaining to microplastic counts, specifically within size ranges >25 µm and within the range of 0.2-25 µm, reveal an absence of discernible trends or consistent patterns in seasonal plastic loads. However, a deeper examination through statistical analysis, specifically employing the one-way MANOVA as detailed in Table 6-17 and Table 6-18, exposes a significant disparity in microplastics quantities across seasons within the same sampling point. This observation implies that seasons exert a discernible influent on the overall microplastic levels, underscoring the dynamic nature of these pollutants in response to temporal variations.

3.1.4 Type of plastics for microplastics size > 25 µm

The identification of microplastic types was constrained to particles >25 µm. Figure 6-39 illustrates the predominant plastics across each sampling point throughout various seasons, with polypropylene (PP) consistently dominating all samples across different seasons. In the case of sludge samples, polyvinyl chloride (PVC) took precedence, followed by ethyl vinyl acetate (EVA), polyethylene terephthalate (PET), polyurethane (PUR), rubber, and other polyesters (PEs). Notably, polyester was absent in all influent samples, surfacing only during the summer seasons of 2022 and 2023. This discrepancy may be attributed to the limitations of grab sampling, which may not fully capture the entirety of influent entering the wastewater treatment plant. It is also noteworthy that PVC was consistently present in all samples, likely originating from the material composition of the pipes used in the wastewater treatment plant.[1] The preliminary analysis conducted using Py-GCMS identified the presence of various types of plastics, including polyethylene (PE), polypropylene (PP), polyester, polyvinyl chloride (PVC), polystyrene, and polyacrylonitrile. These findings are consistent with the 2019 plastic consumption trends in Australia, which were predominantly composed of PP, PE, PVC, and polyethylene terephthalate (PET).[12]

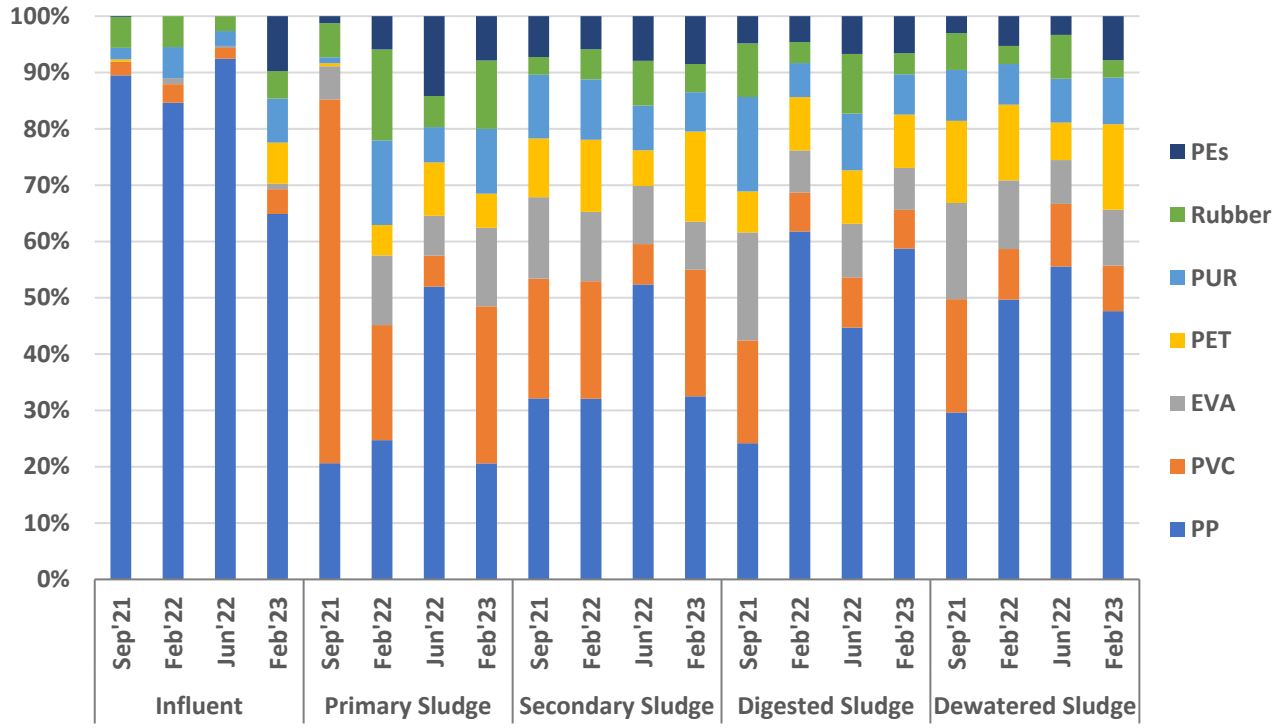

Figure 6-39. Type of plastics for particles >25 µm proportionally per sampling point at different seasons

If we postulate that PET and other polyesters primarily exist in the form of fibers originating from winter clothing, their dominance during the winter in primary sludge, at 24% and 9%, respectively, becomes apparent. This prevalence suggests a propensity for these polymers to settle during the primary sedimentation treatment, given their higher density compared to other plastic types. However, it is crucial to acknowledge that these dynamics are contingent on the size and shape of the particles in question. This study faces limitations in comparing plastic types across sampling points due to the use of grab samples, which do not reflect the actual treatment timeline or period. For instance, the secondary sedimentation process typically spans around ten days, whereas the samples in this study were uniformly collected on the same day across all sampling points. A more in-depth exploration of treatment effects on plastic load is presented in Chapter 7 in this thesis.

3.2 Size trend

Microplastics exhibit a tendency to undergo fragmentation into smaller particles when exposed to various environmental conditions such as UV light, additives and water exposure.[13, 14] Therefore, in this study, we conducted an analysis of samples within three distinct size fractions: >25 µm, 10-25 µm, and 0.2-10 µm. As depicted in Figure 6-40, the overall size distribution of microplastics at the wastewater treatment plant was predominantly characterized by particles in the 10-25 µm (83.72%), followed by 0.2-10 µm (16.24%), and >25 µm (0.04%). Examining seasonal variations, Figure 6-41 reveals that during both the summers of 2022 and

2023, a higher proportion of microplastics in the 10-25 µm size range was evident compared to spring and winter. This observation may be attributed to prolonged exposure to UV sunlight, rendering polymer particles more susceptible to physical or chemical processes during wastewater treatment. It is essential to highlight that different analytical techniques were employed for measurement, specifically FTIR for >25 µm and Flow Cytometer for 0.2-25 µm.

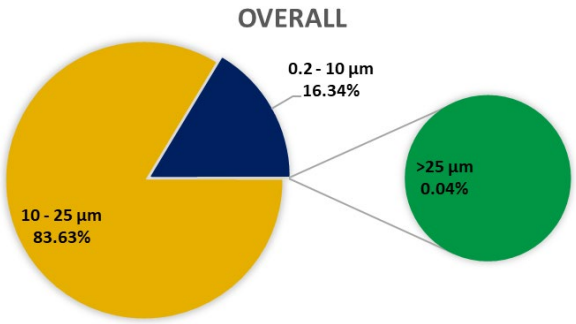

Figure 6-40. Overall size trend

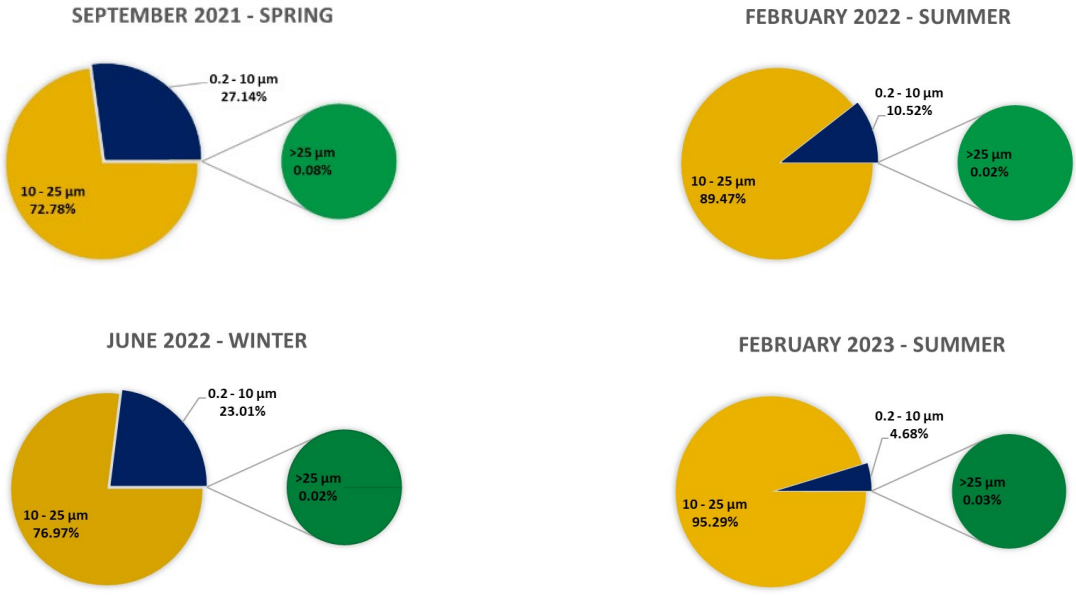

Figure 6-41. Size trend per season

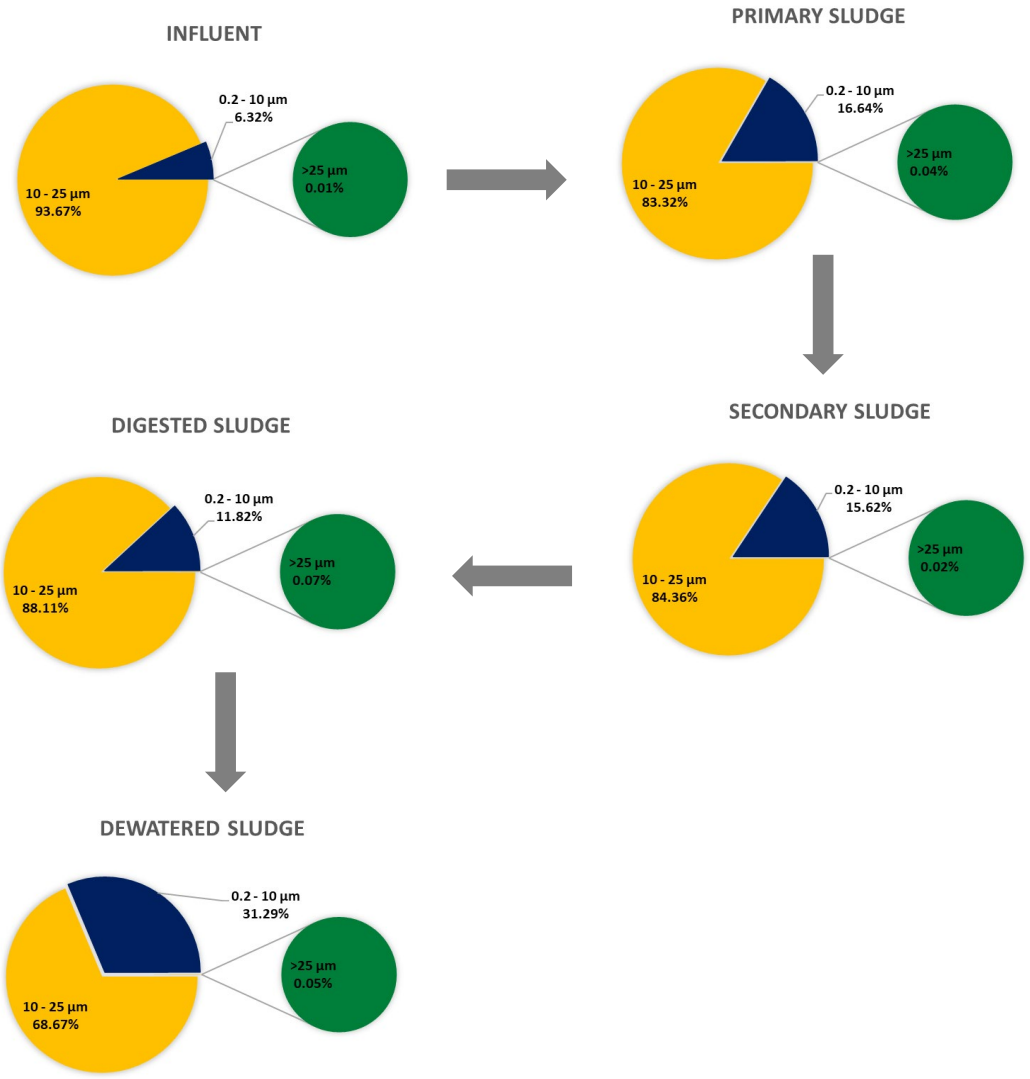

Figure 6-42. Size trend per sampling point

Upon scrutinizing individual sampling points representing distinct treatment stages, as illustrated in Figure 6-42, the proportion of microplastics in the 0.2-10 µm size range exhibited an increase from influent to dewatering processes. Despite the grab sampling technique employed in this study, it is plausible that the treatment processes at the wastewater plant contribute to the fragmentation of microplastics. Comprehensive investigations regarding the treatment effects on microplastics at the wastewater plant are expounded upon in Chapter 7 of this thesis.

3.3 QA/QC

3.3.1 LOD and LOQ

Blank samples, serving as negative field and laboratory controls, played a crucial role in determining the Limit of Detection (LOD) and Limit of Quantification (LOQ) in this study, serving as a quality control measure.

The values for LOD and LOQ for each size fraction are detailed in Table 6-22. The LOD for the size fraction >25 µm was subtracted from the number of identified microplastics in each tested sample, resulting in all final data surpassing its LOQ. This implies that the quantitative values of microplastics size >25 µm derived from the samples were genuine, representing an accurate reflection of the sample content rather than potential contamination from the environment, such as air, sampling tools, or laboratory glassware. However, this approach was not applied to microplastics size 0.2-25 µm due to not all data exceeding the LOD. On average, only approximately 61% and 32% of all data met the minimum LOQ for the 10-25 µm and 0.2-10 µm size bins, respectively. This suggests the possibility of reported data being subject to cross-contamination from the environment during sampling and/or analysis. Further validation of the Flow Cytometry technique is deemed necessary, as elaborated in Chapter 5 of this thesis.

Table 6-22. LOD and LOQ of each analytical technique per size bin

Methods	Size fraction	LOD (particles/tested sample)	LOQ (particles/tested sample)
FTIR	>25 µm	102	311
Flow Cytometry	10-25 µm	2.25×10^{6}	6.34×10^{6}
	0.2-10 µm	6.51×10^{6}	1.80×10^{7}

3.3.2 Recovery rates

Plastic particles introduced into the samples were successfully recovered and subjected to visual examination under a stereomicroscopy, as pictured in Figure 6-43. Subsequently, 20% of these particles underwent analysis using FTIR microspectroscopy, with a confirmation rate of over 65% for the original polymer type, as depicted in Figure 6-44. The comprehensive recovery rate achieved was 96%, with individual recovery rates for samples spiked with 70, 49, and 35 plastic particles standing at 94%, 96%, and 97%, respectively. A more detailed experiment result is presented in Appendix D of this thesis.

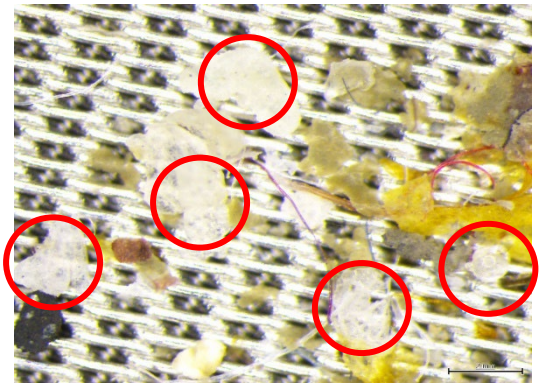

Figure 6-43. Stereomicroscope image of spiked standard reference polymers

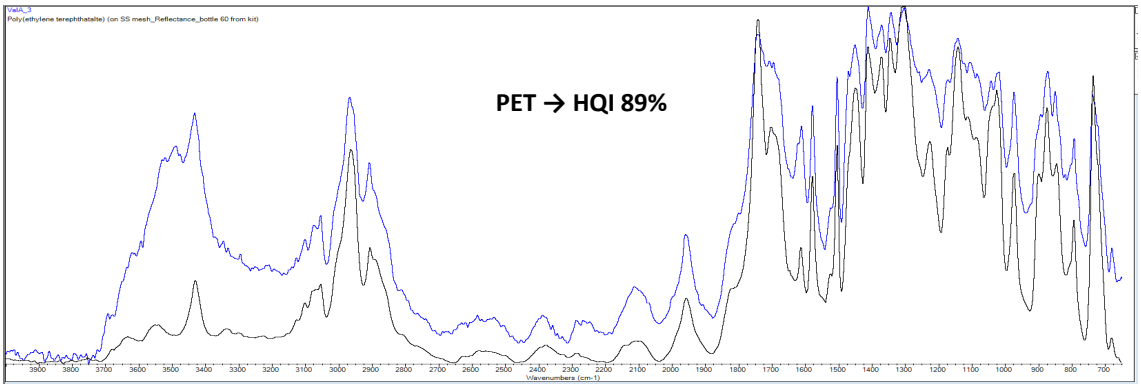

Figure 6-44. Polyethylene terephthalate (PET) IR spectra before (black spectra) and after (blue spectra) digestion or pretreatment procedure

4 Conclusions and Recommendations

Fulfilling the specific aim of this study to observe the influence of seasons on plastic loads at the wastewater treatment plant, it can be concluded that the wet-winter season (9.06 x 10^{11} particles per kg dried solid) exhibited a higher number of microplastics compared to the spring season (5.50 x 10^{11} particles per kg dried solid) and the dry-summer season (4.41 x 10^{11} particles per kg dried solid in 2022, and 7.04 x 10^{11} particles per kg dried solid in 2023). The statistical analysis confirmed a significant difference between seasons within the sampling points, emphasizing the implications of seasonality on plastic loads.

The majority of microplastics measured fell within the 10-25 µm range (83.65%), followed by 0.2-10 µm (16.34%) and >25 µm (0.04%). During summer, a higher proportion of microplastics in the size range of 10-25 µm was observed compared to spring and winter. Furthermore, the treatment processes appeared to contribute to the fragmentation of microplastics into smaller particles, particularly during summer. Prolonged exposure to UV light and slower flow rates during the drier summer months may render the particles more susceptible to physical and chemical treatments.[14] Previous studies have also found a significant number of microplastics in the size fraction of 10-25 µm; however, we acknowledge the limitations of the technique employed, specifically when using two different methods, such as FTIR and Flow Cytometry.

The study refrained from comparing the number of microplastics within seasons between sampling points or treatments due to the grab sampling technique, which does not accurately represent the entire treatment process's timeline. Consequently, a subsequent study was conducted to examine the treatment effects on plastic loads, as detailed in Chapter 7 of this thesis. Preliminary findings revealed that approximately 31% of

the total microplastics entering the wastewater plant were retained in the dewatered sludge, with size distribution of 68.67%, 31.29%, and 0.05% for 10-25 µm, 0.2-10 µm, and >25 µm.

Microplastics larger than 25 µm were predominantly composed of polypropylene (PP) and polyvinyl chloride (PVC), followed by ethyl vinyl acetate (EVA), polyethylene terephthalate (PET), polyurethane (PUR), rubber, and other polyesters (PEs). Seasonal variations were observed, with winter receiving more PET (9%) and/or other PEs (14%) fibers, while summer exhibited higher concentrations of PUR (13%) and rubber (14%) than winter and spring. This highlights the seasonal influence on the types of plastics entering the wastewater treatment plant, including acrylonitrile butadiene styrene (ABS), polystyrene (PS), polyacrylonitrile (PAN) copolymer, synthetic cellulose, polyethylene (PE), polyamide (PA), and polymethyl methacrylate (PMMA).

However, it is crucial to acknowledge certain limitations of this study, particularly the use of different techniques for enumerating plastic particles (>25 µm using FTIR Microspectroscopy and 0.2-25 µm using Flow Cytometry). While FTIR microspectroscopy is restricted to particles of 20 or 25 µm, flow cytometry provides a broader range from 0.2 µm to 100 µm (recommended upper limit of the instrument). It is worth noting that while FTIR Microspectroscopy relies on human identification and counting, flow cytometry minimized this reliance through automatic detection and counting, thereby reducing potential sources of error and bias. Nevertheless, flow cytometry cannot analyse particles larger than 100 µm to mm size, as achievable with FTIR Microspectroscopy. The flow cytometry technique requires further optimization and validation, as discussed in Chapter 5 of this thesis, owing to sample size constraints.

Applying the same techniques for different complex environmental samples requires modifications in the sample pretreatment or preparation steps to ensure that the isolated particles are predominantly microplastics. This necessitates a validation procedure to achieve at least an 80% recovery rate.

Recommendations for future studies include exploring different locations of wastewater treatment plants or conducting spatial trend studies. Such investigations could complement seasonal trend data, offering insights into the correlation between plastic loads and population density, as well as their behaviour across different seasons. These findings are valuable for aiding companies in developing effective techniques and decision-making regarding microplastic treatment at wastewater plants, particularly considering seasonal variations.

References

1. Okoffo, E. D.; O'Brien, S.; O'Brien, J. W.; Tscharke, B. J.; Thomas, K. V., Wastewater treatment plants as a source of plastics in the environment: a review of occurrence, methods for identification, quantification and fate. *Environmental Science: Water Research & Technology* **2019,** *5* (11), 1908-1931.
2. Browne, M. A.; Crump, P.; Niven, S. J.; Teuten, E.; Tonkin, A.; Galloway, T.; Thompson, R., Accumulation of Microplastic on Shorelines Woldwide: Sources and Sinks. *Environmental Science & Technology* **2011,** *45* (21), 9175-9179.
3. Xia, F.; Yao, Q.; Zhang, J.; Wang, D., Effects of seasonal variation and resuspension on microplastics in river sediments. *Environmental Pollution* **2021,** *286*.

4. Alexy, P.; Anklam, E.; Emans, T.; Furfari, A.; Galgani, F.; Hanke, G.; Koelmans, A.; Pant, R.; Saveyn, H.; Sokull Kluettgen, B., Managing the analytical challenges related to micro- and nanoplastics in the environment and food: filling the knowledge gaps. *Food Additives & Contaminants: Part A* **2020,** *37* (1), 1-10.
5. Ziajahromi, S.; Neale, P. A.; Telles Silveira, I.; Chua, A.; Leusch, F. D. L., An audit of microplastic abundance throughout three Australian wastewater treatment plants. *Chemosphere* **2021,** *263*, 128294.
6. Bray, J. H.; Maxwell, S. E., *Multivariate analysis of variance*. Sage Publications: Beverly Hills, 1985.
7. Crichton, N., Wilks' lambda. *Journal of clinical nursing* **2000,** *9*, 369-381.
8. Armbruster, D. A.; Tillman, M. D.; Hubbs, L. M., Limit of detection (LQD)/limit of quantitation (LOQ): comparison of the empirical and the statistical methods exemplified with GC-MS assays of abused drugs. *Clinical Chemistry* **1994,** *40* (7), 1233-1238.
9. Dawson, A. L.; Santana, M. F. M.; Nelis, J. L. D.; Motti, C. A., Taking control of microplastics data: A comparison of control and blank data correction methods. *Journal of Hazardous Materials* **2023,** *443*, 130218.
10. Ziajahromi, S.; Leusch, F. D. L., Systematic assessment of data quality and quality assurance/quality control (QA/QC) of current research on microplastics in biosolids and agricultural soils. *Environmental Pollution* **2022,** *294*, 118629.
11. AOAC, Guidelines for standard method performance requirements-Appendix F. 2016.
12. Granwal, L. *Consumption of plastic in Australia in financial year 2019, by polymer type(in 1,000 metric tons)*; Statista: 2020.
13. He, P.; Chen, L.; Shao, L.; Zhang, H.; Lu, F., Municipal solid waste (MSW) landfill: A source of microplastics?-Evidence of microplastics in landfill leachate. *Water Research* **2019,** *159*, 38-45.
14. Gewert, B.; Plassmann, M. M.; MacLeod, M., Pathways for degradation of plastic polymers floating in the marine environment. *Environmental Science: Processes & Impacts* **2015,** *17* (9), 1513-1521.

CHAPTER 7: INVESTIGATING TREATMENT EFFECT ON PLASTIC LOADS AT WASTEWATER TREATMENT PLANT

The primary objective of this chapter was to investigate the impact of wastewater treatment on plastic loads, focusing on the solid waste stream within a wastewater treatment plant. The chapter provides insights into the quantity, types, and size trends of microplastics at various treatment stages, encompassing influent, primary sedimentation, secondary sedimentation, digestion, and dewatering. A subset of the data in this chapter, specifically pertaining to microplastics larger than 25 µm, is earmarked for future publication.

Abstract

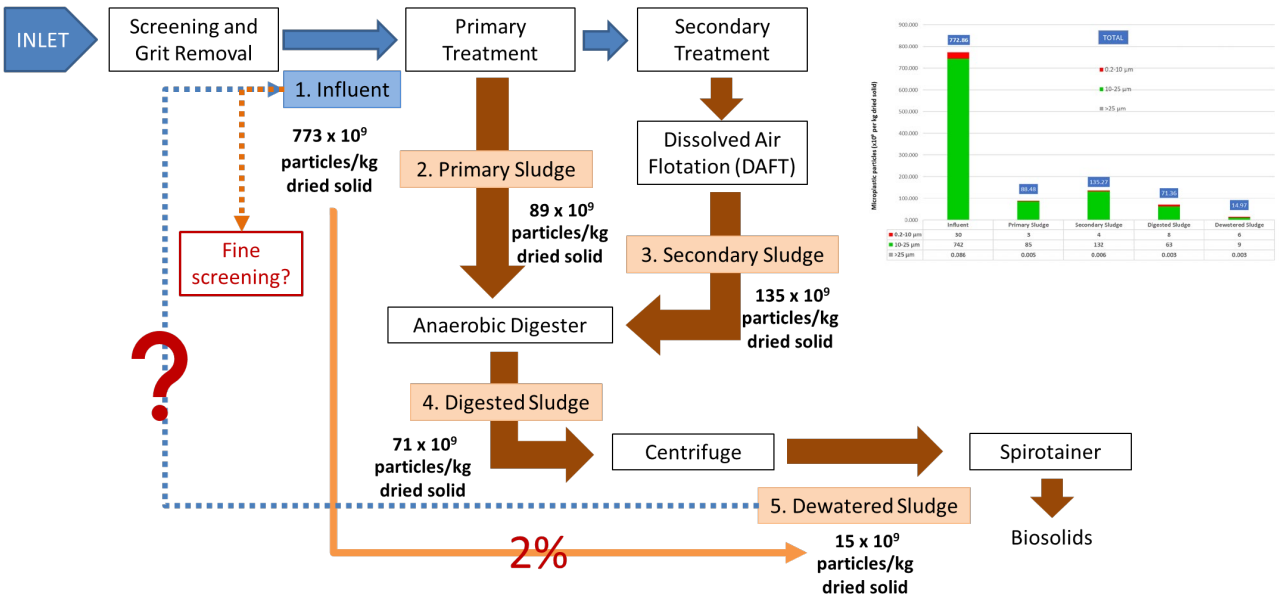

Figure 7-45. Graphical Abstract

Landfill is often considered a critical sink of microplastics coming from the wastewater treatment plant.[1] While some studies have highlighted the abundance of microplastics in such facilities, there remains a limited understanding of the impact of the treatment processes on loads. This study aimed to investigate the effect of treatments on microplastics loads, focusing specifically on the solid waste stream at a local wastewater treatment plant. Samples, collected at different stages (influent, primary sludges, secondary sludge, digested sludge, and dewatered sludge) over a five-week period from February to March 2023, underwent a pretreatment procedure to isolate microplastics. FTIR Microspectroscopy was used to quantify and identify microplastics larger than 25 µm, while Flow Cytometry was employed for quantifying plastic particles in the size ranges of 10-25 µm and 0.2-10 µm.

The comprehensive treatment study revealed a substantial reduction in the number of microplastics from influent (773 x 10^9 particles per kg dried solid) to dewatered sludge (15 x 10^9 particles per kg dried solid). A reducing number of microplastics were found in the dewatered sludge, prompting further investigation into

their fate within the treatment plant, including potential interception at grit/fine screens and the contribution of centrate from the dewatering process back into the inlet. Microplastics in the size range of 10-25 µm dominated treatment points (63-96%), with synthetic/regenerated cellulose prevalent in influent samples, and ethyl vinyl acetate, polyurethane, and polyethylene terephthalate (or polyester) in sludge samples. The digestion process exhibited the highest microplastic counts at day 4 for sizes >25 µm (7×10^6 particles per kg dried solid) and 10-25 µm (97×10^9 particles per kg dried solid), and at day 32 for sizes 0.2-10 µm (8×10^9 particles per kg dried solid).

The treatments in the wastewater plant, particularly in the solid waste stream, tend to fragment plastic particles into smaller sizes. However, the specific treatments triggering this fragmentation effect remain unclear. While an observation during the digestion process did not indicate a distinct fragmentation pattern over the treatment period (day 0 to day 39), it did reveal a decrease in the abundance of microplastics. Due to the continuous nature of this process, the observation's validity is limited. Thus, a more detailed study focusing on the digestion treatment's impact on plastic loads could contribute valuable insights into understanding plastic behavior within treatment plants. This information would be instrumental in technological advancements aimed at reducing and eliminating microplastics before their release into the effluent or land.

1 Introduction

Wastewater treatment plants are effective in removing plastic particles, although their design currently falls short of complete elimination. Various processes are employed to extract plastic particles from wastewater and sludge before their discharge into effluent and land. These processes encompass sedimentation, screening, grit removal, coagulation, aeration, membrane separation, chlorination, filtration, and biological treatment. Primary, secondary, and tertiary treatments have been reported to achieve removal rates ranging from 70% to 98% for plastics larger than 100 µm. However, particles smaller than 100 µm are likely to pass through the effluent.[2-4]

Understanding how treatments effectively reduce or eliminate microplastics is crucial for comprehending the distribution of microplastics within the treatment plant and beyond, while also managing their sources or pathways.[5] Gaining insights into how each treatment affects plastic loads and types involves studying polymer behaviors in wastewater and sludge subjected to different treatments. For instance, polyethylene (PE) has been observed to persist in the soil for extended periods, with degradation requiring several years. Connel at al.'s study revealed that PE remains in biosolids even after three years of storage.[6, 7]

Mahon et al. conducted a study comparing lime stabilization (LS), which generates smaller particles, anaerobic digestion (AD), associated with fewer plastic particles, and thermal drying (TD), leading to melting and blistering particles. However, it is essential that certain treatments may potentially increase the

absorption of other chemicals into microplastics, and therefore pose higher risks to the ecosystem.[4, 7] Additionally, considering the substantial evidence of microbial breakdown of polymers through exoenzyme activity promoting depolymerization and assimilation of smaller particles leading to mineralization, the role of degradation by microorganisms within the AD system warrants further investigation [2, 4]

The ultimate goal of this study was to provide information to the local agency regarding how their treatments influence the abundance and behaviors of microplastics. This knowledge will contribute to more informed decision-making in managing and optimizing wastewater treatment processes to mitigate the environmental impact of microplastics.

2 Materials and Methods

2.1 Sample collection and weather conditions

Samples were collected following the treatment time period, as illustrated in Figure 7-46. Based on this treatment period, sampling was conducted on various dates from 13th February 2023 to 23rd March 2023. Details of sampling dates, time, points, and volume are presented in Table 7-23. The weather during February to March 2023 indicated an average temperature of 21°C (with minimum of 12°C and a maximum of 40°C) accompanied by daily average 0.6 mm rainfall (ranging from 0 mm to 11 mm), a relative humidity fluctuating between 8% to 99%, and wind speeds ranging from 2 km/h to 46 km/h.

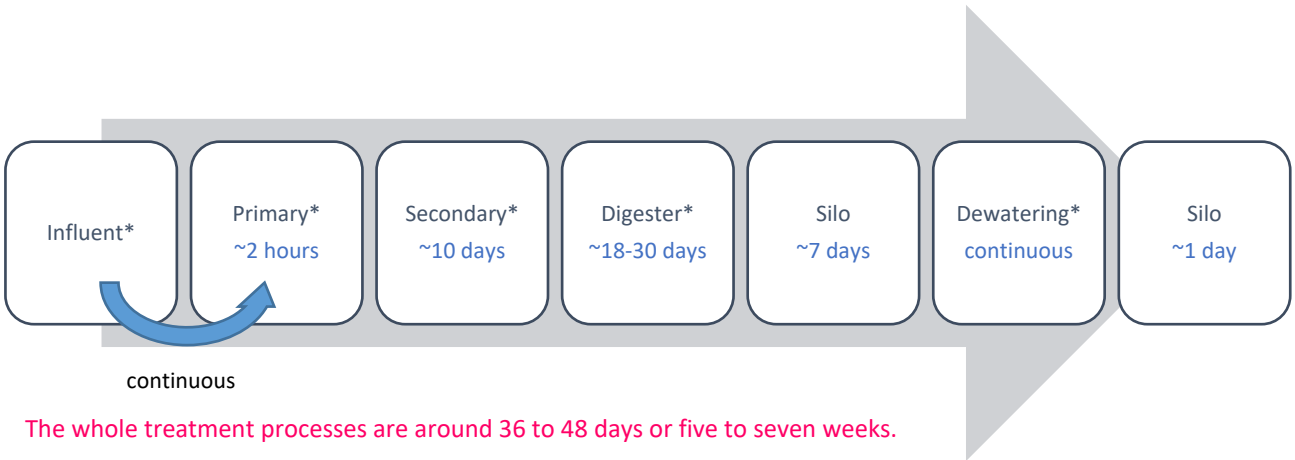

Figure 7-46. Treatments period

Table 7-23. Sampling timeline

Sampling date	Sampling time	Sampling point	Sample volume (L)	Notes
Monday, 13th Feb 23	10am	Influent	5	
	12pm	Influent	5	
		Primary sludge	1	
		Digested sludge	1	Day 0
Tuesday, 14th Feb 23	10am	Influent	5	
Wednesday, 15th Feb 23	10am	Influent	5	
	12pm	Influent	5	
		Primary sludge	1	
		Digested sludge	1	Day 2
Thursday, 16th Feb 23	10am	Influent	5	
Friday, 17th Feb 23	12pm	Influent	5	
		Primary sludge	1	
		Digested sludge	1	Day 4
Thursday, 23rd Feb 23	10am	Secondary sludge	1	10th day after primary sedimentation
		Digested sludge	1	Day 11
Thursday, 16th March 23	10am	Digested sludge	1	Day 32 ;21st day after secondary sedimentation
Thursday, 23rd March 23	10am	Digested sludge	1	Day 39
		Dewatered sludge	1	a week after digestion treatment

2.2 Sample processing and data collection

The collected samples underwent processing following the digestion and microplastics separation procedures as adopted from Ziajahromi et.al.[1] A digestion using 30% H_2O_2 for 48 hours at 60°C was carried out, followed with Fenton reaction involving a mixture of 10 mL 0.05M FeSO4 pH 3 and 20mL of 30% H_2O_2 for approximately 6 hours or until no further reactions were observed. Then, microplastics were isolated with a density separation procedure employing filtered ultrapure water and 4.5M NaI solution both three times. Size fractionation was carried out after the pretreatment process, during which isolated microplastics were filtered through three different filters: a 25 µm-stainless steel mesh, a 10 µm-polycarbonate membrane, and a 0.2 µm-polycarbonate membrane. This size fractionation process resulted in three distinct size bins of microplastics: those >25 µm dried on SS mesh, those sized 10-25 µm suspended in TE Buffer, and those sized 0.2-10 µm suspended in TE Buffer. Subsequently, plastic counts were determined for all size bins, and plastic type identification was performed for the >25 µm size bin. FTIR Microspectroscopy was employed to quantify and characterize microplastics larger than 25 µm, with detailed methods explained in Chapter 4 of this thesis. Meanwhile, Flow Cytometry was used to enumerate plastic counts for sizes 0.2-10 µm and 10-25 µm. The overall analysis flow is illustrated in Figure 7-47.

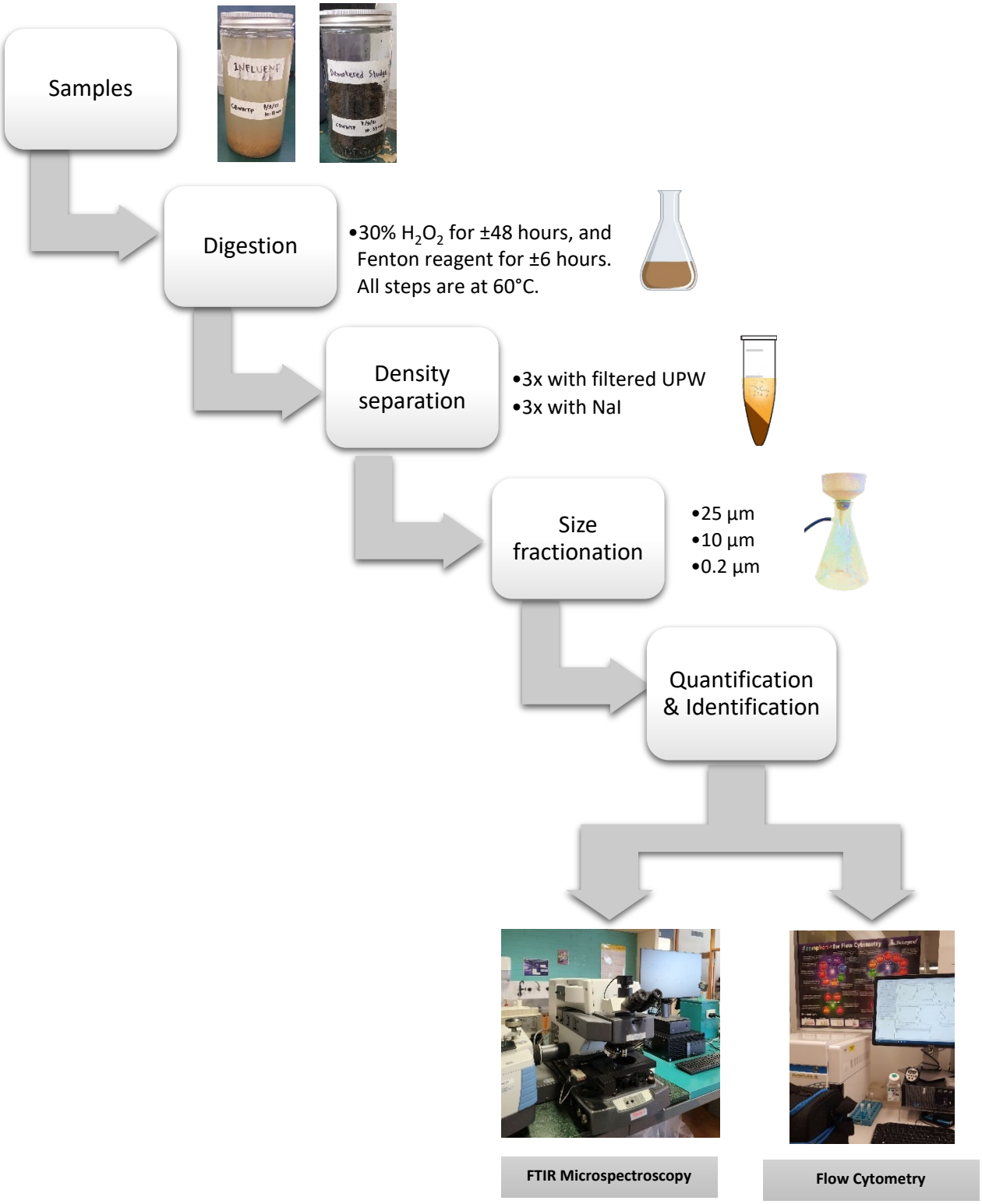

Figure 7-47. Analysis Flow Chart

2.3 Data processing

2.3.1 FTIR Microspectroscopy and Flow Cytometry

The collected IR spectra of each sample were individually identified to determine their polymer type through cross-referencing with the spectrum database, as explained in Chapter 4 of this thesis. This characterization process was specifically applied to microplastics larger than 25 µm. Meanwhile, for microplastics sized 0.2-25 µm, the detected counts of particles in each sample were extrapolated to estimate the actual sample amount. Unfortunately, the Flow Cytometry technique is currently unable to identify the type of plastic.

2.3.2 Microplastics counts

The quantity of microplastics was expressed in kg dried solid and load per day. To derive this figure, the total solids and flow rate (FR, refer to Table 7-24) of each sampling point on various sampling dates were utilized. Incorporating both sets of data provides a more comprehensive understanding of how the treatments at the wastewater plant impact the daily abundance of plastics and their concentration per unit mass.

Table 7-24. Total Solid (TS) and Flow Rate (FR) of each sampling point at different sampling date

Sampling		Sampling point									
		Influent		Primary sludge		Secondary sludge		Digested sludge		Dewatered sludge	
Date	Time	TS (%)	FR	TS (%)	FR	TS (%)	FR	TS (%)	FR	TS (%)	FR
Mon, 13 Feb 23	10am	0.1	518 L/s								
	12pm	0.1	456 L/s	2.27	7.1 L/s			1.5	10 L/s		
Tues, 14 Feb 23	10am	0.1	509 L/s								
Wed, 15 Feb 23	10am	0.1	521 L/s								
	12pm	0.1	398 L/s	2.27	7.0 L/s			1.5	10 L/s		
Thurs, 16 Feb 23	10am	0.1	502 L/s								
Fri, 17 Feb 23	12pm	0.1	248 L/s	2.18	7.0 L/s			1.6	10 L/s		
Thurs, 23 Feb 23	10am					3.26	4.7 m^3/h	1.6	10 L/s		
Thurs, 16 Mar 23	11am							1.35	10 L/s	17.1	1.25 tonne/h
Thurs, 23 Mar 23	11am							1.35	10 L/s	17.1	1.25 tonne/h

TS = Total Solid; FR = Flow Rate

2.3.3 Statistical analysis

A Univariate ANOVA using IBM SPSS Statistics (version 28) was employed to statistically compare the number of microplastics at different stages of treatment. The treatment stage served as the independent variable,

with the number of microplastics per size bin as the dependent variable. Regarding the digestion process, the treatment period in days was designated as the independent variable, and plastic counts were considered the dependent variable.

2.4 Quality Control

To monitor potential cross-contamination of plastic particles during sampling and analysis, five different negative controls, encompassing both field and laboratory settings, were prepared. In each negative control, a liter of filtered ultrapure water was stored in a glass jar, which was then left open either during sampling at the wastewater plant or during analysis in the laboratory. The number of plastic particles detected in these negative controls were calculated and served as the Limit of Detection (LOD=mean+3SD, the lowest concentration where detection is feasible) and Limit of Quantification (LOQ=mean+10SD, values greater than LOQ have a higher likelihood of being true quantitative values and not random fluctuation of the blank).[8-11] The value of LOD was used to correct the number of microplastics counted.

Simultaneously, positive control samples were created by spiking sludge samples with various standard reference polymers, including polypropylene (PP), high density PE (HDPE), low density PE (LDPE), polystyrene, PET, polymethyl methacrylate (PMMA), and polyvinyl chloride (PVC), with particle size ranges between 25 µm and 1 mm. Further details on the preparation and processes of these controls were elucidated in Chapter 6 of this thesis.

3 Results and Discussion

This section is divided into three parts, delving into the overall treatment effect on the abundance of microplastics based on size bins, followed by a more detailed examination of the digestion treatment. These components encompass the size trend and type of plastics larger than 25 µm. The final segment explores the Quality Assurance/Quality Control (QA/QC) results of the experiment. The overall statistics data are presented in Appendix J of this thesis. The sampling documentation and some plastic particles images collected using stereomicroscope are given in Appendix A of this thesis.

3.1 Overall treatment processes

3.1.1 Microplastics >25 µm per kg dried solid and per day

Microplastics larger than 25 µm were quantified using a semi-automated mapping mode of FTIR Microspectroscopy, as detailed in Chapter 4 of this thesis. Figure 7-48 illustrated the abundance of microplastics throughout the overall treatment processes, both per kg dried solid and per day. It showcases the influx of plastic entering the wastewater plant, represented by the influent sample, followed by the subsequent solid waste treatments in primary sedimentation, secondary sedimentation, digestion, and dewatering.

Approximately 12% per kg dried solid or 1% per day of the total amount of plastics from the influent (86 x 10^6 particles per kg dried solid or 742 x 10^9 particles per day) were settled in primary (5 x 10^6 particles per kg dried solid or 85 x 10^9 particles per day) and secondary (6 x 10^6 particles per kg dried solid or 132 x 10^9 particles per day) sedimentations. The subsequent treatments demonstrated a decreased number of microplastics, with only 2.7 x 10^6 particles per kg dried solid or 63 x 10^9 particles per day in digested sludge, and 2.9 x 10^6 particles per kg dried solid or 9 x 10^9 particles per day in dewatered sludge. However, a slight increase, around 6% per kg dried solid, in the number of microplastics was observed between digested and dewatered sludges. Further explanation of the overall treatment effect is discussed in Section 3.1.5 of this chapter.

A univariate ANOVA test (refer to Table 7-25 and Table 7-26) revealed a significant main effect of treatments on microplastics abundance per kg dried solid [$F(1,4) = 15.273$; $p < 0.001$; partial $\eta^2 = 0.694$)], similarly for per day plastic loads [$F(1,4) = 14.667$; $p < 0.001$; partial $\eta^2 = 0.685$)]. However, the Post Hoc analysis showed that the significance was only between Influent and sludges treatments. The solid waste treatments including primary and secondary sedimentations, and digestion and dewatering, did not show a significant difference in number of microplastics larger than 25 µm.

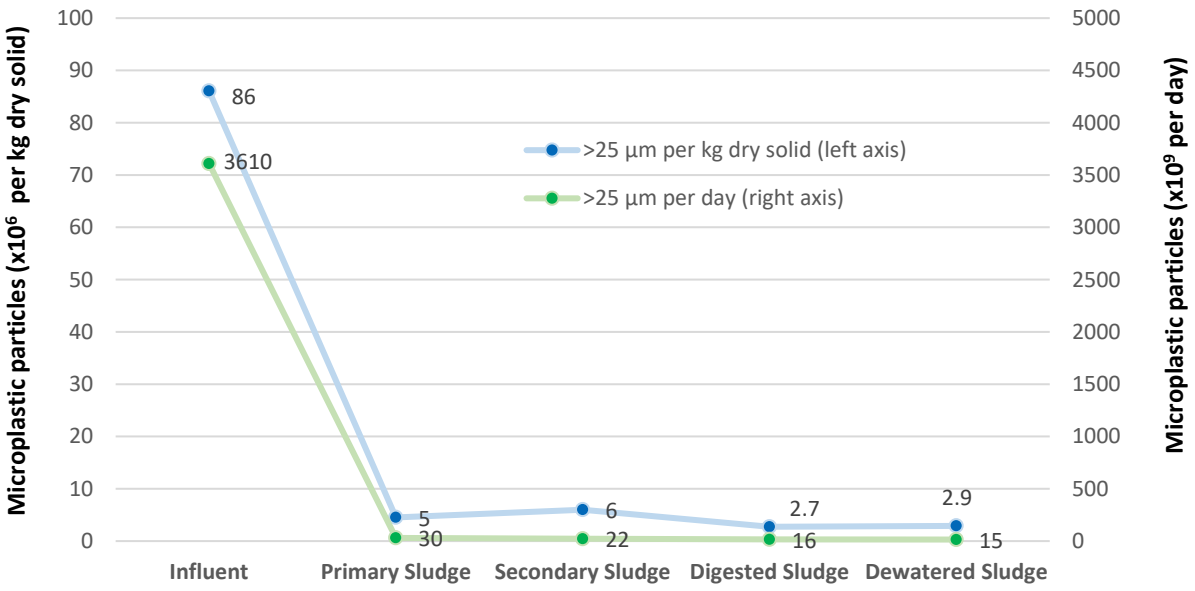

Figure 7-48. Microplastics abundance sizes >25 µm

3.1.2 Microplastics 0.2-25 µm per kg dried solid and per day

Examining microplastics in the smaller size range of 10-25 µm using the Flow Cytometry technique revealed a significantly higher number of plastic particles compared to those larger than 25 µm. In Figure 7-49 and Figure 7-50, the microplastics entering the wastewater plant at the influent sampling point were quantified at 742 x 10^9 particles per kg dried solid or 29,497 x 10^{12} particles per day. Only around 29% per kg dried solid or 4% per day ended up in primary (85 x 10^9 particles per kg dried solid or 564 x 10^{12} particles per day) and secondary (132 x 10^9 particles per kg dried solid or 485 x 10^{12} particles per day) sedimentations. Moreover, the dewatered sludge (9 x 10^9 particles per kg dried solid or 48 x 10^{12} particles per day) contained around 15% per kg dried solid or 13% per day of the microplastics content in the digested sludge.

The statistical analysis of univariate ANOVA for microplastics size 10-25 µm (refer to Table 7-25 and Table 7-26) showed no significant difference [$F(1,4) = 2.109$; $p = 0.103$; partial $\eta^2 = 0.214$)] in microplastics abundance per kg dried solid for all treatments, with a medium effect of the treatment itself. However, considering the flow rate per day, there was a modest influence [$F(1,4) = 3.164$; $p = 0.027$; partial $\eta^2 = 0.290$)] of treatments on the plastic particles daily. This effect was mainly observed between influent and primary sludge and not between influent and secondary, digested, and dewatered sludges.

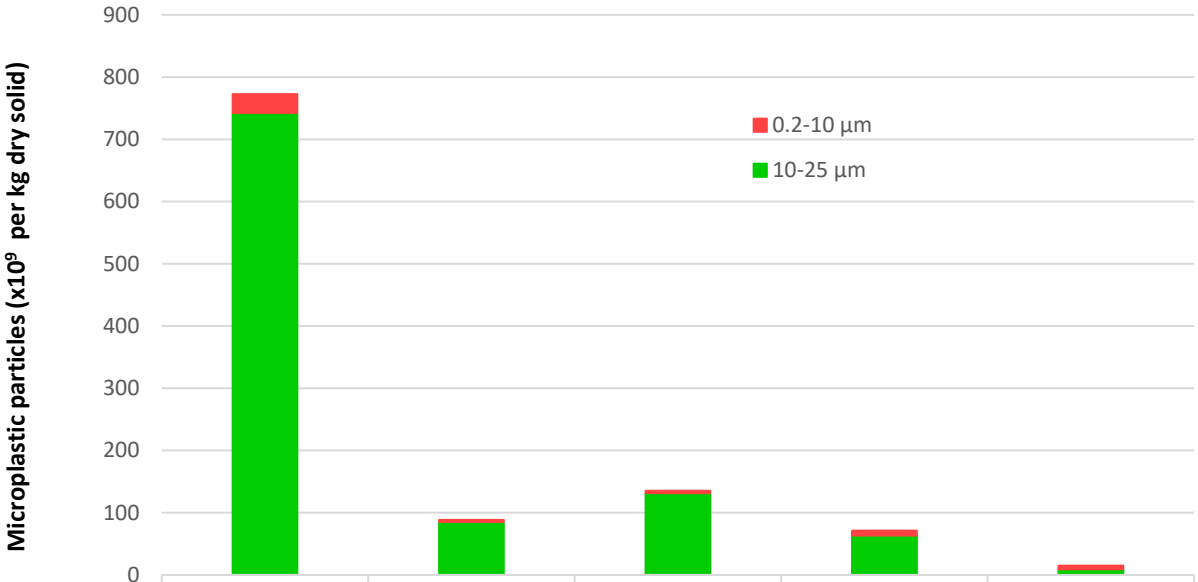

	Influent	Primary Sludge	Secondary Sludge	Digested Sludge	Dewatered Sludge
0.2-10 µm	30	3	4	8	6
10-25 µm	742	85	132	63	9

Figure 7-49. Microplastics abundance sizes 0.2-25 µm per kg dried solid

For the smaller size of plastic particles, 0.2-10 µm, as shown in Figure 7-49 and Figure 7-50, the number of microplastics entering the wastewater plant was 30 x 10^9 particles per kg dried solid or 1130 x 10^{12} particles

per day. Only around 23% per kg dried solid or 3% per day ended up in primary (3 x 10^9 particles per kg dried solid or 23 x 10^{12} particles per day) and secondary (4 x 10^9 particles per kg dried solid or 14 x 10^{12} particles per day) sludges. The following treatment, digestion (8 x 10^9 particles per kg dried solid or 48 x 10^{12} particles per day) posed a higher number of microplastics, around 116% per kg dried solid or 131% per day compared to the previous treatments, primary and secondary sedimentations. This suggests that the digestion process triggered the fragmentation of the plastic particles. Further explanation of the treatment's effect is provided in Section 3.1.5 of this chapter.

A univariate ANOVA test revealed no significant effect of treatments on the microplastics abundance size 0.2-10 µm in both per kg dried solid [F (1,4) = 1.734; p = 0.168; partial η^2 = 0.183)] and per day [F (1,4) = 2.309; p = 0.080; partial η^2 = 0.230)]. A post hoc test showed a slight difference between influent and the sludges but not between the sludges.

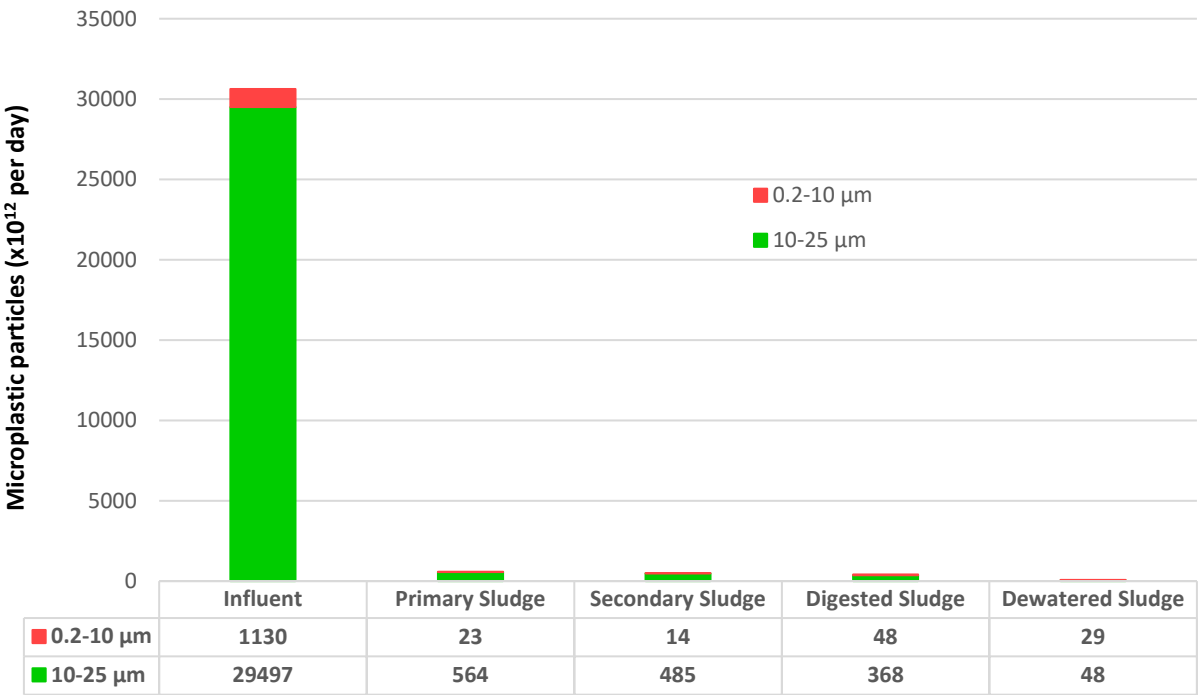

	Influent	Primary Sludge	Secondary Sludge	Digested Sludge	Dewatered Sludge
0.2-10 µm	1130	23	14	48	29
10-25 µm	29497	564	485	368	48

Figure 7-50. Microplastics abundance sizes 0.2-25 µm daily loads

Table 7-25. Univariate ANOVA test result – overall treatments

Size bin_unit	F	df1	df2	Sig./p-value	Partial Eta Squared (η^2)
25 µm_per kg dried solid	15.273	1	4	<0.001	0.694
25 µm_per day	14.667	1	4	<0.001	0.685
10-25 µm_per kg dried solid	2.109	1	4	**0.103**	0.214

10-25 µm_per day	3.164	1	4	0.027	0.290
0.2-10 µm_per kg dried solid	1.734	1	4	**0.168**	0.183
0.2-10 µm_per day	2.309	1	4	**0.080**	0.230

Table 7-26. Univariate ANOVA test result interpretation – overall treatments

Size bin_unit	Sig./p-value*	Partial Eta Squared (η^2)**
25 µm_per kg dried solid	YES	Large
25 µm_per day	YES	Large
10-25 µm_per kg dried solid	**NO**	Medium
10-25 µm_per day	YES	Medium
0.2-10 µm_per kg dried solid	**NO**	Small
0.2-10 µm_per day	**NO**	Medium

** YES/NO = yes/no **significant difference** between treatments

*** Large/Small = treatments had a large/medium/small **influence** on number of microplastics (dependent variable) between treatments (independent variable)

3.1.3 Type of microplastics >25 µm

Figure 7-51 illustrates the proportional distribution of microplastics for each type at various treatment points. The influent sample was predominantly composed of synthetic or regenerated cellulose, mainly in the form of translucent fibers (refer to Figure 7-52), followed by ethyl vinyl acetate (EVA), polyamide (PA), and wood polymer composite (WPC). In primary sedimentation, EVA, polyethylene terephthalate (PET) or polyester (PEs), and PVA were the dominant types, while synthetic/regenerated cellulose was found in secondary sludge, along with polyurethane (PUR) and WPC. It is noteworthy that cellulose, WPC, and PUR tend to pass through primary sedimentation, as their density (around 1 g/mL) is lower than that of PET/PEs and PVC (both having a density around 1.39 g/mL). Digested and dewatered sludges contained a mix of all plastic types, including cellulose, EVA, PUR, WPC, PA, rubber, PET/PEs, and PVC with more or less the same proportion.

Examining the potential sources of these plastics, synthetic/regenerated cellulose primarily identified in the form of translucent fibers or yellowish fragments, could originate from textiles, furnishings, female hygiene products, nappies, toilet papers, and dishwashing fibers and/or fragments. EVA is a material commonly used for shoe soles, insulation, and mat foam. PUR is employed in cosmetics sponges, dishwashing sponges, and

bra foam pads. WPC finds applications in decking tiles, furniture, and building materials; PA may be present in dishwashing sponges (green side fibers), while rubber could stem from car mats and shoe soles.[12-21].

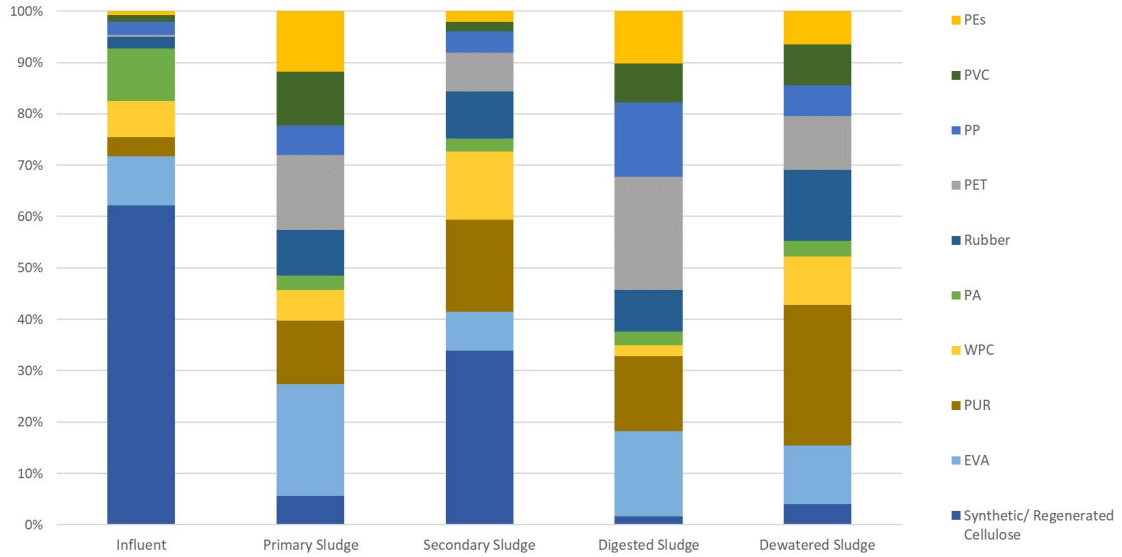

Figure 7-51. Tye of plastics (size >25 µm) proportionally at each treatment point

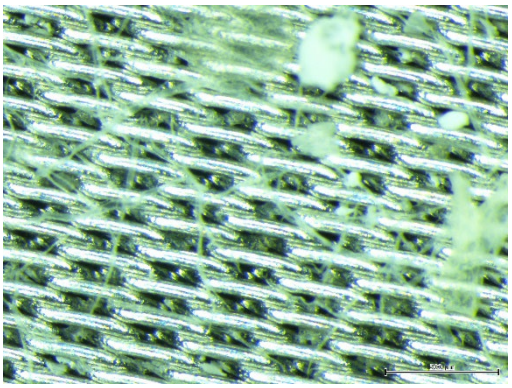

Figure 7-52. Stereomicroscope image of translucent synthetic/regenerated cellulose

3.1.4 Size Trend

The overall size trend among three different size bins (>25 µm, 10-25 µm, and 0.2-10 µm), as depicted in Figure 7-53, reveals that microplastics in the size range of 10-25 µm (88.14%) dominate the microplastic abundance at the wastewater treatment plant. They are followed by microplastics in the size range of 0.2-10

µm (11.85%) and those exceeding 25 µm (0.01%). Analyzing each treatment process individually (Figure 7-54), it becomes evident that microplastics tend to undergo fragmentation throughout the treatment stages. As the particles get smaller, the surface area ratio increases, resulting in a differential size distribution. In dewatered sludge, which represents the final stage of the solid waste stream, approximately 37% of microplastics fall within the size range of 0.2-10 µm. This percentage is 26% higher than that observed in digested sludge (11%), and around 30% higher than in influent, primary, and secondary sludges. The number of microplastics in the size range of 10-25 µm decreases as the size range shifts towards 0.2-10 µm throughout the treatment processes from primary sedimentation to dewatering. However, it is essential to note that different techniques, namely FTIR microspectroscopy and Flow Cytometry, were used to quantify microplastics in the size ranges of >25 µm and 0.2-25 µm, respectively.

This observed trend of fragmentation during the treatment process aligns with expectations, as plastic particles are prone to braking down into smaller sizes when exposed to various conditions, including water, heat, chemicals, and physical interactions.[5] Having this data and understanding the behavior of plastic particles at wastewater treatment plants can contribute to the development of appropriate techniques for minimizing the release of microplastics into the environment.

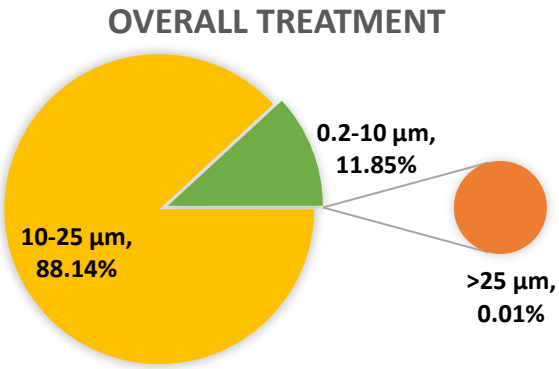

Figure 7-53. Overall treatment size trend

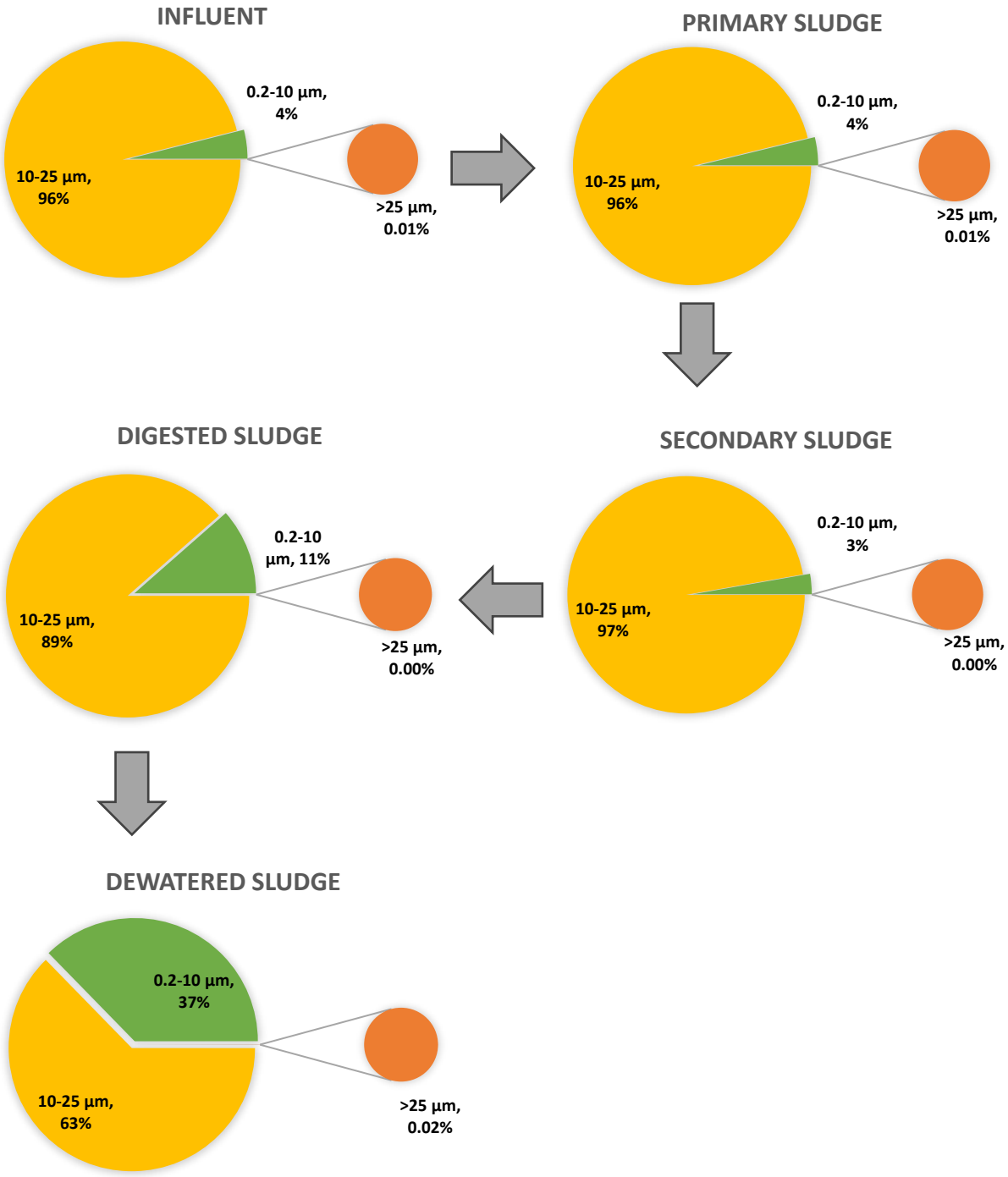

Figure 7-54. Size trend per treatment point

3.1.5 Overall treatment effect on plastic loads

Examining the percentage of microplastics abundance per size bin across treatment points (Table 7-27), it is noted that only 12% of microplastics exceeding 25 µm in the influent end up in primary and secondary sludges, and only 26% of them end up in digested sludge, but with a marginal increase of 6% observed in dewatered sludge. For plastic particles in the size range of 10-25 µm, there is no noticeable increase in

percentage throughout the treatment processes. However, plastic particles in the size range of 0.2-10 µm show a 16% increase from primary and secondary sedimentations to digestion treatment.

Table 7-27. Microplastics abundance fluctuation between treatment point

Treatment point	% microplastics abundance per size bin compared to the previous treatment point					
	>25 µm		10-25 µm		0.2-10 µm	
	per kg	per day	per kg	per day	per kg	per day
Influent						
Primary sedimentation	12	1	29	4	23	3
Secondary sedimentation						
Digestion	26	30	29	35	**116**	**131**
Dewatering	**106**	93	15	13	68	60

When comparing the number of microplastics from influent, the entry point of the treatment plant, to the end of the solid waste stream, dewatering, only 3%, 1%, and 18% of microplastics exceeding 25 µm, 10-25 µm, and 0.2-10 µm, respectively, end up in dewatered sludge per kg dried solid. Despite observing a significant decrease in microplastics abundance from influent to sludges, it is crucial to trace where these microplastics go during the treatment processes. This study did not collect samples from the frit/fine screen, a process before and after the influent sampling point, and did not collect samples from centrate, the liquid separated from the dewatering process, which is connected back to the influent point. Both points could potentially be where plastic particles accumulate and contribute to the overall treatment processes.

Given this observations, further investigation into the treatment process and its effects from sedimentation to digestion and dewatering is necessary. The following sections provide a more in-depth discussion of the digestion process's impact on plastic loads.

3.2 Digestion treatment

Anaerobic digestion is a widely employed technique in wastewater treatment plants, offering several advantages such as the production of biogas, enhanced sludge stabilization, pathogen reduction, reduced odor emissions, and a decrease in sludge dry matter leading to a reduction in the final sludge volume.[22, 23] A study by Mahon et al reported that anaerobic digestion resulted in a lower number of microplastics in the size range of 250-4000 µm.[7] As discussed in the previous section of this chapter on the overall treatment effects, we further investigate the impact of the digestion process on plastic loads over time. Samples collected were not particularly contained in one batch over 39 days instead they were a mix of sludges accumulated as the wastewater continuous enter the treatment plant.

3.2.1 Microplastics >25 µm per kg dried solid

Figure 7-55 depicts the abundance of microplastics sized >25 µm in digested sludge across various time periods: day 0, 2, 4, 11, 32, and 39. The number of microplastics reached its peak on day 4 (7 x 10^6 particles per kg dried solid or 49 x 10^9 particles per day) and subsequently decreased in the following observation days. A univariate ANOVA test was conducted, revealing a significant effect of time on both microplastics abundance per kg dried solid [F (1,5) = 4.228; p = 0.025; partial η^2 = 0.679)] and daily plastic loads [F (1,5) = 6.973; p = 0.005; partial η^2 = 0.777)]. Post hoc test indicated differences between day 0 and 4, as well as day 0 and 39 for both microplastics abundance per kg dried solid, with an additional distinction between day 0 and 32 daily plastic loads.

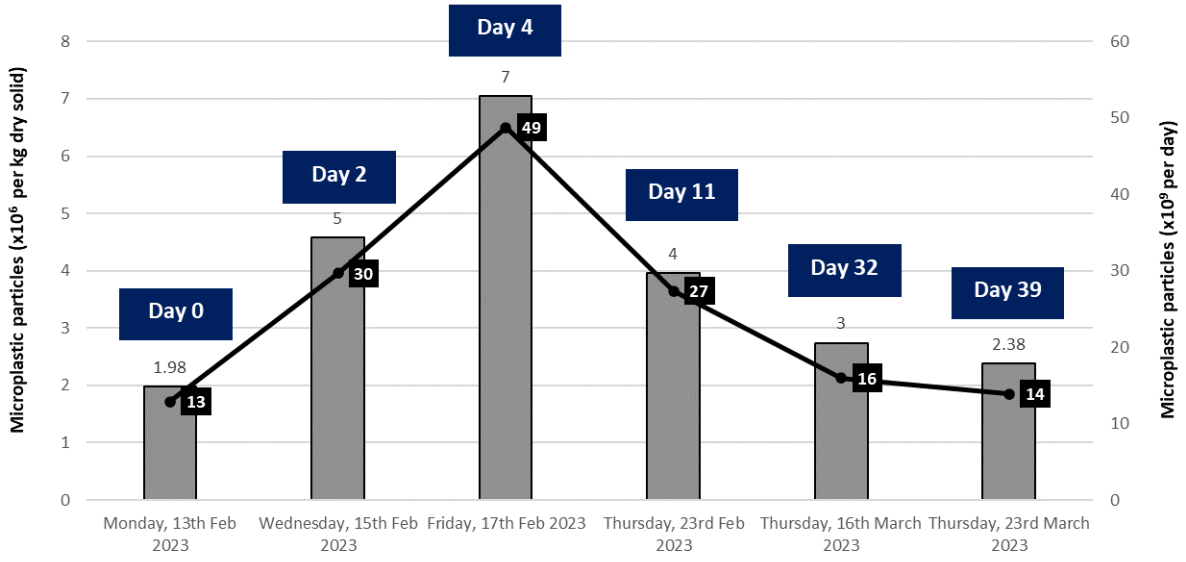

Figure 7-55. Microplastics abundance sizes >25 µm at digestion process over 39 days

3.2.2 Microplastics 0.2-25 µm per kg dried solid

Similar to microplastics size >25 µm, day 4 also exhibit the highest number of microplastics size 10-25 µm µm (97 x 10^6 particles per kg dried solid or 671 x 10^9 particles per day) (Figure 7-56 and Figure 7-57), showing a decrease on day 11 but an increase on day 32 and 39. There was a significant effect of time on microplastics abundance per kg dried solid [F (1,5) = 6.519; p = 0.005; partial η^2 = 0.748)], particularly between day 0, 2, 4, and 11 (Post hoc test result). However, this effect was not applicable for daily plastic loads [F (1,5) = 0.989; p = 0.467; partial η^2 = 0.310)], indicating no significant difference or influent of time on plastic loads.

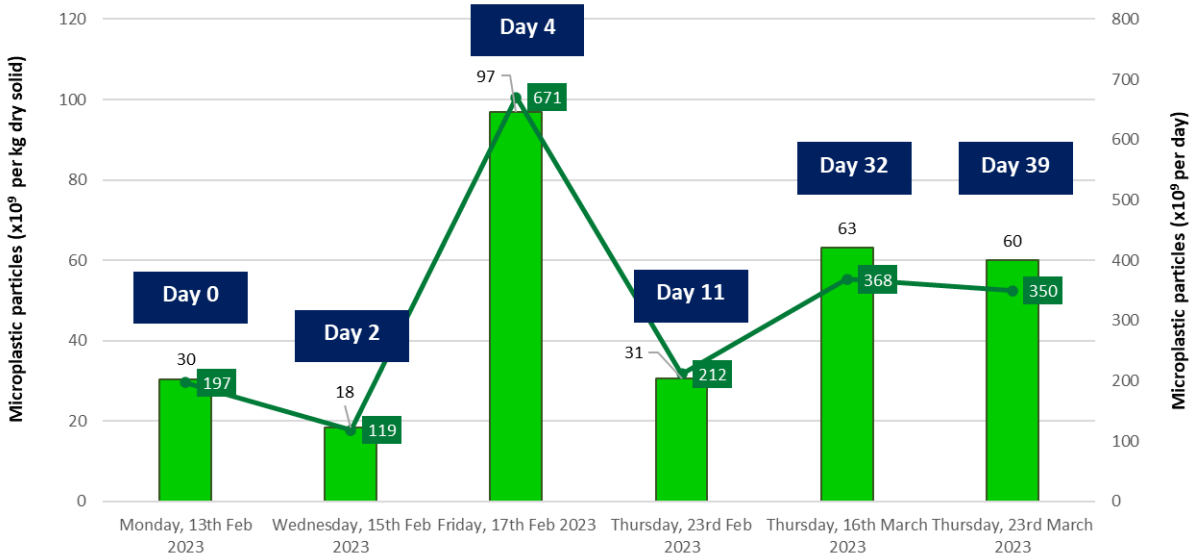

Figure 7-56. Microplastics abundance sizes 0.2-25 um (per kg dried solid) at digestion process over 39 days

In contrast, the smaller size of microplastics (0.2-10 µm) exhibited different patterns, with day 32 showing the highest microplastics abundance (8 x 10^6 particles per kg dried solid or 48 x 10^9 particles per day) (Figure 7-56 and Figure 7-57). A univariate ANOVA test revealed a significant effect of time on the number of microplastics per kg dried solid [F (1,5) = 4.805; p = 0.014; partial η^2 = 0.686)] and daily loads [F (1,5) = 4.560; p = 0.017; partial η^2 = 0.675)], specifically between day 0 and 32, as well as 32 and 39.

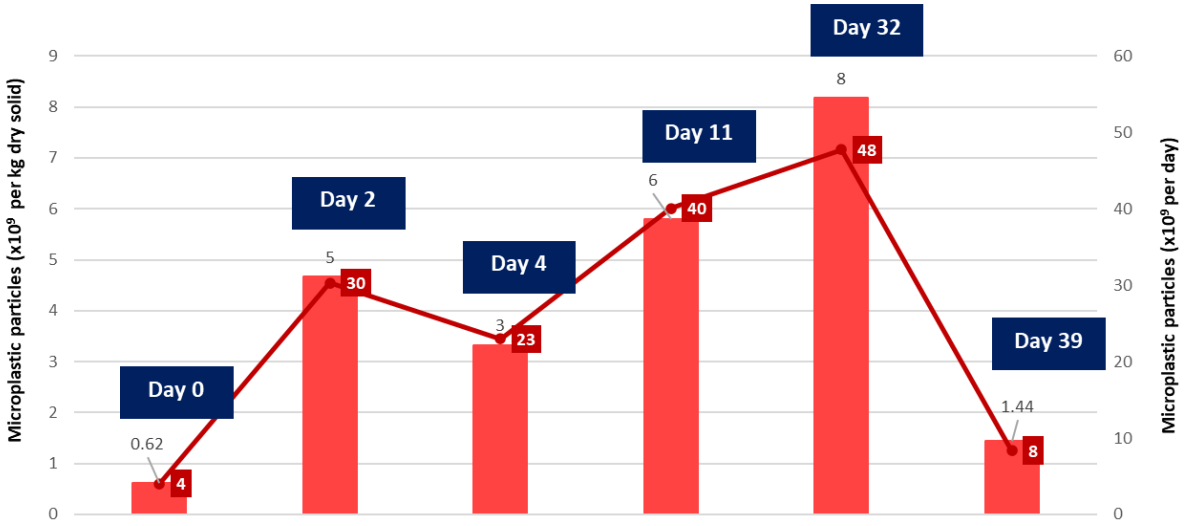

Figure 7-57. Microplastics abundance sizes 0.2-25 um (daily loads) at digestion process over 39 days

Table 7-28. Univariate ANOVA test result - digestion process

Size bin_unit	F	df1	df2	Sig./p-value	Partial Eta Squared (η^2)
25 µm_per kg dried solid	4.228	1	5	0.025	0.679
25 µm_per day	6.973	1	5	0.005	0.777
10-25 µm_per kg dried solid	6.519	1	5	0.005	0.748
10-25 µm_per day	0.989	1	5	**0.467**	0.310
0.2-10 µm_per kg dried solid	4.805	1	5	0.014	0.686
0.2-10 µm_per day	4.560	1	5	0.017	0.675

Table 7-29. Univariate ANOVA test result interpretation - digestion process

Size bin_unit	Sig./p-value*	Partial Eta Squared (η^2)**
25 µm_per kg dried solid	YES	Large
25 µm_per day	YES	Large
10-25 µm_per kg dried solid	YES	Large
10-25 µm_per day	**NO**	Medium
0.2-10 µm_per kg dried solid	YES	Large
0.2-10 µm_per day	YES	Large

** YES/NO = yes/no **significant difference** between treatments
*** Large/Small = treatments had a large/medium/small **influence** on number of microplastics (dependent variable) between treatments (independent variable)

3.2.3 Type of microplastics >25 µm

The analysis of plastics size >25 µm, conducted using FTIR microspectroscopy, revealed a diverse range of polymers, including EVA, PET/PEs, PUR, polypropylene (PP), rubber, PE, synthetic cellulose, PVS, and WPC. Notably, EVA, PET/PEs, PUR, PP, and rubber exhibited persistence throughout the entire 39-day digestion treatment period. Further investigation into the specific effects of digestion on individual types of polymers could yield a more comprehensive understanding of microplastics treatment within wastewater treatment plants.

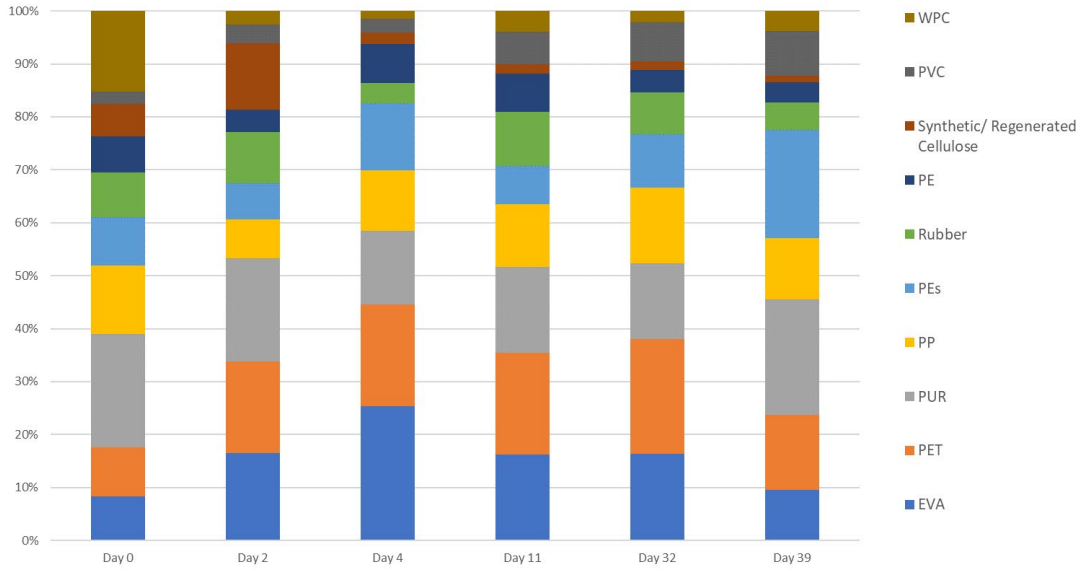

Figure 7-58. Type of plastics at digestion process over 39 days

3.2.4 Size Trend

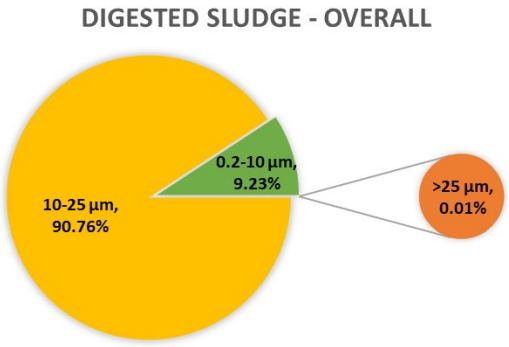

Figure 7-59. Size trend at digestion process

In the digestion process, microplastics abundance was predominantly composed of particles sized 10-25 µm (90.67%), followed by 0.2-10 µm (9.23%) and >25 µm (0.01%). This trend aligns with the overall treatment size trend discussed in Section 3.1.4.

Examining the individual size trends during the treatment days revealed an increase in the number of microplastics sized 0.2-10 µm on day 2 compared to day 0, although this trend was not sustained in the subsequent days. Notably, despite day 4 having the highest overall number of microplastics, it was not dominated by the smallest size category (0.2-10 µm); instead, 97% consisted of microplastics sized 10-25 µm. The subsequent days (11, 32, and 39) did not exhibit specific patterns in terms of size distribution.

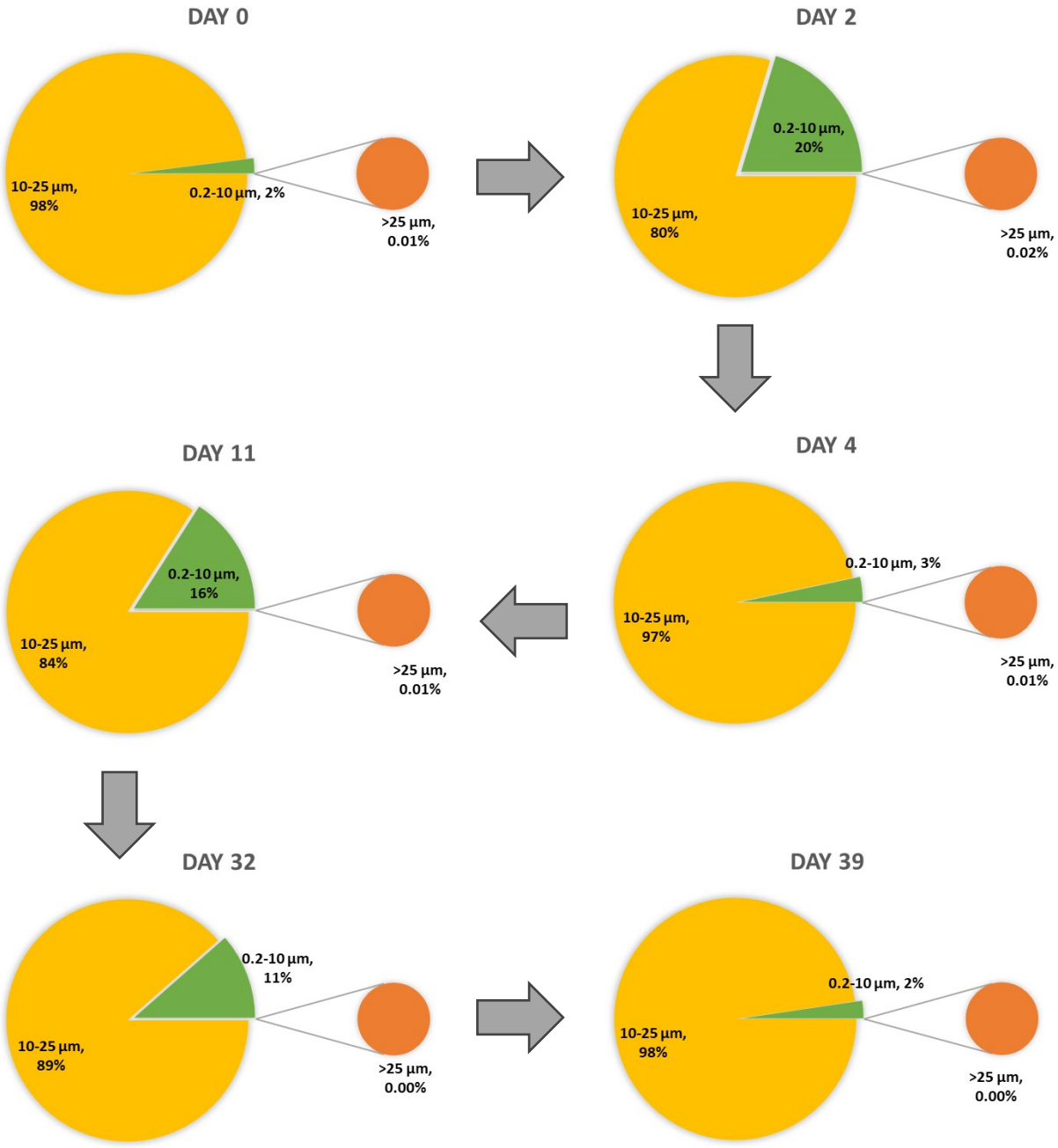

Figure 7-60. Size trend at digestion process over 39 days

3.2.5 Digestion process effect on microplastics abundance

The concentration of microplastics peaked on day 4 for both size categories (>25 µm and 10-25 µm) and on day 32 for size 0.2-10 µm during the digestion process. By day 39, there was a decrease in microplastics abundance. However, due to the continuous and extended nature of the overall digestion process spanning 18 to 30 days, it becomes challenging to pinpoint specific effects on plastic loads over time. Furthermore, the analysis of size trends did not reveal discernible patterns in terms of particle fragmentation resulting from

the digestion process. Given the complexities and continuous nature of digestion, further laboratory-scale studies are warranted to gain a better understanding of the efficacy of the digestion technique in reducing and/or eliminating microplastics, as well as their potential impact on specific polymer types.

3.3 QA/QC

A comprehensive discussion on the Quality assurance/control (QA/QC) procedure implemented in the experiment is provided in Chapter 6 of this thesis. Control negative samples played a crucial role in establishing the Limits of Detection (LOD) and Limits of Quantification (LOQ) for the analysis, as outlined in Table 7-30. In parallel, control positive or spiked samples were instrumental in evaluating the efficacy of the analysis in recovering microplastics from the samples, resulting in an impressive 96% recovery rate.

Table 7-30. LOD and LOQ of the analysis

Methods	Size fraction	LOD (particles/tested sample)	LOQ (particles/tested sample)
FTIR	>25 µm	102	311
Flow Cytometry	10-25 µm	2.25×10^{6}	6.34×10^{6}
	0.2-10 µm	6.51×10^{6}	1.80×10^{7}

The LOD value for size fraction >25 µm was used to correct the number of microplastics counted in each sample, yet not applicable for size fraction <25 µm. After the subtractions, all data of microplastics size >25 µm were above LOQ value, implying that the values representing an accurate reflection of the actual sample rather that potential contamination from the environment. Meanwhile, this was not applied for microplastics <25 µm because only around 50% of the data were above its LOQ value. This means that the number of microplastics counted were possibly from the cross-contamination of the environment during sampling and/or analysis. Further validation of the Flow Cytometry method is needed, as explained in Chapter 5 of this thesis.

4 Conclusions and Further studies

The primary objective of this study was to investigate the impact of wastewater treatment processes on the abundance and characteristics of microplastics at a wastewater treatment plant. The findings revealed a significant reduction in microplastic abundance from influent (86×10^{6} particles per kg dried solid or 3610×10^{9} particles per day) to the dewatering stage (2.9×10^{6} particles per kg dried solid or 15×10^{9} particles per day). However, a nuanced analysis of size trends indicated that the plastic particles underwent fragmentation into smaller sizes during the treatment processes. While only 4% of plastic particles were in the 0.2-10 µm range in the influent, this percentage increased to 37% in the dewatered sludge. The observed fragmentation pattern was also evident in the increase of 6% in microplastic size >25 µm between digestion and dewatering, as well as a 16% increase in microplastics size 0.2-10 µm between sedimentation and digestion processes.

Statistical analysis demonstrated a significant treatment effect on microplastic abundance for sizes >25 µm and 10-25 µm, but not for size 0.2-10 µm.

In terms of types, the influent was dominated by synthetic/regenerated cellulose, which mainly passed through the secondary sedimentation. In sludges, EVA, PUR, and PET were identified as dominant polymers.

A focused investigation into the digestion treatment revealed a significant time-dependent effect on microplastics. Notably, day 4 exhibited the highest concentration of microplastics for sizes >25 µm (7×10^6 particles per kg dried solid or 49×10^9 particles per day), and 10-25 µm (97×10^9 particles per kg dried solid or 671×10^{12} particles per day), while day 32 presented the highest number for microplastics size 0.2-10 µm (8×10^9 particles per kg dried solid or 48×10^{12} particles per day). However, the size trend analysis did not reveal a clear pattern of particle's fragmentation over the treatment period (day 0 to day 39). It is plausible that the particles underwent both fragmentation and elimination or digestion[24], given the overall decrease in microplastic numbers during the treatment period. Based on the polymer composition, Tthe persistence of all identified polymers from day 0 to day 39 in the digestion process suggests that plastics tend to endure throughout this treatment phase.

This study underscores the need for further investigations to trace the fate of plastic particles in wastewater treatment processes, especially considering that only 2% of microplastics were found in the dewatered sludge. Potential scenarios include fragmentation into smaller sizes (below 0.2 µm, for which standard methods are not yet established), separation in the fine/grit screen, or elimination during the digestion process. This additional knowledge will contribute to a more comprehensive understanding of addressing microplastics-related challenges in wastewater treatment plants.

Reference

1. Ziajahromi, S.; Neale, P. A.; Telles Silveira, I.; Chua, A.; Leusch, F. D. L., An audit of microplastic abundance throughout three Australian wastewater treatment plants. *Chemosphere* **2021,** *263*, 128294.
2. Okoffo, E. D.; O'Brien, S.; O'Brien, J. W.; Tscharke, B. J.; Thomas, K. V., Wastewater treatment plants as a source of plastics in the environment: a review of occurrence, methods for identification, quantification and fate. *Environmental Science: Water Research & Technology* **2019,** *5* (11), 1908-1931.
3. Bayo, J.; Olmos, S.; López-Castellanos, J., Removal of Microplastics from Wastewater. *Handbook of Microplastics in the Environment* **2020**, 1-20.
4. Zhang, Z.; Chen, Y., Effects of microplastics on wastewater and sewage sludge treatment and their removal: A review. *Chemical Engineering Journal* **2020,** *382*, 122955.
5. He, P.; Chen, L.; Shao, L.; Zhang, H.; Lu, F., Municipal solid waste (MSW) landfill: A source of microplastics?-Evidence of microplastics in landfill leachate. *Water Research* **2019,** *159*, 38-45.
6. Bläsing, M.; Amelung, W., Plastics in soil: Analytical methods and possible sources. *Science of The Total Environment* **2018,** *612*, 422-435.
7. Mahon, A. M.; Connell, B.; Healy, M.; O'Connor, I.; Officer, R.; Nash, R.; Morrison, L., Microplastics in Sewage Sludge: Effects of Treatment. *Environmental Science & Technology* **2016,** *51*.
8. Armbruster, D. A.; Tillman, M. D.; Hubbs, L. M., Limit of detection (LQD)/limit of quantitation (LOQ): comparison of the empirical and the statistical methods exemplified with GC-MS assays of abused drugs. *Clinical Chemistry* **1994,** *40* (7), 1233-1238.

9. Dawson, A. L.; Santana, M. F. M.; Nelis, J. L. D.; Motti, C. A., Taking control of microplastics data: A comparison of control and blank data correction methods. *Journal of Hazardous Materials* **2023,** *443*, 130218.
10. AOAC, Guidelines for standard method performance requirements-Appendix F. 2016.
11. Ziajahromi, S.; Leusch, F. D. L., Systematic assessment of data quality and quality assurance/quality control (QA/QC) of current research on microplastics in biosolids and agricultural soils. *Environmental Pollution* **2022,** *294*, 118629.
12. Luo, Y.; Qi, F.; Gibson, C. T.; Lei, Y.; Fang, C., Investigating kitchen sponge-derived microplastics and nanoplastics with Raman imaging and multivariate analysis. *Science of The Total Environment* **2022,** *824*, 153963.
13. Wu, L.; Yick, K. L.; Ng, S.; Sun, Y., Modeling of Flexible Polyurethane Foam Shrinkage for Bra Cup Moulding Process Control. *Polymers (Basel)* **2018,** *10* (5).
14. Niaounakis, M., 1 - The Problem of Marine Plastic Debris. In *Management of Marine Plastic Debris*, Niaounakis, M., Ed. William Andrew Publishing: 2017; pp 1-55.
15. Robbins, S.; Waked, E., Balance and vertical impact in sports: Role of shoe sole materials. *Archives of Physical Medicine and Rehabilitation* **1997,** *78* (5), 463-467.
16. Zhang, H.; Liu, H.; Ferro, A. R.; Vivian; Lai, A. C. K., Effects of triboelectric charging, flooring materials, relative humidity, and shoe sole materials on human walking-induced particle resuspension. *Building and Environment* **2023,** *244*, 110838.
17. Dang, M.; Li, M.; Li, J.; Liu, R.; Guo, Y.; Hou, K., Emissions of Formamide and Ammonia from Foam Mats: Online Measurement Based on Dopant-Assisted Photoionization TOFMS and Assessment of Their Exposure for Children. *Environmental Science & Technology* **2023,** *57* (14), 5646-5654.
18. Henderson, A. M., Ethylene-vinyl acetate (EVA) copolymers: a general review. *IEEE Electrical Insulation Magazine* **1993,** *9* (1), 30-38.
19. Haider, A.; Eder, A., Markets, applications, and processes for wood polymer composites (WPC) in Europe. *Processing technologies for the forest and biobased product industries* **2010**, 146-151.
20. Niska, K. O.; Sain, M., *Wood-polymer composites*. Elsevier: 2008.
21. Ghasimi, D. S. M.; Zandvoort, M. H.; Adriaanse, M.; van Lier, J. B.; de Kreuk, M., Comparative analysis of the digestibility of sewage fine sieved fraction and hygiene paper produced from virgin fibers and recycled fibers. *Waste Management* **2016,** *53*, 156-164.
22. Hanum, F.; Yuan, L. C.; Kamahara, H.; Aziz, H. A.; Atsuta, Y.; Yamada, T.; Daimon, H., Treatment of Sewage Sludge Using Anaerobic Digestion in Malaysia: Current State and Challenges. *Frontiers in Energy Research* **2019,** *7*.
23. Ward, A. J.; Hobbs, P. J.; Holliman, P. J.; Jones, D. L., Optimisation of the anaerobic digestion of agricultural resources. *Bioresource Technology* **2008,** *99* (17), 7928-7940.
24. Tang, K. H. D., Bioaugmentation of anaerobic wastewater treatment sludge digestion: A perspective on microplastics removal. *Journal of Cleaner Production* **2023,** *387*, 135864.

CHAPTER 8: CONCLUSIONS AND FUTURE STUDIES

1 Significance of this research

The proliferation of microplastics contamination in the environment has become an increasingly pressing issue over the past few decades. Research efforts aimed at understanding their impact on ecosystems have heightened awareness, leading to initiatives to monitor their abundance, particularly at wastewater treatment plants that serve as significant pathways for microplastics entering the environment. This collaborative research with South Australia (SA) Water was geared towards developing techniques for recovery, enumeration, and identification of microplastics within wastewater treatment plant systems.

This research has provided valuable insights into the presence of plastic contaminants in wastewater treatment plants. We have introduced techniques for analysing microplastics in wastewater and sludge, including a semi-automated mapping mode of FTIR Microspectroscopy (Chapter 4), which can effectively enumerate and characterize microplastics sized above 25 µm. Additionally, Flow Cytometry (Chapter 5) offers a reliable method for detecting and counting microplastics sized below 25 µm. These validated techniques have proven to be efficient for analysing microplastics in both seasonal (Chapter 6) and treatment (Chapter 7) studies, revealing the contributions of seasons and treatments to plastic loads at wastewater treatment plants. The following figure summarise this final chapter of the thesis.

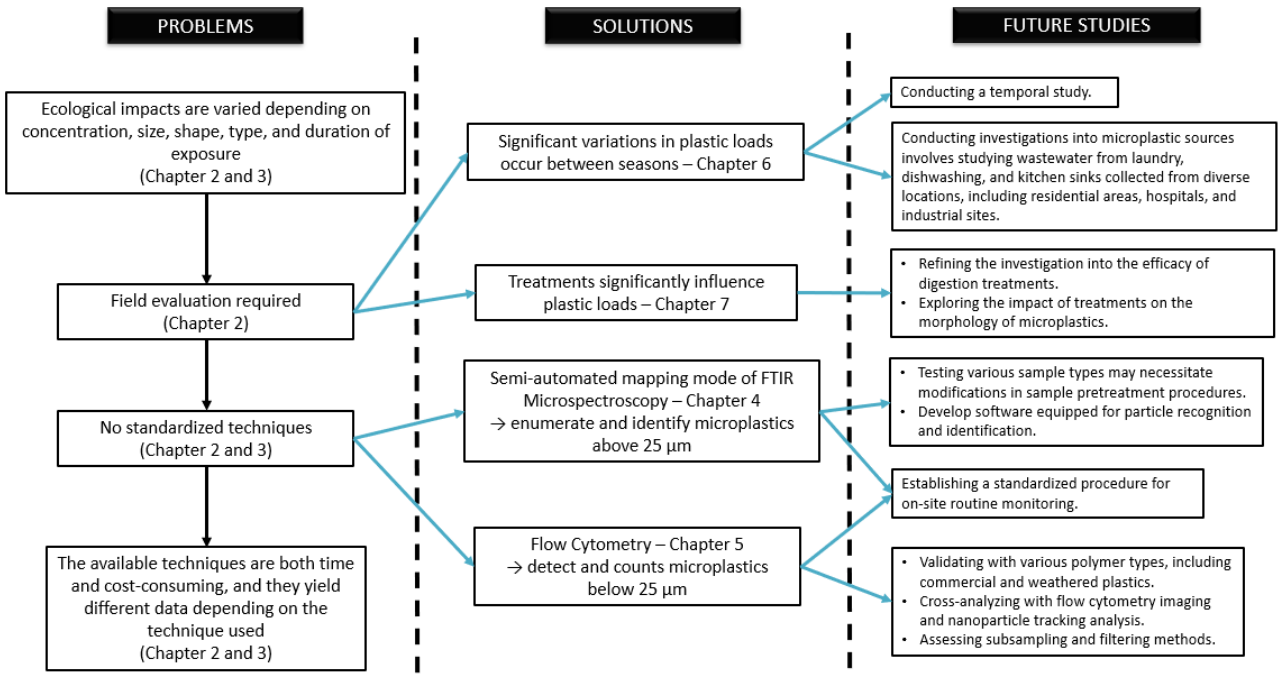

Figure 8-61. Summary of the thesis - Tracing microplastics at the wastewater treatment plant

2 Key Findings and Contributions

Key findings underscore the importance of tailored approaches for microplastic analysis, depending on particle size and environmental context. The development of a semi-automatic FTIR mapping technique for particle larger than 25 µm successfully reduced analysis time and maintained a high level of sensitivity, despite sample variability. Similarly, the introduction of Flow Cytometry for microplastics smaller than 25 µm demonstrated high recovery rates, although polymer identification remains a challenge. These technical advancements represent significant steps toward microplastics monitoring, particularly at wastewater treatment plant.

This study also revealed notable seasonal variations in microplastics abundance at wastewater treatment plants, with higher loads observed during wet seasons. Seasonal and treatment effects were shown to influence microplastics fragmentation and abundance. However, limitations such as the reliance on grab sampling techniques and the need for more efficient filtration methods were identified. Future research should aim to refine these methodologies and explore the fate of microplastics during the digestion process, particularly in relation to fragmentation and removal efficiency.

As discussed in Chapter 2, concerns about the ecological impact of microplastics, particularly in relation to biosolids applications for land use such as composting and landfill, have prompted extensive research efforts. Browne et al. [1] have suggested hypothetical modelling to assess potential ecological impacts, emphasizing the need for experimental testing to establish causality and direct effects. Existing research underscores the significance of various factors, including concentration, size, type, and duration of exposure, in determining the extent of these effects. However, establishing lethal limits for microplastics in ecosystems remains challenging due to the complexity of organism behaviours and soil compositions.

Field evaluations are essential for understanding the spatial and temporal distribution of microplastics, with geographical data coverage being crucial for comprehending their occurrence and accumulation, as noted by Rolsky et al. (2020). [2] Continuous monitoring and detailed characterization methods are vital, especially in agricultural contexts where microplastics are inevitable contaminants. Furthermore, recognizing interactions with other pollutants and identifying alternative sources of microplastics beyond biosolid applications are critical steps in mitigating their adverse effects.

Chapter 2 also reviews a variety of analytical instruments suitable for microplastics analysis, ranging from spectroscopy-based methods such as FTIR and Raman to thermoanalytical techniques such as Pyrolysis-GC/MS. The absence of standardized methods may pose challenges for practical applications, particularly in industries and analytical laboratories concerned about time and cost constraints. Therefore, a tailored approach based on specific data or information required, such as the amount (by items or mass units), type, size, and shape of microplastics, is recommended.

Chapter 3 provides a foundational background on microplastics categorization and characterization, essential for understanding their impact on the environment. It delineates a comprehensive framework for categorizing microplastics based on size, shape, colour, and origin, aiming to bring coherence and consistency to the classification of plastic debris. Essential procedures for identifying microplastics in solid samples, including collection, processing, and analysis. It emphasizes the importance of representative sample collection, which varies based on the sample's phase and source, with different tools and techniques recommended for liquid and solid samples. Sample processing involves pretreatment to isolate microplastics from their original matrices, biochemical treatments, and preconcentration to enhance the concentration of plastic particles for analysis. Density separation emerges as a time-efficient method for isolating microplastics from environmental samples, ensuring reliable analysis results.

Advanced techniques such as FTIR Microspectroscopy and Flow Cytometry are highlighted for their pivotal roles in quantifying and characterizing microplastics within various environmental matrices. These methods play significant roles in providing insights into the presence and distribution of microplastics, contributing to a comprehensive understanding of their impact on diverse ecosystem. Fourier Transform Infrared (FTIR) Microspectroscopy is effective in identifying and characterizing microplastics based on their chemical composition, though challenges such as varied shapes and thicknesses can influence spectral accuracy. Flow Cytometry, traditionally used for analysing microorganisms and cells, has emerged as a valuable tool for microplastics analysis, offering precise particle detection through light scattering and fluorescence.

3 CHAPTER 4 AND 5: Technical solutions and Future directions for reliable and robust analysis

In Chapter 4, we introduced a semi-automatic mapping technique utilizing FTIR Microspectroscopy for microplastics analysis, specifically for particles size above 25 µm in samples with high organic content such as sludge. The technique elaborated the automatic mapping and IR spectrum collection capability of the instrument with manual pin-pointing particles and a combination of software library search with human justification to interpret the collected spectrum. The technique notably reduced analysis time to 1-2 hours per sample without requiring additional investments in advanced instruments or software. Statistical analysis indicated no significant difference between small and large mapping modes, with approximately 47% of the dataset meeting a minimal 20% subsampling error criterion, showcasing reasonable accuracy despite sample variability. The investigation revealed a random and non-uniform particle distribution on filters, with over 80% of plastic types consistently detected in both mapping modes, demonstrating high sensitivity. Adherence to certain conditions, including confirming at least 80% of particles as microplastic/fibers and reporting estimated counts alongside subsampling error and plastics distribution, ensures analysis reliability.

To improve accuracy, we suggested broader sample testing, potential modifications to pretreatment processes, and the development of compatible built-in software for automatic spectrum identification, requiring collaboration with data scientists and software engineers for database integration. We also recommended conducting a study using selected polymers to evaluate the reliability of the identification process. This should involve collecting reflectance spectra at various sizes and thicknesses across multiple replicates and analysing the variance. Different search algorithms should also be considered, as they can impact the hit index, particularly those that emphasize broad peaks, which may pose challenges for reflectance spectra with broad features.

To measure microplastics size below 25 µm, we introduce Flow Cytometry technique in Chapter 5. This method, with a recovery rate of approximately 96% and tailored gating distribution settings, proves to be an effective method for providing counts of microplastics, especially those sized below 25 µm, albeit without polymer identification. However, further investigations are necessary to confirm the absence of non-plastic particles in the gating distribution set for plastic particles. Recommendations include conducting recovery rate tests with various polymer types and cross-analysing with alternative instruments like Flow Cytometry imaging and Nanoparticle Tracking Analysis to validate accuracy in detecting and counting microplastics. To mitigate the impact of subsampling, it is advised to filter all filtrate collected after 10 µm filtration through 0.2 µm and analyse it. Yet, the current filtration method may be time-consuming, prompting the exploration of more efficient techniques. Using a 96-well plate for Flow Cytometer analysis is proposed for efficient sample analysis compared to individual flow cytometry tubes, which require frequent changes for each sample. Building on these findings, further research into the effects of treatment processes on microplastics morphology is essential to understand how they behave, persist, and degrade during wastewater treatment. These insights would inform the development of more effective strategies for microplastics removal, especially in systems dealing with biosolids and organic waste.

Implementing advanced techniques such as the semi-automated mapping mode of FTIR microspectroscopy and Flow Cytometry for routine analysis at wastewater treatment plants would require an established standard operating procedure (SOP). Regular method validation, including weekly and inter-day assessments of the Limit of Detection (LOD) and Limit of Quantification (LOQ) values, would ensure that the methodologies remain accurate and reliable. These quality control measures are vital for maintaining the precision of data collected over time.

Additionally, targeted research on specific commercial and weathered microplastics like wood plastid composites (WPC) would improve the accuracy of identification and characterization. Comparing transmission mode and micro reflectance more in FTIR analysis would allow for better particle detection. Exploring potential sources of microplastics, such as wastewater from household appliances and industrial

processes, and investigating their presence in different environments such as residential, industrial, and hospital settings, would provide valuable insights into the role of urbanization in microplastics pollution.

4 CHAPTER 6 AND 7: Seasonal and treatments effects on plastic loads - Standardisation and technological advancements

To ensure reliability of micro/nanoplastics analysis, the field needs standardized protocols that can be applied globally. This includes developing universal methods for sample collection, preparation, and analysis, ensuring that results are comparable across different studies.[1] In particular, the use of both semi-automated FTIR and Flow Cytometry in routine monitoring at wastewater plants will help to standardise detection and reduce human error, increasing efficiency and accuracy. Collaborative research as in global inter-laboratory comparison should be carried out to validate methods and assess the reproducibility of results. Moreover, development of reference materials for different type of micro/nanoplastics, in different matrices (water, soil, sediment, etc), to allow for collaboration and comparison across studies.

The harmonisation of methodologies for both large and small particles, combined with advanced in software and automation, will play crucial role in shaping future monitoring systems. This direction is preferred as it will reduce the variability currently seen in microplastics research, allowing researchers, water utilities, and regulators to make more informed decisions based on robust, comparable data.

Chapter 6 examines the impacts of seasons on plastic loads at a wastewater treatment plant, revealing significant variations between seasons and treatments. Results indicate higher microplastic concentrations during wet-winter seasons (9.06×10^{11} particles per kg dried solid) compared to spring (5.50×10^{11} particles per kg dried solid) and the dry-summer season (4.41×10^{11} particles per kg dried solid in 2022, and 7.04×10^{11} particles per kg dried solid in 2023). Most of the microplastics measured fell within the 10-25 µm range (83.65%), with summer exhibiting a higher proportion in this size range. Treatment processes, particularly during summer, appeared to contribute to microplastics fragmentation, possibly to prolonged exposure to UV light and slower flow rates. Microplastics larger than 25 µm were mainly composed of polypropylene (PP) and polyvinyl chloride (PVC), with seasonal variations observed in types entering the plant. The study highlighted the seasonal influence on plastic types, including polyethylene terephthalate (PET), polyurethane (PUR), and rubber, among others.

However, comparing microplastic numbers within seasons between sampling points or treatments was limited due to the grab sampling technique used. This prompted a subsequent study to examine treatment effects, revealing that a significant portion of microplastics entering the plants were retained in dewatered sludge, with seasonal variations observed in the types of plastics. Despite these insights, it is important to acknowledge limitations such as using different techniques for enumerating plastic particles and the need for further optimization and validation of the flow cytometry technique due to sample size constraints. Future

studies should explore different plant locations or conduct spatial trend studies to complement seasonal trend data, offering valuable insights for improving microplastic treatment techniques at wastewater plants, especially considering seasonal variations.

Chapter 7 assesses how wastewater treatment processes affect microplastic abundance and characteristics, demonstrating a significant decrease in abundance from influent (86 x 10^6 particles per kg dried solid or 3610 x 10^9 particles per day) to dewatering stages (2.9 x 10^6 particles per kg dried solid or 15 x 10^9 particles per day), with plastic particles showing a trend of fragmentation into smaller size during treatment. Statistical analysis revealed a notable treatment effect on microplastic abundance for sizes >25 µm and 10-25 µm, but not for size 0.2-10 µm. The influent was predominantly composed of synthetic/regenerated cellulose, while ethyl vinyl acetate (EVA), polyurethane (PUR), and polyethylene terephthalate (PET) were dominant polymers in sludges.

Further investigation into the digestion treatment demonstrated a significant time-dependent effect on microplastics, with varying concentrations observed over the treatment period (from 1.98 x 10^6 to 7 x 10^6 per kg dry solid for size above 25 µm; and from 18 x 10^9 to 97 x 10^9 per kg dry solid for size below 25 µm) . Despite the lack of a clear pattern in particle fragmentation, the persistence of all identified polymers throughout the digestion process suggests plastic endurance during this treatment phase. Given that only 2% of microplastics were found in dewatered sludge, there is a pressing need for additional research to track the fate of plastic particles in wastewater treatment processes, potentially involving fragmentation into smaller sizes or elimination during digestion. This enhanced understanding will aid in addressing microplastics-related challenges effectively in wastewater treatment plants.

5 Future studies and Implications for Stakeholders

Some fundamental studies related to the treatments' effect on the microplastics morphology would provide some insights into microplastics' behaviour, how they could persist during the treatment processes, and what factors influencing these conditions.

Implementing both techniques, semi-automated mapping mode of FTIR microspectroscopy and Flow Cytometry, for a routine analysis at the wastewater treatment plant, requires an established standard operating procedure in place. A method verification to obtain the LOD and LOQ values needs to be performed regularly such as the beginning of each week, and inter-day variations. These values serve as a quality control system and ensure the accuracy of the data.

Further study on specific commercial or weathered microplastics such as wood plastic composites (WPC), are recommended to improve the accuracy of identification and characterization. This should include collecting spectra of specific particle using transmission mode in comparison to micro reflectance mode. Additionally,

investigating potential sources of microplastics is worthwhile, such as identifying types of microplastics/fibers in wastewater from laundry and dishwashing machines, as well as kitchen sinks. Examining different locations, such as residential, industrial, or hospital settings could provide further insights into how urbanization influences the occurrence of microplastics in the environment. Reliable quantification of microplastics has significant implications for stakeholders:

- Researchers can produce more consistent and comparable data, enhancing the reliability of studies that assess the ecological and health impacts of microplastics. For instance, analytical chemists could focus on standardizing detection and quantification techniques, microbiologist could contribute by studying the potential use of microorganisms for plastics digestion, and engineers could assist with mechanical improvements at the treatment plants to monitor and control microplastics loads entering and being discharged from the plant.[2-4]
- Water utilities and environmental organisations can develop monitoring programs that utilize multiple detection methods, allowing for more comprehensive assessment of microplastics pollution. These programs could be guided by set achievable detection limits based on validated methods and adjust protocols as newer technologies emerge. This ensuring consistent monitoring of water and waste streams.[5]
- Policy makers and regulators can establish regulations based on more accurate and reliable data, setting permissible limits for microplastics contamination in water, air, and soil.[6-8]

Public awareness and everyday practices can play a critical role in reducing the presence of microplastics in the environment.[9] One approach is to reduce the use of plastic water pies, which may release microplastics over time. Alternatives such as metal pipes, particularly those made from stainless steel or other non-corrosive materials, offer a more durable solution without the risk of microplastic contamination. For gardening, using plant pots made from natural materials like clay or wood instead of plastic pots can minimise plastic waste and contribute to a more sustainable lifestyle.

In daily activities, switching from plastic utensils to those made of glass, metal, or other eco-friendly materials is another effective practice. Glass and metal utensils are not only more durable but also reduce the demand for disposable plastic items that contribute to pollution. Encouraging these small yet impactful changes in everyday life can help reduce the overall reliance on plastic and contribute to long-term environmental sustainability. Public education on the environmental and health impacts of microplastics, along with practical alternatives, can significantly influence consumer behaviour and reduce plastic waste at the source.

This research contributes valuable insights into the detection, characterization, and treatment of microplastics in environmental systems. The technique developed and applied here, combined with an understanding of seasonal and treatment-related influences, provide a foundation for improving

microplastics monitoring and mitigation strategies. Future work should focus on enhancing the identification of smaller microplastics[10] and exploring long-term solutions for reducing their presence in the environment, particularly within wastewater systems.

By addressing the methodological gaps and further exploring the behaviour of microplastics during treatment processes, this research advances the field toward more reliable, standardised, and actionable approaches for tackling microplastics pollution.

References

1. Schymanski, D.; Oßmann, B. E.; Benismail, N.; Boukerma, K.; Dallmann, G.; von der Esch, E.; Fischer, D.; Fischer, F.; Gilliland, D.; Glas, K.; Hofmann, T.; Käppler, A.; Lacorte, S.; Marco, J.; Rakwe, M. E. L.; Weisser, J.; Witzig, C.; Zumbülte, N.; Ivleva, N. P., Analysis of microplastics in drinking water and other clean water samples with micro-Raman and micro-infrared spectroscopy: minimum requirements and best practice guidelines. *Analytical and Bioanalytical Chemistry* **2021,** *413* (24), 5969-5994.
2. Rochman, C. M.; Regan, F.; Thompson, R. C., On the harmonization of methods for measuring the occurrence, fate and effects of microplastics. *Analytical Methods* **2017,** *9* (9), 1324-1325.
3. Tang, K. H. D., Bioaugmentation of anaerobic wastewater treatment sludge digestion: A perspective on microplastics removal. *Journal of Cleaner Production* **2023,** *387*, 135864.
4. Kim, K. T.; Park, S., Enhancing microplastics removal from wastewater using electro-coagulation and granule-activated carbon with thermal regeneration. *Processes* **2021,** *9* (4).
5. Lv, X.; Dong, Q.; Zuo, Z.; Liu, Y.; Huang, X.; Wu, W.-M., Microplastics in a municipal wastewater treatment plant: Fate, dynamic distribution, removal efficiencies, and control strategies. *Journal of Cleaner Production* **2019,** *225*, 579-586.
6. Gbor, L. A. a. N. *Plastic waste in Australia and the recycling greenwash*; Australia Institute: Australia, 2024.
7. Wagner, T. P., Policy instruments to reduce consumption of expanded polystyrene food service ware in the USA. *Detritus* **2020,** *9* (March 2020), 11-26.
8. Guerranti, C.; Martellini, T.; Perra, G.; Scopetani, C.; Cincinelli, A., Microplastics in cosmetics: Environmental issues and needs for global bans. *Environmental Toxicology and Pharmacology* **2019,** *68*, 75-79.
9. Alexy, P.; Anklam, E.; Emans, T.; Furfari, A.; Galgani, F.; Hanke, G.; Koelmans, A.; Pant, R.; Saveyn, H.; Sokull Kluettgen, B., Managing the analytical challenges related to micro- and nanoplastics in the environment and food: filling the knowledge gaps. *Food Additives & Contaminants: Part A* **2020,** *37* (1), 1-10.
10. Schwaferts, C.; Niessner, R.; Elsner, M.; Ivleva, N. P., Methods for the analysis of submicrometer- and nanoplastic particles in the environment. *TrAC Trends in Analytical Chemistry* **2019,** *112*, 52-65.

APPENDIX A. SAMPLING AND COLLECTED MICROPLASTICS IMAGES

This section serves as the collection of evidence on the sampling done for this research.

All samples were collected in glass jars with metal lids, which were stored in eskies during transport and sampling. Prior to use, the jars were cleaned three times with ethanol and acetone, then dried using nitrogen gas (N_2). Nitrile gloves were worn during sampling, and both the outside of the jars and gloves were sprayed with 70% ethanol before and after sampling. Pre-treatment processes were conducted in a fume hood while wearing a cotton lab coat. All lab glassware and non-plastic labware were used, with the exception of the centrifuge tubes.

Blanks were prepared by storing 1 liter of filtered ultrapure water in a glass jar, which was then left open either during sampling at the wastewater plant or during analysis in the laboratory. The number of plastic particles detected in these negative controls was calculated and used to determine the Limit of Detection (LOD = mean +3SD), the lowest concentration where detection is feasible) and Limit of Quantification (LOQ = mean +10SD), values greater than LOQ have a higher likelihood of being true quantitative values and not random fluctuations from the blank. The LOD value was used to correct the number of microplastics counted.

Four different times of sampling for the seasonal study (Chapter 6), from September 2021 to February 2023 representing different seasons, and one sampling period, February-March 2023, for the treatment study (Chapter 7). Additionally, for each sampling period or batch, some isolated microplastics, size >25 µm, on a stainless-steel mesh were captured using an optical stereomicroscope, Olympus SZX10.

1. Seasonal study

1.1. Batch 1 - 7th September 2021 – Spring

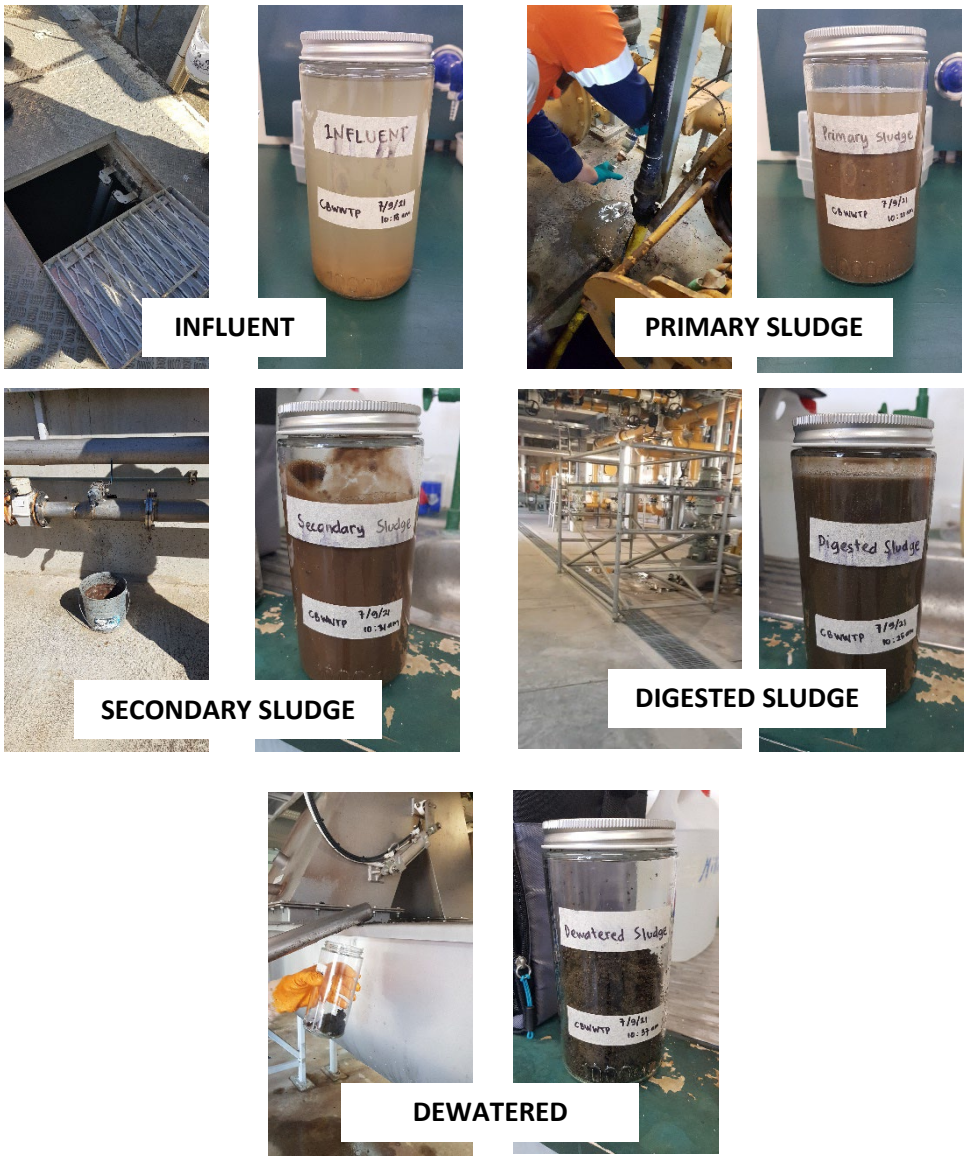

Figure A-62. Sampling points and respected samples as labelled in the captured photos for Batch 1 (September 2021 – Spring)

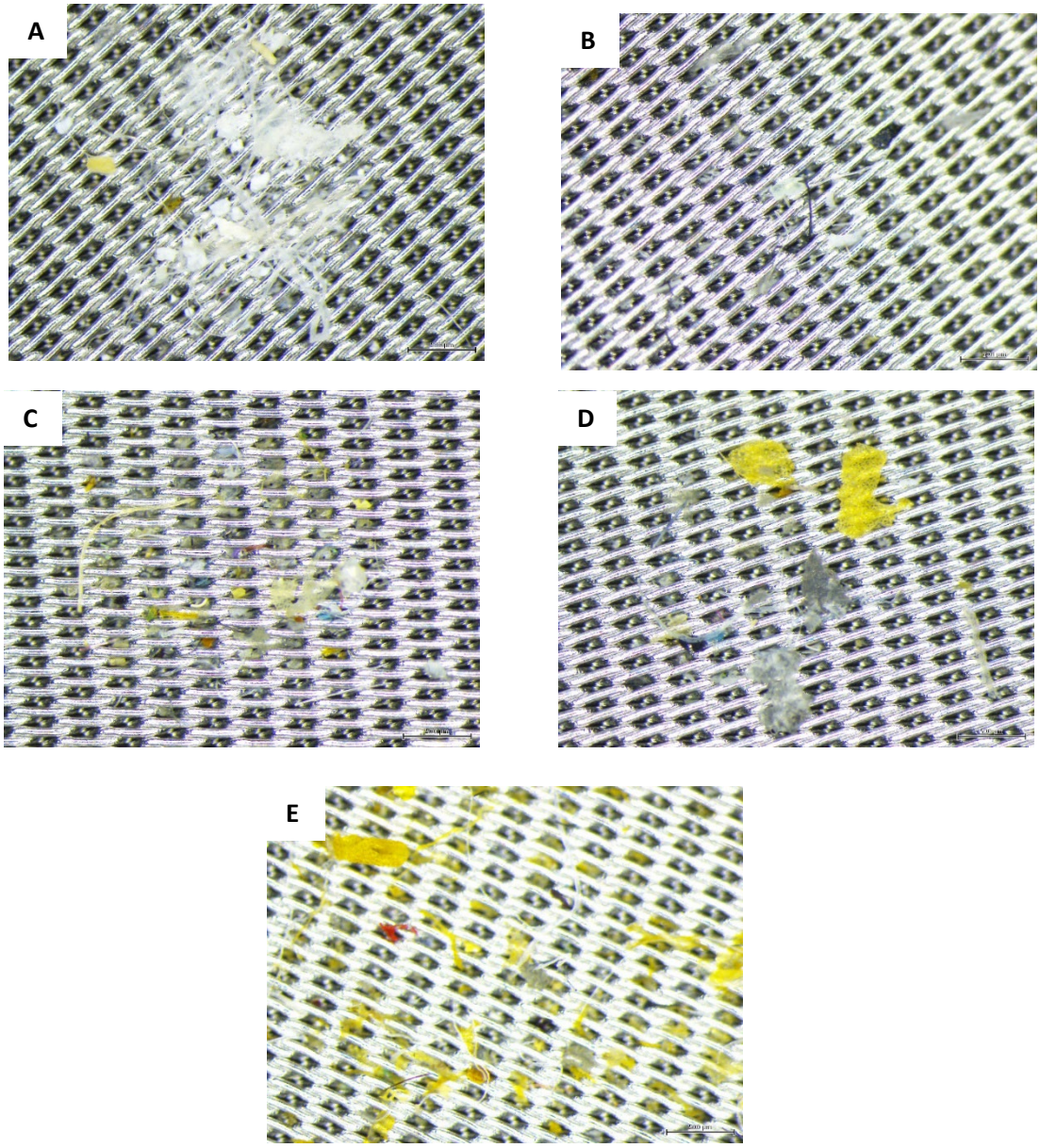

Figure A-63. Isolated plastic particles under stereomicroscope (63X; 500 µm scale bar) of (A) Influent; (B) Primary sludge; (C) Secondary sludge; (D) Digested sludge; (E) Dewatered sludge for Batch 1 (September 2021 – Spring)

1.2. Batch 2 - 24th February 2022 - Summer

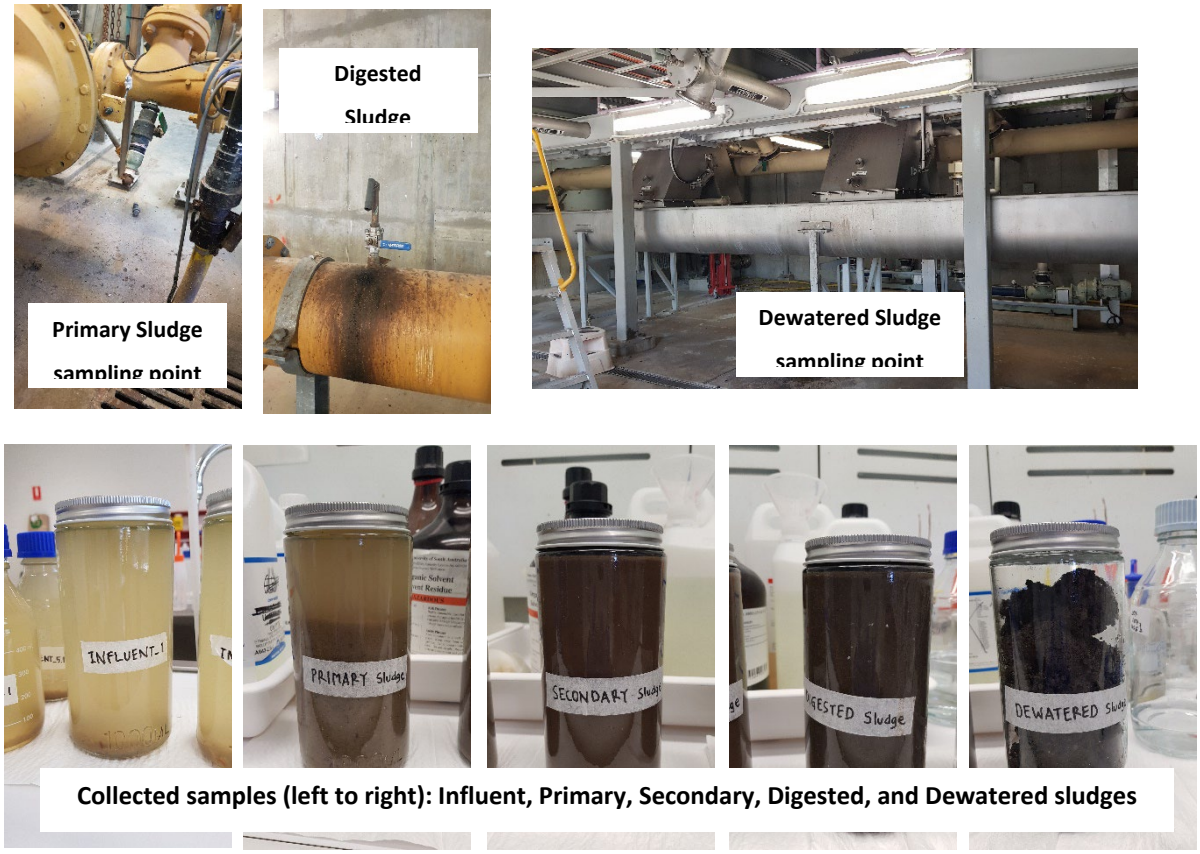

Figure A-64. Sampling points and respected samples as labelled in the captured photos for

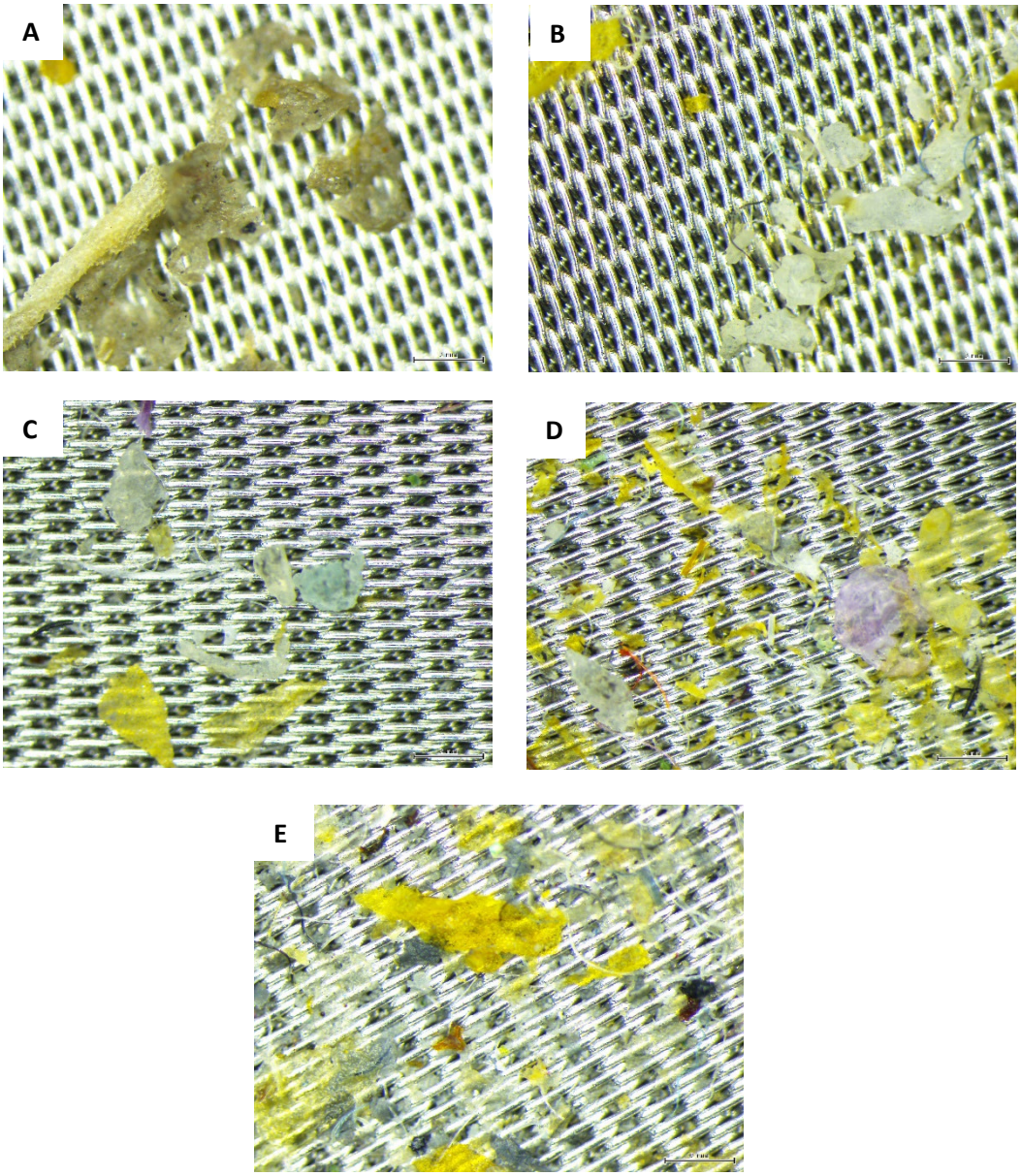

Figure A-65. Isolated plastic particles under stereomicroscope (63X; 500 µm scale bar) of (A) Influent; (B) Primary sludge; (C) Secondary sludge; (D) Digested sludge; (E) Dewatered sludge for Batch 2 (February 2022 – Summer)

1.3. Batch 3 - 8th June 2022 – Winter

Collected samples (left to right):

Influent, Primary, Secondary, Digested, Dewatered sludges, and negative field control

Figure A- 66. Collected samples as labelled in the captured photos for Batch 3 (June 2022 – Winter)

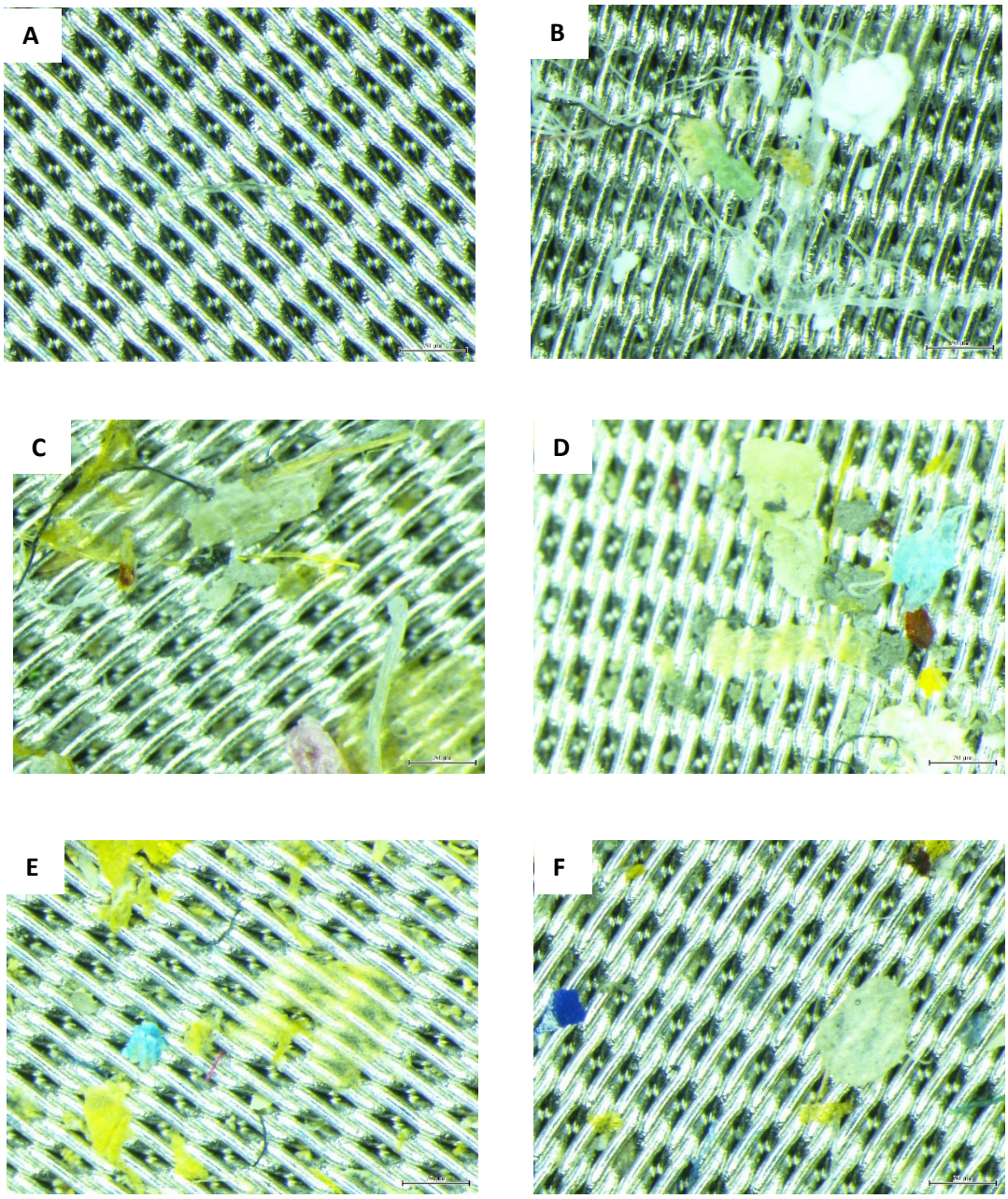

Figure A-67. Isolated plastic particles under stereomicroscope (63X; 500 µm scale bar) of (A) Negative field control; (B) Influent; (C) Primary sludge; (D) Secondary sludge; (E) Digested sludge; (F) Dewatered sludge for Batch 3 (June 2022 - Winter)

1.4. Batch 4 - 8th February 2023 – Summer

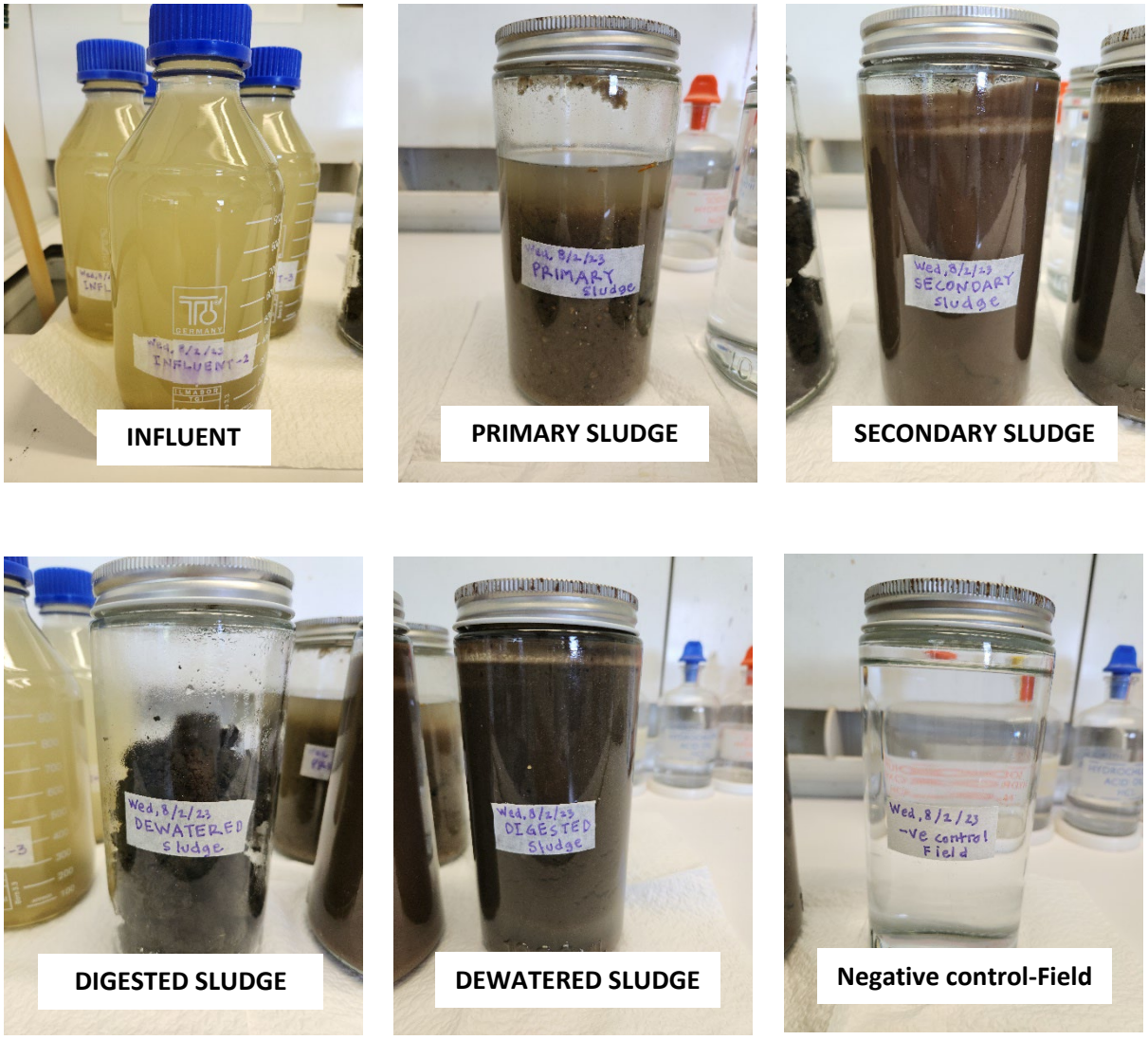

Figure A-68. Collected samples as labelled in the captured photos for Batch 4 (February 2023 - Summer)

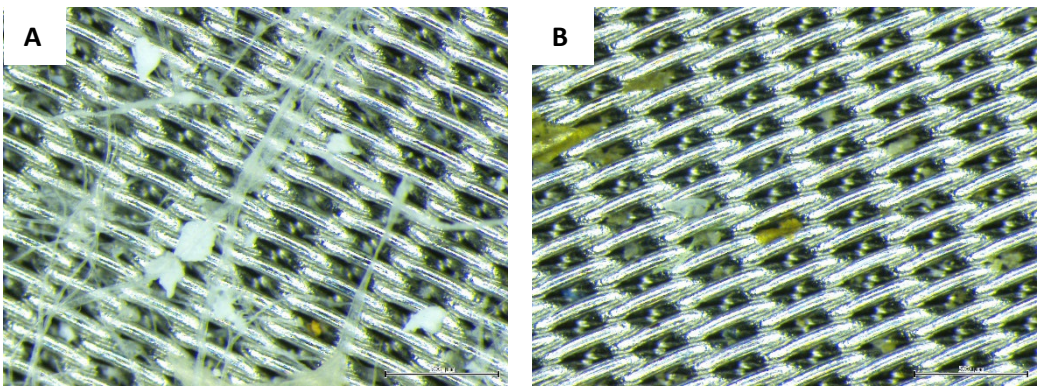

Figure A-69. Isolated plastic particles under stereomicroscope (63X; 500 µm scale bar) of (A) Influent; (B) Primary sludge for Batch 4 (February 2023 – Summer)

2. Treatment study

A set of samples representing different sampling points was collected for this study, from 13th February to 23rd March 2023. They were collected following the treatment period as presented in Figure A-9 and shown in the Table A-1 below.

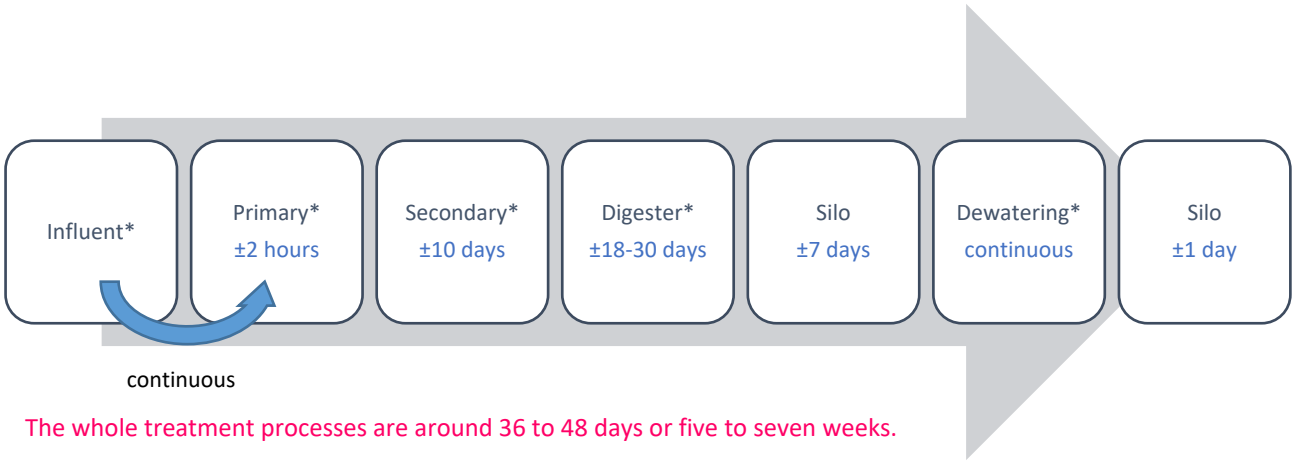

Figure A-70. Common treatments timeline at the wastewater treatment plants

Table A-31. Sampling date, time, points, and amount of collected samples respected to the treatments' timeline

Sampling date	Sampling time	Sampling point	Sample volume (L)	Notes
Monday, 13th Feb 23	10am	Influent	5	
	12pm	Influent	5	
		Primary sludge	1	
		Digested sludge	1	Day 0
Tuesday, 14th Feb 23	10am	Influent	5	
Wednesday, 15th Feb 23	10am	Influent	5	
	12pm	Influent	5	
		Primary sludge	1	
		Digested sludge	1	Day 2
Thursday, 16th Feb 23	10am	Influent	5	
Friday, 17th Feb 23	12pm	Influent	5	

		Primary sludge	1	
		Digested sludge	1	Day 4
Thursday, 23rd Feb 23	10am	Secondary sludge	1	10th day after primary sedimentation
		Digested sludge	1	Day 11
Thursday, 16th March 23	10am	Digested sludge	1	Day 32 ;21st day after secondary sedimentation
Thursday, 23rd March 23	10am	Digested sludge	1	Day 39
		Dewatered sludge	1	a week after digestion treatment

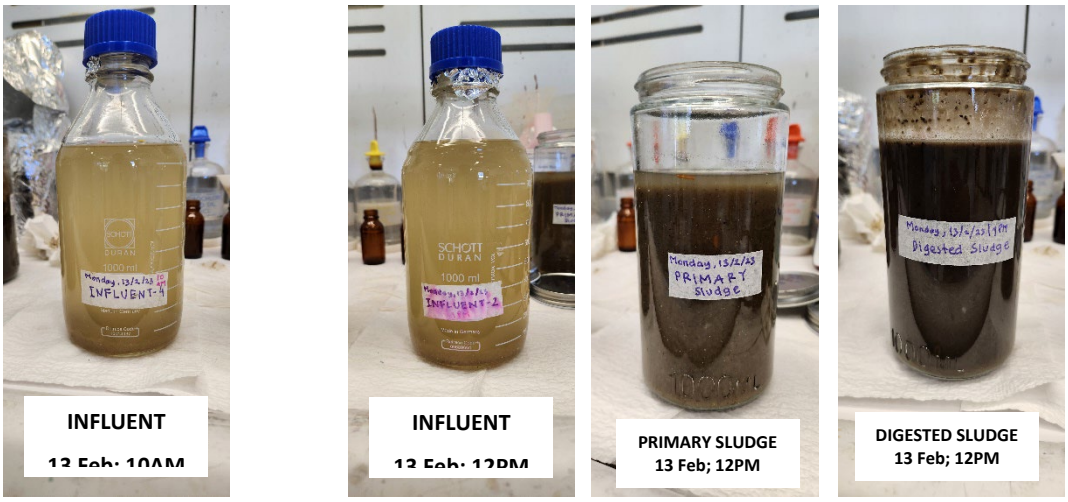

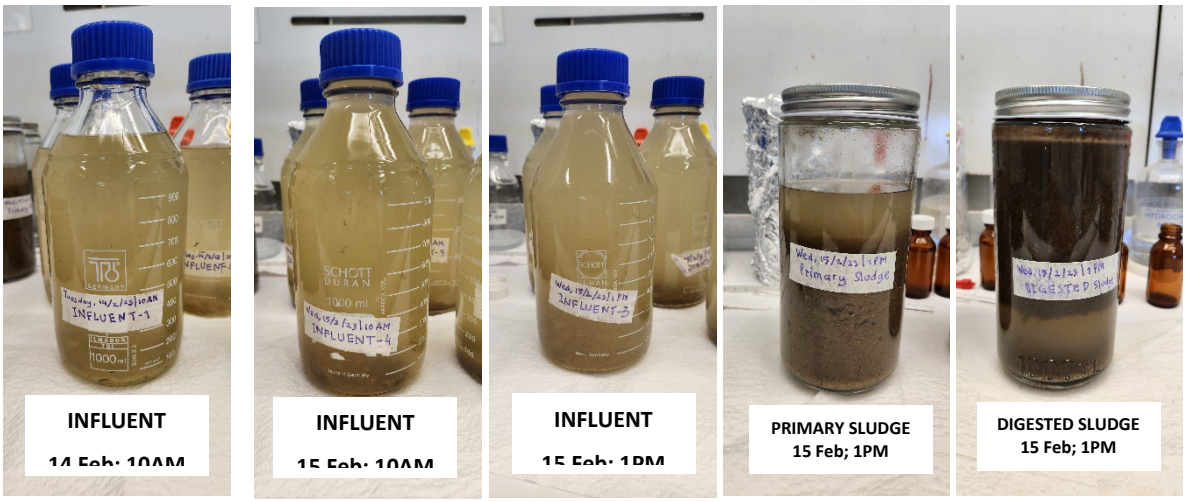

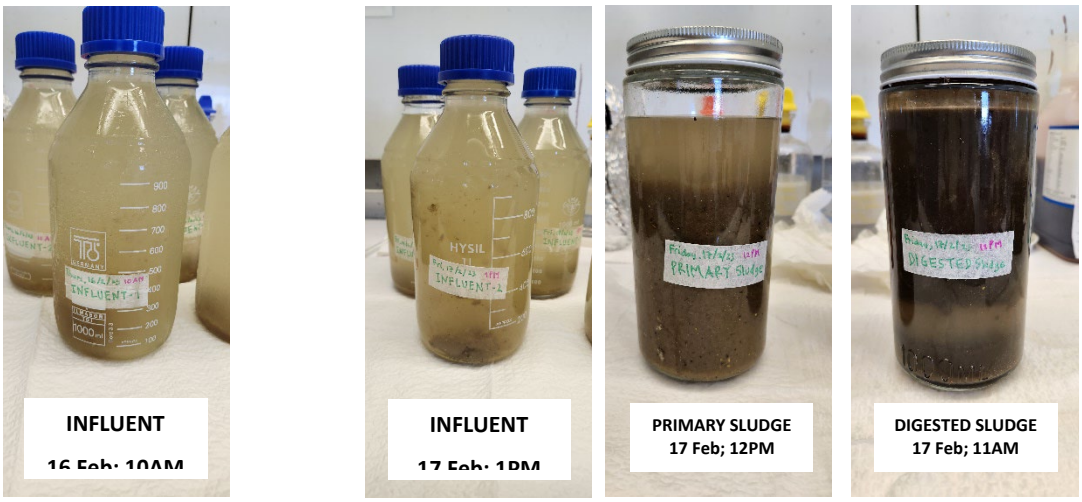

Figure A-71. Samples collected on February 13 to February 17, 2023, as labelled on each photo for treatment study (Chapter 7)

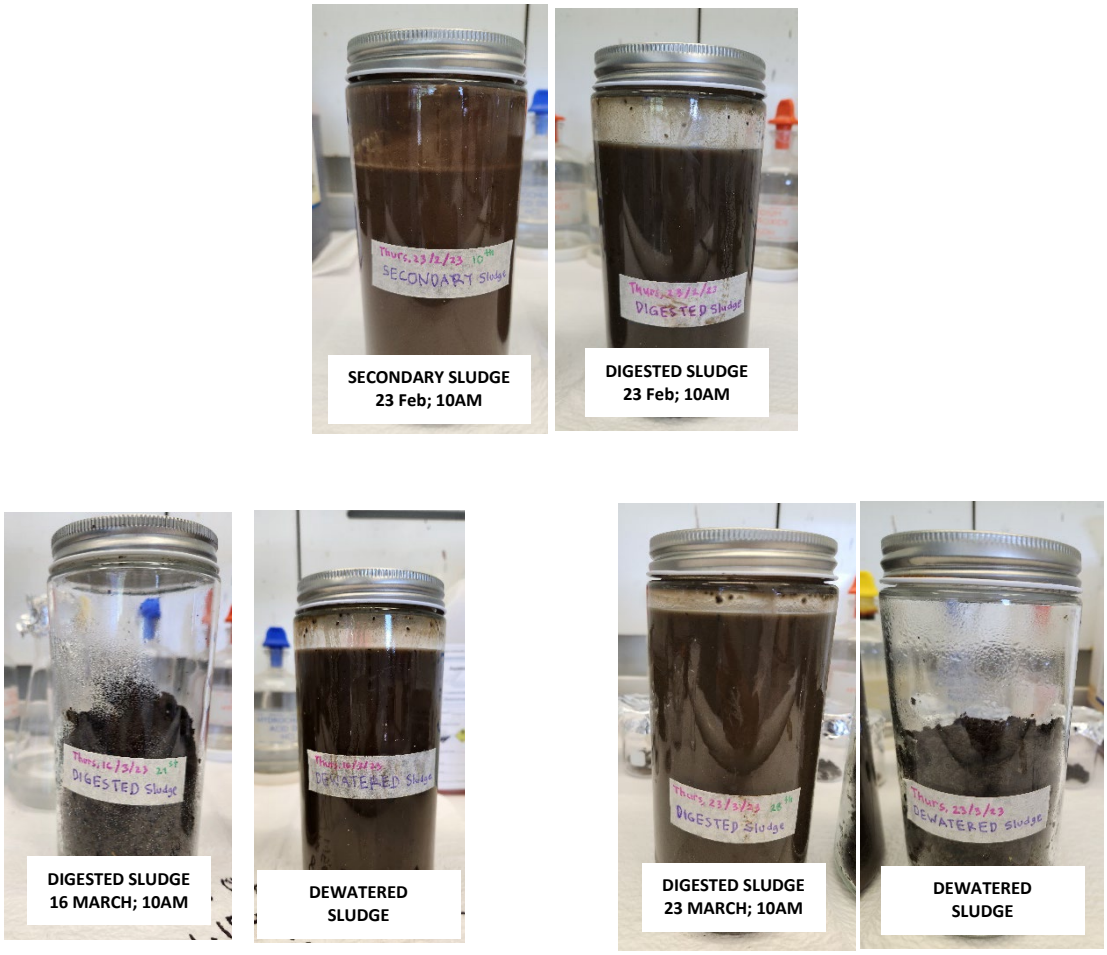

Figure A-72. Samples collected on February 23, March 16, and March 23, 2023, as labelled on each photo for treatment study (Chapter 7)

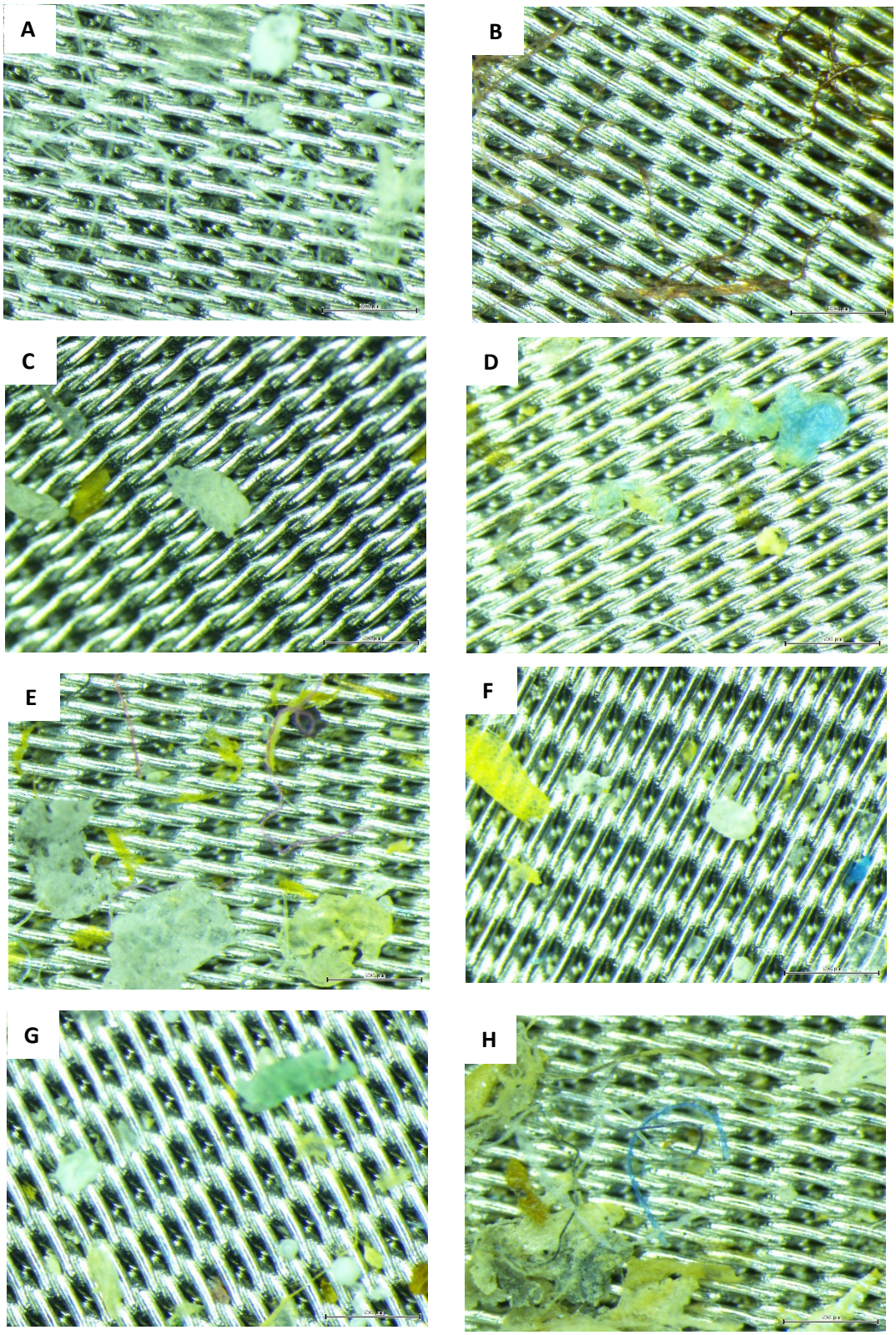

Figure A-73. Isolated plastic particles under stereomicroscope (63X; 500 µm scale bar) of (A) and (B) Influent; (C) and (D) Primary sludge; (E) and (F) Secondary sludge; (G) Digested sludge; (H) Dewatered sludge for treatment study (Chapter 7)

APPENDIX B. PRELIMINARY EXPERIMENT

A preliminary experiment was undertaken to explore various techniques commonly employed for microplastics analysis, with a specific focus on wastewater and sludge samples. The procedures encompassed sample pretreatment involving digestion and density separation, along with microplastics quantification and identification. Stereomicroscopy, FTIR microspectroscopy, and Pyrolysis-GC/MS were employed to enumerate and characterize plastic particles sized above 25 µm, while the Flow Cytometry method was tested for quantifying and identifying plastic particles sized 0.2-25 µm.

B. 1. Samples

Three distinct samples were collected and prepared for the preliminary test, labelled as A and B, representing BASR digested sludge 11.5.21 rep-1 and rep-2, respectively. Additionally, a positive control sample was prepared from the same source (400°C pre-heat), incorporating various plastic fragments including six small balls dark blue color of polyester fiber, ten white fragments of polypropylene/PP, ten blue fragments of polyethylene, and ten pink fragments of poly(lactic) acid, for calibration.

B. 2. Pretreatment

Pretreatment procedures were conducted at SA Water, involving digestion with 30% H_2O_2, Fenton reagent, and density separation using NaI, detailed as explained in Chapter 4 of this thesis. Microplastics were subsequently isolated into three size bins: >25 µm, 10-25 µm, and 0.2-10 µm.

B. 3. Stereomicroscopy and FTIR Microspectroscopy

Stereomicroscope was used to collect images of microplastics and manually count the number of particles, then some of the particles were identified using FTIR microspectroscopy. Table B-2 summarizing the results.

Table B-2. Number and type of microplastics/fibers in sludge A and B

Particles/Fibers	Image	Sludge A (items)	Sludge B (items)	Microplastics	Chemicals composition / possible sources
Blue particles	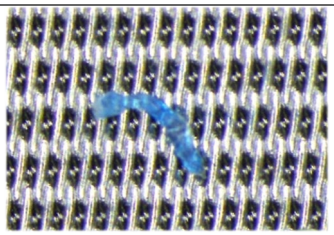	39	24	✓	Polypropylene / Various difference sources
Green particles	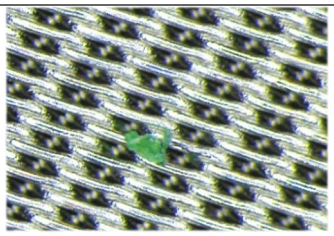	75	87	✓	Polystyrene - acrylate ester / Fiber turf
Light blue particles	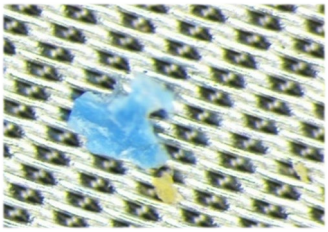	15	2	✓	Poly(vinylidene fluoride) / piping products, sheet, tubing, films, plate and an insulator for premium wire
Red particles (few different shapes)	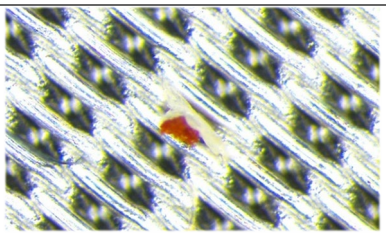	4	6	✗	Benzene / Quartz sand beach
Clear particles	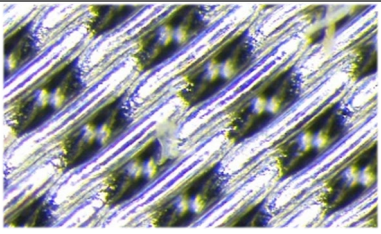	>4 (many on membrane, not counted)	many on membrane, not counted	✓	Naphthalene / Windscreen wiper rubber

Particles/Fibers	Image	Sludge A (items)	Sludge B (items)	Microplastics	Chemicals composition / possible sources
White particles	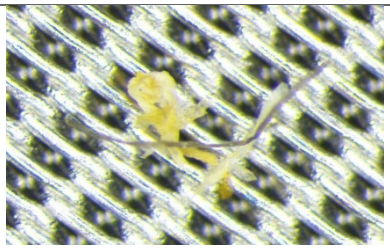	>3 (many on membrane, not counted)	Many on membrane, not counted	✓	Thrichloro acetonitrile / Sealing ring
Grey particle (long irregular shape-big)	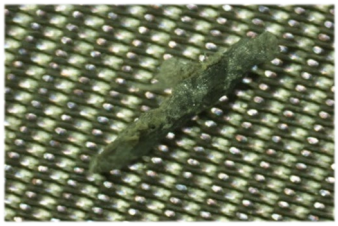	Many on membrane, not counted	2 (1 big, 1 small); many on membrane, not counted	✓	Bycyclonona-3,6(1)-diene / Synthetic rubber – commonly used for tires
Dark blue particles	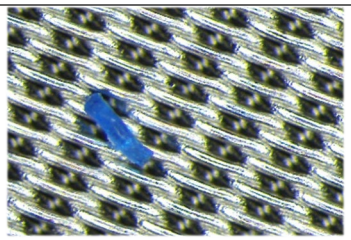	0	3	✓	Methacrylic acid / sealing ring
Shiny blue-green particles	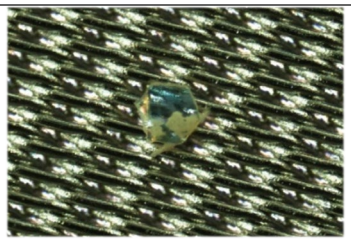	1	0	✓	Alkyd resin / paints, glitters
Black particles	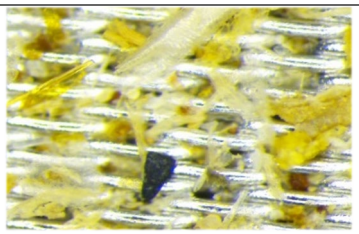	Many on membrane, not counted	Many on membrane, not counted	✓	Styrene acrylonitrile / tire rubber

Particles/Fibers	Image	Sludge A (items)	Sludge B (items)	Microplastics	Chemicals composition / possible sources
Brown particles	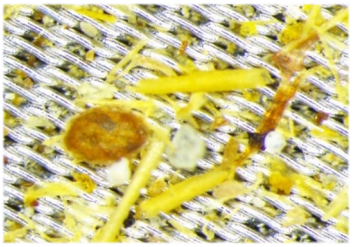	Many on membrane, not counted	Many on membrane, not counted	✓	Poly(styrene : vinylidene chloride) / food packaging coating, filters, etc
Dull-red particles	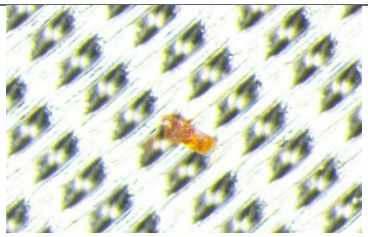	Many on membrane, not counted	Many on membrane, not counted	✓	Poly(ethylene : propylene) / various difference sources
White beads	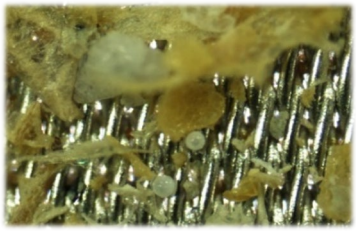	Many on membrane, not counted	Many on membrane, not counted	✓	Poly(ethylene : propylene) / microbeads – commonly used in toothpaste or personal care products
Blue fibers	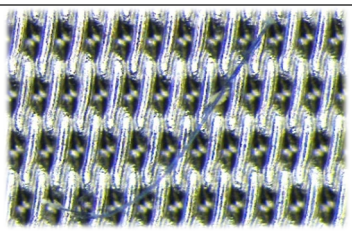	4	2	✓	Polyester satin / fabrics
Red fibers	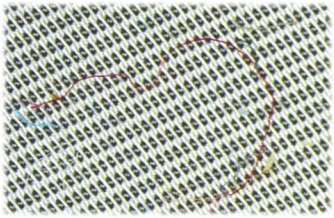	31	19	✓	Polyacrylonitrile – modified acrylics / sweater, tracksuits, boots, gloves, carpets

Particles/Fibers	Image	Sludge A (items)	Sludge B (items)	Microplastics	Chemicals composition / possible sources
Green fibers	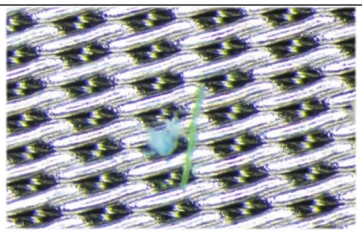	8	11	✓	Phenyl phosphate / used as flame-retardant additive
Black fibers	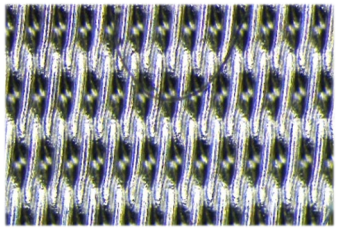	80	81	✓	Vinyl chloride_vinyl acetate_maleic acid – modified acrylics / sweater, tracksuits, boots, gloves, carpets
Clear fibers	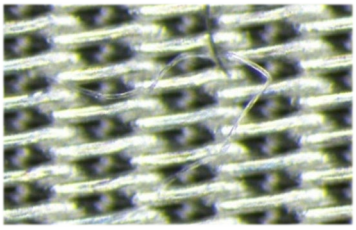	110	64	✓	Polypropylene + poly(ethylene : propylene) / clothing, apparel, ropes, food labels and packaging
Brown fibers	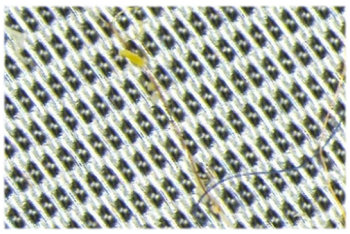	2	5	✓	Polyurethane acrylic resin / insulation, elastomers, adhesives, and foam liners for clothing
	TOTAL microplastics/fibers	>365	>298	In 500mL of digested sludge	

Stereomicroscopy was utilized to capture images and manually count microplastics, with subsequent identification using FTIR microspectroscopy. However, the time-consuming nature of manual counting

prompted the exploration of alternatives, such as the "siMPle" software developed by Primpke et.al. (2020). [1] While this software was incompatible with our instruments, we developed a semi-automated mapping technique to expedite particle counting as presented in Chapter 4 of this thesis.

B. 4. Pyrolysis-GC/MS

Pyrolysis-GC/MS, chosen for its time efficiency, provided insights into total plastic mass and polymer types. The instrument setting as follows:

Pyrolysis → 700ºC for 20 seconds; Interface 300ºC

Split ratio → 1:50

Flow rate → 1.3 mL/min

Pressure → 9.8 psi

Oven → from 40ºC (2 min hold) to 300ºC at 10ºC/min (30 min run time)

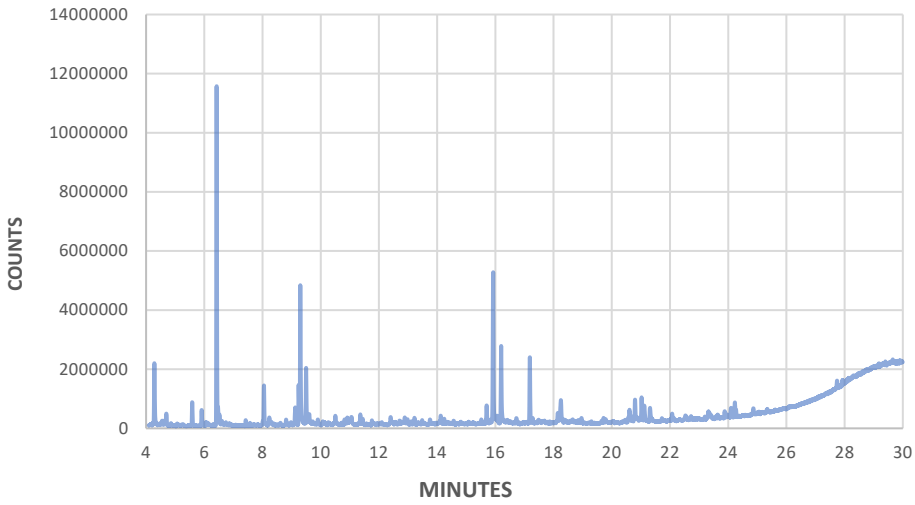

Figure B-13. Pyrograms of sludge A

Table B-3. Type of microplastics found in sludge A based on the pyrogram indicator compound

Indicator compound	RT (min)	Type of polymer	Ref
2,4-dimethyl-1-heptene	5.582	Polypropylene	In house
o-xylene	6.065	Vinyl chloride/vinyl acetate	Watanabe, et al (2011)[2]
Styrene	6.425	Polystyrene	In house

α-Methylstyrene	8.051	Polystyrene	In house
Pentanedinitrile, 2-methylene-	9.298	Polyacrylonitrile	Watanabe, et al (2011)[2]
Naphthalene	11.362	Polyvinyl chloride	Watanabe, et al (2011)[2]
Biphenyl	14.122	Polyester fiber	In house

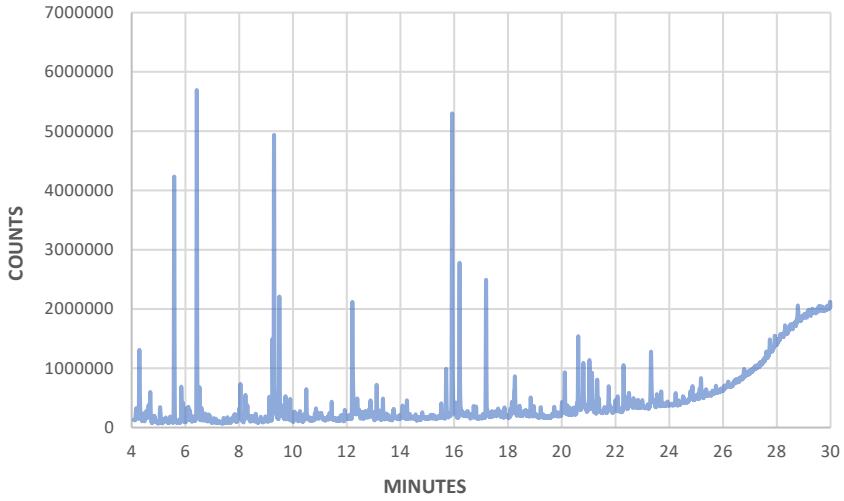

Figure B-14. Pyrograms of sludge B

Table B-4. Type of microplastics found in sludge B based on the pyrogram indicator compound

Indicator compound	RT (min)	Type of polymer	Ref
2,4-dimethyl-1-heptene	5.34	Polypropylene	In house
Styrene	6.421	Polystyrene	In house
α-Methylstyrene	8.046	Polystyrene	In house
Pentanedinitrile, 2-methylene-	9.298	Polyacrylonitrile	Watanabe, et al (2011)[2]
1-Undecene	9.898	Polyethylene (HDPE)	Watanabe, et al (2011)[2]
1-Tetradecene	11.441	Polyethylene (HDPE)	Watanabe, et al (2011)[2]

As shown in Figure B-13 and Table B-3, some microplastics were found in sludge A including polypropylene, vinyl chloride, polystyrene, polyacrylonitrile, and polyester. Similar type of microplastics found in sludge B,

with additional polyethylene, but not for polyester and vinyl chloride (Figure B-14 and Type of microplastics found in sludge B based on the pyrogram indicator compound. This technique, pyrolysis-GC/MS, had been proven to be used to detect microplastics in sludge samples. We were planning to progress using the method for quantifying microplastics.

The technique, while successful in detecting various microplastics in sludge samples, faced challenges related to instrument sensitivity (1 µg), sample transfer (manually using tweezer), and pyrolyzer temperature (could not reached desired temperature, 700°C).

B. 5. Flow Cytometry

Flow Cytometry was employed to count and identify microplastics sized 0.2-10 µm. Although it successfully detected and counted standard polymer references as shown in Figure B-15 (5633 counts/mL, 6733 counts/mL, and 1775 counts/mL of LDPE, PMMA, and PVC, respectively), it could not differentiate between polymer types based on their distribution (Figure B-16).

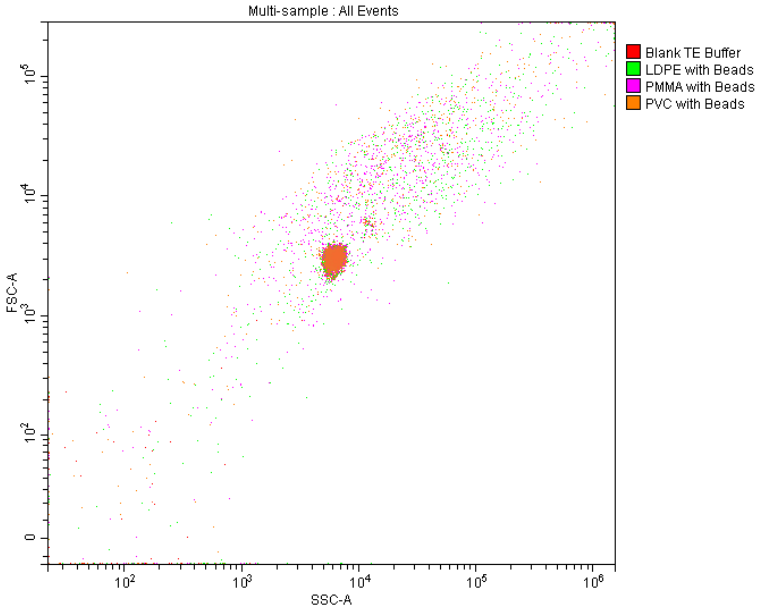

Figure B-15. Cytograms of LDPE, PMMA, and PVC standard reference polymers

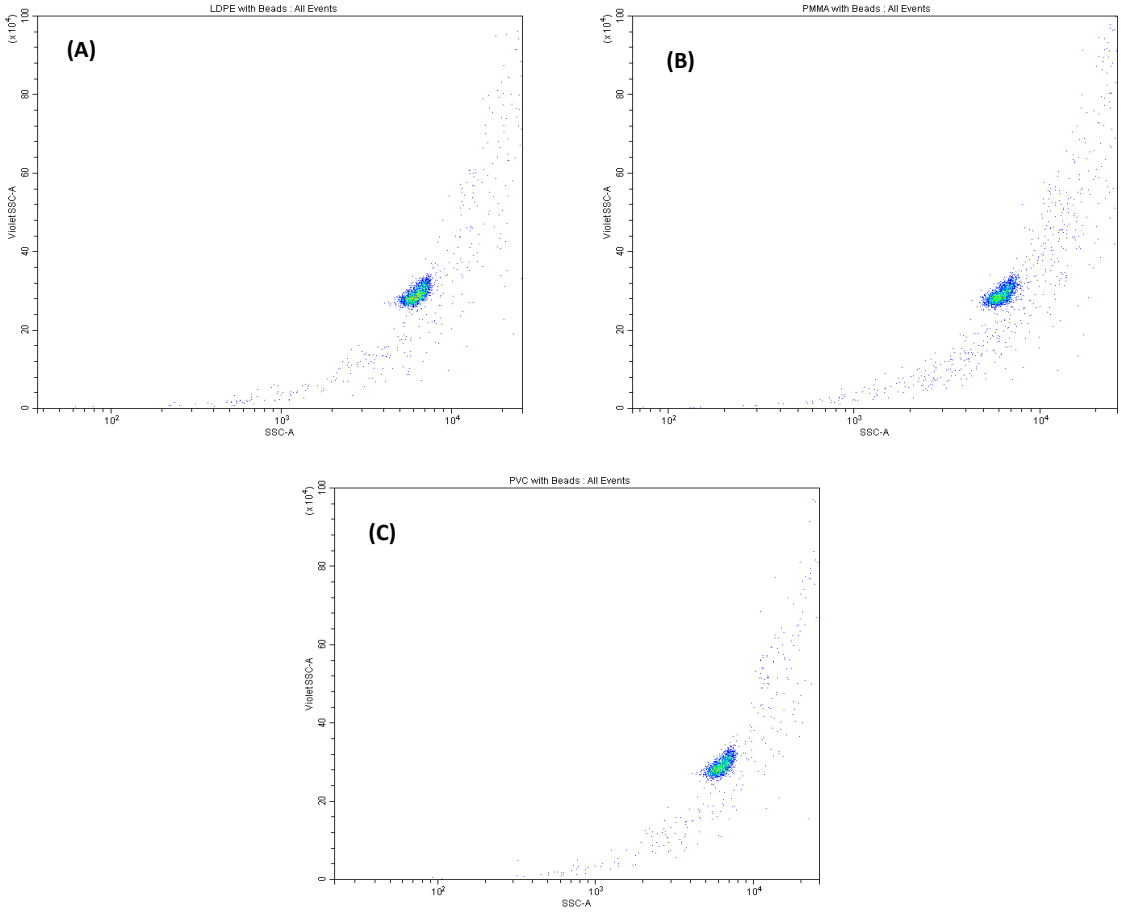

Figure B-16. Individual cytogram of (A) LDPE; (B) PMMA; and (C) PVC

B. 6. Evaluations

Observations from the preliminary experiments, summarized in Table B-5, guided decisions on progressing with the development and optimization of FTIR microspectroscopy with a mapping mode Chapter 4 of this thesis) and Flow Cytometry (Chapter 5 of this thesis). Both methods were deemed suitable for covering the size bins of isolated microplastics/fibers, specifically above 25 µm and 0.2-25 µm, respectively.

Table B-5. Summary of preliminary experiments results and evaluations of each possible techniques for analysing microplastics in wastewater and sludge samples

Methods	Mode	Data	Time (per sample)	Validation (recovery rate)	Verification (LOD & LOQ)	Cost
FTIR Microspectroscopy	Single spectrum	• Type/chemical characteristics • Counts (in combination with stereomicroscope)	1 week	90%	For MPs >25 µm	Instruments available, but need to calculate consumables and analysis costs
	Mapping 1 (without "siMPle" image analysis	• Type/chemical characteristics • Counts (pin-point MPs using FTIR imaging program)	2-3 days	Not tested yet	For MPs >25 µm	Instrument available, but need to calculate consumables and analysis costs
	Mapping 2 (with "siMPle" image analysis	• Type/chemical characteristics • Counts • Size	2-3 days	Not tested yet	For Mos >25 µm	Instrument available, but need to calculate consumables and analysis costs
Pyrolysis-GC/MS	Resuspend MPs in solvents i.e., dichloromethane	• Total mass/concentration • Type of polymers	1 hour	Not tested yet, some MPs/MFs still left on the filter	Less than 0.1 mg (need further test)	Instrument available, but need to calculate consumables and analysis costs
	Without solvent	• Type of polymers	1 hour	Not tested yet	Less than 0.1 mg (need further test)	Instrument available, but need to calculate consumables and analysis costs
	In combination with ASE (Accelerated Solvent Extraction)	• Total mass/concentration • Type of polymers	Need to be tested when the	>80%[3]	Less than 2 µg[3]	$71.8K (Thermo Fisher)

			instrument available			
Flow Cytometry	Violet/Blue lasers-FITC green beads	• Type of polymers (limited) • Counts • Size range	15 minutes	Not tested yet	0.2 – 150 µm (need further test)	Instrument available, but need to calculate consumables and analysis costs

For FTIR microspectroscopy, the need for a representative database led to efforts in enriching the spectrum database with commercial and weathered plastics. The open library published by De Frond et.al (2021) [4] was added, and some spectrum to the in-house library database were shared in Appendix G of this thesis. Additionally, challenges encountered in Py-GC/MS, including sample transfer and identifying plastic sources, prompted considerations for further improvement.

References

1. Primpke, S.; Cross, R. K.; Mintenig, S. M.; Simon, M.; Vianello, A.; Gerdts, G.; Vollertsen, J., Toward the Systematic Identification of Microplastics in the Environment: Evaluation of a New Independent Software Tool (siMPle) for Spectroscopic Analysis. *Applied Spectroscopy* **2020,** *74* (9), 1127-1138.
2. Watanabe, C.; Ohtani, H.; Tsuge, S. In *Pyrolysis - GC/MS Data Book of Synthetic Polymers: Pyrograms, Thermograms and MS of Pyrolyzates*, 2011.
3. Okoffo, E. D.; Ribeiro, F.; O'Brien, J. W.; O'Brien, S.; Tscharke, B. J.; Gallen, M.; Samanipour, S.; Mueller, J. F.; Thomas, K. V., Identification and quantification of selected plastics in biosolids by pressurized liquid extraction combined with double-shot pyrolysis gas chromatography–mass spectrometry. *Science of The Total Environment* **2020,** *715*.
4. De Frond, H.; Rubinovitz, R.; Rochman, C. M., µATR-FTIR Spectral Libraries of Plastic Particles (FLOPP and FLOPP-e) for the Analysis of Microplastics. *Anal Chem* **2021,** *93* (48), 15878-15885.

APPENDIX C. EFFECT OF DIGESTION ON PLASTIC IDENTIFICATION

The aim was to study the effect of the digestion procedure, using H_2O_2 and Fenton reagent, on the identification of plastic particles. Six different standard polymers namely LDPE, PP, PET, PS, PVC, and PMMA, with size range from 25 µm to 1 mm, were used in this experiment.

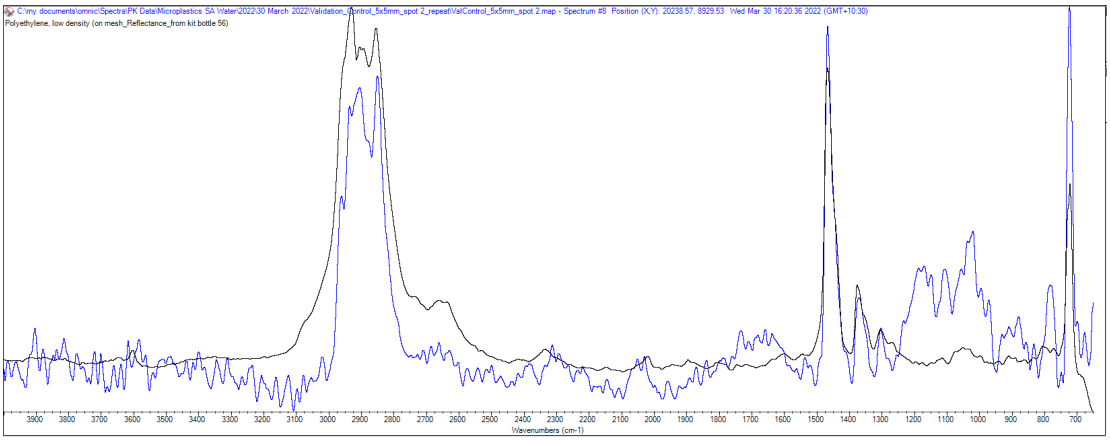

Figure C-17. IR spectrum of LDPE, with (blue spectrum) and without (black spectrum) digestion. HQI = 81%

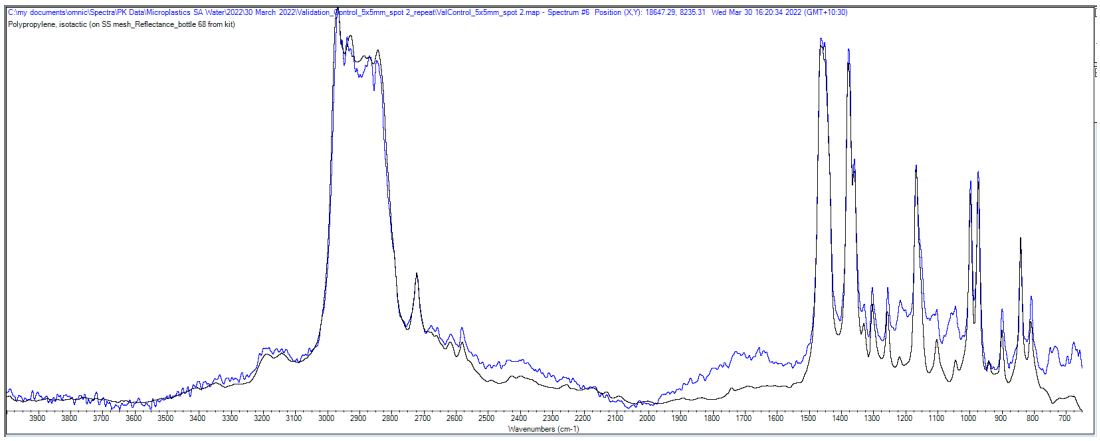

Figure C-18. IR spectrum of PP, with (blue spectrum) and without (black spectrum) digestion. HQI = 96%

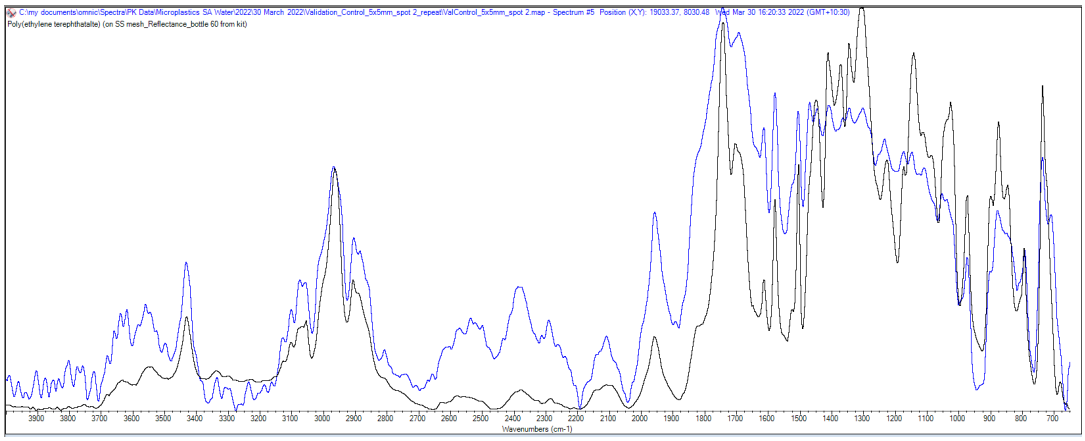

Figure C-19. IR spectrum of PET, with (blue spectrum) and without (black spectrum) digestion. HQI = 69%

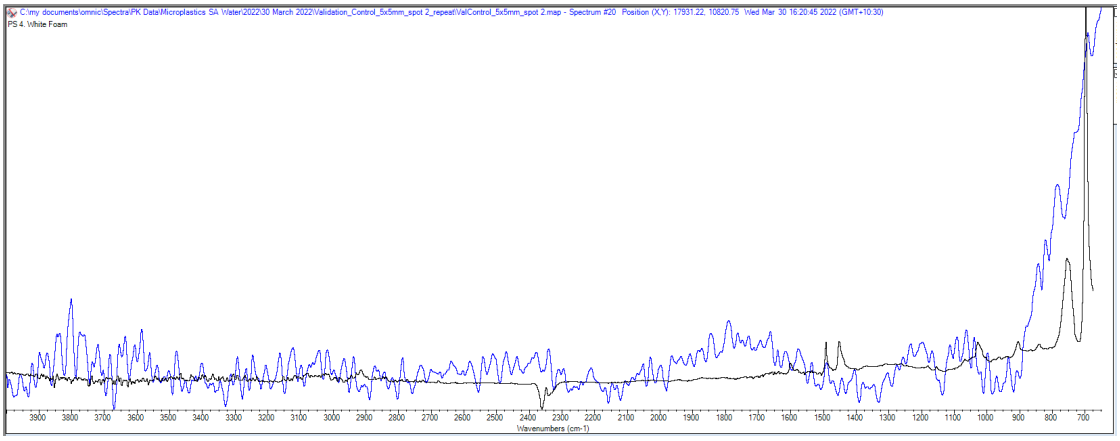

Figure C-20. IR spectrum of PS, with (blue spectrum) and without (black spectrum) digestion. HQI = 82%

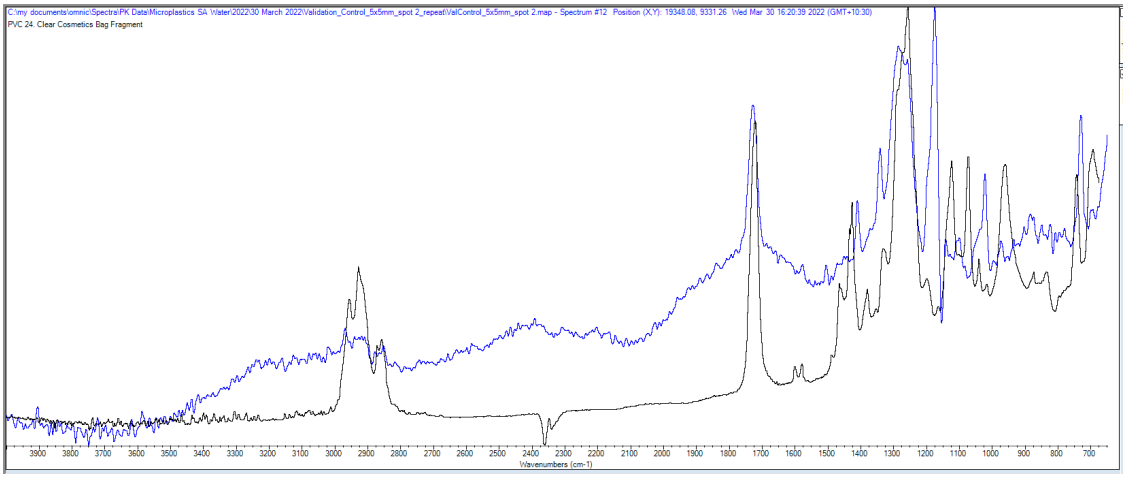

Figure C-21. IR spectrum of PVC, with (blue spectrum) and without (black spectrum) digestion. HQI = 79%

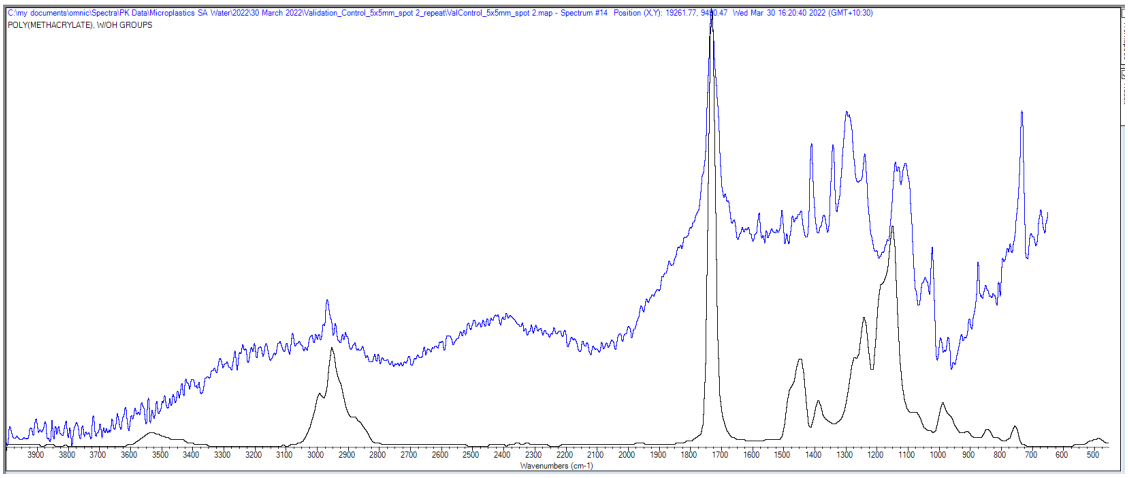

Figure C-22. IR spectrum of PMMA, with (blue spectrum) and without (black spectrum) digestion. HQI 88%

APPENDIX D. CHAPTER 6 - RECOVERY RATE

Experiments dates: April-May 2022.

Pure standard polymer references used from kit: PP, HDPE, LDPE, PS, PET, PMMA, and PVC. Particles with size range from 25 µm to 1 mm were prepared using a metal coffee grinder and/or nail file to fragment the pellets, then suspended in ethanol, followed by filtration with 1 mm and 25 µm. Collected particles were washed with ethanol and air-dried before used. These particles were spiked into one gram of dried sludge and treated following the pretreatment procedure involving the hydrogen peroxide and Fenton reaction. Collected particles were observed under the microscope and their infrared spectrum were collected with FTIR microspectroscopy (Figure D-23). The spectrum before and after the pretreatment processes were compared and the HQI (Hit Quality Index) percentage were all above 65% (Table D-6)

Sample: Digested sludge

Validation A: 70 particles (10 each type) → 66 particles (**94%**) detected → 14 particles (**20%**) confirmed as spiked polymers

Validation B: 49 particles (7 each type) → 47 particles (**96%**) detected → 10 particles (**20%**) confirmed as spiked polymers

Validation C: 35 particles (5 each type) → 34 particles (**97%**) detected → 8 particles (**20%**) confirmed as spiked polymers

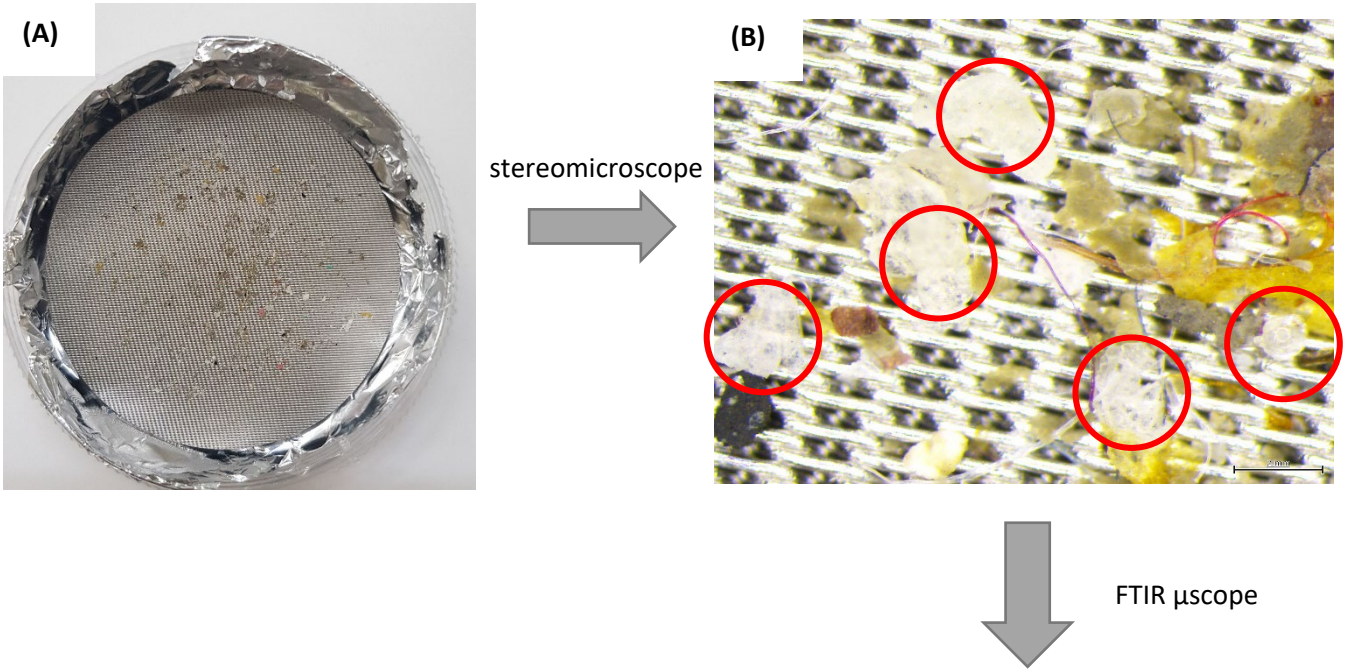

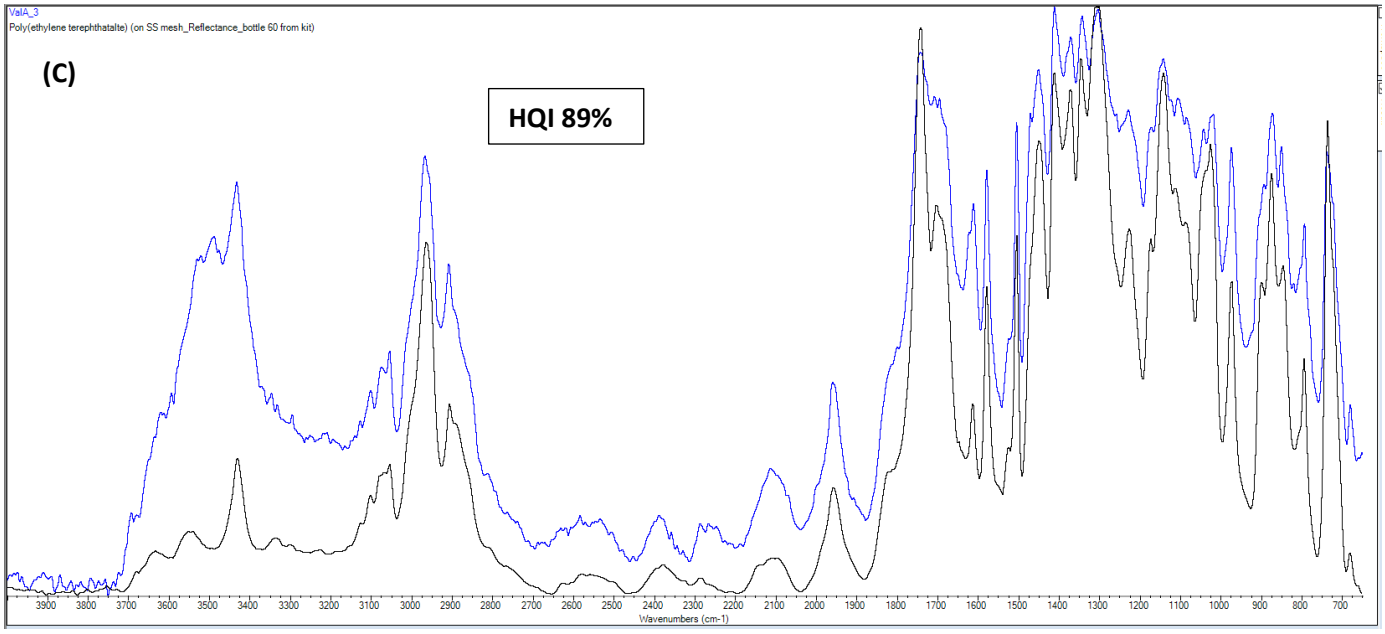

Figure D-23. (A) Particles on the mesh; (B) Reference polymers (red circle); (C) Spectrum of PET before and after treatment

<u>Physical and chemical changes showed in the following table:</u>

black spectrum = before treatment; blue spectrum = after treatment

Table D-6. Polymers standard before and after treatments

Polymer type	Before pretreatment	After pretreatment	IR spectrum
Polypropylene / PP	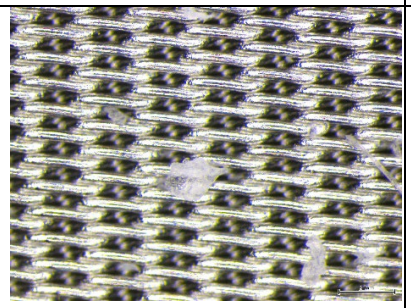	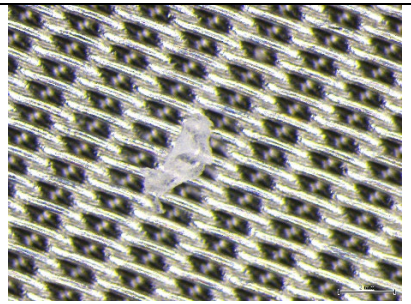	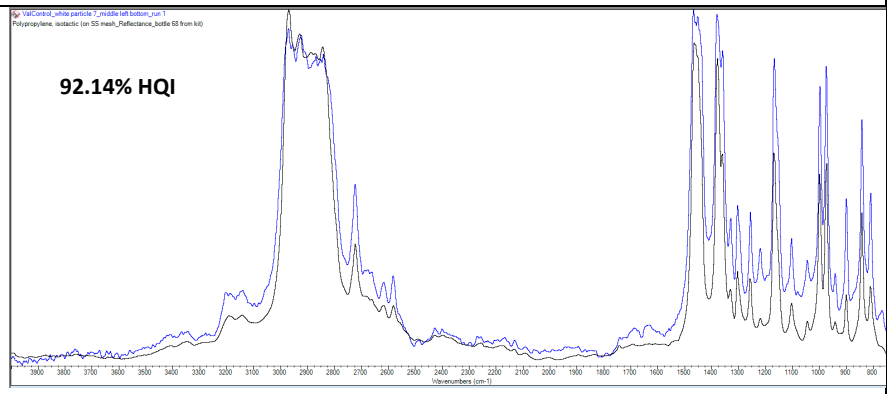
Polyethylene Terephthalate / PET	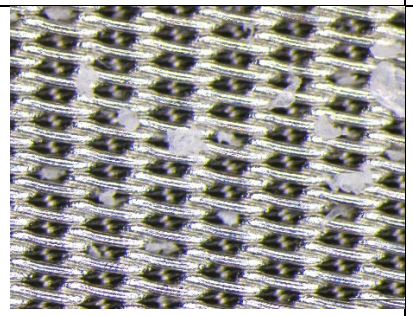	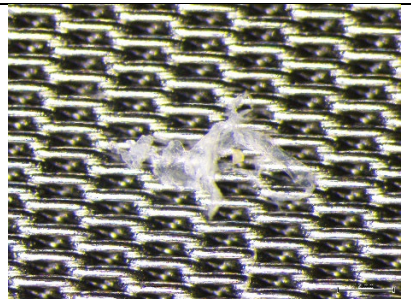	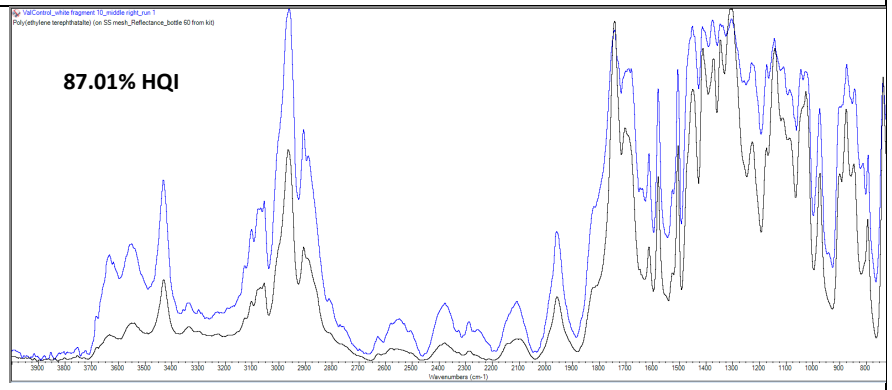

Polymer type	Before pretreatment	After pretreatment	IR spectrum
Low density Polyethylene/ LDPE	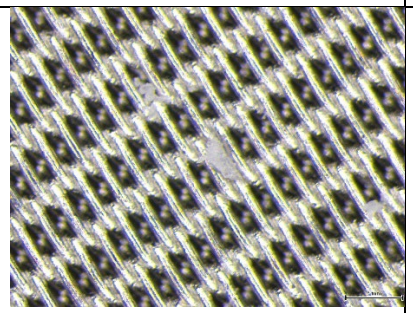	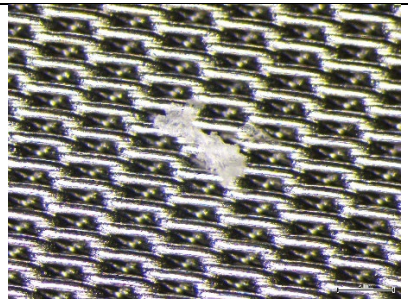	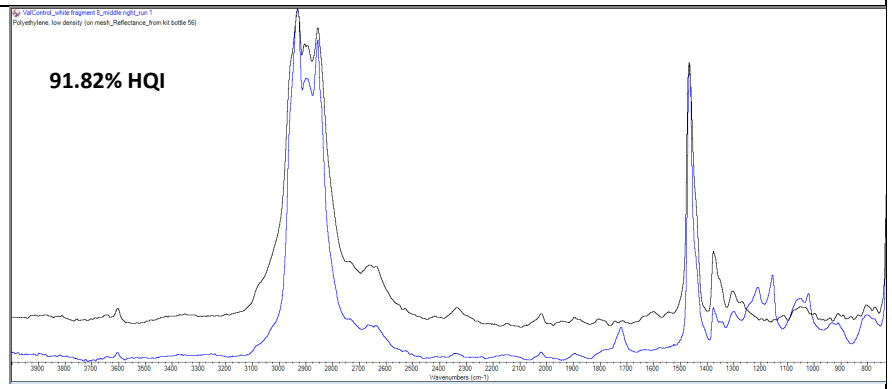
High density Polyethylene/ HDPE	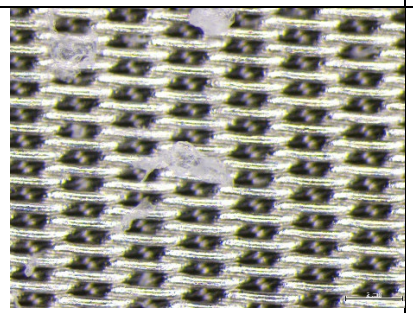	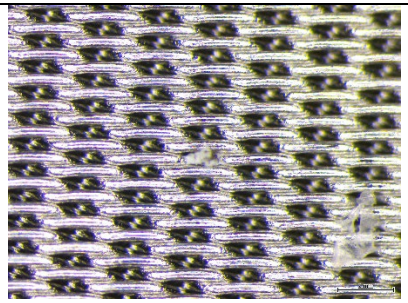	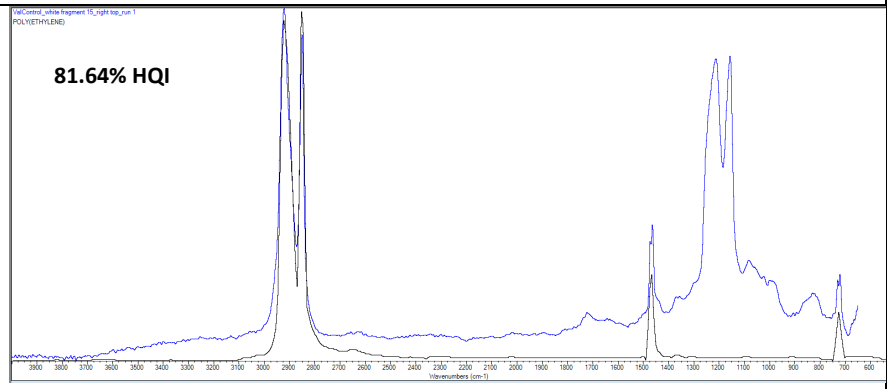

Polymer type	Before pretreatment	After pretreatment	IR spectrum
Polystyrene/ PS	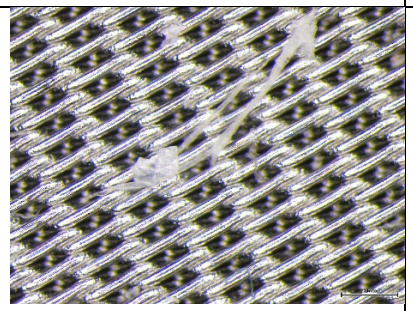	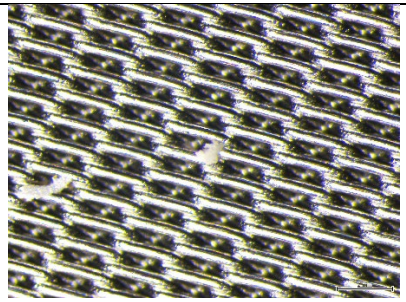	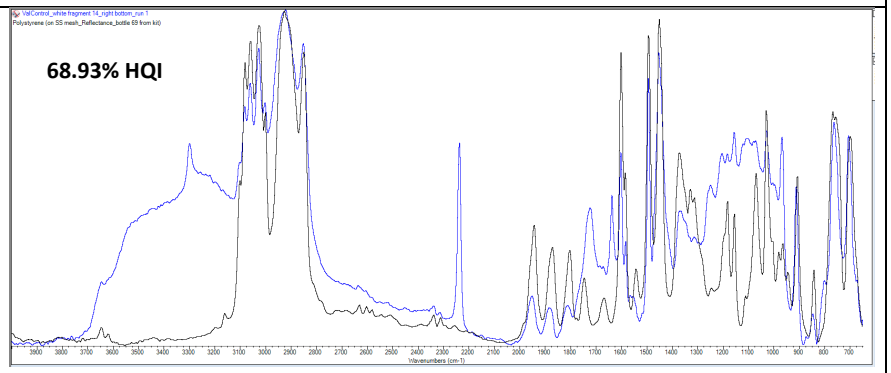
Poly Vinyl Chloride/PVC	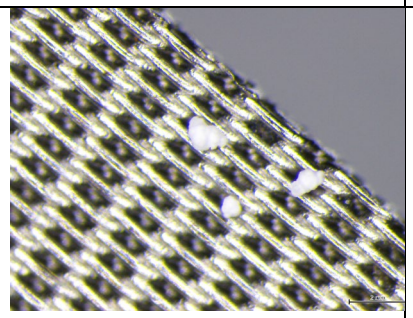	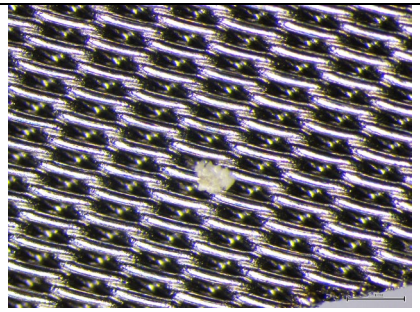	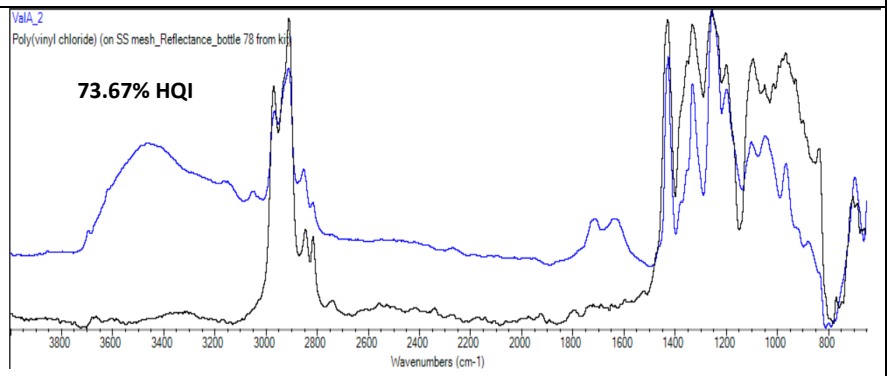

Polymer type	Before pretreatment	After pretreatment	IR spectrum
Poly Methyl Methacrylate/ PMMA	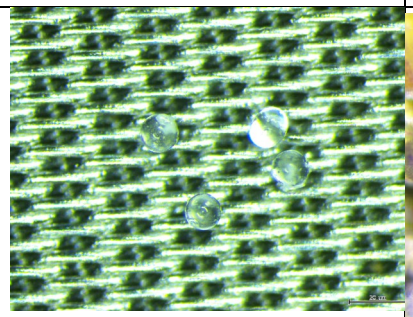	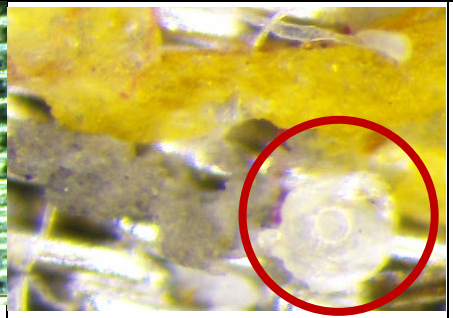	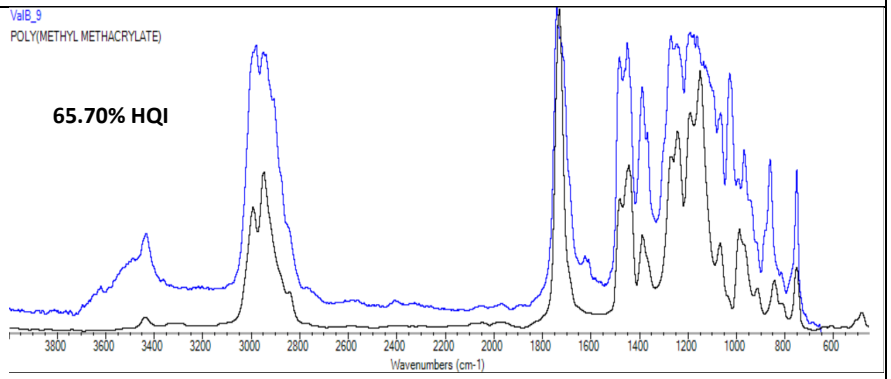

APPENDIX E. EXPERIMENT ON A 23.5X23.5 MM MAPPED AREA

This experiment was conducted in November 2021, as part of a technique development of semi-automated mapping mode of FTIR Microspectroscopy. Sample used was dewatered sludge collected on September 7, 2021. The mesh was mapped in 23.5 x 23.5 mm area, as illustrated in Figure E-24 .This area represents a quarter of the total mesh area.

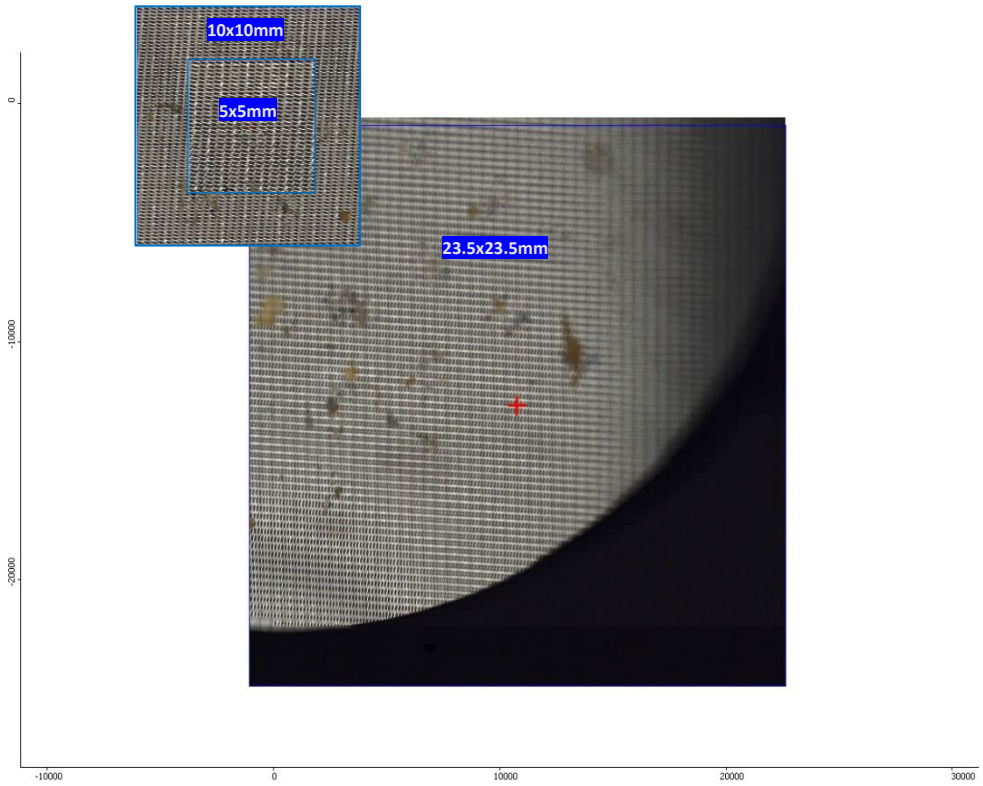

Figure E-24. Illustration on the mapped area of 23.5 x 23.5 mm in comparison with 5x5mm and 10x10mm. Not the actual ratio.

The total time required to collect and identify the particles' spectra was around 2.5 days. An overnight process to collect a map of 23.5x23.5 mm of the mesh, then, another six hours was needed to manually pin-point the particles on the mesh. The infrared spectrum collection of each particle needed additional three hours to finish, and around ten hours was to identify 1170 collected particle's spectrum. 70% of the total collected spectrum was confirmed as microplastics, with average 86% Hit Quality Index (HQI), and extrapolated into 4404 microplastics/fibers per kg dry solid of sample.

One sample t-test was conducted to analyse the difference between the "5x5mm" and "10x10mm" mapping area with the "23.5x23.5mm" ones as the test value. *Table E. 1* summarise the data collected and percentage

of the represented area of total mesh. The test showed that no significant difference (p>0.05) between the "5x5mm" and the "23.5x23.5mm" as well as between the "10x10mm" and the "23.5x23.5mm" (Table E-7 and Table E-8).

Table E-7. Number of microplastics/fibers in a gram of dried sludge tested on different mapped areas

	5x5 mm	10x10 mm	23.5x23.5 mm
Represented area of total mesh (Ø 47 mm)	2%	6%	27% - used as **Hypothesized mean.** A minimum of 10% of total mesh is required as representative of total mesh area.[1]
Mapping spot:			
1	5755	6111	4404
2	5271	7698	

Table E-8. One sample t-test statistics of "5x5mm" and "10x10mm" mapped areas

	N	Mean	Std. Deviation	Std. Error Mean
5x5	2	5513.0000	342.23968	242.00000
10x10	2	6904.5000	1122.17846	793.50000

Table E-9. One sample t-test result of "5x5mm" and "10x10mm" in comparison with test value from "23.5x23.5mm" mapping area

	Test Value = 4044						
	t	df	Significance		Mean Difference	95% Confidence Interval of the Difference	
			One-Sided p	**Two-Sided p**		Lower	Upper
5x5	6.070	1	0.052	**0.104**	1469.00000	-1605.9015	4543.9015
10x10	3.605	1	0.086	**0.172**	2860.50000	-7221.8735	12942.8735

Considering the time required for finishing the analysis, from mapping to identifying the spectrum, and based on the statistical analysis result using one sample t-test (Table E-9), we proceed the development of the mapping technique using "5x5mm" and "10x10mm" mapping areas as presented in Chapter 4 of this thesis.

References

1. Schymanski, D.; Oßmann, B. E.; Benismail, N.; Boukerma, K.; Dallmann, G.; von der Esch, E.; Fischer, D.; Fischer, F.; Gilliland, D.; Glas, K.; Hofmann, T.; Käppler, A.; Lacorte, S.; Marco, J.; Rakwe, M. E. L.; Weisser, J.; Witzig, C.; Zumbülte, N.; Ivleva, N. P., Analysis of microplastics in drinking water and other clean water samples with micro-Raman and micro-infrared spectroscopy: minimum requirements and best practice guidelines. *Analytical and Bioanalytical Chemistry* **2021,** *413* (24), 5969-5994.

APPENDIX F. CHAPTER 4 - BOXPLOT STATISTICAL ANALYSIS

The following graphs are the boxplot statistics analysis result for evaluating distribution of microplastics on the mapped mesh, small and big area, based on the type of plastics. This served as attachment for section 3.5 of Chapter 4 of this thesis.

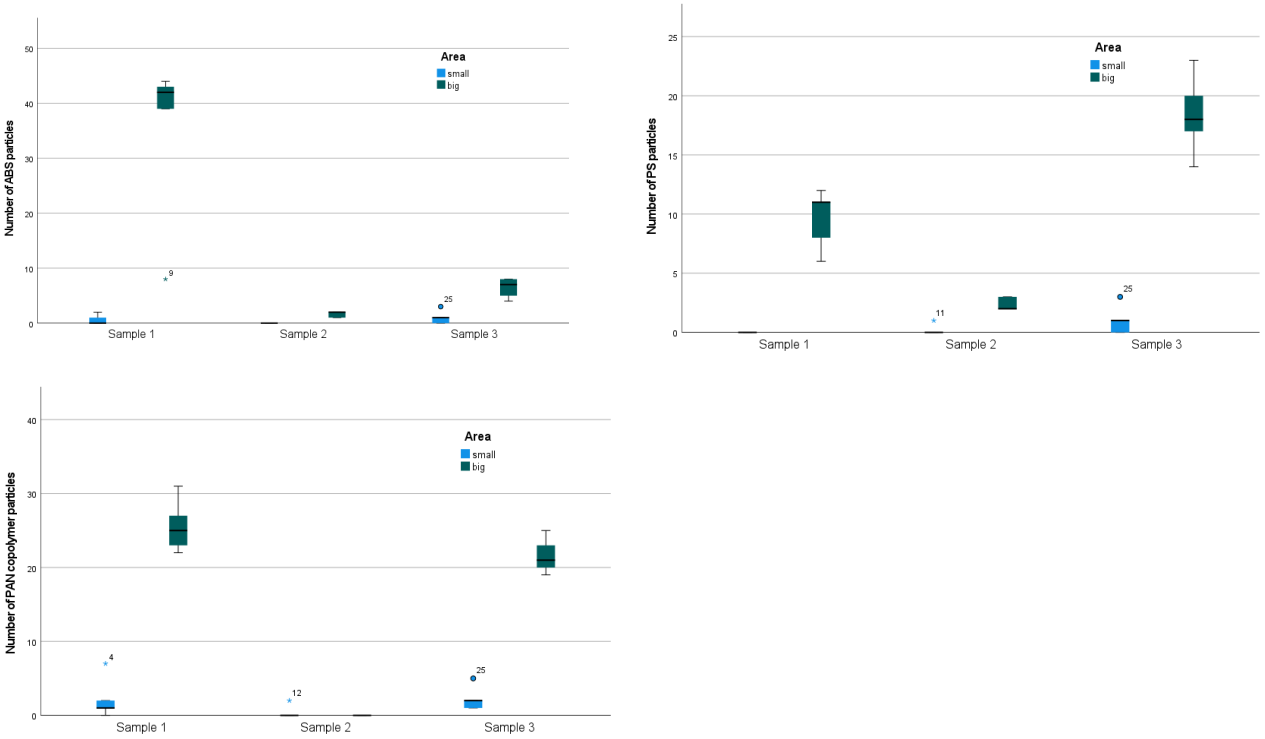

Figure F-25. Boxplots of ABS, PS, and PAN copolymer

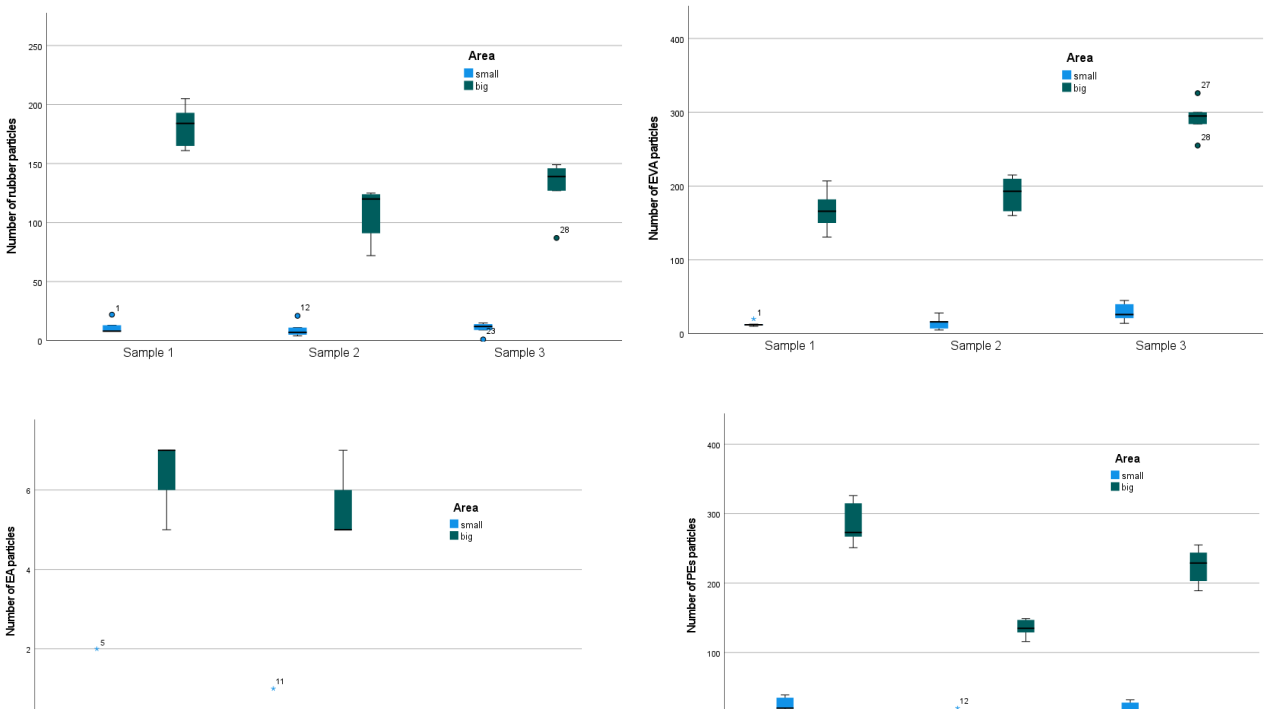

Figure F-26. Boxplots of rubber, EVA, EA, and PEs

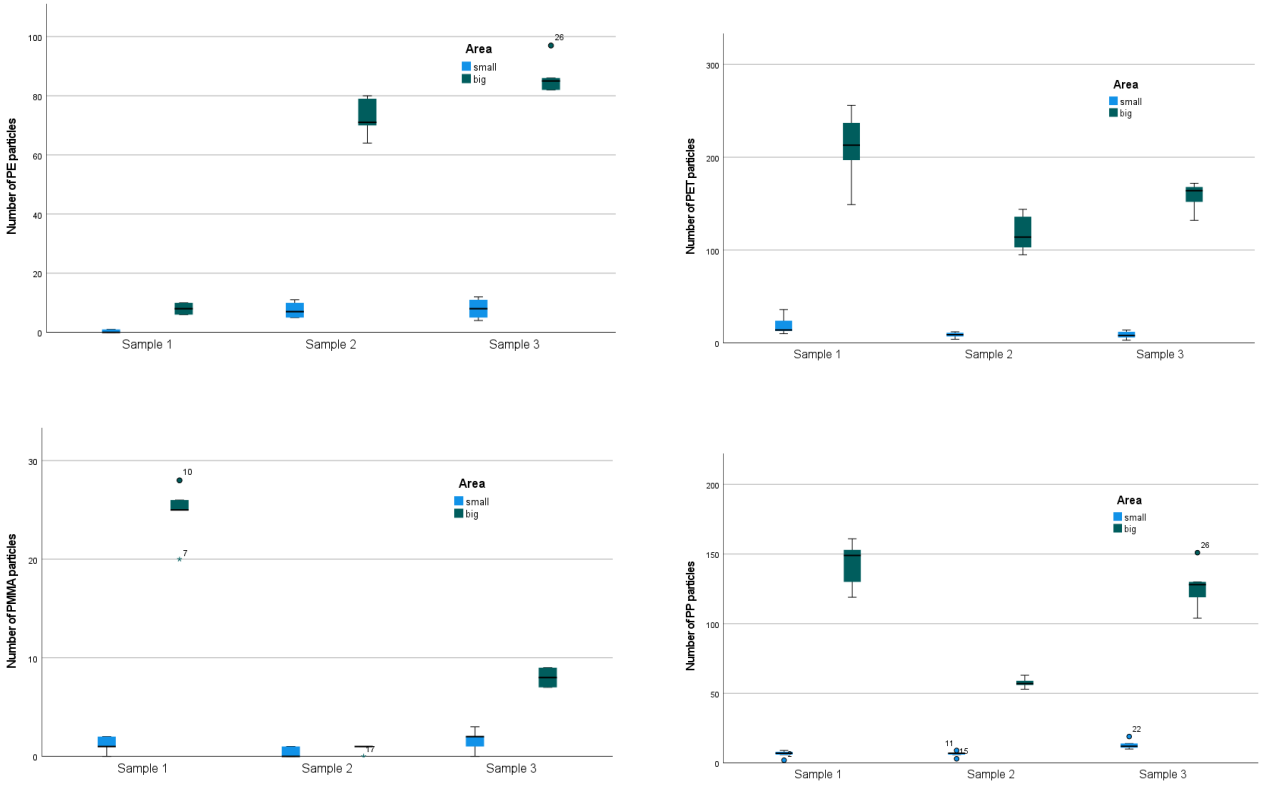

Figure F-27. Boxplots of PE, PET, PMMA, and PP

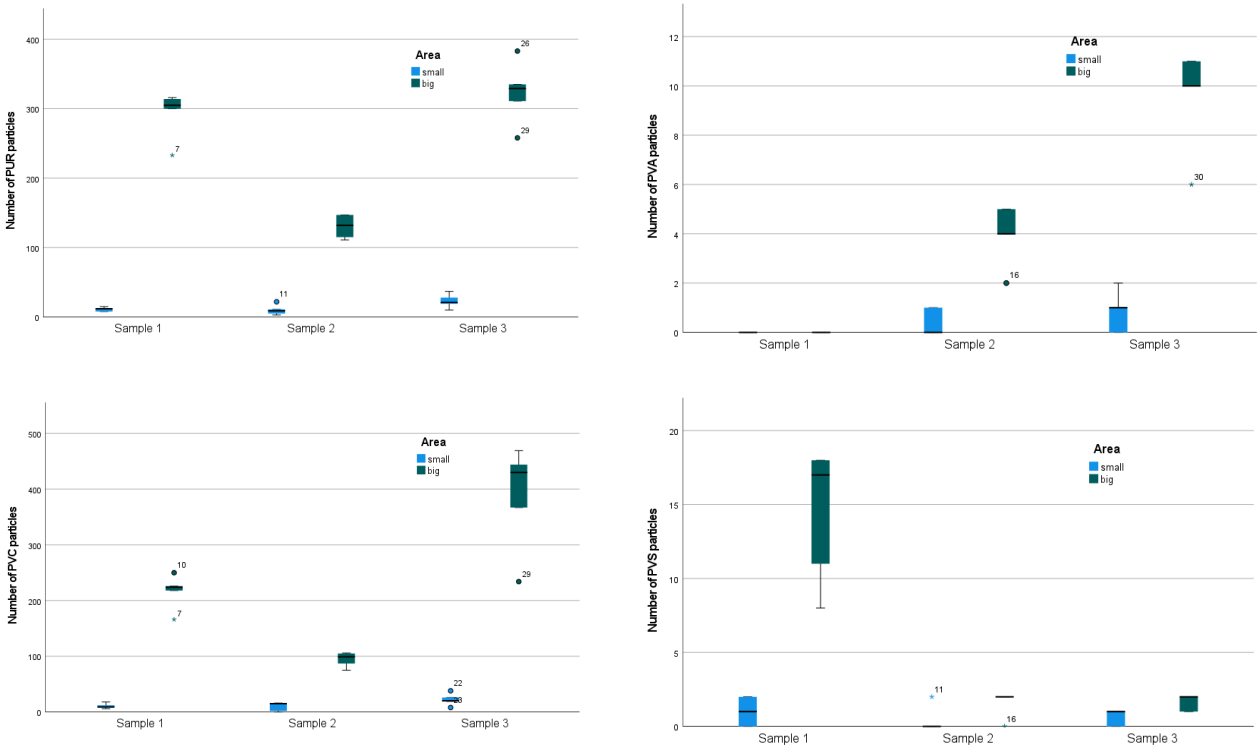

Figure F-28. Boxplots of PUR, PVA, PVS, and PVS

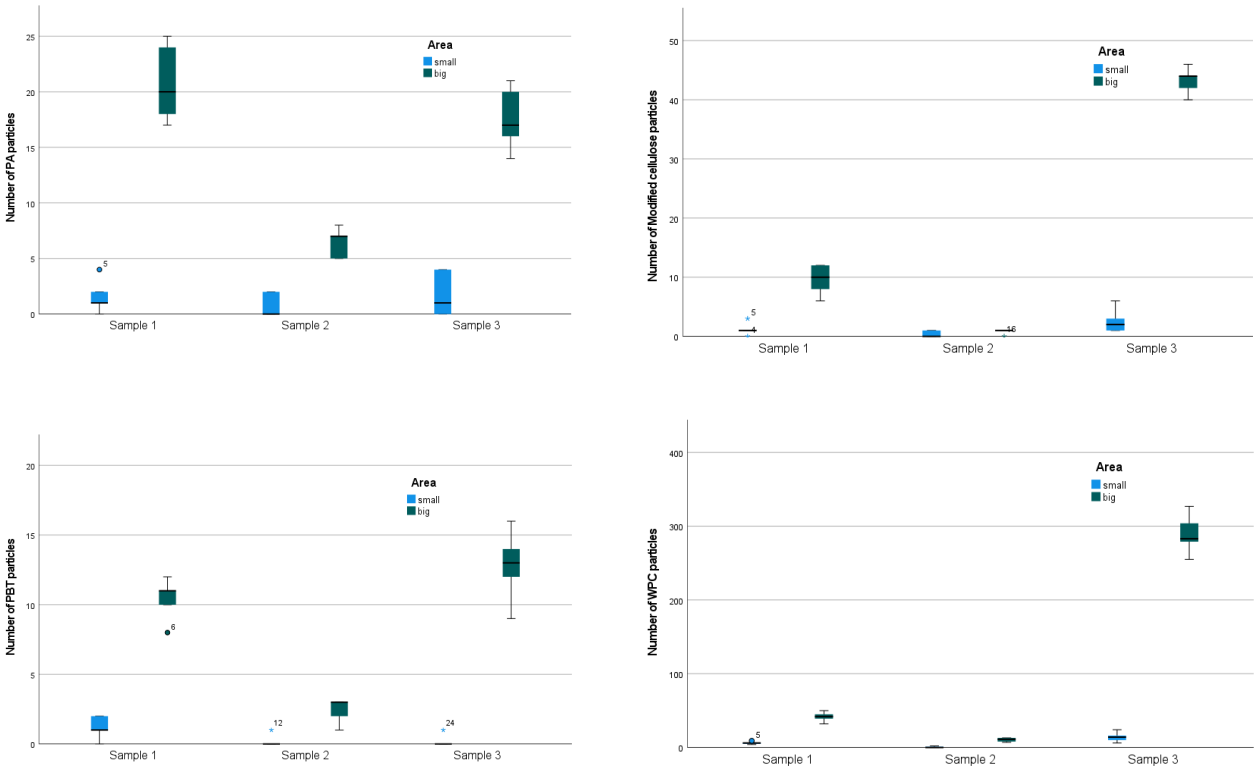

Figure F-29. Boxplots of PA, modified cellulose, PBT, and WPC

APPENDIX G. MODIFICATION OF MESH HOLDER

Throughout the refinement of the semi-automated mapping mode in FTIR microspectroscopy, an identified challenge surfaced in the form of discontinuous images within the collected map, as depicted in Figure G. 1-A. This anomaly was attributed to an unstable mesh holder, causing movement during image capture, as illustrated in *Figure G. 2*-A. Additionally, scrutiny revealed an irregular surface on the mesh itself, as evident in *Figure G. 2*-B. These factors collectively compromised the quality of spectrum collection and subsequent identification, leading to the displacement and defocused appearance of certain pointed particles, thereby diminishing the intensity of the obtained spectra.

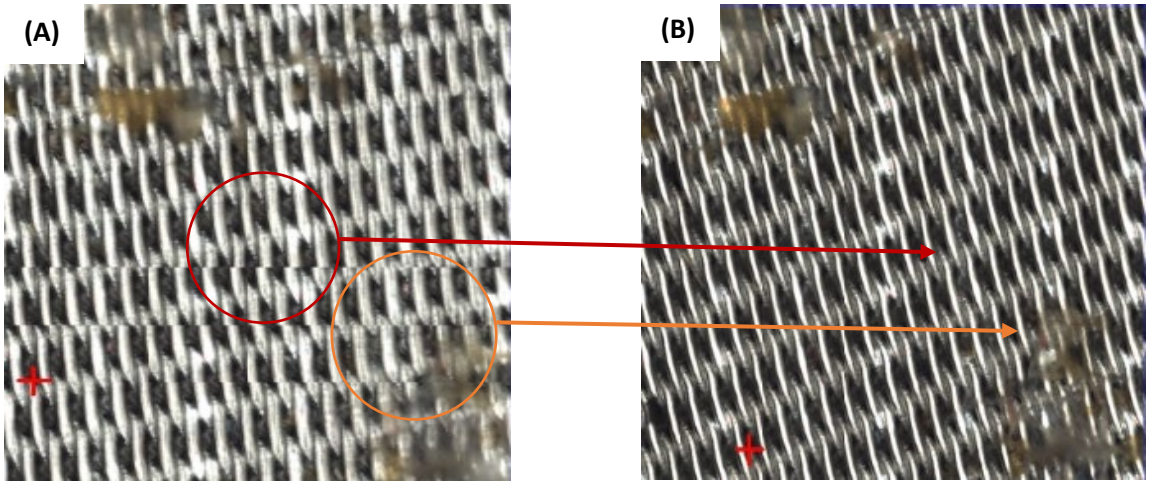

Figure G-30. Mapped mesh (A) Without and (B) With mesh holder

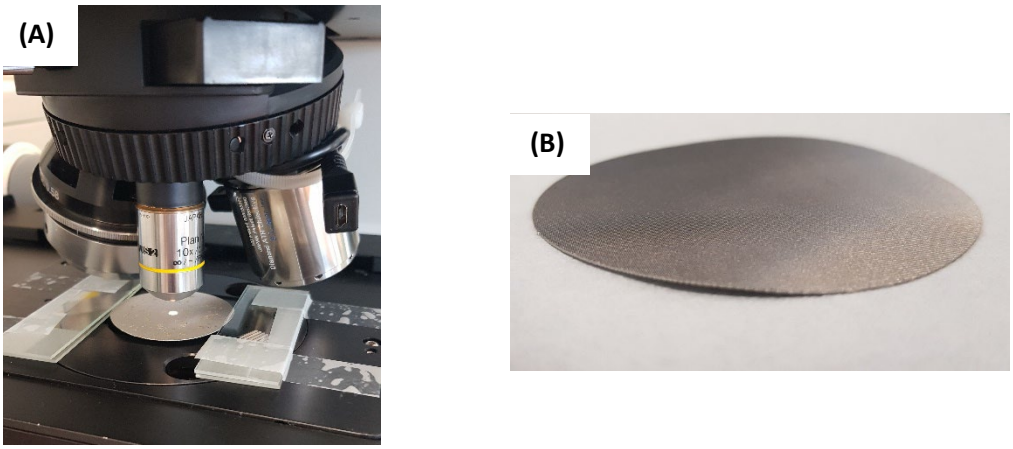

Figure G-31. (A) microscope stage without the mesh holder; (B) uneven stainless-steel mesh

In our pursuit of refining the mapping mode technique and elevating the quality of collected spectra, a strategic modification was implemented on the microscope stage, involving the incorporation of a purpose-built mesh holder, as illustrated in *Figure G. 3*-A. This modification successfully mitigated the challenges associated with a dynamic mesh, eliminating issues such as interrupted mapping Figure G. 1-B), particle displacement, and minimizing surface irregularities on the mesh. Notably, the intensity of the collected spectra witnessed a significant improvement (*Figure G. 4*), consequently yielding a heightened Hit Quality Index (HQI).

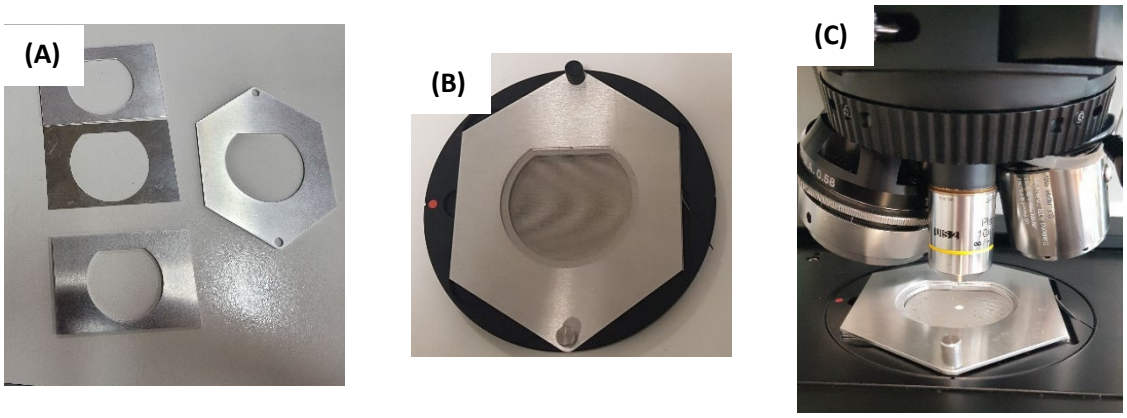

Figure G-32. (A) mesh holder; (B) stainless-steel mesh on the mesh holder; (C) mesh holder on the microscope stage

Prior to the integration of the mesh holder, spectra HQI stood at 64.45%, falling below the minimum threshold required for the identified plastic type (65%), thereby resulting in the classification of the spectra as non-microplastics. However, with the incorporation of the mesh holder, the HQI surged to 71.11%, surpassing the established minimum requirement and meriting the categorization of the spectra as microplastics. This enhancement underscores the efficacy of the modified microscope stage in achieving more accurate and reliable microplastics identification.

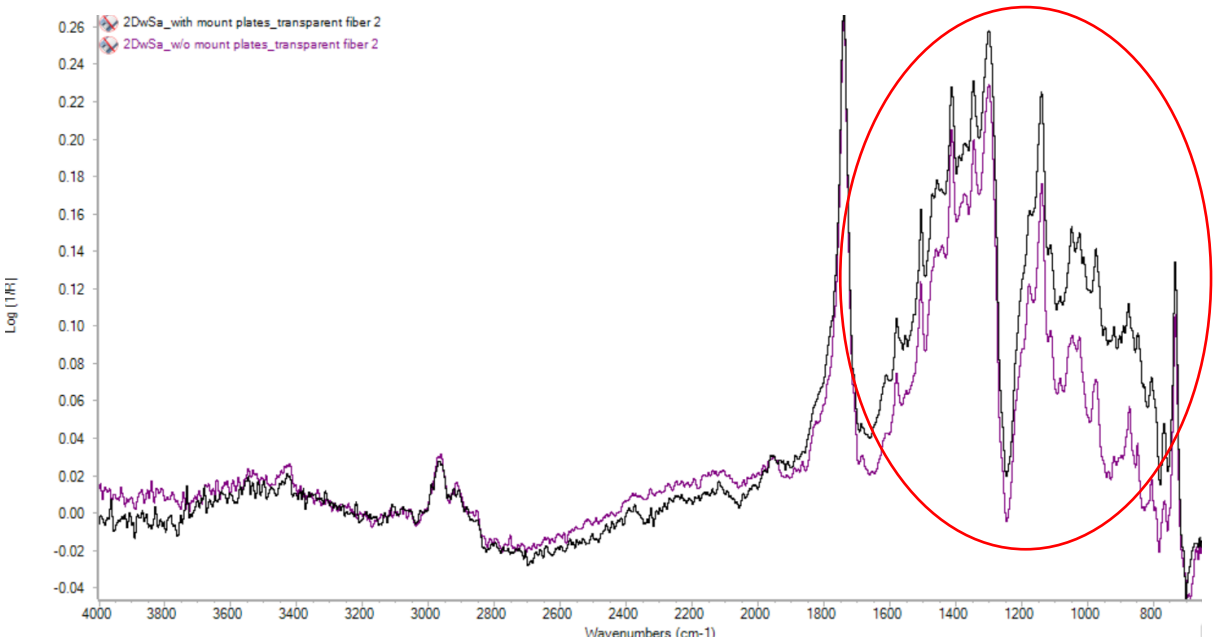

Figure G-33. IR spectrum of a transparent fiber on a stainless-steel mesh without mesh holder (purple spectra) and with mesh holder (black spectra). The fiber identified as poly(ethylene terephthalate) with 64.45% and 71.11% HQI without and with mesh holder, respectively. Area with a red circle showed an increase of intensity of the spectra of the fiber on the mesh with mesh holder.

APPENDIX H. SPECTRUM OF STANDARD POLYMER REFERENCE, COMMERCIAL AND WEATHERED PLASTICS

Table H-10. List of standard polymer references and plastics. Each is hyperlinked to the details on the sources and spectrum

Plastics sources	New/used/weathered	Colour	type of polymer/classification
COMMERCIAL PLASTICS			
Floor decking	new	dark grey	Wood-Plastic Composite (WPC)
Floor tiles	new	black	Ethyl Vinyl Acetate (EVA)
Sink stopper	used	dark orange	Rubber
Multipurpose liner	new	white	Polyester
Dishwashing sponge-Scott Brite	new	yellow	Synthetic or Regenerated cellulose
	new	dark green	Nylon/Polyamide
Toothbrush bristle	used	white	Poly(butylene terephthalate)
	used	light purple	Poly(butylene terephthalate)
Car mats	used	black	Rubber
Shoes' outer sole-Nike	used	white	Ethyl Vinyl Acetate (EVA)
Shoes' outer sole-Adidas	used	black	Rubber
Cleaning gloves	used	yellow	Rubber

Plastics sources	New/used/weathered	Colour	type of polymer/classification
Cosmetic sponge	used	dark purple	Polyurethane (PUR)
Artificial grass	weathered	dark green	Polyethylene (PE)
Firewood	weathered	brown	Natural cellulose
Water pipe	weathered	white	Poly(vinyl chloride) (PVC)
Laundry wastewater bag trim	new	white	Polyester
STANDARD POLYMER REFERENCES			
Poly(butylene terephthalate)	new		NA
Polyethylene, high density	New		NA
Polyethylene, low density	New		NA
Polystyrene	New		NA
Polypropylene	New		NA
Poly(ethylene terephthalate)	New		NA
Poly(vinyl stearate)	New		NA
Poly(methyl methacrylate)	New		NA
Polyacrylamide	New		NA
Poly(tetrafluoroethylene)/Teflon	New		NA
Poly(vinyl alcohol)	New		NA
Poly(vinyl chloride)	New		NA

Plastics sources	New/used/weathered	Colour	type of polymer/classification
Poly(vinyl acetate)	New		NA
Polyamide resin	New		NA

1. Wood-Plastic Composite (WPC) – floor decking _ new_ grey

Figure H-34. Decking tiles. Materials: Wood plastic composite board and polypropylene (PP) base. Source: Kmart

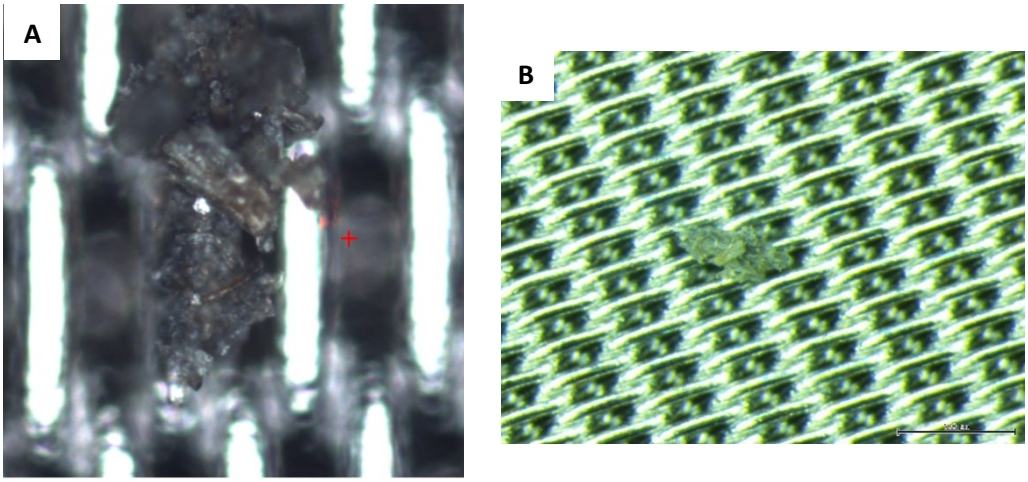

Figure H-35. Microscope image of decking tiles' fragment under (A) FTIR microscope; (B) Stereomicroscope

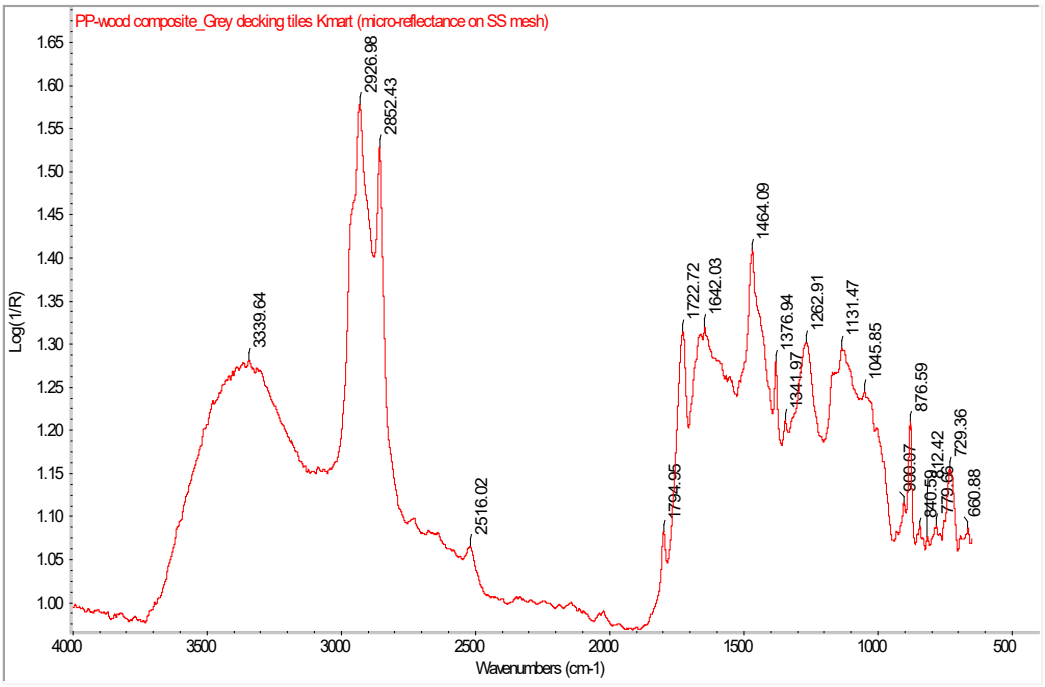

Figure H-36. Spectra of decking tiles - wood plastic composite (WPC) on stainless steel mesh - micro reflectance mode

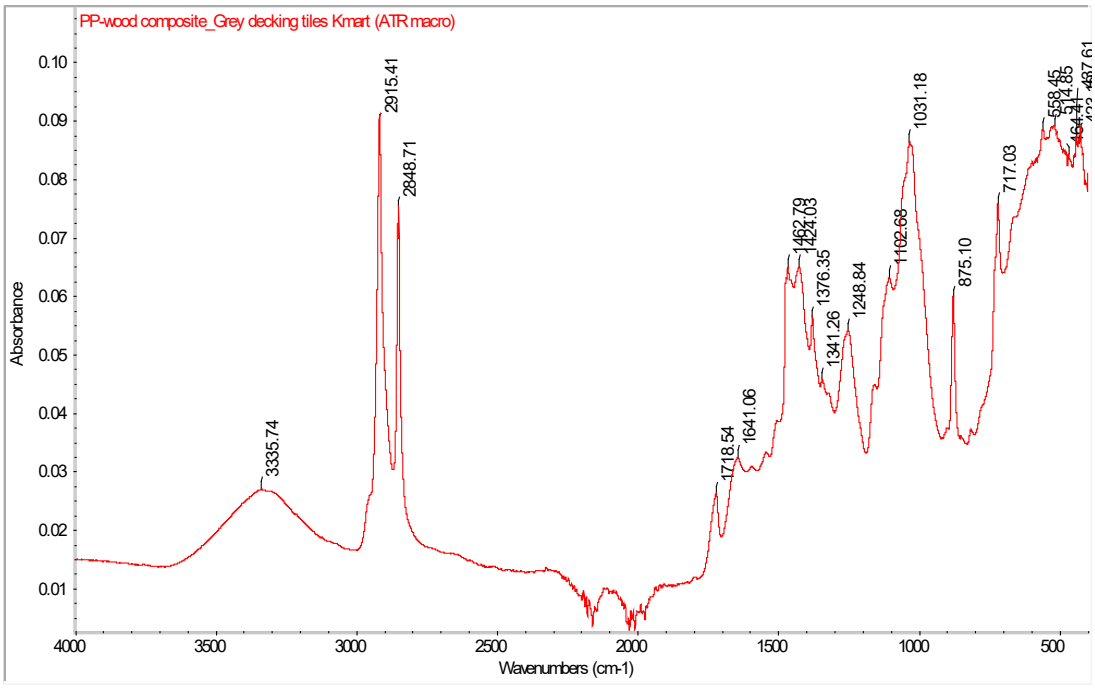

Figure H-37. Spectra of decking tiles - wood plastic composite (WPC) - ATR mode

2. Ethyl Vinyl Acetate (EVA)_floor tiles_new_black

Figure H-38. Floor tiles. Material: Ethyl Vinyl Acetate (EVA) foam. Source: Kmart

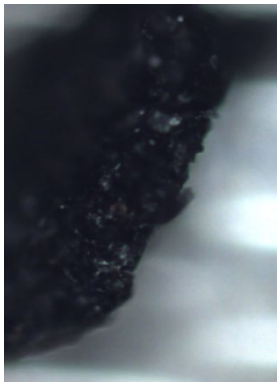

Figure H-39. Image of floor tiles fragment under FTIR microscope

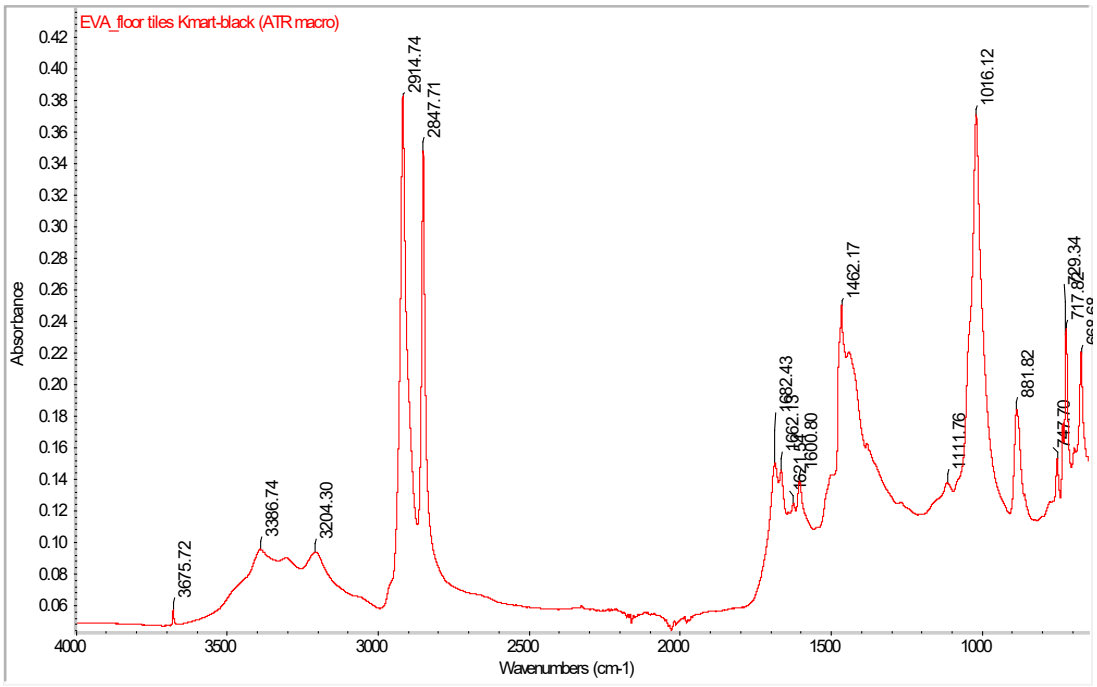

Figure H-40. Spectra of floor tiles - Ethyl Vinyl Acetate (EVA) - ATR mode

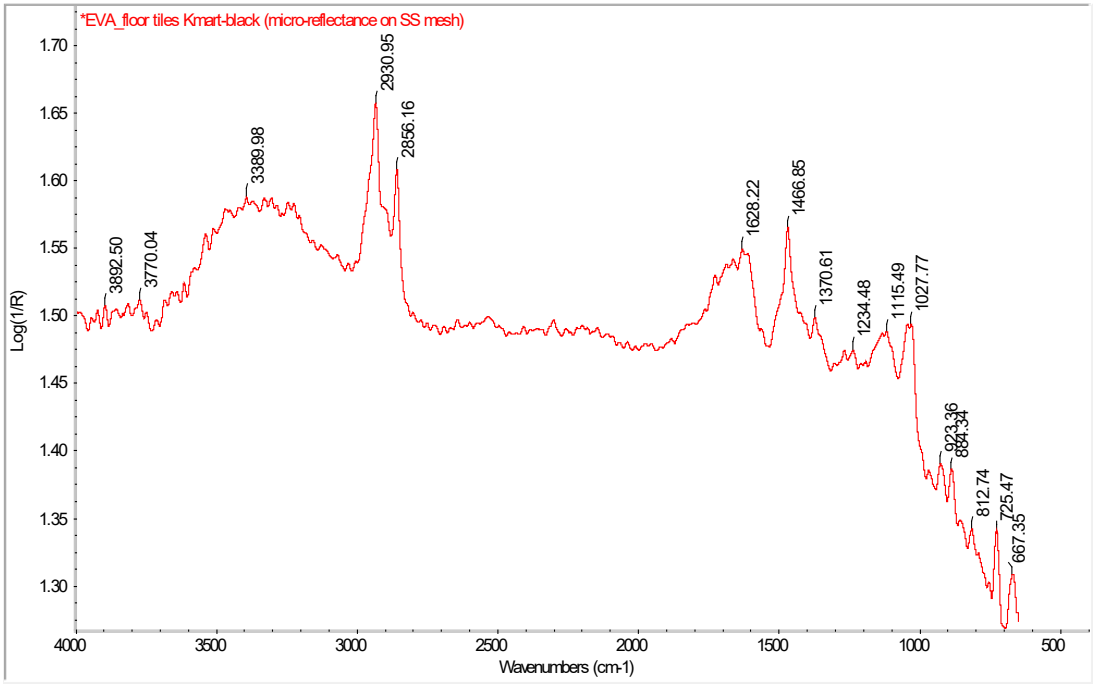

Figure H-41. Spectra of floor tiles - Ethyl Vinyl Acetate (EVA) on stainless steel mesh - micro reflectance mode

3. Sink stopper_used_dark orange

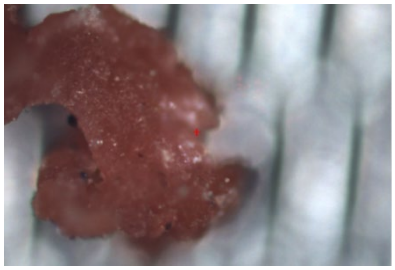

Figure H-42. Image of sink stopper fragment under FTIR microscope

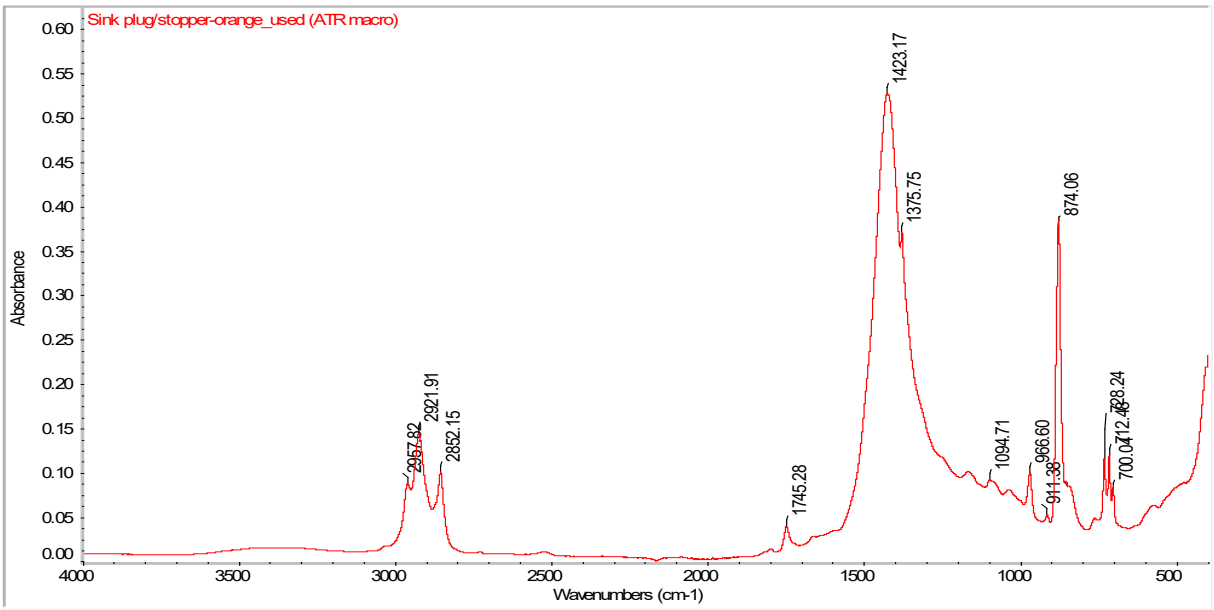

Figure H-43. Spectra of sink stopper - ATR mode

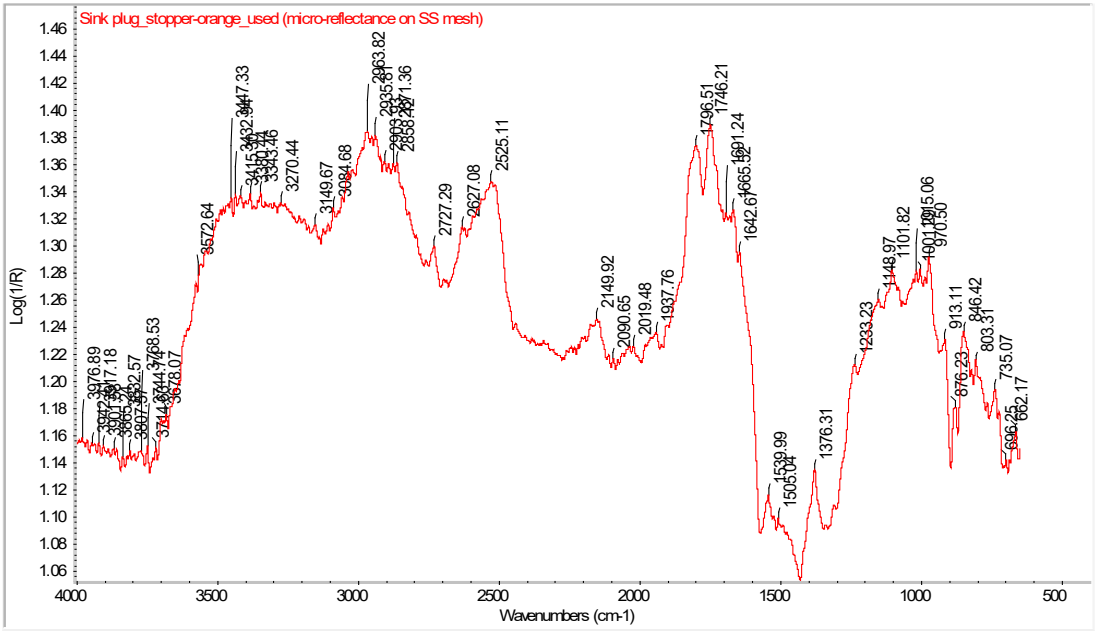

Figure H-44. Spectra of sink stopper on stainless steel - micro reflectance mode

4. Mutipurpose liner_new_white

Figure H-45. Multipurpose liner. Material: polyester and polyvinyl chloride. Source: Kmart

Figure H-46. Image of multipurpose liner under FTIR microscope

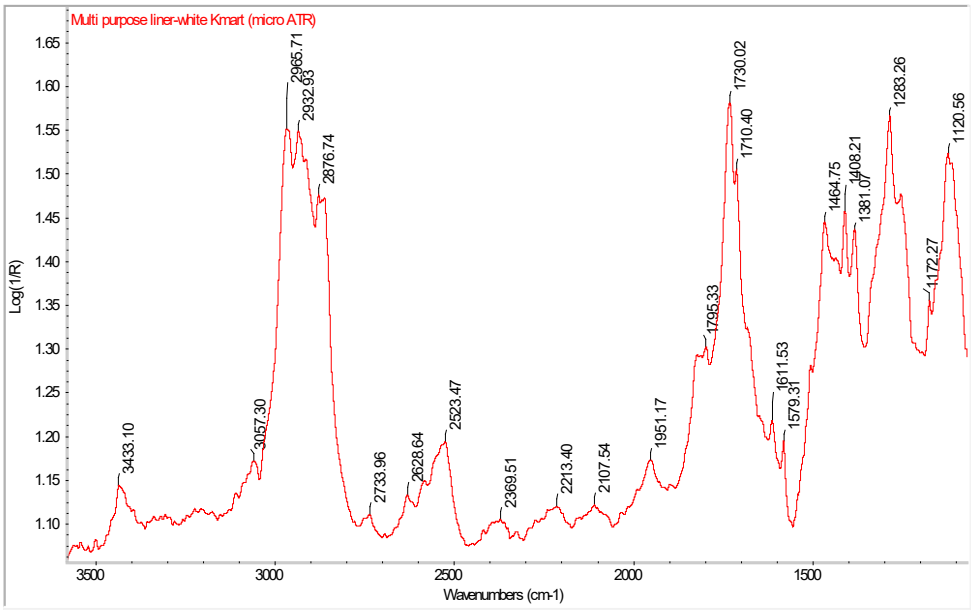

Figure H-47. Spectra of multipurpose liner on stainless steel mesh - micro reflectance mode

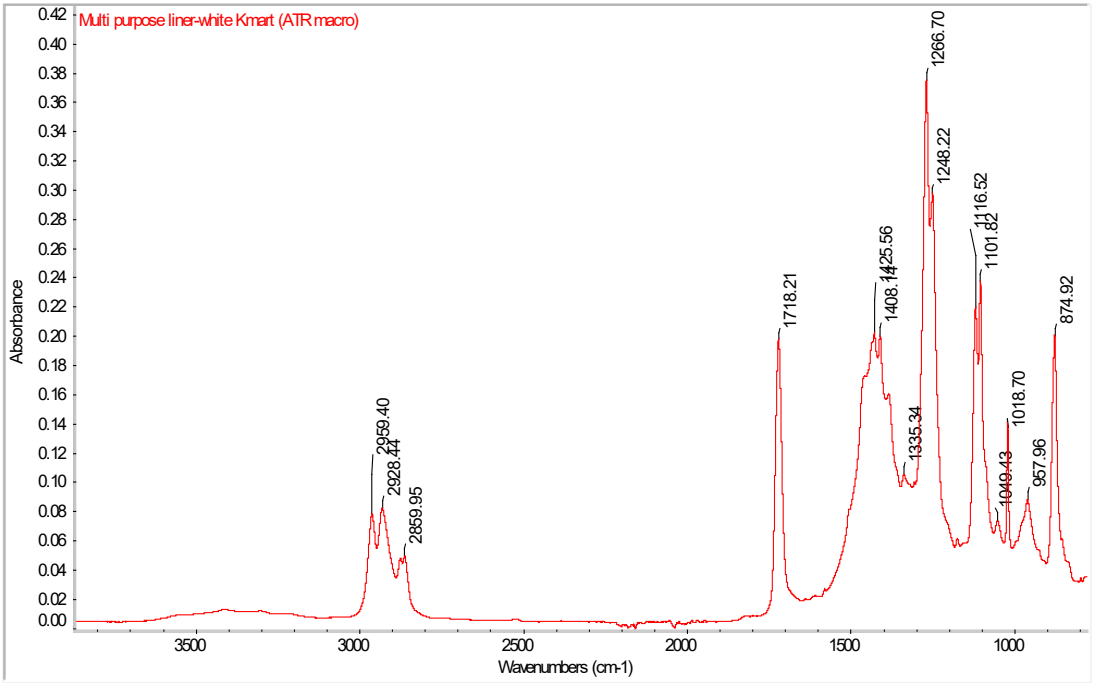

Figure H-48. Spectra of multipurpose liner - ATR mode

5. Dishwashing sponge_Scotch Brite_new_yellow side

Figure H-49. Dishwashing sponge – 3M Scotch Brite Heavy Duty

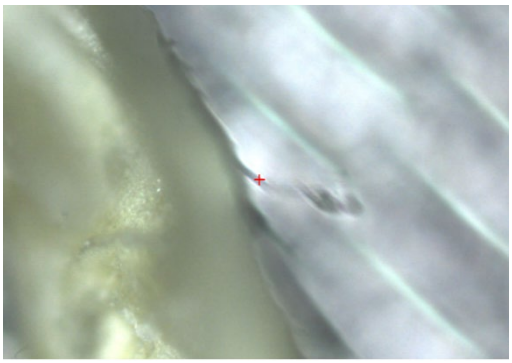

Figure H-50. Image of dishwashing sponge fragment - yellow side under FTIR microscope

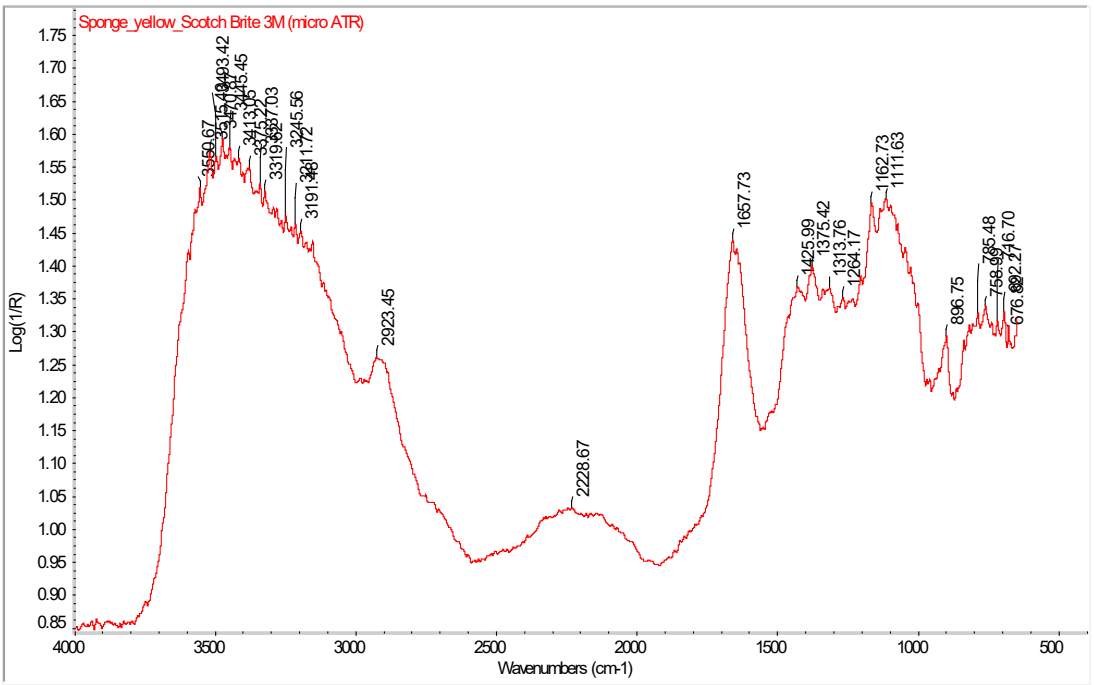

Figure H-51. Spectra of dishwashing sponge - yellow side on stainless steel mesh - micro reflectance mode

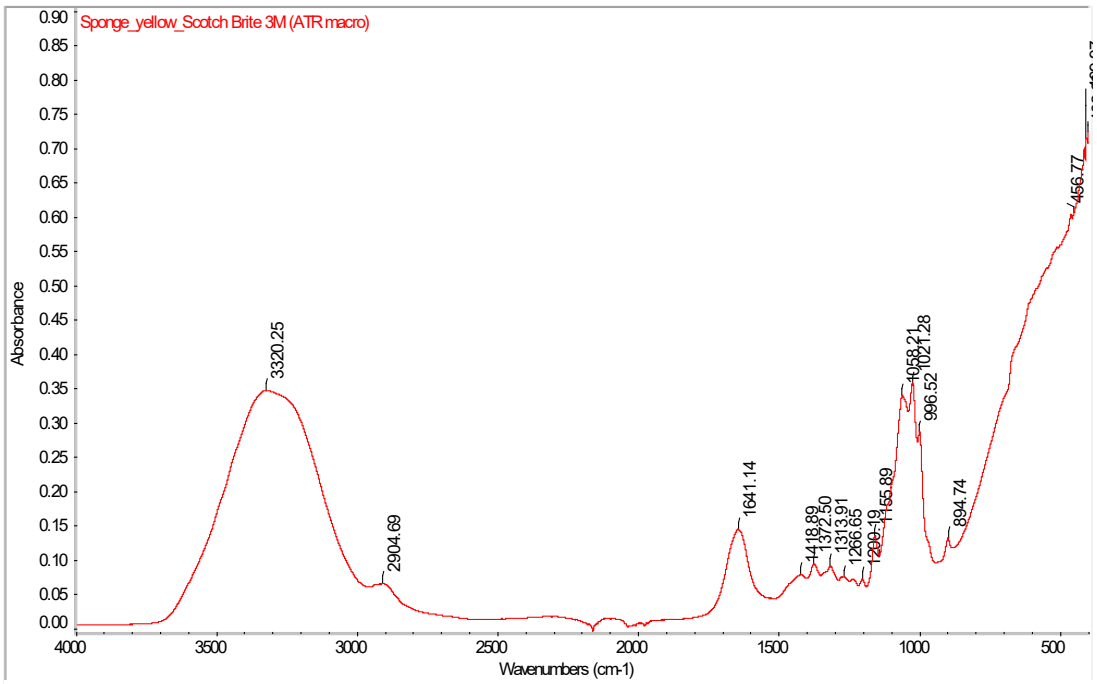

Figure H-52. Spectra of dishwashing sponge - yellow side - ATR mode

6. Dishwashing sponge_Scotch Brite_new_dark green side

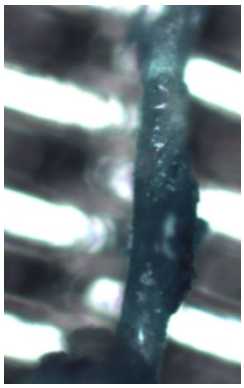

Figure H-53. Image of dishwashing sponge- green side fragment under FTIR microscope

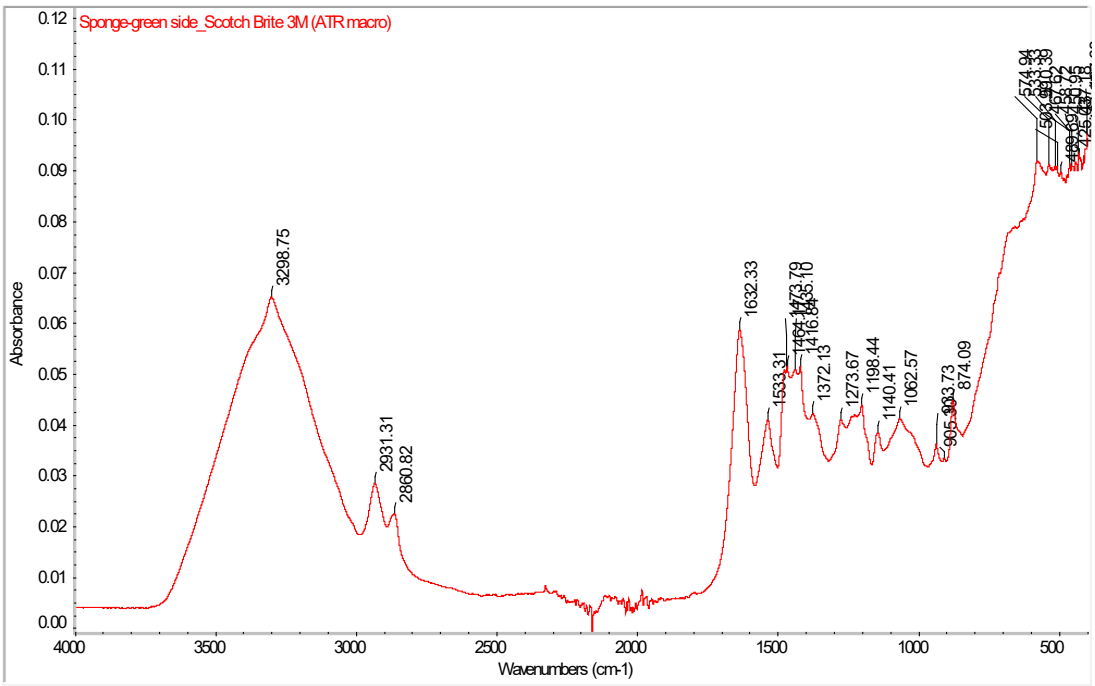

Figure H-54. Spectra of dishwashing sponge - green side - ATR mode

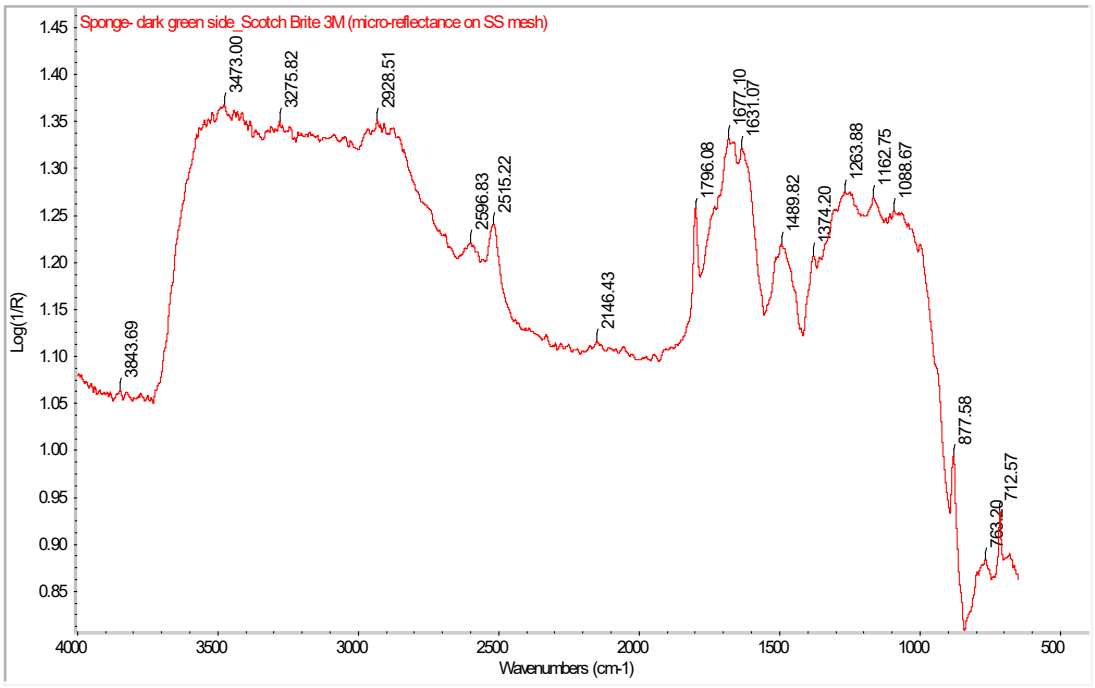

Figure H-55. Spectra of dishwashing sponge - green side on stainless steel mesh - micro reflectance mode

7. Toothbrush bristle_used_white

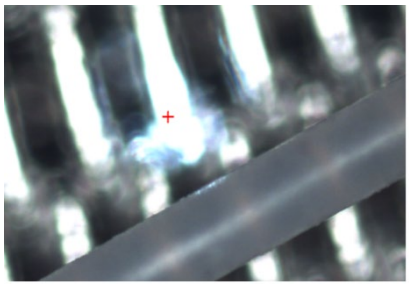

Figure H-56. Image of white toothbrush bristle under FTIR microscope

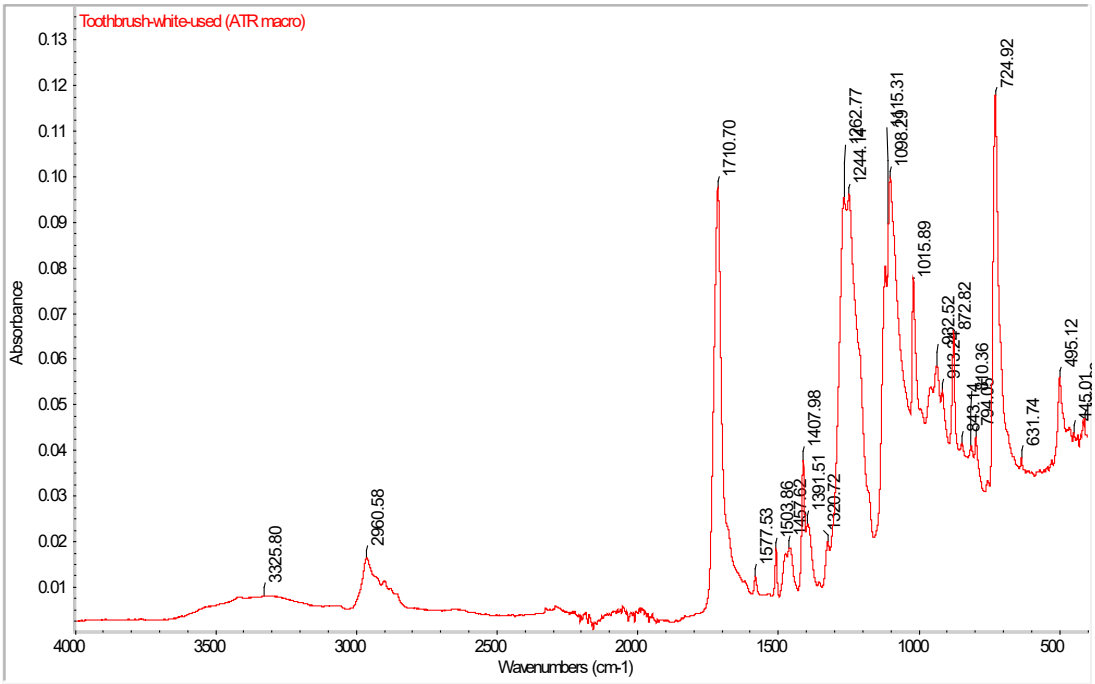

Figure H-57. Spectra of white toothbrush bristle - ATR mode

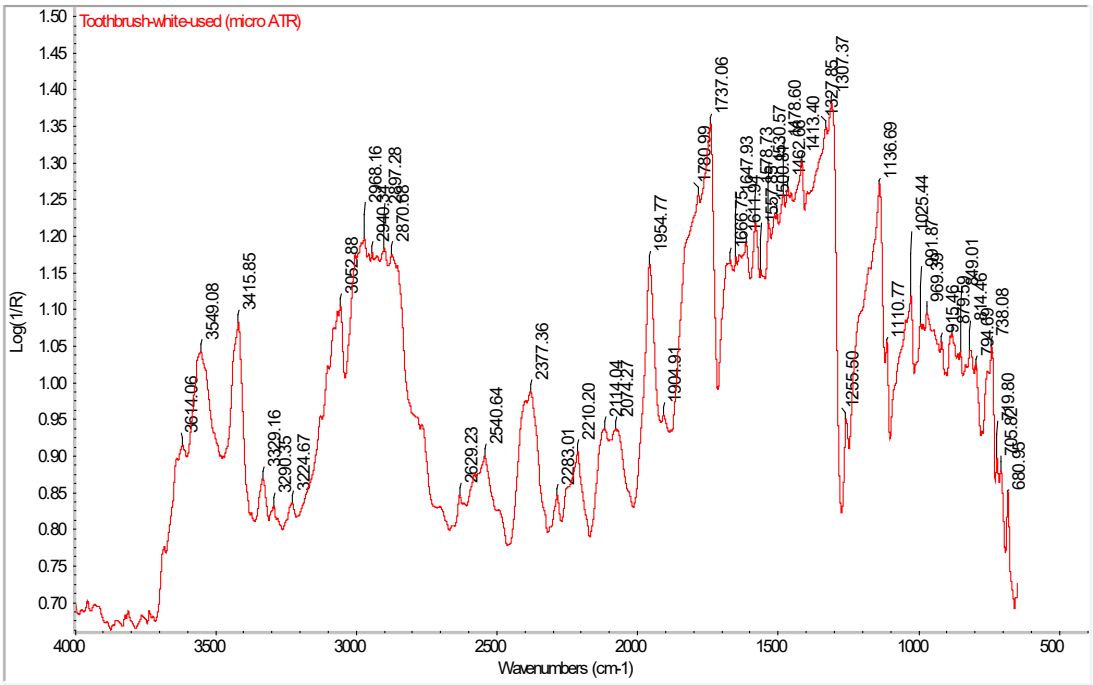

Figure H-58. Spectra of white toothbrush bristle on stainless steel mesh - micro reflectance mode

8. Toothbrush bristle_used_light purple

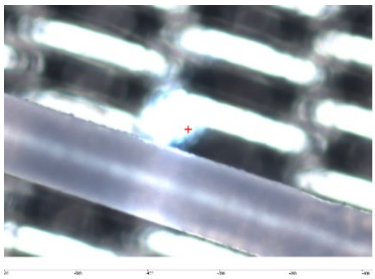

Figure H-59. Image of a light purple toothbrush bristle under FTIR microscope

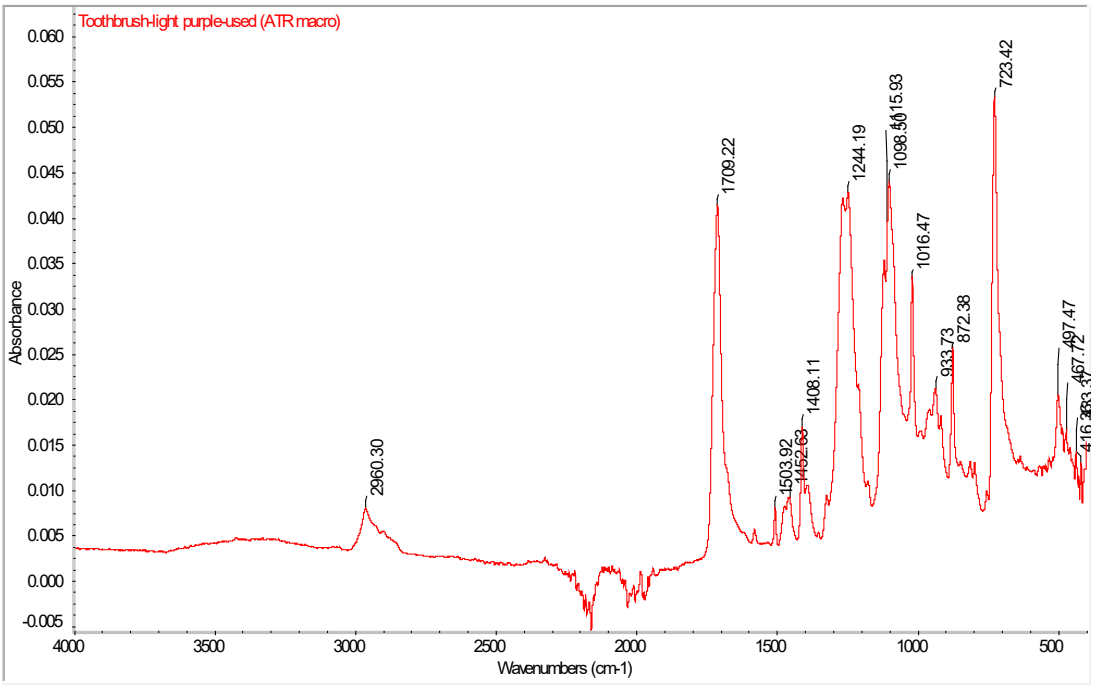

Figure H-60. Spectra of a light purple toothbrush bristle - ATR mode

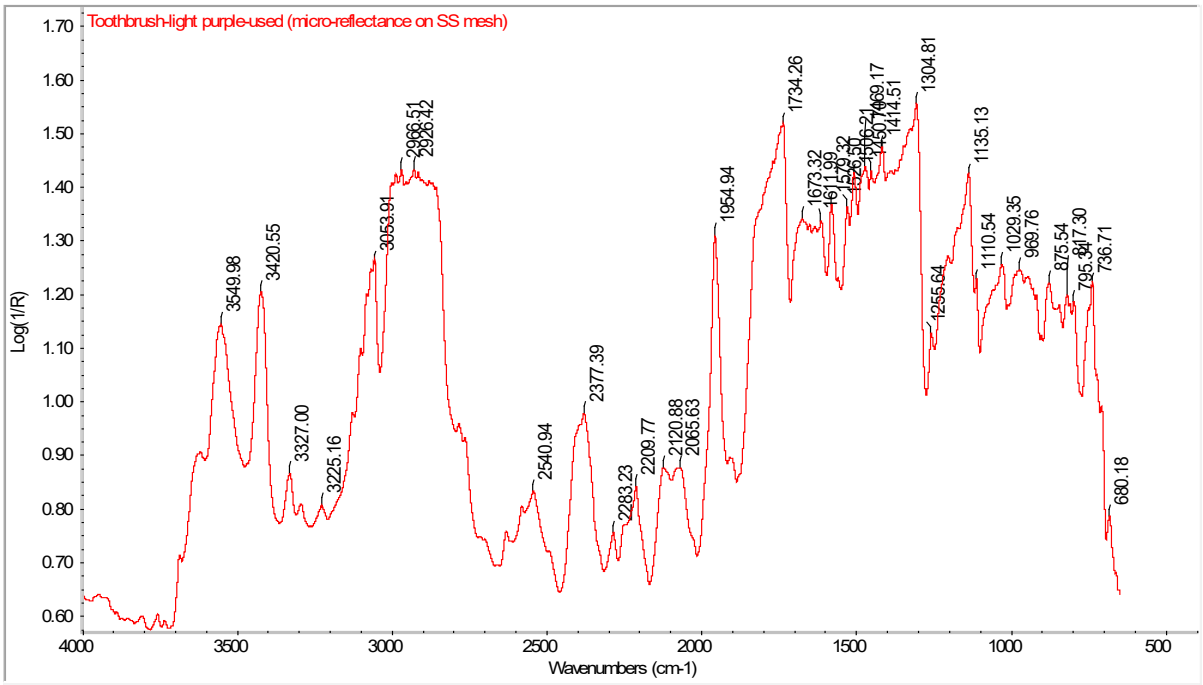

Figure H-61. Spectra of a light purple toothbrush bristle on stainless steel mesh - micro reflectance mode

9. Car rubber mat_used_black

Figure H-62. Car rubber mat. Brand: Michelin

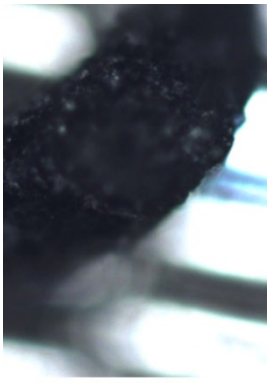

Figure H-63. Image of car rubber mat fragment under FTIR microscope

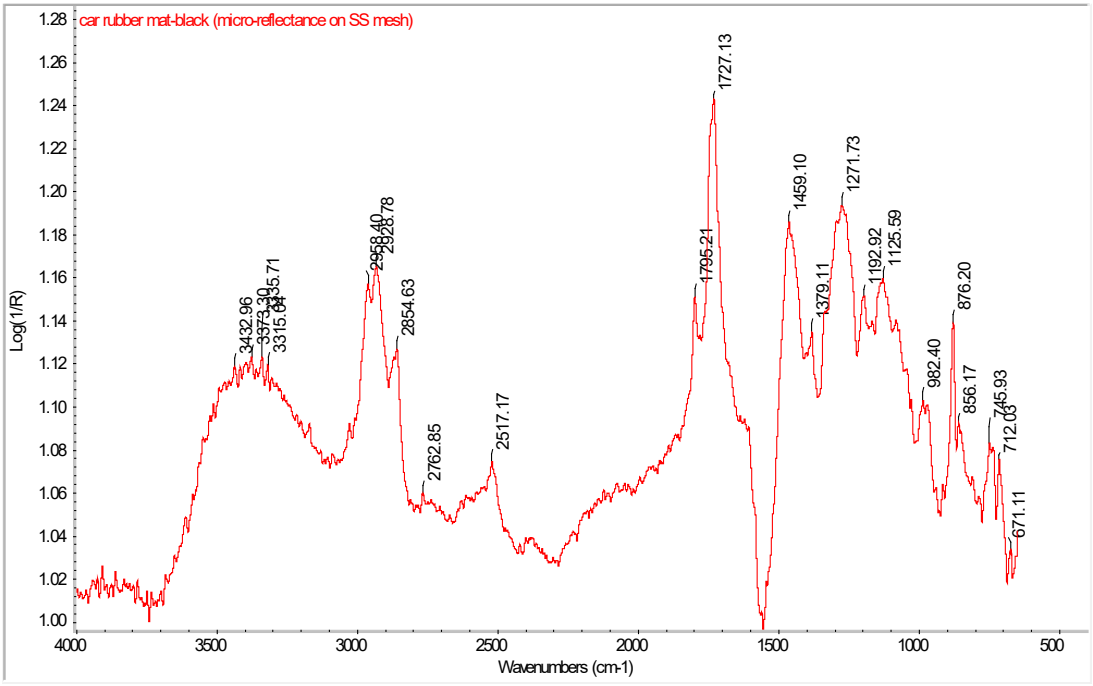

Figure H-64. Spectra of car rubber mat on stainless steel mesh - micro reflectance mode

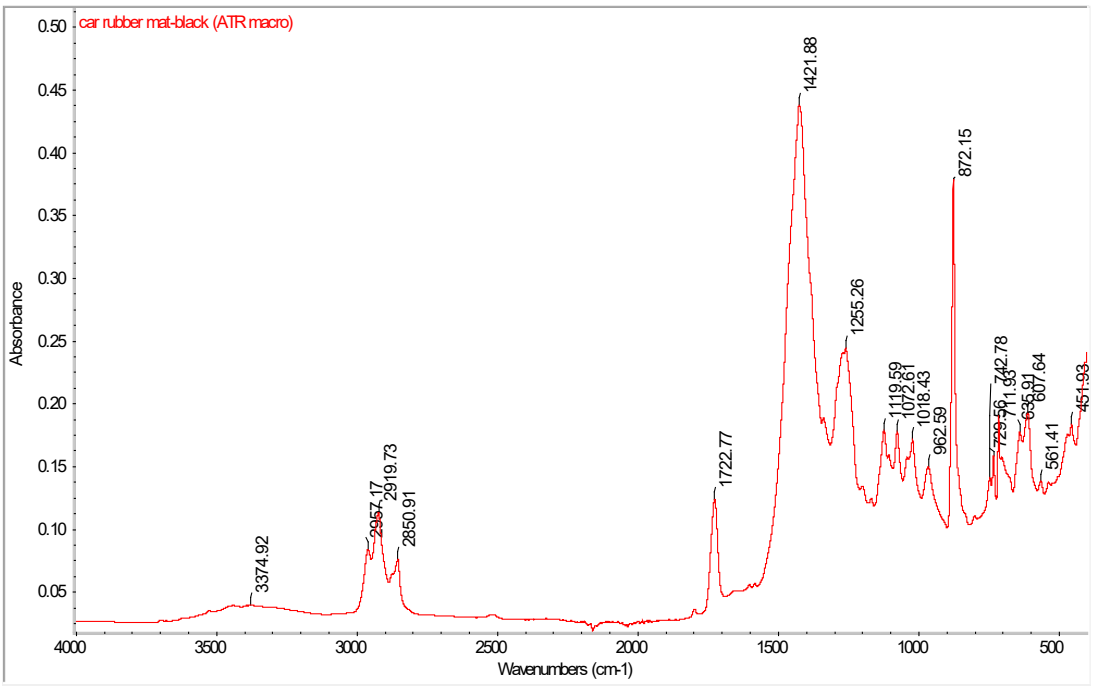

Figure H-65. Spectra of car rubber mat - ATR mode

10.Shoes' outer sole_Nike_used_white

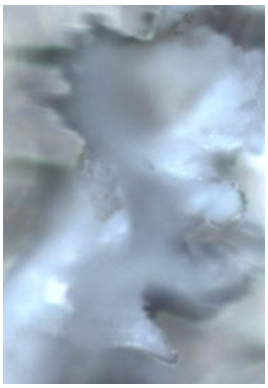

Figure H-66. Image of shoes' outer sole fragment (Nike brand) under FTIR microscope

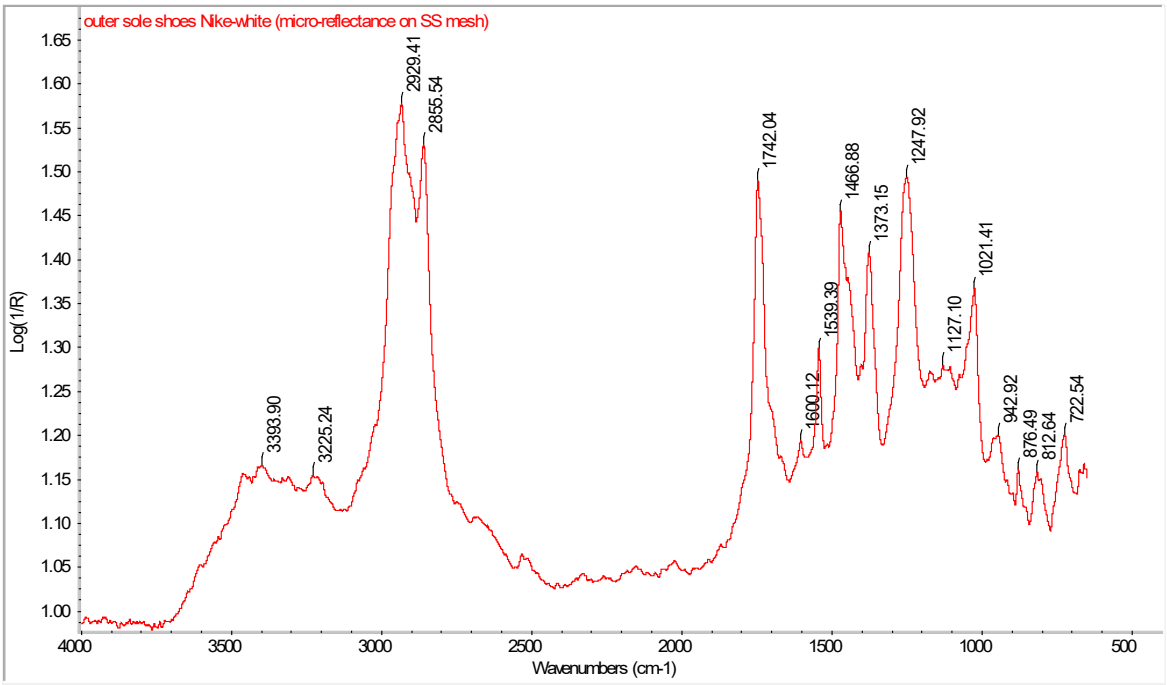

Figure H-67. Spectra of shoes' outer sole fragment (Nike) on stainless steel mesh - micro reflectance mode

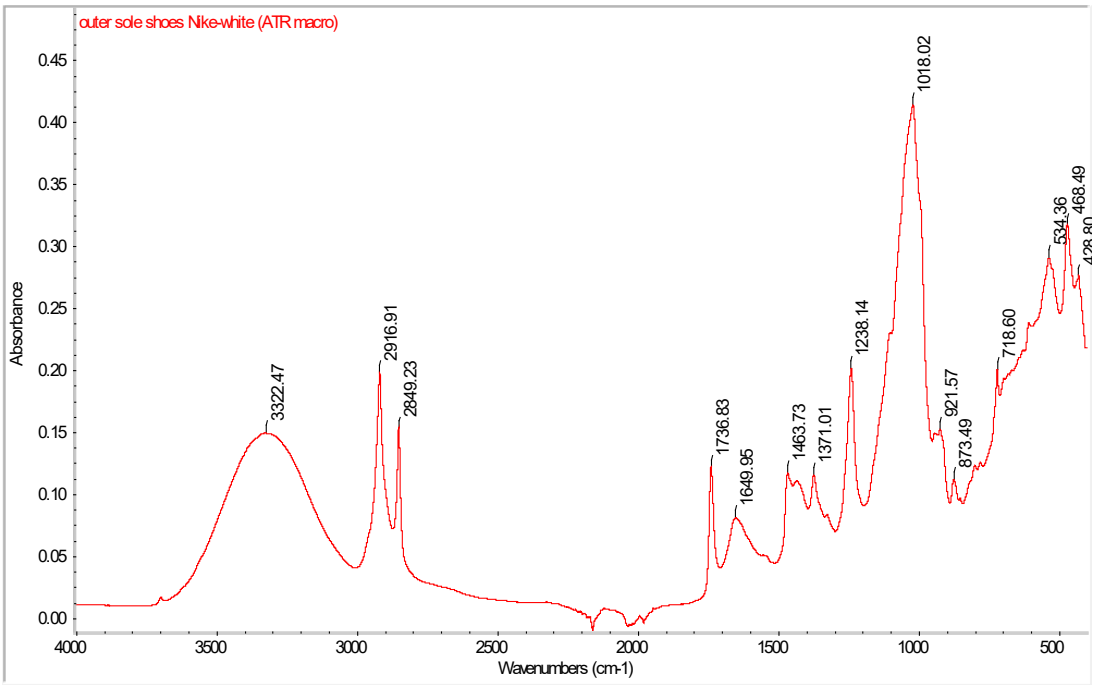

Figure H-68. Spectra of shoes' outer sole fragment (Nike) - ATR mode

11.Shoes' outer sole_Adidas_used_black

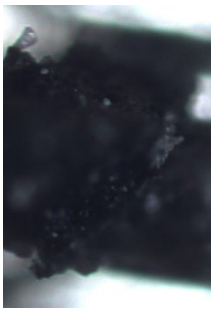

Figure H-69. Image of shoes' outer sole fragment (Adidas brand) under FTIR microscope

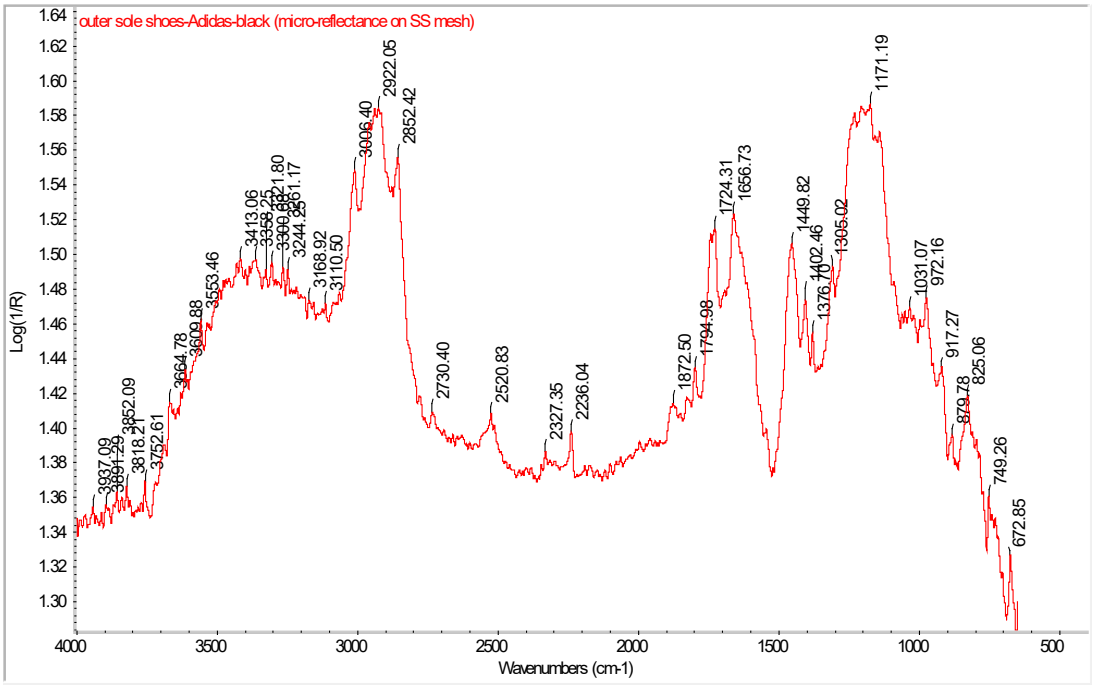

Figure H-70. Spectra of shoes' outer sole fragment (Adidas) on stainless steel mesh - micro reflectance mode

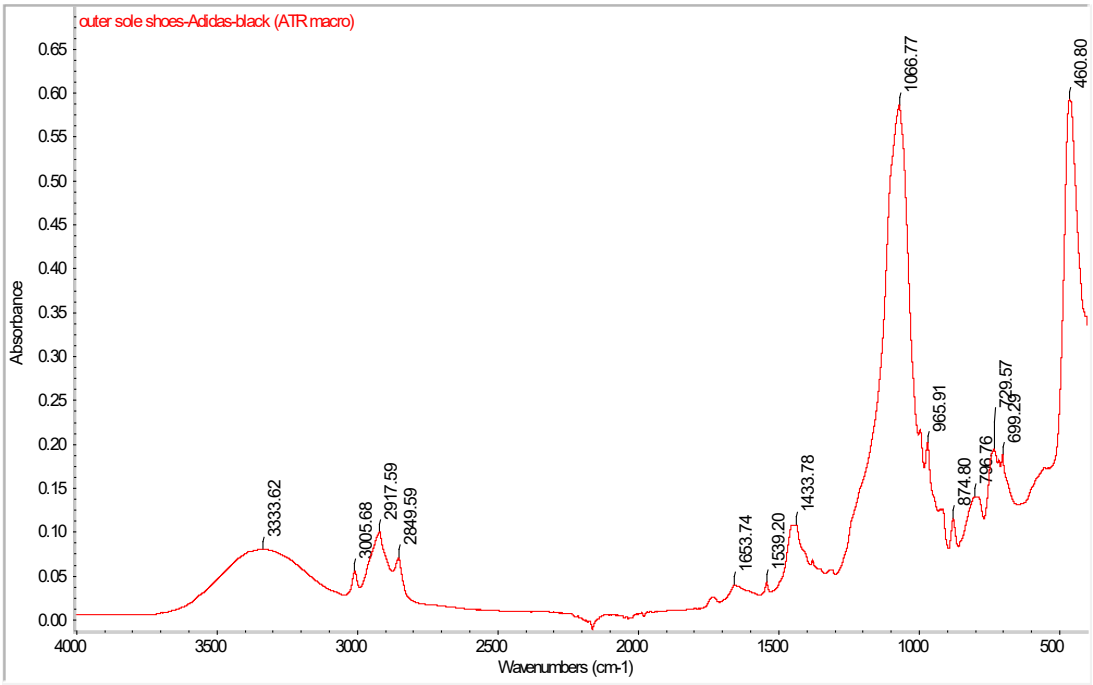

Figure H-71. Spectra of shoes' outer sole fragment (Adidas) - ATR mode

12.Cleaning gloves_used_bright yellow

Figure H-72. Image of rubber cleaning gloves fragment under FTIR microscope

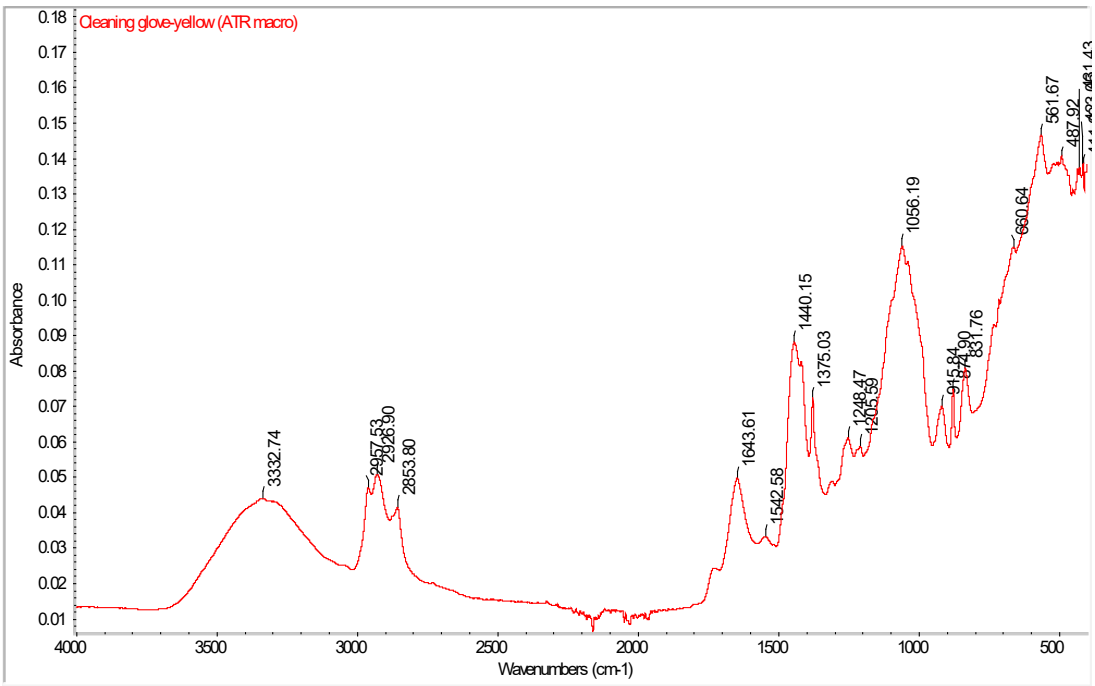

Figure H-73. Spectra of cleaning gloves fragment - ATR mode

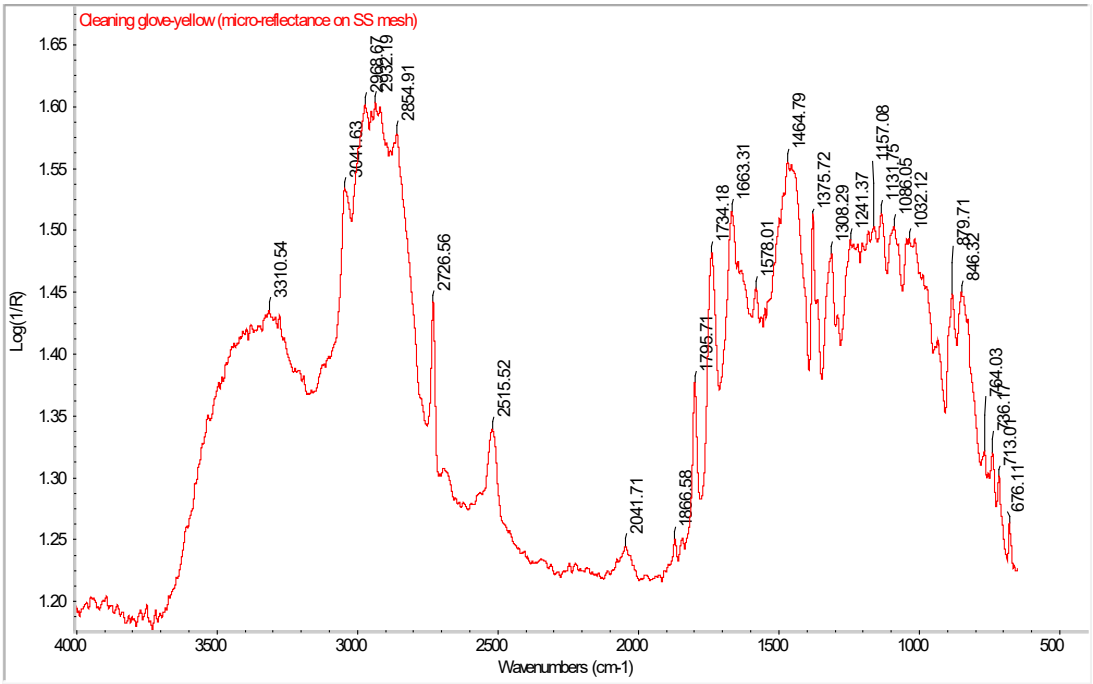

Figure H-74. Spectra of cleaning gloves fragment on stainless steel mesh - micro reflectance mode

13.Cosmetic sponge_used_dark purple

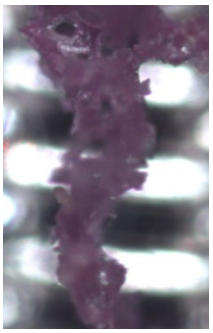

Figure H-75. Image of cosmetics sponge fragment under FTIR microscope

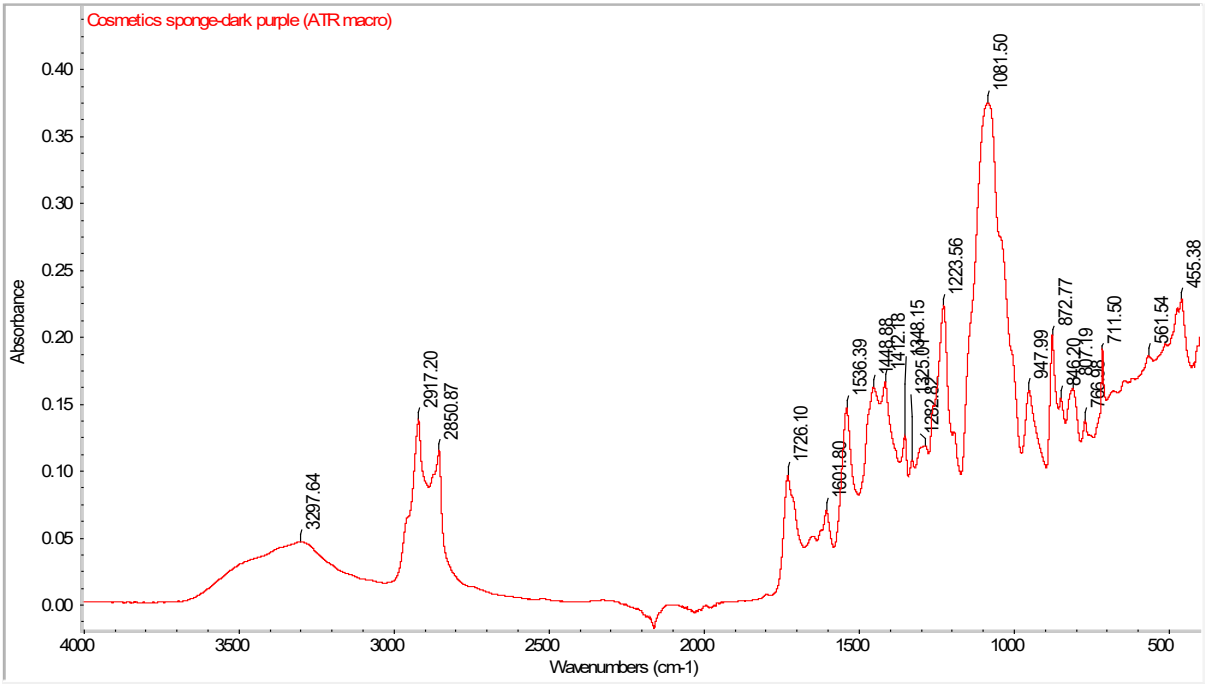

Figure H-76. Spectra of cosmetics sponge fragment - ATR mode

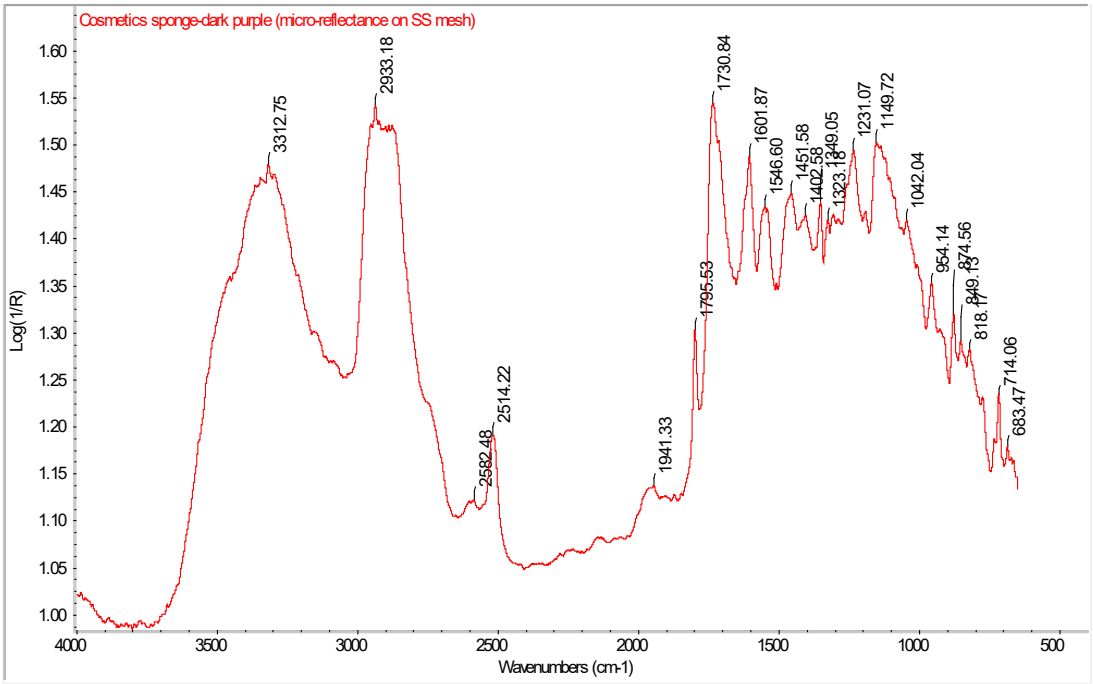

Figure H-77. Spectra of cosmetics sponge fragment on stainless steel mesh - micro reflectance mode

14.Artificial grass

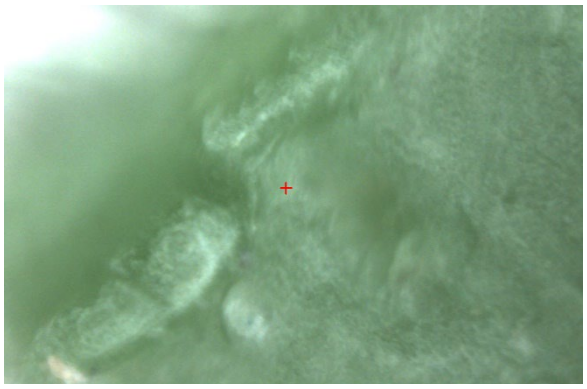

Figure H-78. Image of artificial grass fragment under FTIR microscope

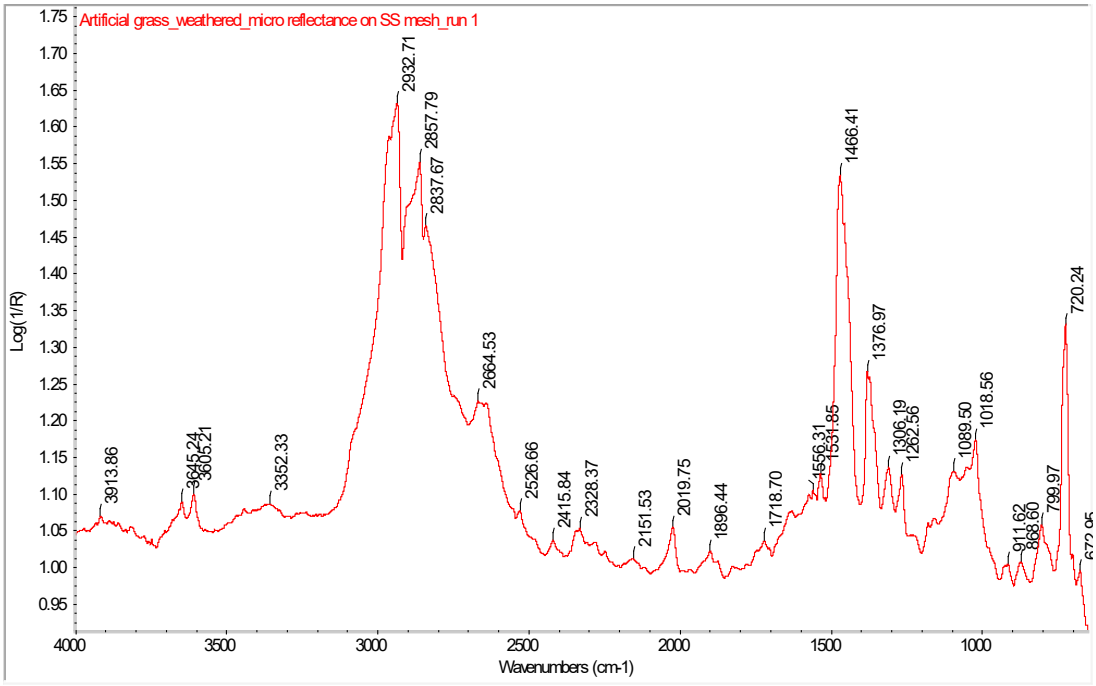

Figure H-79. Spectra of artificial grass fragment on stainless steel mesh - micro reflectance mode

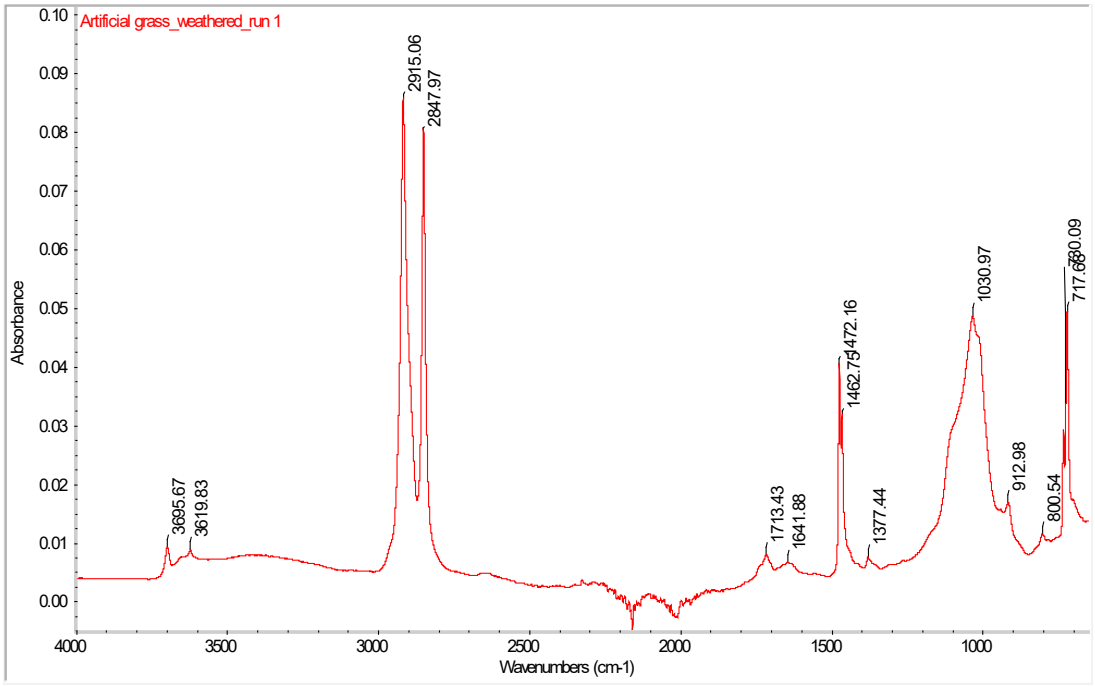

Figure H-80. Spectra of artificial grass fragment - ATR mode

15.Weathered firewood

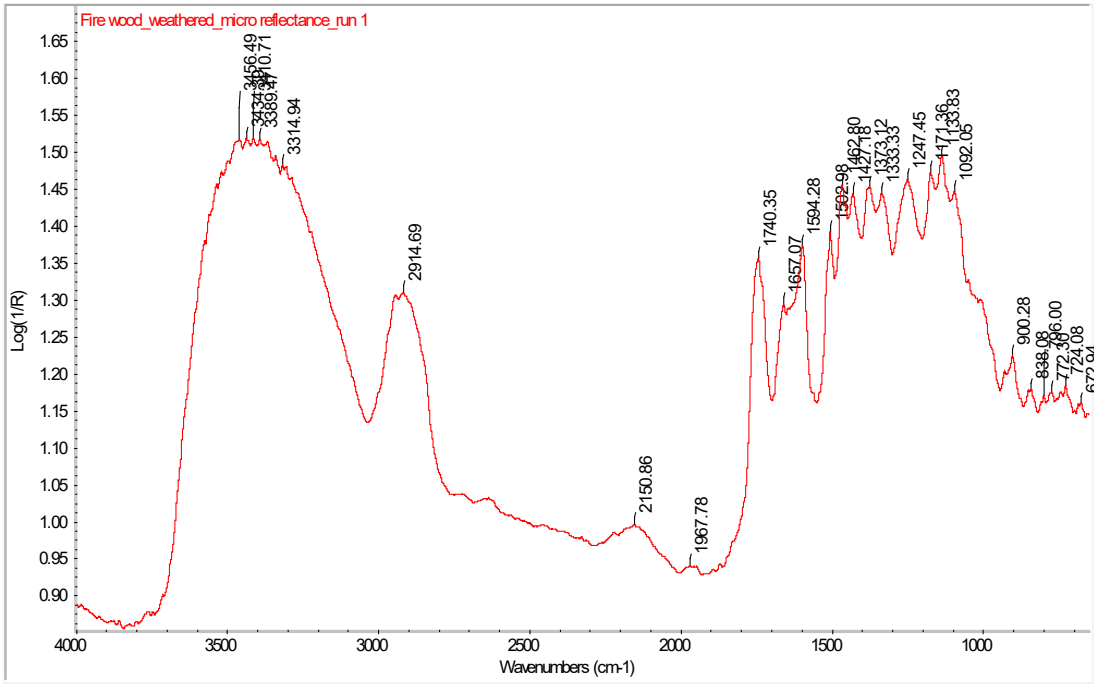

Figure H-81. Spectra of weathered firewood fragment on stainless steel mesh - micro reflectance mode

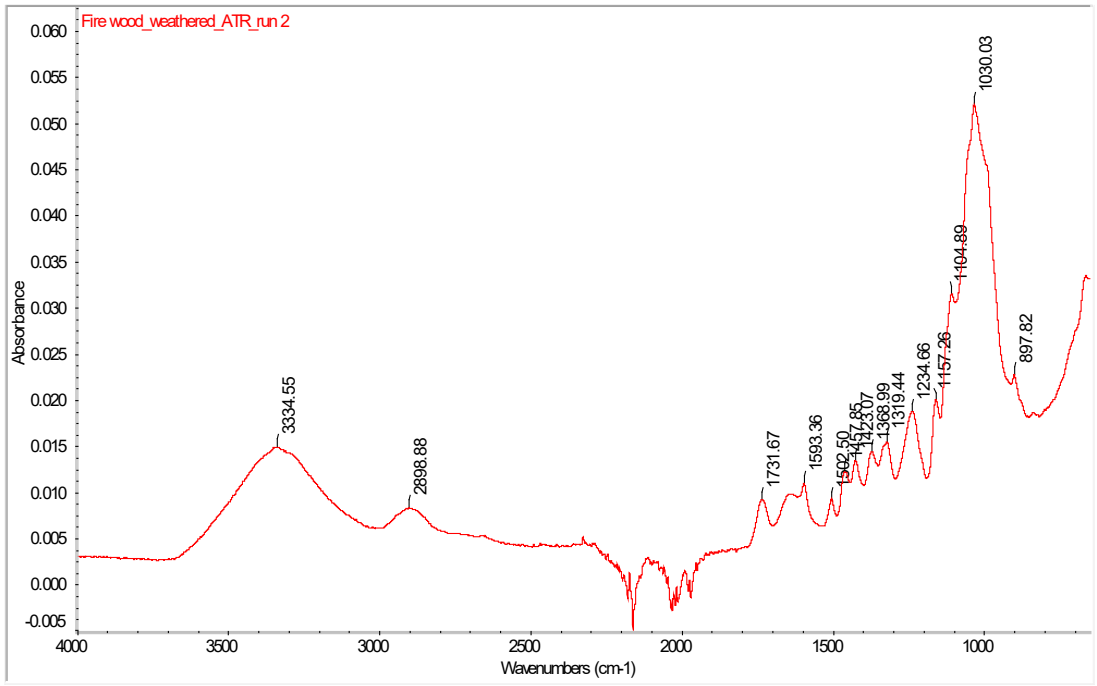

Figure H-82. Spectra of weathered firewood fragment - ATR mode

16.Water pipe

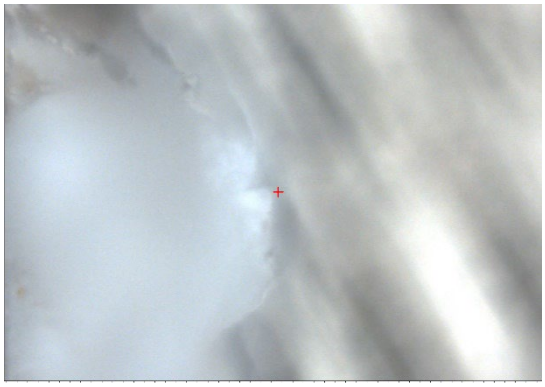

Figure H-83. Image of used water pipe fragment under FTIR microscope

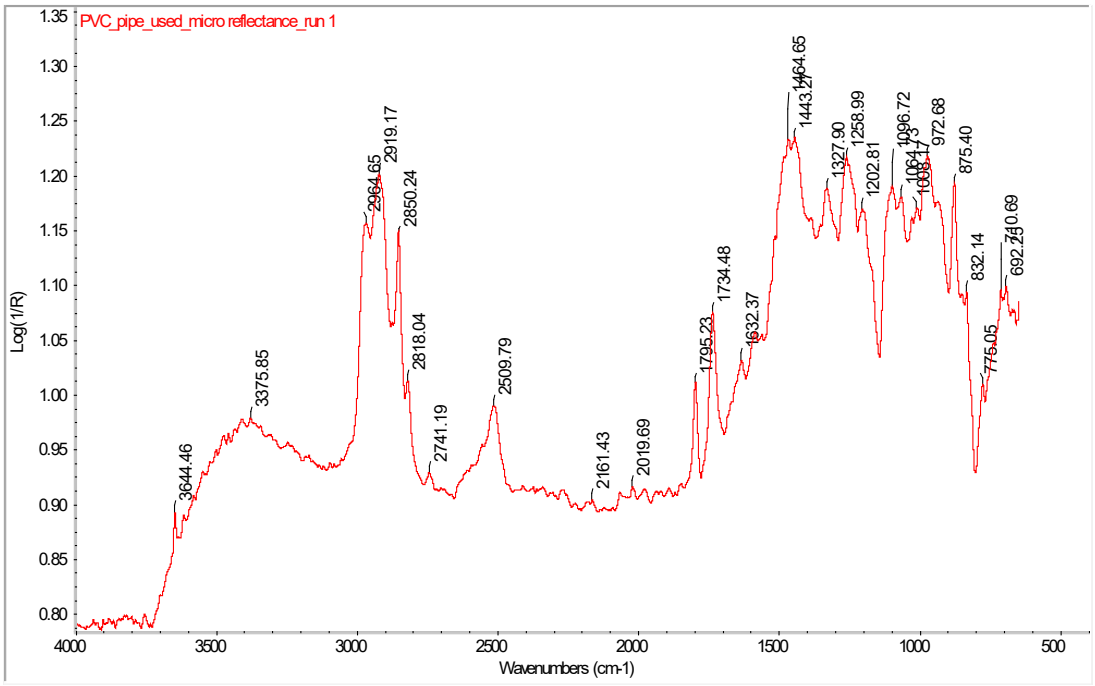

Figure H-84. Spectra of used water pipe fragment on stainless steel mesh - micro reflectance mode

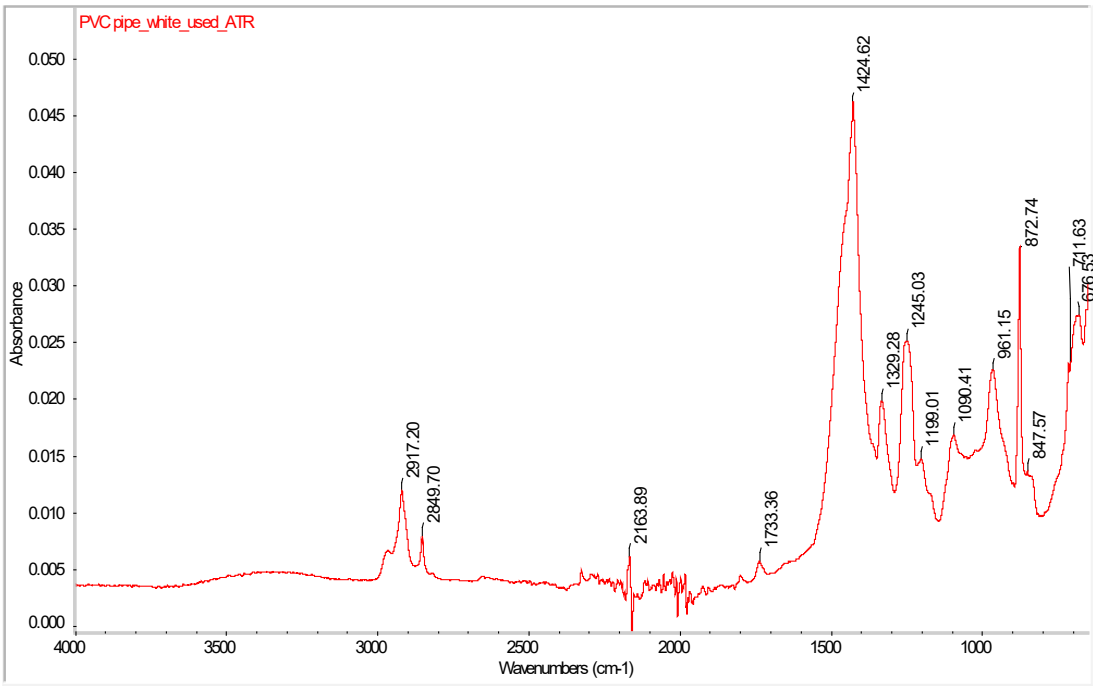

Figure H-85. Spectra of used water pipe fragment - ATR mode

17.Laundry wastewater bag trim

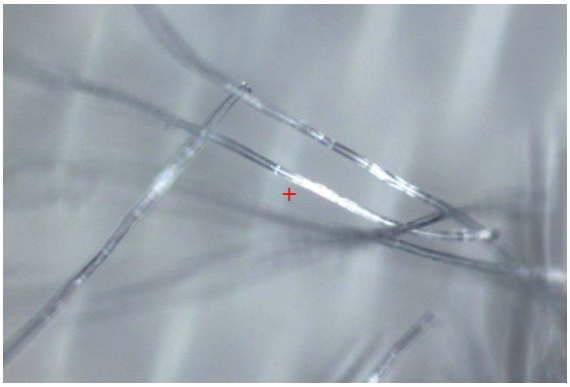

Figure H-86. Image of laundry wastewater bag trim fiber under FTIR microscope

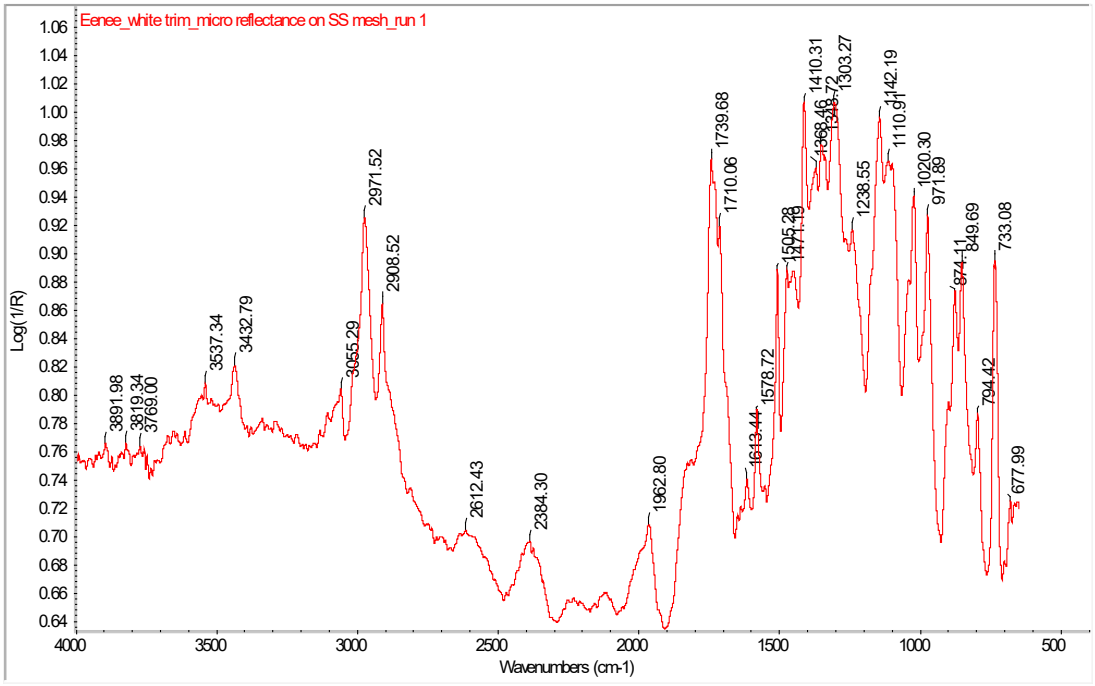

Figure H-87. Spectra of laundry wastewater bag trim fiber on stainless steel mesh - micro reflectance mode

18.Poly(butylene terephthalate)

Figure H-88. Image of poly(butylene terephthalate) fragment under FTIR microscope

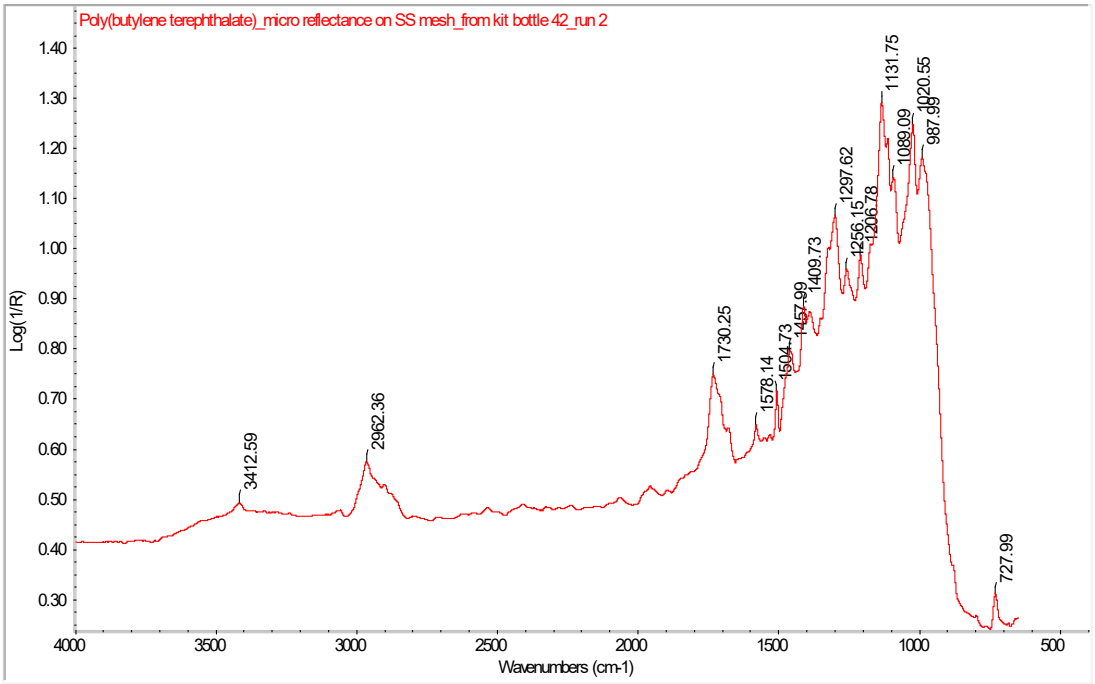

Figure H-89. Spectra of PBT fragment on stainless steel mesh - micro reflectance mode

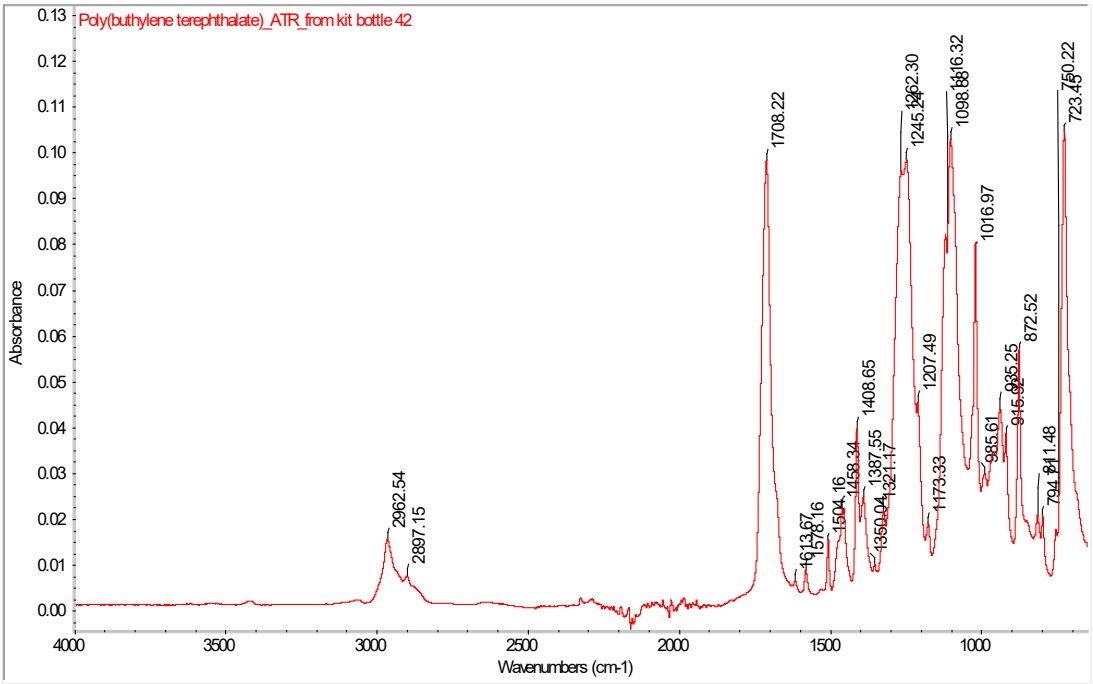

Figure H-90. Spectra of PBT fragment - ATR mode

19.Polyethylene, high density

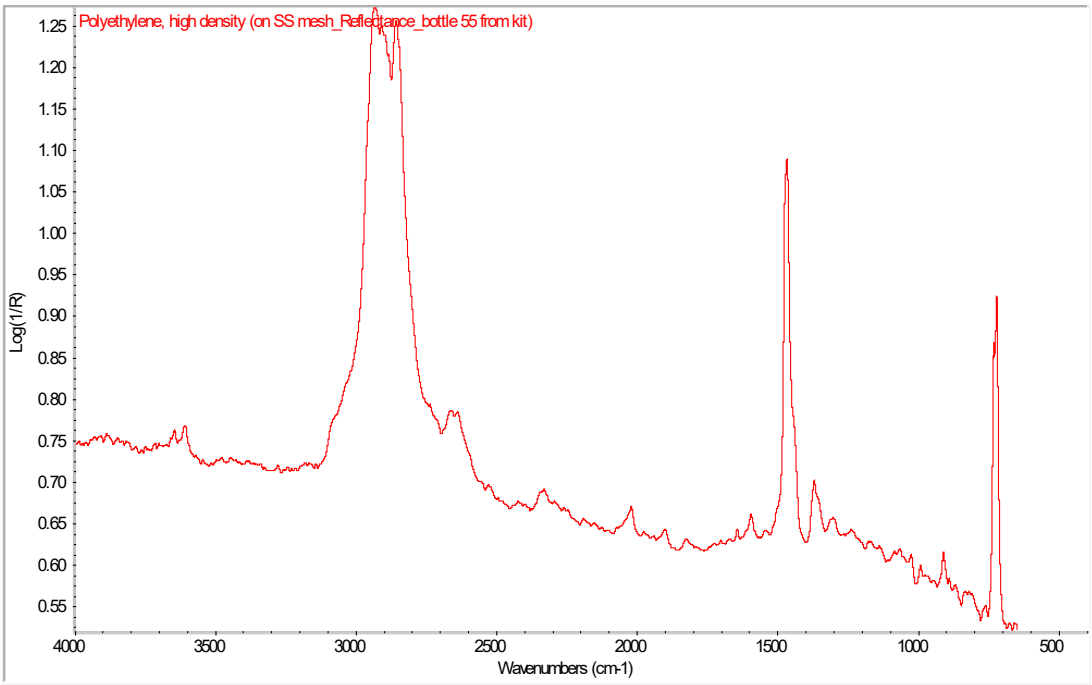

Figure H-91. Spectra of high-density polyethylene fragment on stainless steel mesh - micro reflectance mode

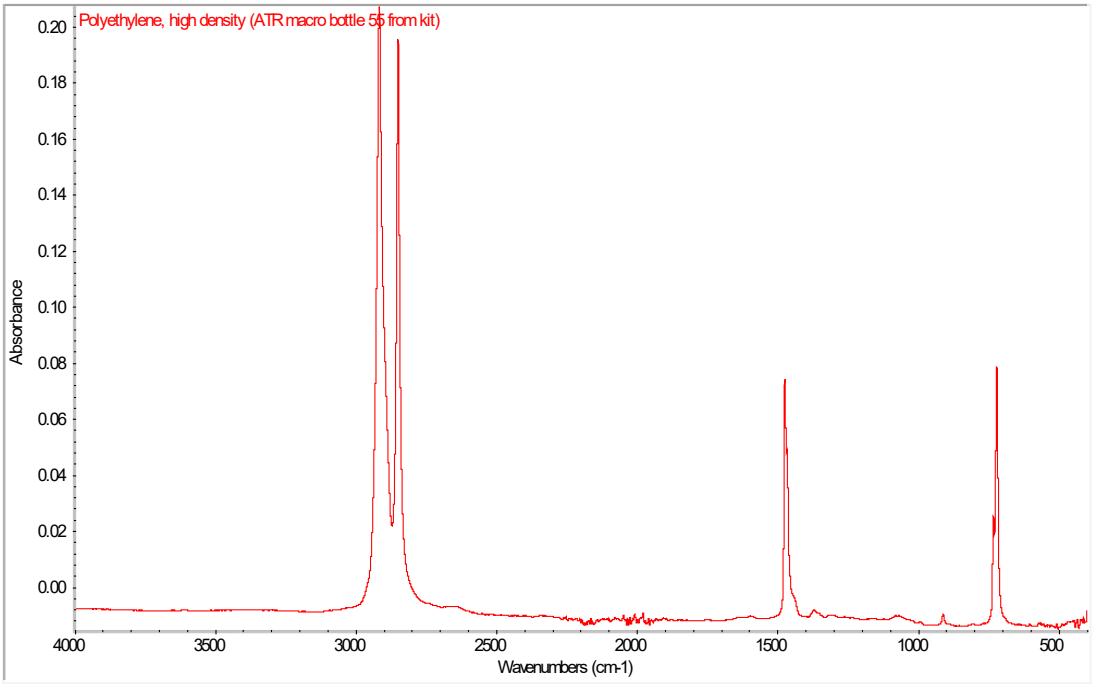

Figure H-92. Spectra of high-density polyethylene fragment - ATR mode

20.Polyethylene, low density

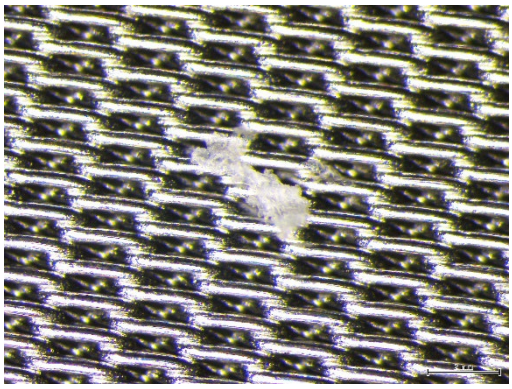

Figure H-93. Image of low-density polyethylene fragment under stereomicroscope

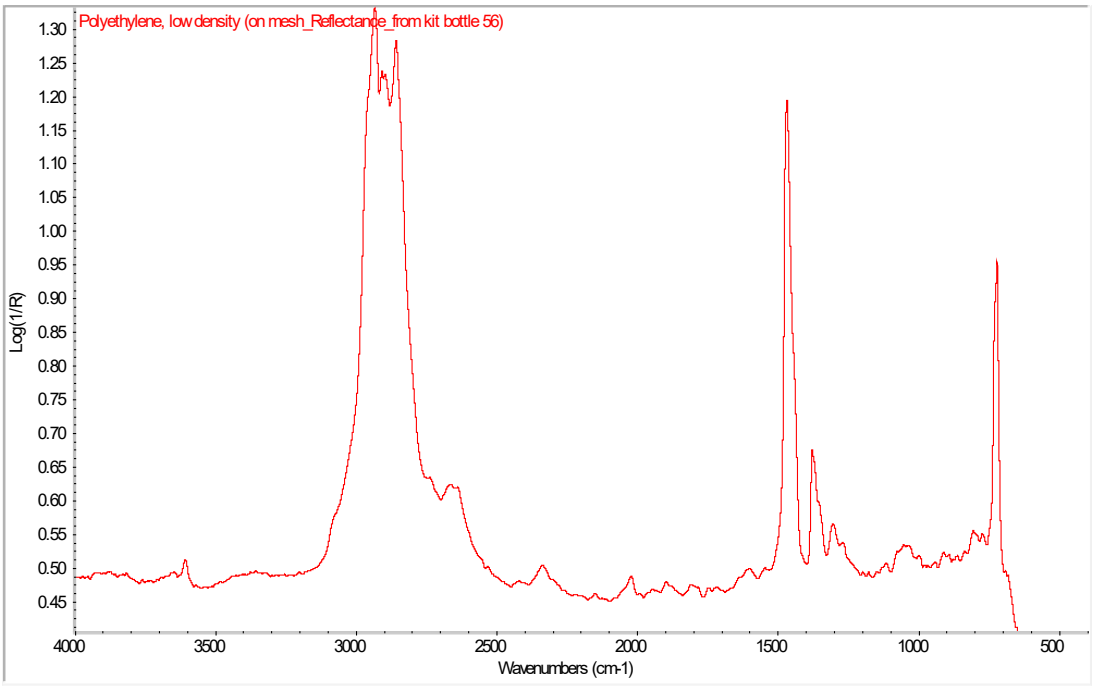

Figure H-94. Spectra of low-density polyethylene fragment - micro reflectance mode

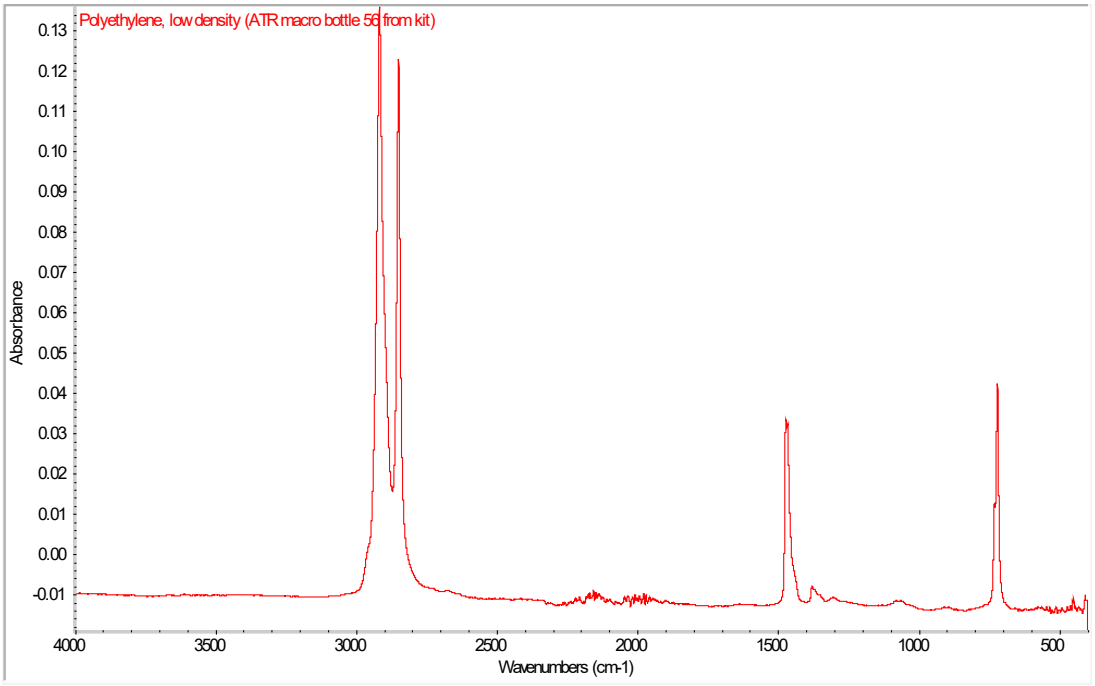

Figure H-95. Spectra of low-density polyethylene fragment - ATR mode

21.Polystyrene

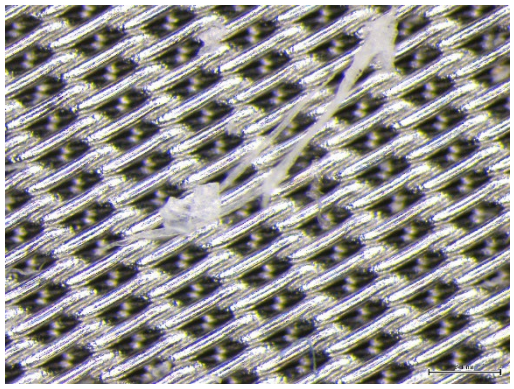

Figure H-96. Image of polystyrene fragment under stereomicroscope

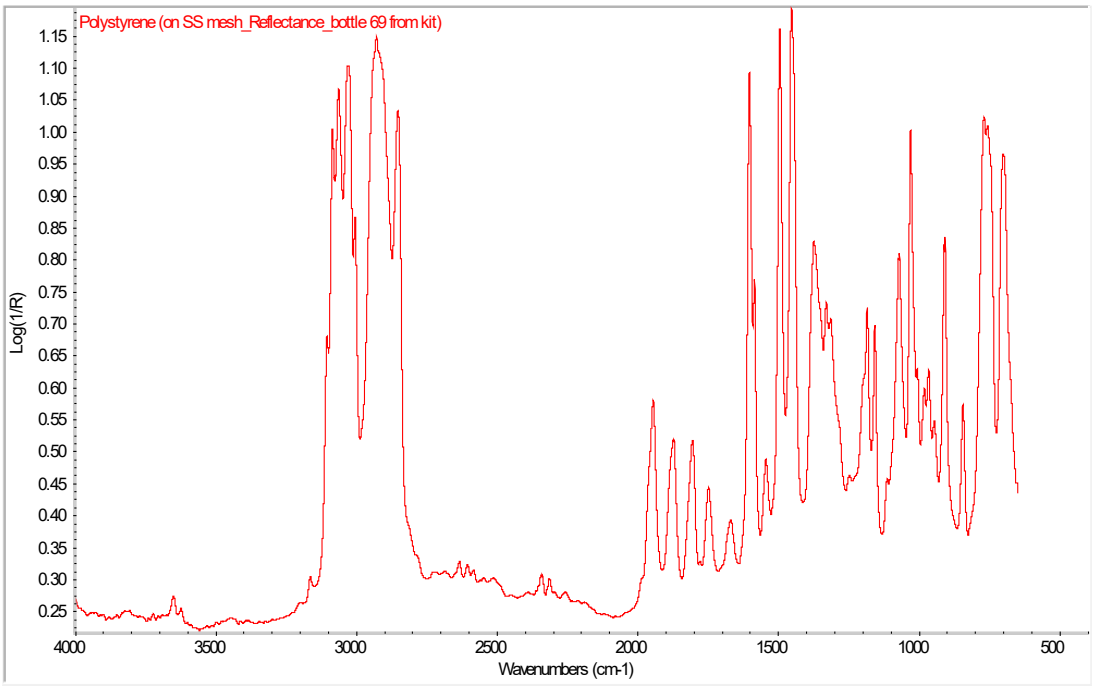

Figure H-97. Spectra of polystyrene fragment on stainless steel mesh - micro reflectance mode

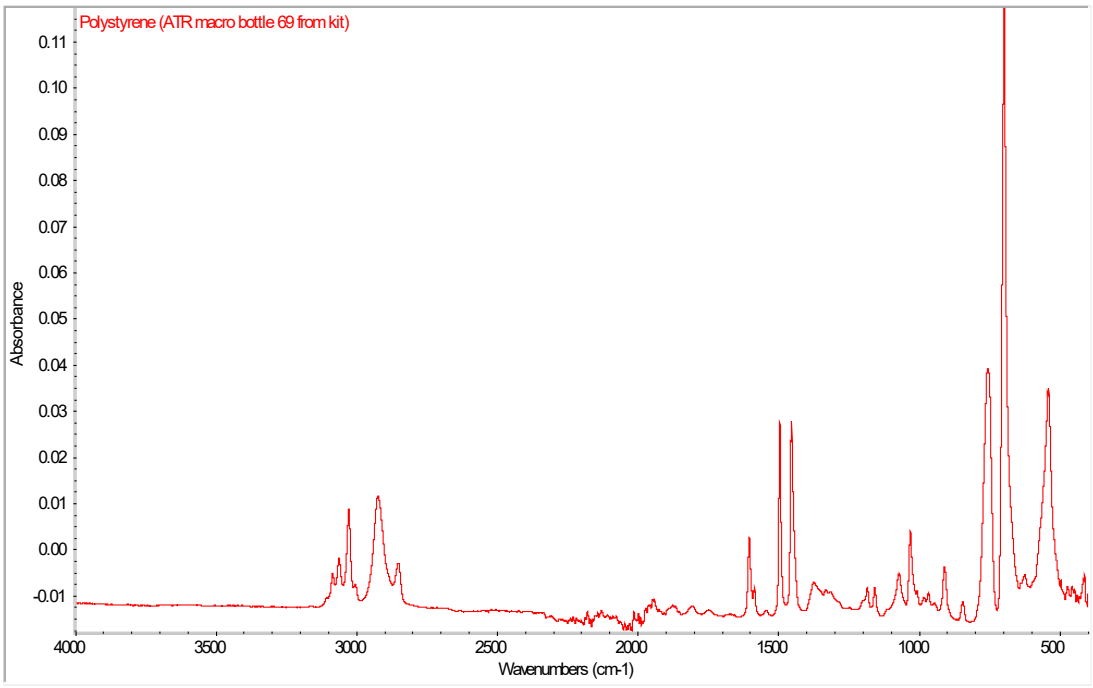

Figure H-98. Spectra of polystyrene fragment - ATR mode

22.Polypropylene

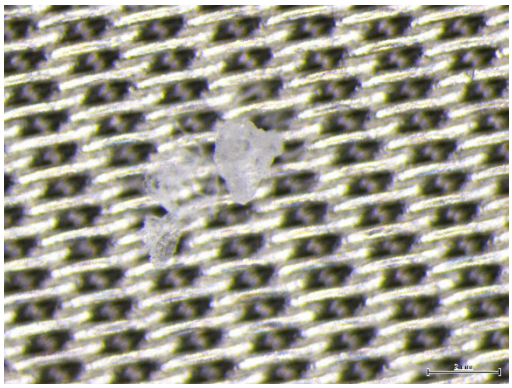

Figure H-99. Image of polypropylene fragment under stereomicroscope

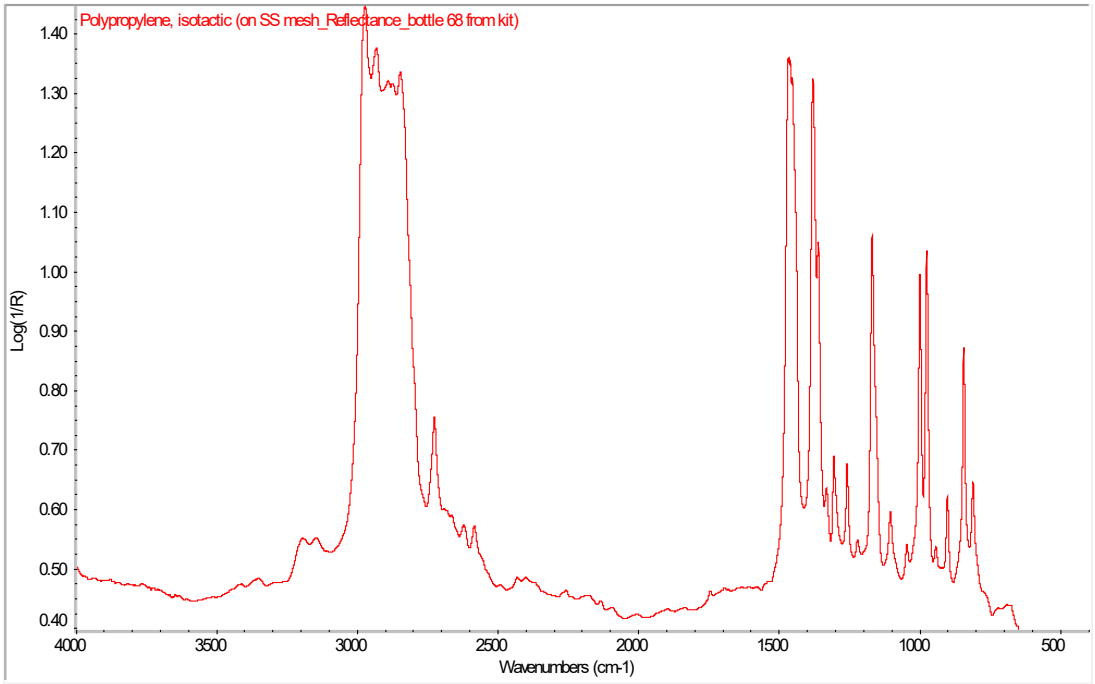

Figure H-100. Spectra of polypropylene on stainless steel mesh - micro reflectance mode

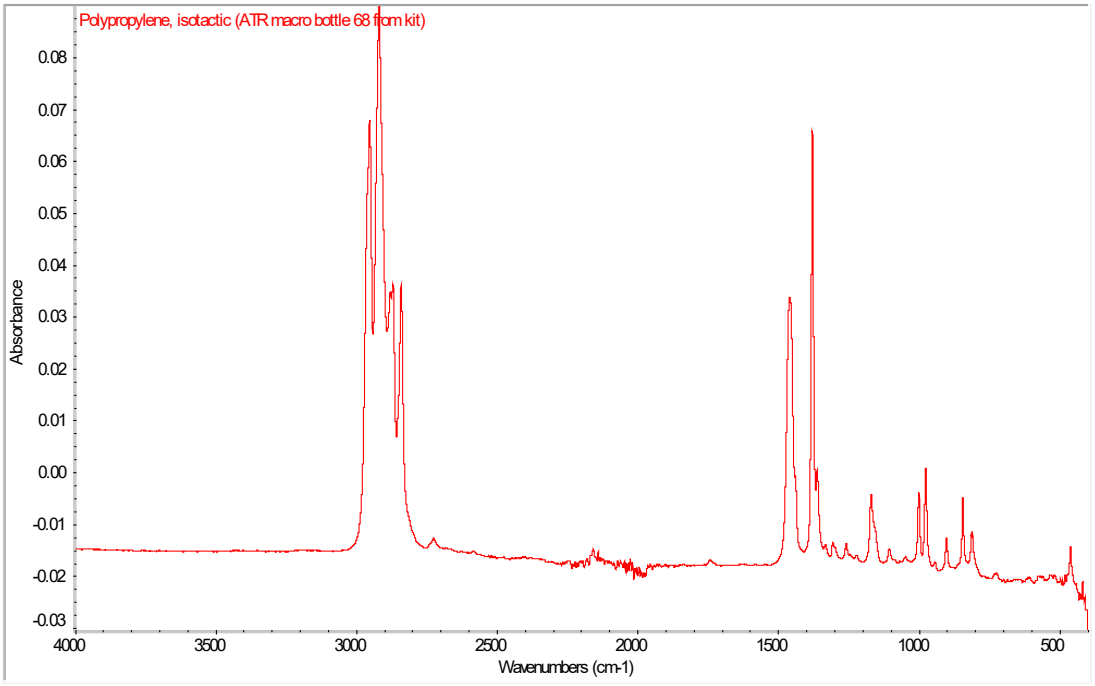

Figure H-101. Spectra of polypropylene - ATR mode

23.Poly(ethylene terephthalate)

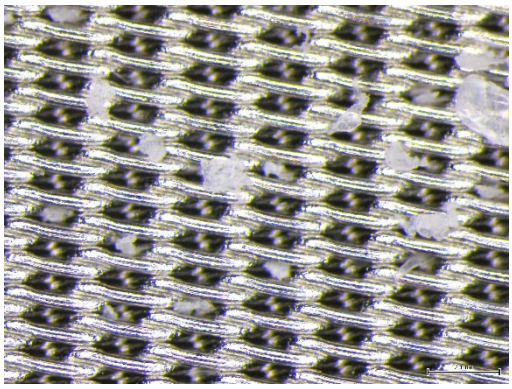

Figure H-102. Poly(ethylene terephthalate) fragment under stereomicroscope

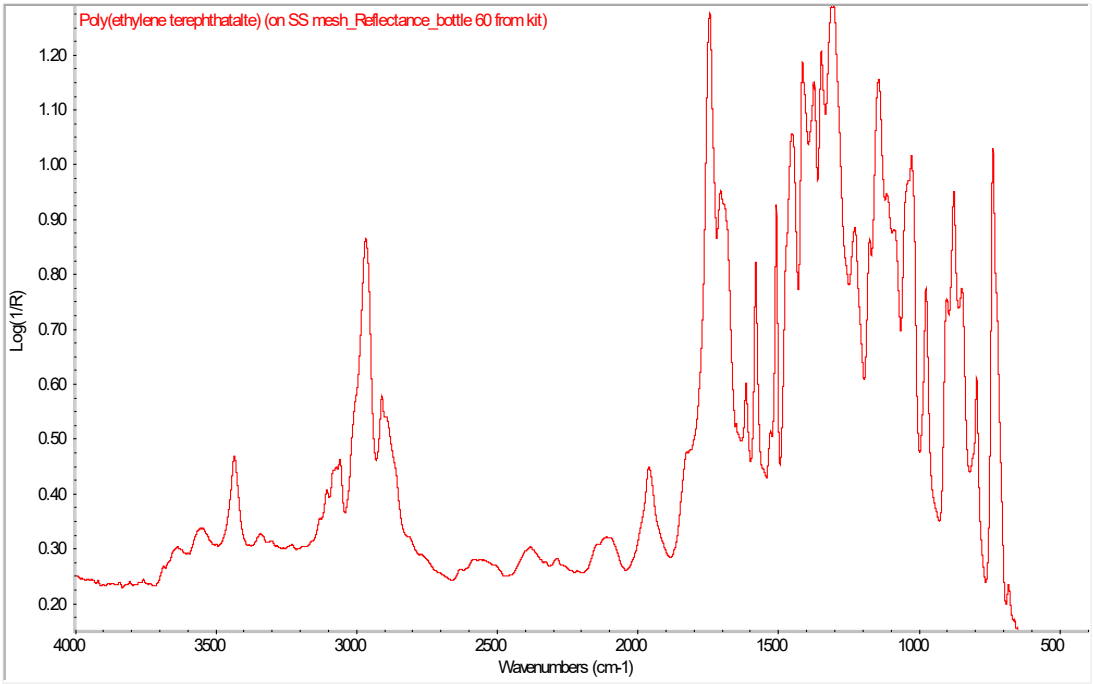

Figure H-103. Spectrum of poly(ethylene terephthalate) on stainless steel mesh - micro reflectance mode

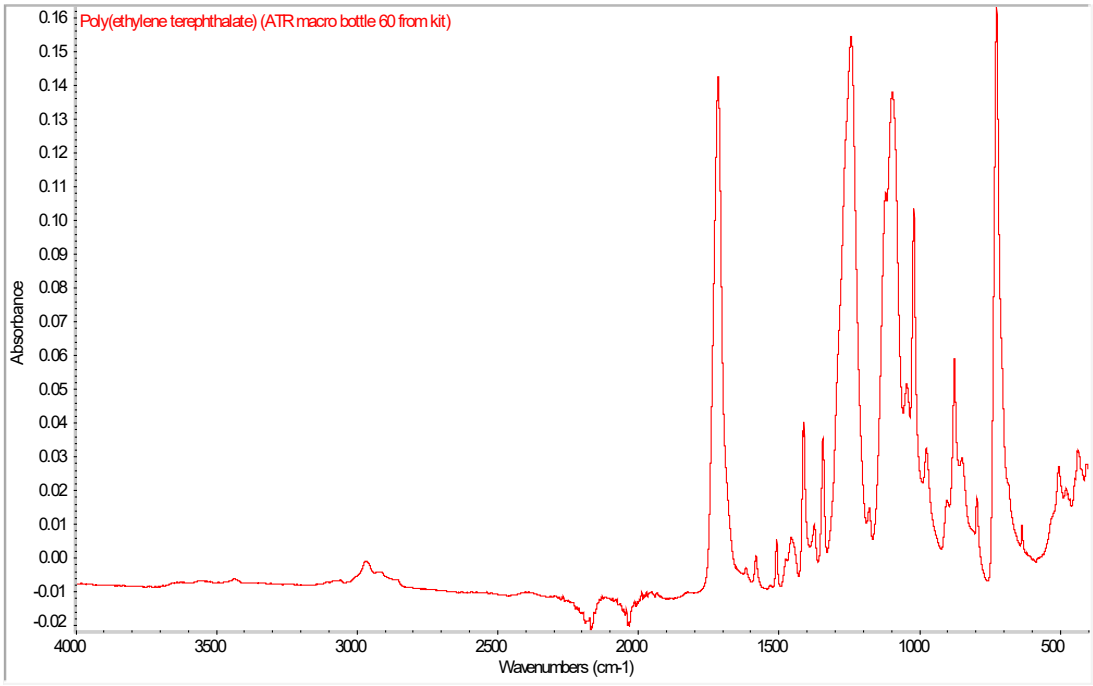

Figure H-104. Spectrum of poly(ethylene terephthalate) - ATR mode

24.Poly(vinyl stearate)

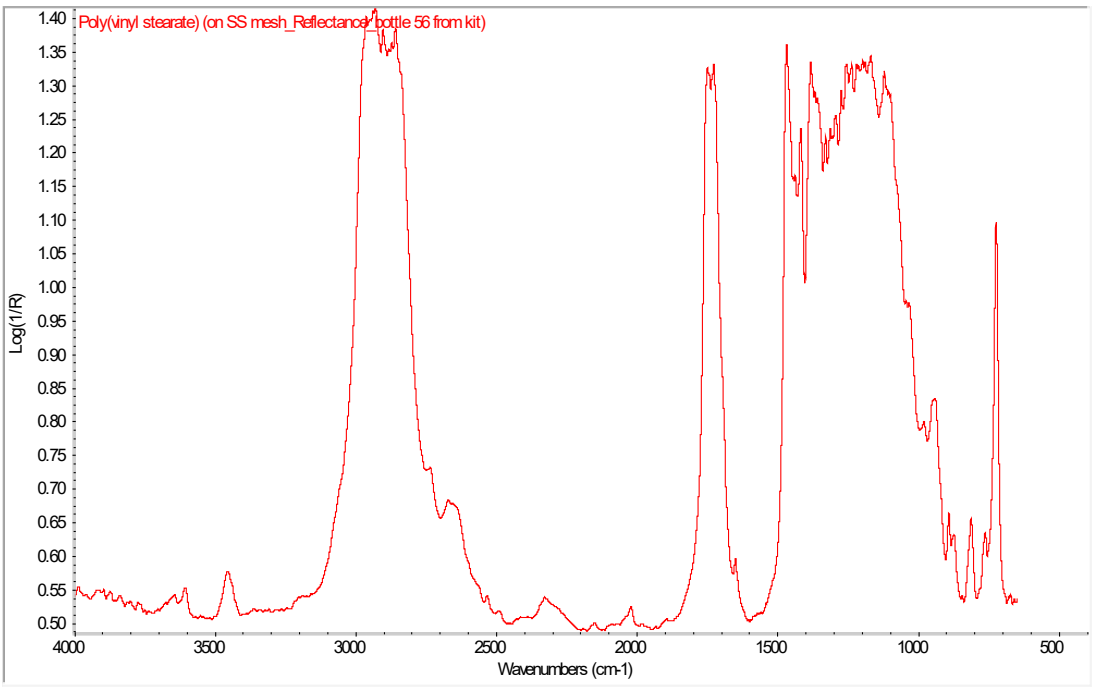

Figure H-105. Spectra of poly(vinyl stearate) on stainless steel mesh - micro reflectance mode

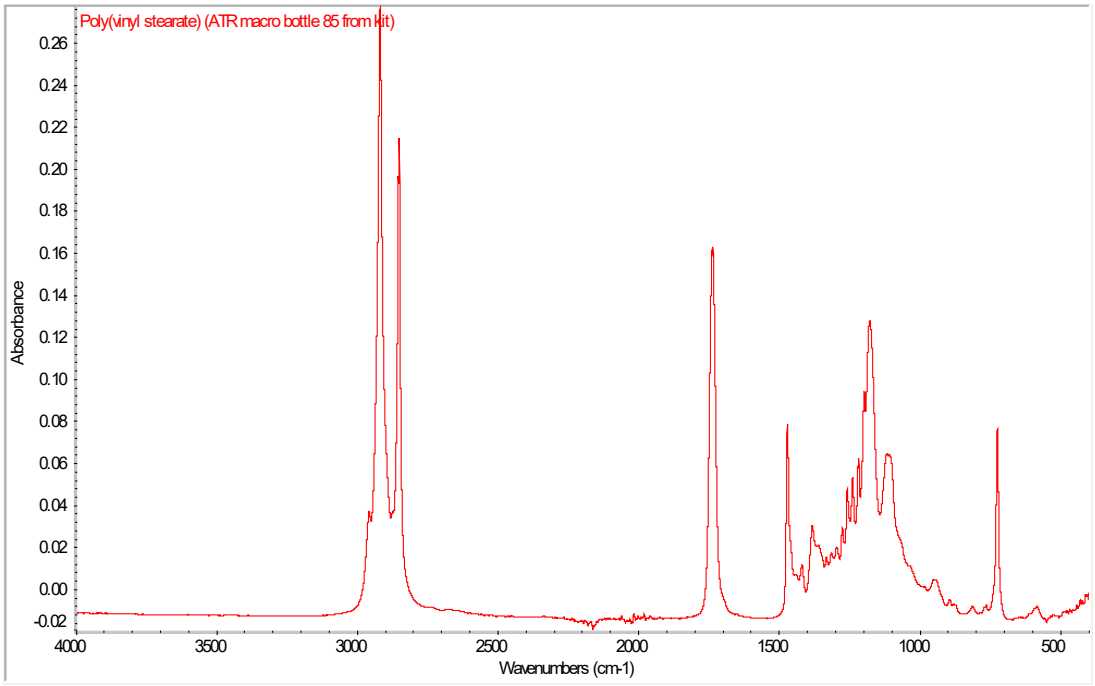

Figure H-106. Spectra of poly(vinyl stearate) - ATR mode

25.Poly(methyl methacrylate)

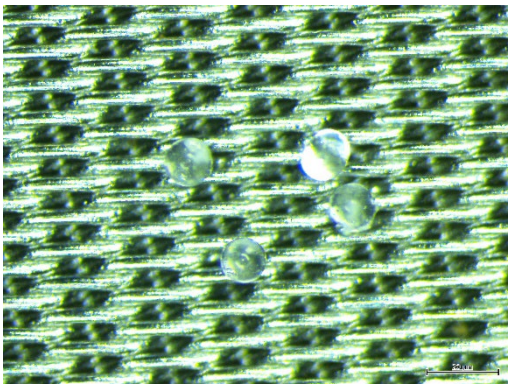

Figure H-107. Image of poly(methyl methacrylate) under stereomicroscope

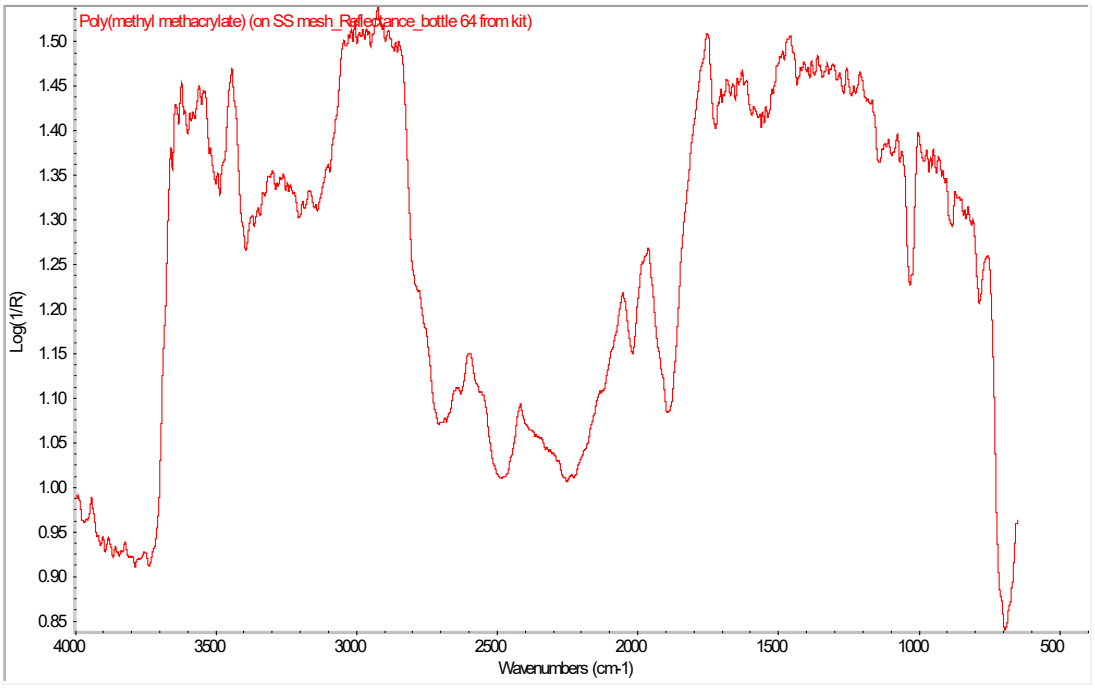

Figure H-108. Spectra of poly(methyl methacrylate) on stainless steel mesh - micro reflectance mode

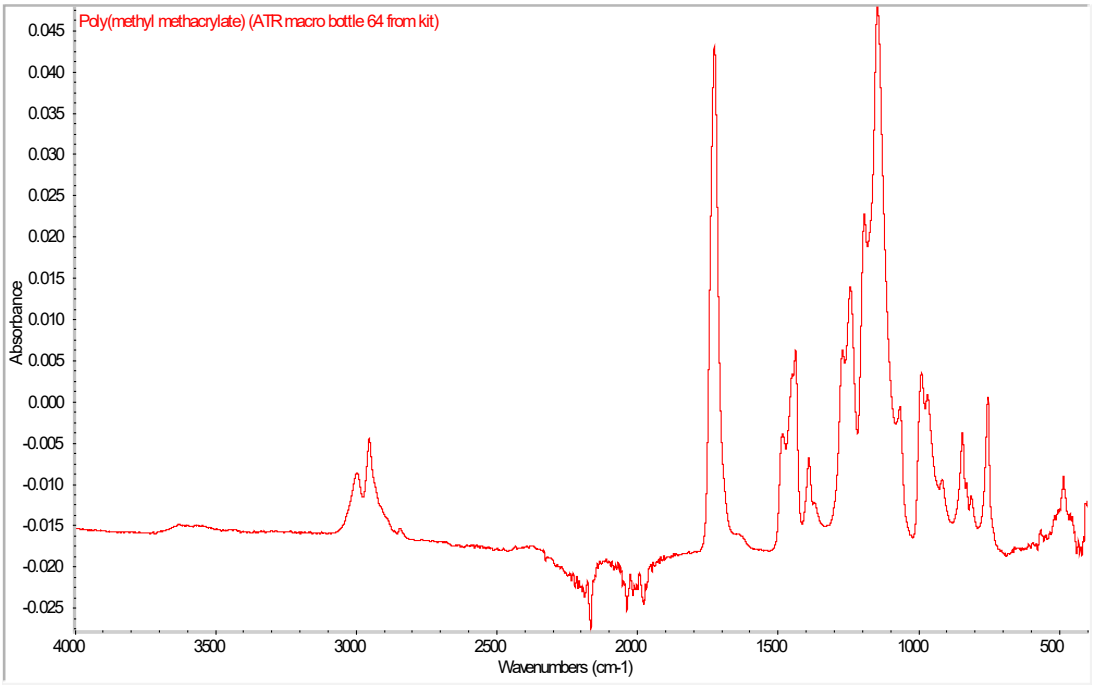

Figure H-109. Spectra of poly(methyl methacrylate) - ATR mode

26.Polyacrylamide

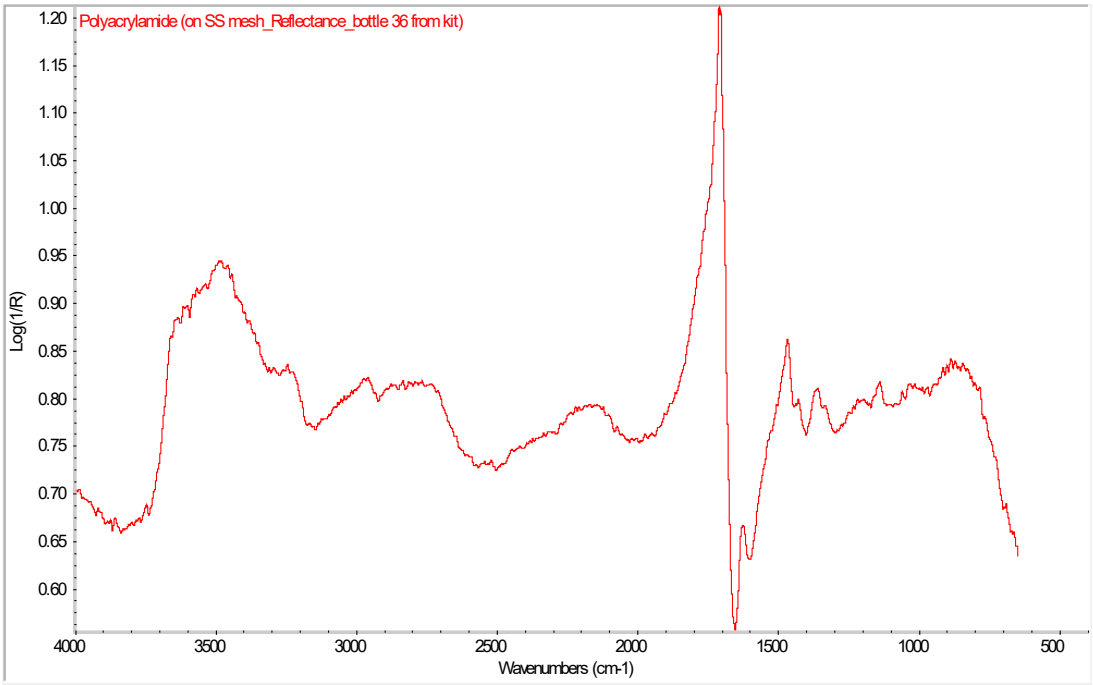

Figure H-110. Spectra of polyacrylamide on stainless steel mesh - micro reflectance mode

27.Poly(tetrafluoroethylene)_Teflon

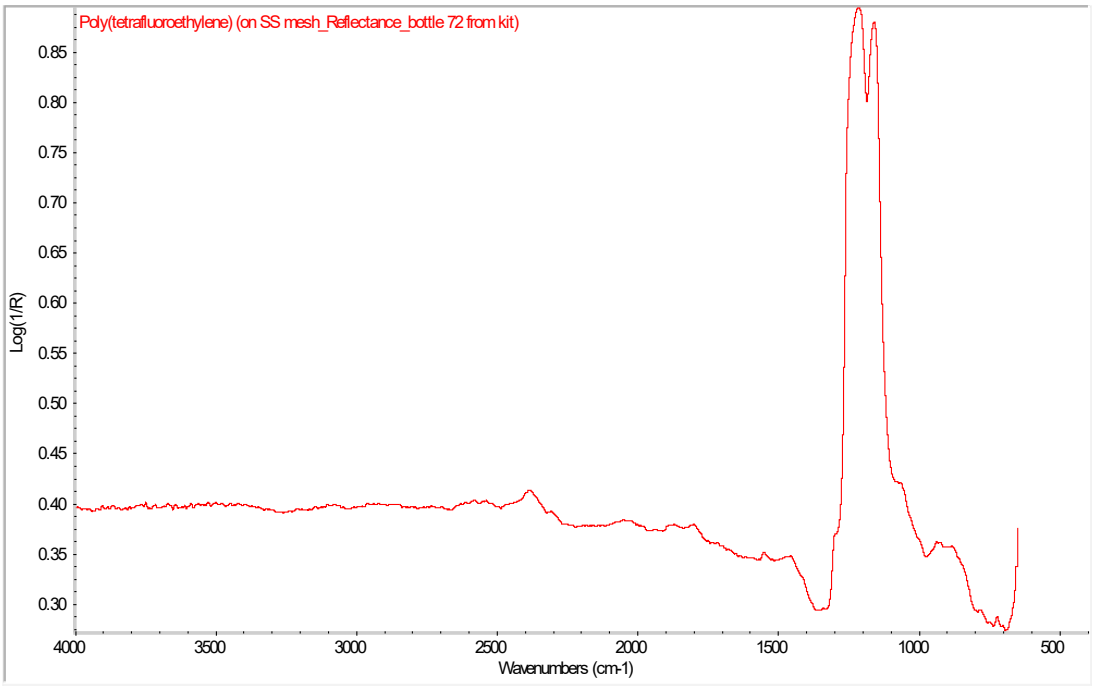

Figure H-111. Spectra of poly(tetrafluoroethylene) on stainless steel mesh - micro reflectance mode

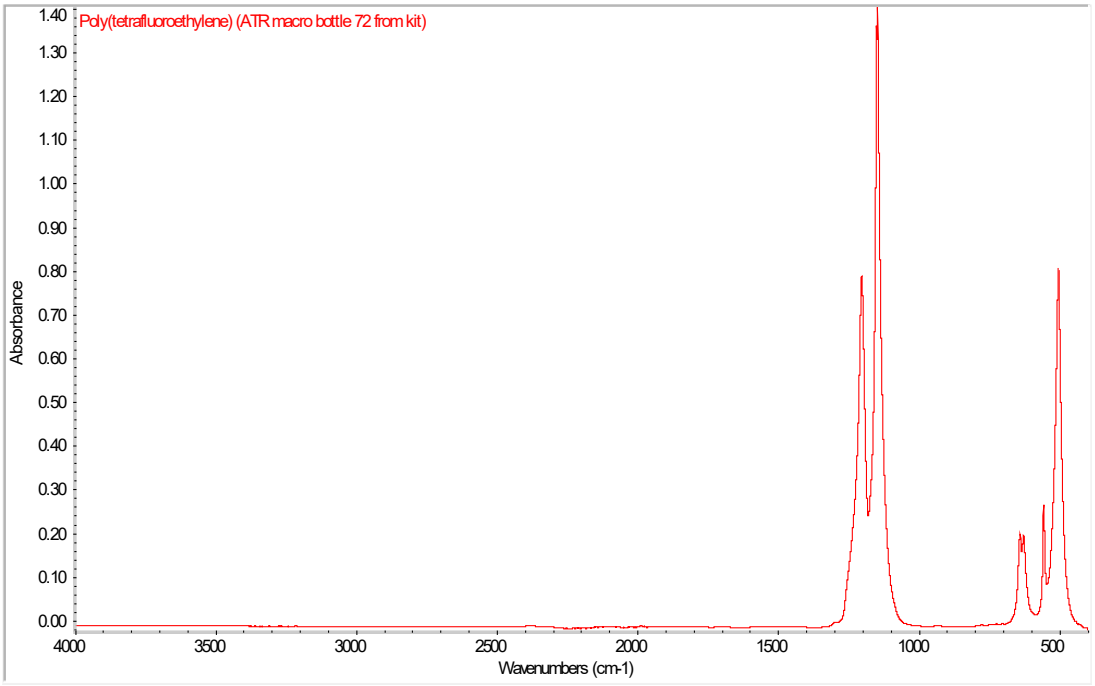

Figure H-112. Spectra of poly(tetrafluoroethylene) - ATR mode

28.Poly(vinyl alcohol)

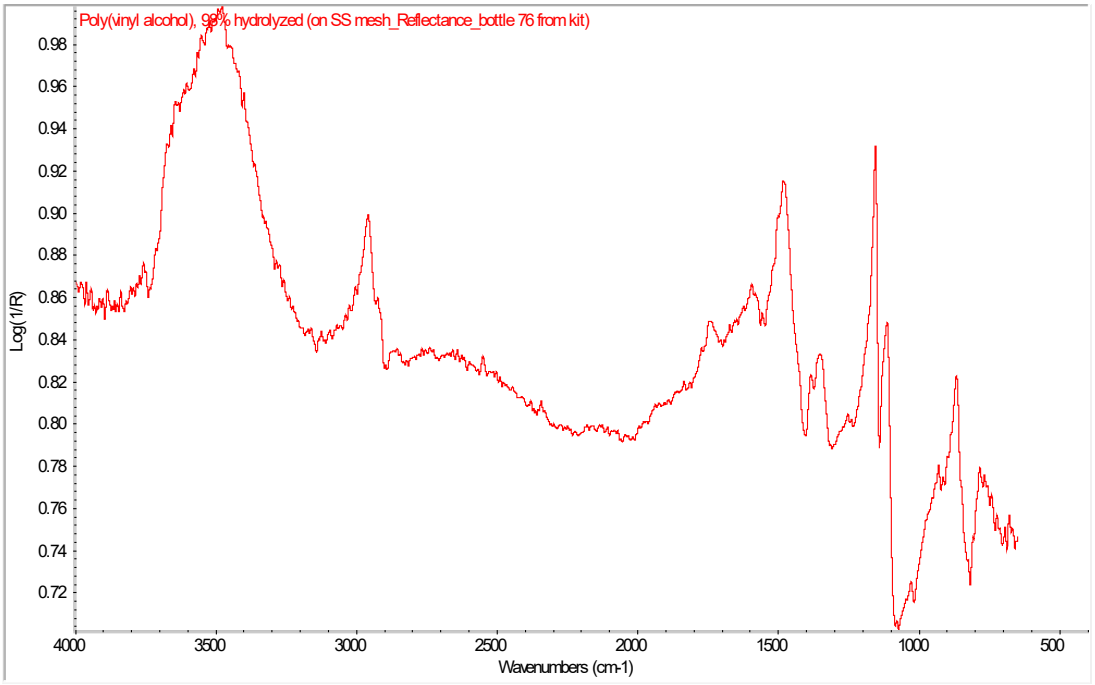

Figure H-113. Spectra of poly(vinyl alcohol) on stainless steel mesh - micro reflectance mode

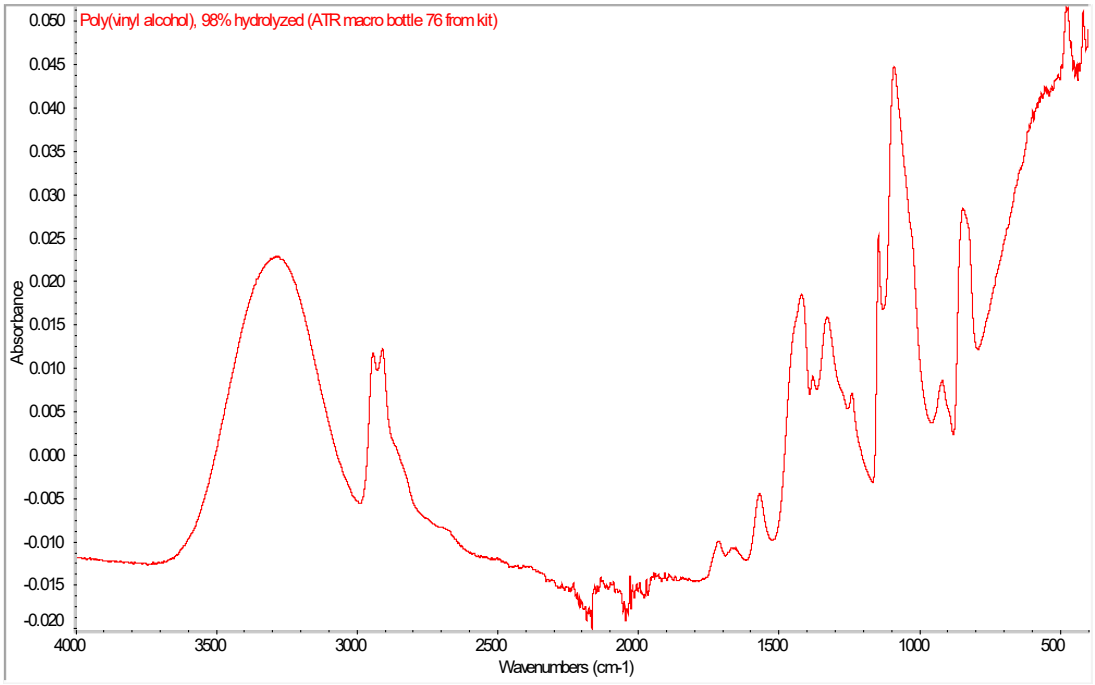

Figure H-114. Spectra of poly(vinyl alcohol) - ATR mode

29.Poly(vinyl chloride)

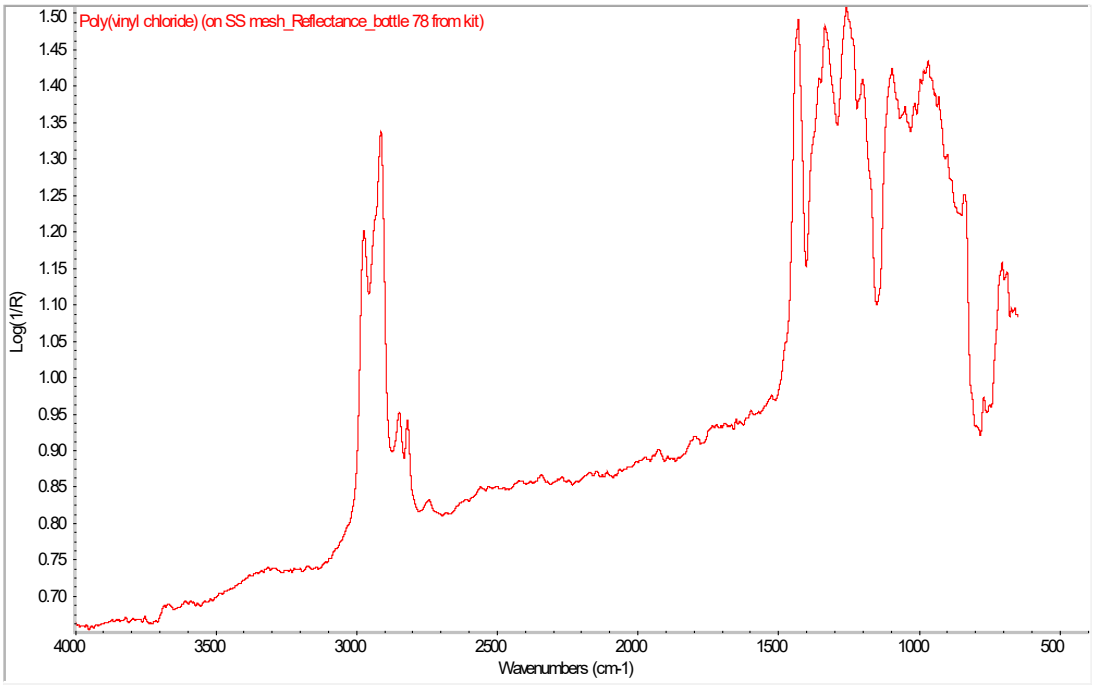

Figure H-115. Spectra of poly(vinyl chloride) on stainless steel mesh - micro reflectance mode

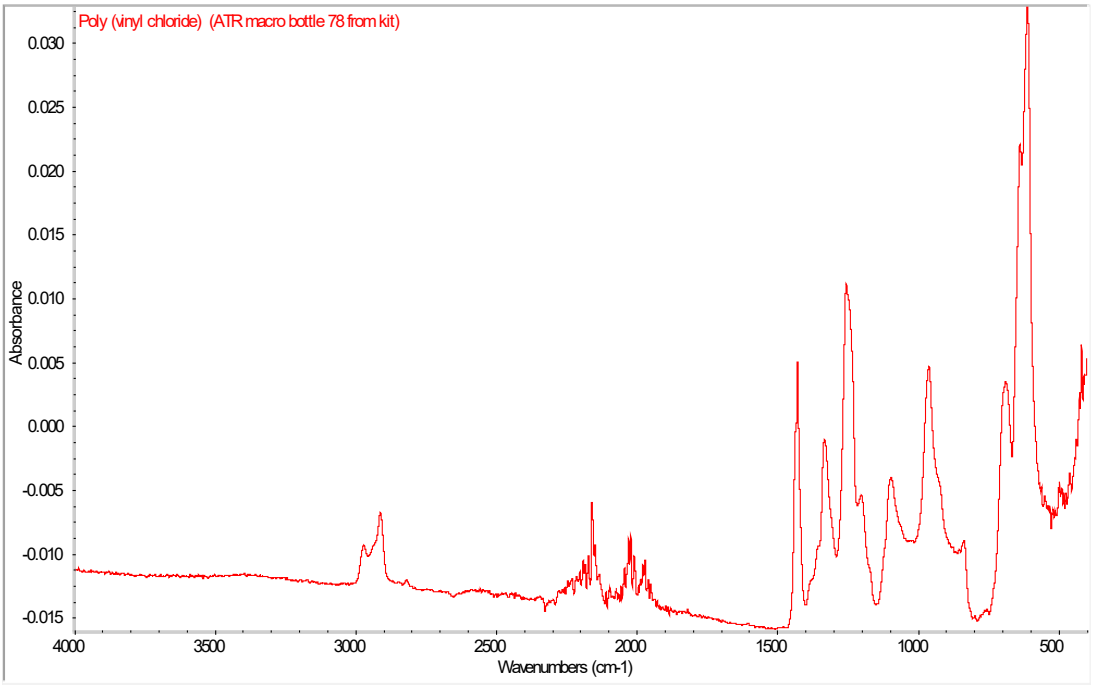

Figure H-116. Spectra of poly(vinyl chloride) - ATR mode

30.Poly(vinyl acetate)

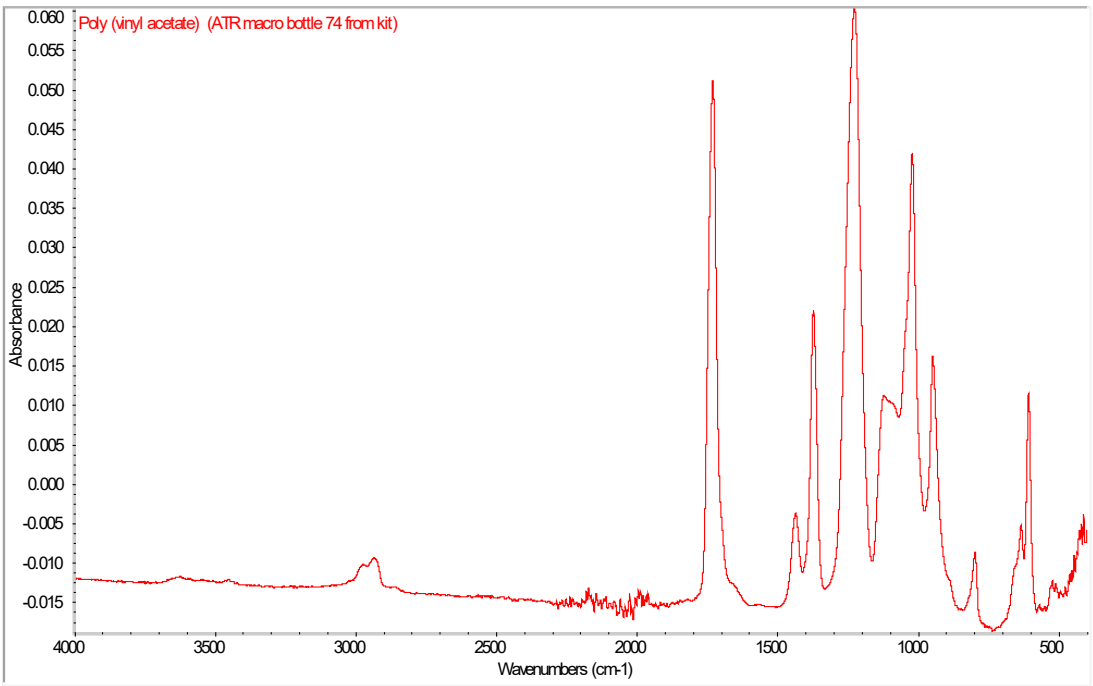

Figure H-117. Spectra of poly(vinyl acetate) - ATR mode

31.Polyamide resin

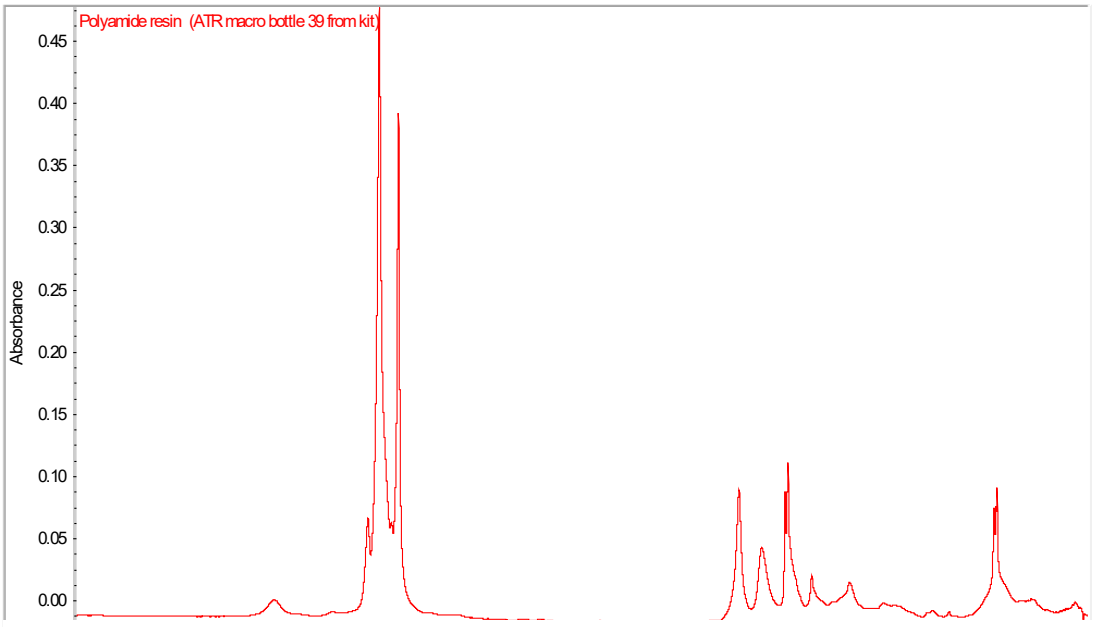

Figure H-118. Spectra of polyamide resin - ATR mode

APPENDIX I. CHAPTER 6 -SEASONAL TREND DATA STATISTICAL ANALYSIS

1. Statistical analysis result for microplastics size above 25 µm in unit of particles per kg dry solid

Table I-11. Descriptive Statistics of microplastics size >25 µm (particles per kg dry solid)

	Seasons	Mean	Std. Deviation	N
Influent_25_per_kg	Spring_2021	66780000.00	14085567.081	2
	Summer_2022	6180000.00	1909188.309	2
	Winter_2022	83625000.00	32491556.596	2
	Summer_2023	37990000.00	6979369.599	3
	Total	47460000.00	32393346.925	9
Primary_25_per_kg	Spring_2021	34870000.00	3705239.533	2
	Summer_2022	4155000.00	332340.187	2
	Winter_2022	6685000.00	1534421.715	2
	Summer_2023	3560000.00	323573.794	3
	Total	11344444.44	13471713.060	9
Secondary_25_per_kg	Spring_2021	5870000.00	480832.611	2
	Summer_2022	4195000.00	261629.509	2
	Winter_2022	7280000.00	919238.816	2
	Summer_2023	4656666.67	448367.409	3
	Total	5406666.67	1304731.773	9
Digested_25_per_kg	Spring_2021	18005000.00	912167.748	2
	Summer_2022	7980000.00	98994.949	2
	Winter_2022	10590000.00	975807.358	2
	Summer_2023	9090000.00	1135825.691	3
	Total	11157777.78	4059118.678	9
Dewatered_25_per_kg	Spring_2021	6100000.00	579827.561	2
	Summer_2022	14185000.00	1944543.648	2
	Winter_2022	5610000.00	777817.459	2
	Summer_2023	8170000.00	1806765.065	3
	Total	8477777.78	3613103.852	9

Table I-12. Multivariate Testa of microplastics size >25 µm (particles per kg dry solid)

Effect		Value	F	Hypothesis df	Error df	Sig.	Partial Eta Squared
Intercept	Pillai's Trace	.998	87.169[b]	5.000	1.000	.081	.998
	Wilks' Lambda	.002	87.169[b]	5.000	1.000	.081	.998
	Hotelling's Trace	435.843	87.169[b]	5.000	1.000	.081	.998
	Roy's Largest Root	435.843	87.169[b]	5.000	1.000	.081	.998
Seasons	Pillai's Trace	2.613	4.049	15.000	9.000	.020	.871
	Wilks' Lambda	.000	10.745	15.000	3.162	.033	.974
	Hotelling's Trace	.	.	15.000	.	.	.
	Roy's Largest Root	1179.022	707.413[c]	5.000	3.000	<.001	.999

a. Design: Intercept + Seasons

b. Exact statistic

c. The statistic is an upper bound on F that yields a lower bound on the significance level.

Table I-13. Tests of Between-Subjects Effects of microplastics size >25 µm (particles per kg dry solid)

Source	Dependent Variable	Type III Sum of Squares	df	Mean Square	F	Sig.	Partial Eta Squared
Corrected Model	Influent_25_per_kg	7.039E+15[a]	3	2.346E+15	8.658	.020	.839
	Primary_25_per_kg	1.435E+15[b]	3	4.785E+14	145.856	<.001	.989
	Secondary_25_per_kg	1.207E+13[c]	3	4.024E+12	13.008	.008	.886
	Digested_25_per_kg	1.274E+14[d]	3	4.248E+13	48.556	<.001	.967
	Dewatered_25_per_kg	9.318E+13[e]	3	3.106E+13	13.804	.007	.892
Intercept	Influent_25_per_kg	2.065E+16	1	2.065E+16	76.192	<.001	.938
	Primary_25_per_kg	1.324E+15	1	1.324E+15	403.615	<.001	.988
	Secondary_25_per_kg	2.640E+14	1	2.640E+14	853.550	<.001	.994
	Digested_25_per_kg	1.137E+15	1	1.137E+15	1300.145	<.001	.996
	Dewatered_25_per_kg	6.330E+14	1	6.330E+14	281.284	<.001	.983
Seasons	Influent_25_per_kg	7.039E+15	3	2.346E+15	8.658	.020	.839
	Primary_25_per_kg	1.435E+15	3	4.785E+14	145.856	<.001	.989
	Secondary_25_per_kg	1.207E+13	3	4.024E+12	13.008	.008	.886
	Digested_25_per_kg	1.274E+14	3	4.248E+13	48.556	<.001	.967
	Dewatered_25_per_kg	9.318E+13	3	3.106E+13	13.804	.007	.892
Error	Influent_25_per_kg	1.355E+15	5	2.710E+14			
	Primary_25_per_kg	1.640E+13	5	3.281E+12			
	Secondary_25_per_kg	1.547E+12	5	3.093E+11			
	Digested_25_per_kg	4.374E+12	5	8.749E+11			
	Dewatered_25_per_kg	1.125E+13	5	2.250E+12			
Total	Influent_25_per_kg	2.867E+16	9				
	Primary_25_per_kg	2.610E+15	9				
	Secondary_25_per_kg	2.767E+14	9				
	Digested_25_per_kg	1.252E+15	9				
	Dewatered_25_per_kg	7.513E+14	9				
Corrected Total	Influent_25_per_kg	8.395E+15	8				
	Primary_25_per_kg	1.452E+15	8				
	Secondary_25_per_kg	1.362E+13	8				
	Digested_25_per_kg	1.318E+14	8				
	Dewatered_25_per_kg	1.044E+14	8				

a. R Squared = .839 (Adjusted R Squared = .742)

b. R Squared = .989 (Adjusted R Squared = .982)

c. R Squared = .886 (Adjusted R Squared = .818)

d. R Squared = .967 (Adjusted R Squared = .947)

e. R Squared = .892 (Adjusted R Squared = .828)

Table I-14. Multiple Comparisons (Turkey HSD) of microplastics size >25 µm (particles per kg dry solid)

Dependent Variable	(I) Seasons	(J) Seasons	Mean Difference (I-J)	Std. Error	Sig.	95% Confidence Interval	
						Lower Bound	Upper Bound
Influent_25_per_kg	Spring_2021	Summer_2022	60600000.00	16463126.374	.050	-147502.47	121347502.47
		Winter_2022	-16845000.00	16463126.374	.745	-77592502.47	43902502.47
		Summer_2023	28790000.00	15028709.470	.329	-26664629.02	84244629.02
	Summer_2022	Spring_2021	-60600000.00	16463126.374	.050	-121347502.47	147502.47
		Winter_2022	-77445000.00*	16463126.374	.020	-138192502.47	-16697497.53
		Summer_2023	-31810000.00	15028709.470	.265	-87264629.02	23644629.02
	Winter_2022	Spring_2021	16845000.00	16463126.374	.745	-43902502.47	77592502.47
		Summer_2022	77445000.00*	16463126.374	.020	16697497.53	138192502.47
		Summer_2023	45635000.00	15028709.470	.098	-9819629.02	101089629.02
	Summer_2023	Spring_2021	-28790000.00	15028709.470	.329	-84244629.02	26664629.02
		Summer_2022	31810000.00	15028709.470	.265	-23644629.02	87264629.02
		Winter_2022	-45635000.00	15028709.470	.098	-101089629.02	9819629.02
Primary_25_per_kg	Spring_2021	Summer_2022	30715000.00*	1811248.188	<.001	24031651.94	37398348.06
		Winter_2022	28185000.00*	1811248.188	<.001	21501651.94	34868348.06
		Summer_2023	31310000.00*	1653435.817	<.001	25208965.84	37411034.16
	Summer_2022	Spring_2021	-30715000.00*	1811248.188	<.001	-37398348.06	-24031651.94
		Winter_2022	-2530000.00	1811248.188	.551	-9213348.06	4153348.06
		Summer_2023	595000.00	1653435.817	.982	-5506034.16	6696034.16
	Winter_2022	Spring_2021	-28185000.00*	1811248.188	<.001	-34868348.06	-21501651.94
		Summer_2022	2530000.00	1811248.188	.551	-4153348.06	9213348.06
		Summer_2023	3125000.00	1653435.817	.338	-2976034.16	9226034.16
	Summer_2023	Spring_2021	-31310000.00*	1653435.817	<.001	-37411034.16	-25208965.84
		Summer_2022	-595000.00	1653435.817	.982	-6696034.16	5506034.16
		Winter_2022	-3125000.00	1653435.817	.338	-9226034.16	2976034.16
Secondary_25_per_kg	Spring_2021	Summer_2022	1675000.00	556186.420	.100	-377279.45	3727279.45
		Winter_2022	-1410000.00	556186.420	.168	-3462279.45	642279.45
		Summer_2023	1213333.33	507726.414	.197	-660132.91	3086799.58
	Summer_2022	Spring_2021	-1675000.00	556186.420	.100	-3727279.45	377279.45
		Winter_2022	-3085000.00*	556186.420	.010	-5137279.45	-1032720.55
		Summer_2023	-461666.67	507726.414	.802	-2335132.91	1411799.58
	Winter_2022	Spring_2021	1410000.00	556186.420	.168	-642279.45	3462279.45
		Summer_2022	3085000.00*	556186.420	.010	1032720.55	5137279.45
		Summer_2023	2623333.33*	507726.414	.013	749867.09	4496799.58
	Summer_2023	Spring_2021	-1213333.33	507726.414	.197	-3086799.58	660132.91
		Summer_2022	461666.67	507726.414	.802	-1411799.58	2335132.91
		Winter_2022	-2623333.33*	507726.414	.013	-4496799.58	-749867.09
Digested_25_per_kg	Spring_2021	Summer_2022	10025000.00*	935334.165	<.001	6573698.39	13476301.61
		Winter_2022	7415000.00*	935334.165	.002	3963698.39	10866301.61
		Summer_2023	8915000.00*	853839.368	<.001	5764407.10	12065592.90
	Summer_2022	Spring_2021	-10025000.00*	935334.165	<.001	-13476301.61	-6573698.39
		Winter_2022	-2610000.00	935334.165	.127	-6061301.61	841301.61
		Summer_2023	-1110000.00	853839.368	.600	-4260592.90	2040592.90
	Winter_2022	Spring_2021	-7415000.00*	935334.165	.002	-10866301.61	-3963698.39
		Summer_2022	2610000.00	935334.165	.127	-841301.61	6061301.61
		Summer_2023	1500000.00	853839.368	.388	-1650592.90	4650592.90
	Summer_2023	Spring_2021	-8915000.00*	853839.368	<.001	-12065592.90	-5764407.10
		Summer_2022	1110000.00	853839.368	.600	-2040592.90	4260592.90
		Winter_2022	-1500000.00	853839.368	.388	-4650592.90	1650592.90
Dewatered_25_per_kg	Spring_2021	Summer_2022	-8085000.00*	1500083.331	.011	-13620176.84	-2549823.16
		Winter_2022	490000.00	1500083.331	.987	-5045176.84	6025176.84
		Summer_2023	-2070000.00	1369382.464	.495	-7122902.03	2982902.03
	Summer_2022	Spring_2021	8085000.00*	1500083.331	.011	2549823.16	13620176.84
		Winter_2022	8575000.00*	1500083.331	.009	3039823.16	14110176.84
		Summer_2023	6015000.00*	1369382.464	.026	962097.97	11067902.03
	Winter_2022	Spring_2021	-490000.00	1500083.331	.987	-6025176.84	5045176.84
		Summer_2022	-8575000.00*	1500083.331	.009	-14110176.84	-3039823.16
		Summer_2023	-2560000.00	1369382.464	.345	-7612902.03	2492902.03
	Summer_2023	Spring_2021	2070000.00	1369382.464	.495	-2982902.03	7122902.03
		Summer_2022	-6015000.00*	1369382.464	.026	-11067902.03	-962097.97
		Winter_2022	2560000.00	1369382.464	.345	-2492902.03	7612902.03

Based on observed means.
The error term is Mean Square(Error) = 2250250000000.000.

*. The mean difference is significant at the .05 level.

2. Statistical analysis result for microplastics size above 25 µm in unit of particles per day

Table I-15. Descriptive Statistics of microplastics size above 25 µm in unit of particles per day

	Seasons	Mean	Std. Deviation	N
	Seasons	Mean	Std. Deviation	N
Influent_25_per_day	Spring_2021	2.27E+12	4.788E+11	2
	Summer_2022	1.92E+11	59340401077	2
	Winter_2022	2.84E+12	1.105E+12	2
	Summer_2023	3.59E+11	65967192098	3
	Total	1.30E+12	1.286E+12	9
Primary_25_per_day	Spring_2021	1.91E+11	20315177823	2
	Summer_2022	17825000000	1407142494.6	2
	Winter_2022	36490000000	8372144289.2	2
	Summer_2023	12900000000	1172859752.9	3
	Total	58788888889	75873436795	9
Secondary_25_per_day	Spring_2021	32255000000	2637508293.8	2
	Summer_2022	18810000000	1173797256.8	2
	Winter_2022	32430000000	4101219330.9	2
	Summer_2023	23006666667	2220593013.9	3
	Total	26223333333	6381414420.0	9
Digested_25_per_day	Spring_2021	1.20E+11	6074047250.4	2
	Summer_2022	43105000000	544472221.51	2
	Winter_2022	70540000000	6462955980.0	2
	Summer_2023	41450000000	5194160182.4	3
	Total	65721111111	33252298584	9
Dewatered_25_per_day	Spring_2021	32040000000	3040559159.1	2
	Summer_2022	75325000000	10330830073	2
	Winter_2022	28615000000	3981011178.1	2
	Summer_2023	29706666667	6582555228.3	3
	Total	40120000000	20669660737	9

Table I-16. Multivariate Tests[a] of microplastics size above 25 µm in unit of particles per day

Effect		Value	F	Hypothesis df	Error df	Sig.	Partial Eta Squared
Intercept	Pillai's Trace	.998	81.879[b]	5.000	1.000	.084	.998
	Wilks' Lambda	.002	81.879[b]	5.000	1.000	.084	.998
	Hotelling's Trace	409.397	81.879[b]	5.000	1.000	.084	.998
	Roy's Largest Root	409.397	81.879[b]	5.000	1.000	.084	.998
Seasons	Pillai's Trace	2.770	7.226	15.000	9.000	.003	.923
	Wilks' Lambda	.000	15.271	15.000	3.162	.019	.981
	Hotelling's Trace	.	.	15.000	.	.	.
	Roy's Largest Root	1180.663	708.398[c]	5.000	3.000	<.001	.999

a. Design: Intercept + Seasons

b. Exact statistic

c. The statistic is an upper bound on F that yields a lower bound on the significance level.

Effect		Value	F	Hypothesis df	Error df	Sig.	Partial Eta Squared
Intercept	Pillai's Trace	1.000	1410.790[b]	5.000	1.000	.020	1.000
	Wilks' Lambda	.000	1410.790[b]	5.000	1.000	.020	1.000
	Hotelling's Trace	7053.948	1410.790[b]	5.000	1.000	.020	1.000
	Roy's Largest Root	7053.948	1410.790[b]	5.000	1.000	.020	1.000
Seasons	Pillai's Trace	2.719	5.796	15.000	9.000	.006	.906
	Wilks' Lambda	.000	21.390	15.000	3.162	.012	.986
	Hotelling's Trace	.	.	15.000	.	.	.
	Roy's Largest Root	4549.388	2729.633[c]	5.000	3.000	<.001	1.000

a. Design: Intercept + Seasons

b. Exact statistic

c. The statistic is an upper bound on F that yields a lower bound on the significance level.

Table I-17. Tests of Between-Subjects Effects of microplastics size above 25 µm in unit of particles per day

Source	Dependent Variable	Type III Sum of Squares	df	Mean Square	F	Sig.	Partial Eta Squared
Corrected Model	Influent_25_per_day	1.176E+25[a]	3	3.920E+24	13.407	.008	.889
	Primary_25_per_day	4.557E+22[b]	3	1.519E+22	155.774	<.001	.989
	Secondary_25_per_day	2.908E+20[c]	3	9.692E+19	13.839	.007	.893
	Digested_25_per_day	8.713E+21[d]	3	2.904E+21	109.250	<.001	.985
	Dewatered_25_per_day	3.199E+21[e]	3	1.066E+21	24.407	.002	.936
Intercept	Influent_25_per_day	1.750E+25	1	1.750E+25	59.849	<.001	.923
	Primary_25_per_day	3.634E+22	1	3.634E+22	372.651	<.001	.987
	Secondary_25_per_day	6.187E+21	1	6.187E+21	883.428	<.001	.994
	Digested_25_per_day	4.126E+22	1	4.126E+22	1551.924	<.001	.997
	Dewatered_25_per_day	1.497E+22	1	1.497E+22	342.683	<.001	.986
Seasons	Influent_25_per_day	1.176E+25	3	3.920E+24	13.407	.008	.889
	Primary_25_per_day	4.557E+22	3	1.519E+22	155.774	<.001	.989
	Secondary_25_per_day	2.908E+20	3	9.692E+19	13.839	.007	.893
	Digested_25_per_day	8.713E+21	3	2.904E+21	109.250	<.001	.985
	Dewatered_25_per_day	3.199E+21	3	1.066E+21	24.407	.002	.936
Error	Influent_25_per_day	1.462E+24	5	2.924E+23			
	Primary_25_per_day	4.875E+20	5	9.751E+19			
	Secondary_25_per_day	3.502E+19	5	7.003E+18			
	Digested_25_per_day	1.329E+20	5	2.658E+19			
	Dewatered_25_per_day	2.185E+20	5	4.370E+19			
Total	Influent_25_per_day	2.840E+25	9				
	Primary_25_per_day	7.716E+22	9				
	Secondary_25_per_day	6.515E+21	9				
	Digested_25_per_day	4.772E+22	9				
	Dewatered_25_per_day	1.790E+22	9				
Corrected Total	Influent_25_per_day	1.322E+25	8				
	Primary_25_per_day	4.605E+22	8				
	Secondary_25_per_day	3.258E+20	8				
	Digested_25_per_day	8.846E+21	8				
	Dewatered_25_per_day	3.418E+21	8				

a. R Squared = .889 (Adjusted R Squared = .823)

b. R Squared = .989 (Adjusted R Squared = .983)

c. R Squared = .893 (Adjusted R Squared = .828)

d. R Squared = .985 (Adjusted R Squared = .976)

e. R Squared = .936 (Adjusted R Squared = .898)

Source	Dependent Variable	Type III Sum of Squares	df	Mean Square	F	Sig.	Partial Eta Squared
Corrected Model	Influent_25_per_day	1.354E+29[a]	3	4.515E+28	1.304	.370	.439
	Primary_25_per_day	4.557E+22[b]	3	1.519E+22	155.774	<.001	.989
	Secondary_25_per_day	2.908E+20[c]	3	9.692E+19	13.839	.007	.893
	Digested_25_per_day	8.713E+21[d]	3	2.904E+21	109.250	<.001	.985
	Dewatered_25_per_day	3.199E+21[e]	3	1.066E+21	24.407	.002	.936
Intercept	Influent_25_per_day	4.892E+28	1	4.892E+28	1.413	.288	.220
	Primary_25_per_day	3.634E+22	1	3.634E+22	372.651	<.001	.987
	Secondary_25_per_day	6.187E+21	1	6.187E+21	883.428	<.001	.994
	Digested_25_per_day	4.126E+22	1	4.126E+22	1551.924	<.001	.997
	Dewatered_25_per_day	1.497E+22	1	1.497E+22	342.683	<.001	.986
Seasons	Influent_25_per_day	1.354E+29	3	4.515E+28	1.304	.370	.439
	Primary_25_per_day	4.557E+22	3	1.519E+22	155.774	<.001	.989
	Secondary_25_per_day	2.908E+20	3	9.692E+19	13.839	.007	.893
	Digested_25_per_day	8.713E+21	3	2.904E+21	109.250	<.001	.985
	Dewatered_25_per_day	3.199E+21	3	1.066E+21	24.407	.002	.936
Error	Influent_25_per_day	1.731E+29	5	3.461E+28			
	Primary_25_per_day	4.875E+20	5	9.751E+19			
	Secondary_25_per_day	3.502E+19	5	7.003E+18			
	Digested_25_per_day	1.329E+20	5	2.658E+19			
	Dewatered_25_per_day	2.185E+20	5	4.370E+19			
Total	Influent_25_per_day	3.484E+29	9				
	Primary_25_per_day	7.716E+22	9				
	Secondary_25_per_day	6.515E+21	9				
	Digested_25_per_day	4.772E+22	9				
	Dewatered_25_per_day	1.790E+22	9				
Corrected Total	Influent_25_per_day	3.085E+29	8				
	Primary_25_per_day	4.605E+22	8				
	Secondary_25_per_day	3.258E+20	8				
	Digested_25_per_day	8.846E+21	8				
	Dewatered_25_per_day	3.418E+21	8				

a. R Squared = .439 (Adjusted R Squared = .102)

b. R Squared = .989 (Adjusted R Squared = .983)

c. R Squared = .893 (Adjusted R Squared = .828)

d. R Squared = .985 (Adjusted R Squared = .976)

e. R Squared = .936 (Adjusted R Squared = .898)

Table I-18. Multiple Comparisons (Turkey HSD) of microplastics size above 25 um in unit of particles per

Dependent Variable	(I) Seasons	(J) Seasons	Mean Difference (I-J)	Std. Error	Sig.	95% Confidence Interval	
						Lower Bound	Upper Bound
Influent_25_per_day	Spring_2021	Summer_2022	2.08E+12*	5.408E+11	.043	83671498532	4.07E+12
		Winter_2022	-5.73E+11	5.408E+11	.726	-2.57E+12	1.42E+12
		Summer_2023	1.91E+12*	4.936E+11	.042	90088847876	3.73E+12
	Summer_2022	Spring_2021	-2.08E+12*	5.408E+11	.043	-4.07E+12	-83671498532
		Winter_2022	-2.65E+12*	5.408E+11	.016	-4.65E+12	-6.56E+11
		Summer_2023	-1.67E+11	4.936E+11	.985	-1.99E+12	1.65E+12
	Winter_2022	Spring_2021	5.73E+11	5.408E+11	.726	-1.42E+12	2.57E+12
		Summer_2022	2.65E+12*	5.408E+11	.016	6.56E+11	4.65E+12
		Summer_2023	2.48E+12*	4.936E+11	.015	6.63E+11	4.31E+12
	Summer_2023	Spring_2021	-1.91E+12*	4.936E+11	.042	-3.73E+12	-90088847876
		Summer_2022	1.67E+11	4.936E+11	.985	-1.65E+12	1.99E+12
		Winter_2022	-2.48E+12*	4.936E+11	.015	-4.31E+12	-6.63E+11
Primary_25_per_day	Spring_2021	Summer_2022	1.73E+11*	9874517709.7	<.001	1.37E+11	2.09E+11
		Winter_2022	1.54E+11*	9874517709.7	<.001	1.18E+11	1.91E+11
		Summer_2023	1.78E+11*	9014160156.8	<.001	1.45E+11	2.11E+11
	Summer_2022	Spring_2021	-1.73E+11*	9874517709.7	<.001	-2.09E+11	-1.37E+11
		Winter_2022	-18665000000	9874517709.7	.338	-55101110329	17771110329
		Summer_2023	4925000000.0	9014160156.8	.944	-28336465892	38186465892
	Winter_2022	Spring_2021	-1.54E+11*	9874517709.7	<.001	-1.91E+11	-1.18E+11
		Summer_2022	18665000000	9874517709.7	.338	-17771110329	55101110329
		Summer_2023	23590000000	9014160156.8	.153	-9671465892	56851465892
	Summer_2023	Spring_2021	-1.78E+11*	9014160156.8	<.001	-2.11E+11	-1.45E+11
		Summer_2022	-4925000000	9014160156.8	.944	-38186465892	28336465892
		Winter_2022	-23590000000	9014160156.8	.153	-56851465892	9671465892.0
Secondary_25_per_day	Spring_2021	Summer_2022	13445000000*	2646367951.2	.014	3680132744.9	23209867255
		Winter_2022	175000000.00	2646367951.2	1.000	-9939867255	9589867255.1
		Summer_2023	9248333333*	2415792370.6	.044	334269888.91	18162396778
	Summer_2022	Spring_2021	-1.34E+10*	2646367951.2	.014	-23209867255	-3680132745
		Winter_2022	-1.36E+10*	2646367951.2	.013	-23384867255	-3855132745
		Summer_2023	-4196666667	2415792370.6	.396	-13110730111	4717396777.8
	Winter_2022	Spring_2021	175000000.00	2646367951.2	1.000	-9589867255	9939867255.1
		Summer_2022	13620000000*	2646367951.2	.013	3855132744.9	23384867255
		Summer_2023	9423333333*	2415792370.6	.041	509269888.91	18337396778
	Summer_2023	Spring_2021	-9248333333*	2415792370.6	.044	-18162396778	-334269888.91
		Summer_2022	4196666666.7	2415792370.6	.396	-4717396778	13110730111
		Winter_2022	-9423333333*	2415792370.6	.041	-18337396778	-509269888.91
Digested_25_per_day	Spring_2021	Summer_2022	76820000000*	5155946082.0	<.001	57795008014	95844991986
		Winter_2022	49385000000*	5155946082.0	<.001	30360008014	68409991986
		Summer_2023	78475000000*	4706713290.6	<.001	61107637888	95842362112
	Summer_2022	Spring_2021	-7.68E+10*	5155946082.0	<.001	-95844991986	-57795008014
		Winter_2022	-2.74E+10*	5155946082.0	.012	-46459991986	-8410008014
		Summer_2023	1655000000.0	4706713290.6	.983	-15712362112	19022362112
	Winter_2022	Spring_2021	-4.94E+10*	5155946082.0	<.001	-68409991986	-30360008014
		Summer_2022	27435000000*	5155946082.0	.012	8410008013.9	46459991986
		Summer_2023	29090000000*	4706713290.6	.006	11722637888	46457362112
	Summer_2023	Spring_2021	-7.85E+10*	4706713290.6	<.001	-95842362112	-61107637888
		Summer_2022	-1655000000	4706713290.6	.983	-19022362112	15712362112
		Winter_2022	-2.91E+10*	4706713290.6	.006	-46457362112	-11722637888
Dewatered_25_per_day	Spring_2021	Summer_2022	-4.33E+10*	6610288445.5	.005	-67676388642	-18893611358
		Winter_2022	3425000000.0	6610288445.5	.951	-20966388642	27816388642
		Summer_2023	2333333333.3	6034340155.4	.978	-19932856280	24599522947
	Summer_2022	Spring_2021	43285000000*	6610288445.5	.005	18893611358	67676388642
		Winter_2022	46710000000*	6610288445.5	.003	22318611358	71101388642
		Summer_2023	45618333333*	6034340155.4	.002	23352143720	67884522947
	Winter_2022	Spring_2021	-3425000000	6610288445.5	.951	-27816388642	20966388642
		Summer_2022	-4.67E+10*	6610288445.5	.003	-71101388642	-22318611358
		Summer_2023	-1091666667	6034340155.4	.998	-23357856280	21174522947
	Summer_2023	Spring_2021	-2333333333	6034340155.4	.978	-24599522947	19932856280
		Summer_2022	-4.56E+10*	6034340155.4	.002	-67884522947	-23352143720
		Winter_2022	1091666666.7	6034340155.4	.998	-21174522947	23357856280

Based on observed means.
The error term is Mean Square(Error) = 43695913333333330000.000.

*. The mean difference is significant at the .05 level.

Dependent Variable	(I) Seasons	(J) Seasons	Mean Difference (I-J)	Std. Error	Sig.	95% Confidence Interval	
						Lower Bound	Upper Bound
Influent_25_per_day	Spring_2021	Summer_2022	2.96E+14	1.860E+14	.459	-3.91E+14	9.82E+14
		Winter_2022	2.93E+14	1.860E+14	.465	-3.93E+14	9.80E+14
		Summer_2023	2.96E+14	1.698E+14	.394	-3.31E+14	9.22E+14
	Summer_2022	Spring_2021	-2.96E+14	1.860E+14	.459	-9.82E+14	3.91E+14
		Winter_2022	-2.65E+12	1.860E+14	1.000	-6.89E+14	6.84E+14
		Summer_2023	-1.67E+11	1.698E+14	1.000	-6.27E+14	6.26E+14
	Winter_2022	Spring_2021	-2.93E+14	1.860E+14	.465	-9.80E+14	3.93E+14
		Summer_2022	2.65E+12	1.860E+14	1.000	-6.84E+14	6.89E+14
		Summer_2023	2.48E+12	1.698E+14	1.000	-6.24E+14	6.29E+14
	Summer_2023	Spring_2021	-2.96E+14	1.698E+14	.394	-9.22E+14	3.31E+14
		Summer_2022	1.67E+11	1.698E+14	1.000	-6.26E+14	6.27E+14
		Winter_2022	-2.48E+12	1.698E+14	1.000	-6.29E+14	6.24E+14
Primary_25_per_day	Spring_2021	Summer_2022	1.73E+11*	9874517709.7	<.001	1.37E+11	2.09E+11
		Winter_2022	1.54E+11*	9874517709.7	<.001	1.18E+11	1.91E+11
		Summer_2023	1.78E+11*	9014160156.8	<.001	1.45E+11	2.11E+11
	Summer_2022	Spring_2021	-1.73E+11*	9874517709.7	<.001	-2.09E+11	-1.37E+11
		Winter_2022	-18665000000	9874517709.7	.338	-55101110329	17771110329
		Summer_2023	4925000000.0	9014160156.8	.944	-28336465892	38186465892
	Winter_2022	Spring_2021	-1.54E+11*	9874517709.7	<.001	-1.91E+11	-1.18E+11
		Summer_2022	18665000000	9874517709.7	.338	-17771110329	55101110329
		Summer_2023	23590000000	9014160156.8	.153	-9671465892	56851465892
	Summer_2023	Spring_2021	-1.78E+11*	9014160156.8	<.001	-2.11E+11	-1.45E+11
		Summer_2022	-4925000000	9014160156.8	.944	-38186465892	28336465892
		Winter_2022	-23590000000	9014160156.8	.153	-56851465892	9671465892.0
Secondary_25_per_day	Spring_2021	Summer_2022	13445000000*	2646367951.2	.014	3680132744.9	23209867255
		Winter_2022	-175000000.00	2646367951.2	1.000	-9939867255	9589867255.1
		Summer_2023	9248333333*	2415792370.6	.044	334269888.91	18162396778
	Summer_2022	Spring_2021	-1.34E+10*	2646367951.2	.014	-23209867255	-3680132745
		Winter_2022	-1.36E+10*	2646367951.2	.013	-23384867255	-3855132745
		Summer_2023	-4196666667	2415792370.6	.396	-13110730111	4717396777.8
	Winter_2022	Spring_2021	175000000.00	2646367951.2	1.000	-9589867255	9939867255.1
		Summer_2022	13620000000*	2646367951.2	.013	3855132744.9	23384867255
		Summer_2023	9423333333*	2415792370.6	.041	509269888.91	18337396778
	Summer_2023	Spring_2021	-9248333333*	2415792370.6	.044	-18162396778	-334269888.91
		Summer_2022	4196666666.7	2415792370.6	.396	-4717396778	13110730111
		Winter_2022	-9423333333*	2415792370.6	.041	-18337396778	-509269888.91
Digested_25_per_day	Spring_2021	Summer_2022	76820000000*	5155946082.0	<.001	57795008014	95844991986
		Winter_2022	49385000000*	5155946082.0	<.001	30360008014	68409991986
		Summer_2023	78475000000*	4706713290.6	<.001	61107637888	95842362112
	Summer_2022	Spring_2021	-7.68E+10*	5155946082.0	<.001	-95844991986	-57795008014
		Winter_2022	-2.74E+10*	5155946082.0	.012	-46459991986	-8410008014
		Summer_2023	1655000000.0	4706713290.6	.983	-15712362112	19022362112
	Winter_2022	Spring_2021	-4.94E+10*	5155946082.0	<.001	-68409991986	-30360008014
		Summer_2022	27435000000*	5155946082.0	.012	8410008013.9	46459991986
		Summer_2023	29090000000*	4706713290.6	.006	11722637888	46457362112
	Summer_2023	Spring_2021	-7.85E+10*	4706713290.6	<.001	-95842362112	-61107637888
		Summer_2022	-1655000000	4706713290.6	.983	-19022362112	15712362112
		Winter_2022	-2.91E+10*	4706713290.6	.006	-46457362112	-11722637888
Dewatered_25_per_day	Spring_2021	Summer_2022	-4.33E+10*	6610288445.5	.005	-67676388642	-18893611358
		Winter_2022	3425000000.0	6610288445.5	.951	-20966388642	27816388642
		Summer_2023	2333333333.3	6034340155.4	.978	-19932856280	24599522947
	Summer_2022	Spring_2021	43285000000*	6610288445.5	.005	18893611358	67676388642
		Winter_2022	46710000000*	6610288445.5	.003	22318611358	71101388642
		Summer_2023	45618333333*	6034340155.4	.002	23352143720	67884522947
	Winter_2022	Spring_2021	-3425000000	6610288445.5	.951	-27816388642	20966388642
		Summer_2022	-4.67E+10*	6610288445.5	.003	-71101388642	-22318611358
		Summer_2023	-1091666667	6034340155.4	.998	-23357856280	21174522947
	Summer_2023	Spring_2021	-2333333333	6034340155.4	.978	-24599522947	19932856280
		Summer_2022	-4.56E+10*	6034340155.4	.002	-67884522947	-23352143720
		Winter_2022	1091666666.7	6034340155.4	.998	-21174522947	23357856280

Based on observed means.
The error term is Mean Square(Error) = 43695913333333330000.000.

*. The mean difference is significant at the .05 level.

6 Statistical analysis result for microplastics size 10-25 µm in unit of particles per kg dry solid

Table I-19. Descriptive Statistics of microplastics size 10-25 µm in unit of particles per kg dry solid

	Seasons	Mean	Std. Deviation	N
Influent_10_per_kg	Spring_2021	3.69E+11	84944737624	2
	Summer_2022	77640000000	5656854249.5	2
	Winter_2022	6.49E+11	3.759E+11	2
	Summer_2023	3.27E+11	55939217460	2
	Total	3.56E+11	2.620E+11	8
Primary_10_per_kg	Spring_2021	26995000000	10585388514	2
	Summer_2022	1.79E+11	62656731881	2
	Winter_2022	21670000000	1117228714.3	2
	Summer_2023	23220000000	5444722215.1	2
	Total	62780000000	75841495992	8
Secondary_10_per_kg	Spring_2021	1.04E+11	42405193668	2
	Summer_2022	9225000000.0	2976919548.8	2
	Winter_2022	10150000000	1428355698.0	2
	Summer_2023	3.01E+11	1.423E+11	2
	Total	1.06E+11	1.390E+11	8
Digested_10_per_kg	Spring_2021	4530000000.0	2856711396.0	2
	Summer_2022	55490000000	15315932881	2
	Winter_2022	1.40E+11	9892423868.8	2
	Summer_2023	71035000000	10557104243	2
	Total	67870000000	52550630824	8
Dewatered_10_per_kg	Spring_2021	4045000000.0	1039446968.3	2
	Summer_2022	79075000000	39746472170	2
	Winter_2022	33400000000	29161083656	2
	Summer_2023	6330000000.0	254558441.23	2
	Total	30712500000	37292143849	8

Table I-20. Multivariate Tests[a] of microplastics size 10-25 µm in unit of particles per kg dry solid

Effect		Value	F	Hypothesis df	Error df	Sig.	Partial Eta Squared
Intercept	Pillai's Trace	1.000	1189.610[b]	4.000	1.000	.022	1.000
	Wilks' Lambda	.000	1189.610[b]	4.000	1.000	.022	1.000
	Hotelling's Trace	4758.441	1189.610[b]	4.000	1.000	.022	1.000
	Roy's Largest Root	4758.441	1189.610[b]	4.000	1.000	.022	1.000
Seasons	Pillai's Trace	2.704	6.852	12.000	9.000	.004	.901
	Wilks' Lambda	.000	16.200	12.000	2.937	.022	.976
	Hotelling's Trace	.	.	12.000	.	.	.
	Roy's Largest Root	1082.949	812.211[c]	4.000	3.000	<.001	.999

a. Design: Intercept + Seasons

b. Exact statistic

c. The statistic is an upper bound on F that yields a lower bound on the significance level.

Table I-21. Tests of Between-Subjects Effects of microplastics size 10-25 µm in unit of particles per kg dry solid

Source	Dependent Variable	Type III Sum of Squares	df	Mean Square	F	Sig.	Partial Eta Squared
Corrected Model	Influent_10_per_kg	3.290E+23[a]	3	1.097E+23	2.891	.166	.684
	Primary_10_per_kg	3.619E+22[b]	3	1.206E+22	11.861	.018	.899
	Secondary_10_per_kg	1.133E+23[c]	3	3.776E+22	6.843	.047	.837
	Digested_10_per_kg	1.888E+22[d]	3	6.293E+21	55.684	.001	.977
	Dewatered_10_per_kg	7.304E+21[e]	3	2.435E+21	4.005	.107	.750
Intercept	Influent_10_per_kg	1.012E+24	1	1.012E+24	26.689	.007	.870
	Primary_10_per_kg	3.153E+22	1	3.153E+22	30.997	.005	.886
	Secondary_10_per_kg	9.004E+22	1	9.004E+22	16.320	.016	.803
	Digested_10_per_kg	3.685E+22	1	3.685E+22	326.075	<.001	.988
	Dewatered_10_per_kg	7.546E+21	1	7.546E+21	12.415	.024	.756
Seasons	Influent_10_per_kg	3.290E+23	3	1.097E+23	2.891	.166	.684
	Primary_10_per_kg	3.619E+22	3	1.206E+22	11.861	.018	.899
	Secondary_10_per_kg	1.133E+23	3	3.776E+22	6.843	.047	.837
	Digested_10_per_kg	1.888E+22	3	6.293E+21	55.684	.001	.977
	Dewatered_10_per_kg	7.304E+21	3	2.435E+21	4.005	.107	.750
Error	Influent_10_per_kg	1.517E+23	4	3.793E+22			
	Primary_10_per_kg	4.069E+21	4	1.017E+21			
	Secondary_10_per_kg	2.207E+22	4	5.517E+21			
	Digested_10_per_kg	4.521E+20	4	1.130E+20			
	Dewatered_10_per_kg	2.431E+21	4	6.078E+20			
Total	Influent_10_per_kg	1.493E+24	8				
	Primary_10_per_kg	7.179E+22	8				
	Secondary_10_per_kg	2.254E+23	8				
	Digested_10_per_kg	5.618E+22	8				
	Dewatered_10_per_kg	1.728E+22	8				
Corrected Total	Influent_10_per_kg	4.807E+23	7				
	Primary_10_per_kg	4.026E+22	7				
	Secondary_10_per_kg	1.353E+23	7				
	Digested_10_per_kg	1.933E+22	7				
	Dewatered_10_per_kg	9.735E+21	7				

a. R Squared = .684 (Adjusted R Squared = .448)

b. R Squared = .899 (Adjusted R Squared = .823)

c. R Squared = .837 (Adjusted R Squared = .715)

d. R Squared = .977 (Adjusted R Squared = .959)

e. R Squared = .750 (Adjusted R Squared = .563)

Table I-22. Multiple Comparisons (Turkey HSD) of microplastics size 10-25 µm in unit of particles per kg dry

Dependent Variable	(I) Seasons	(J) Seasons	Mean Difference (I-J)	Std. Error	Sig.	95% Confidence Interval	
						Lower Bound	Upper Bound
Influent_10_per_kg	Spring_2021	Summer_2022	2.92E+11	1.947E+11	.514	-5.01E+11	1.08E+12
		Winter_2022	-2.80E+11	1.947E+11	.542	-1.07E+12	5.13E+11
		Summer_2023	42750000000	1.947E+11	.996	-7.50E+11	8.36E+11
	Summer_2022	Spring_2021	-2.92E+11	1.947E+11	.514	-1.08E+12	5.01E+11
		Winter_2022	-5.72E+11	1.947E+11	.132	-1.36E+12	2.21E+11
		Summer_2023	-2.49E+11	1.947E+11	.619	-1.04E+12	5.44E+11
	Winter_2022	Spring_2021	2.80E+11	1.947E+11	.542	-5.13E+11	1.07E+12
		Summer_2022	5.72E+11	1.947E+11	.132	-2.21E+11	1.36E+12
		Summer_2023	3.23E+11	1.947E+11	.446	-4.70E+11	1.12E+12
	Summer_2023	Spring_2021	-42750000000	1.947E+11	.996	-8.36E+11	7.50E+11
		Summer_2022	2.49E+11	1.947E+11	.619	-5.44E+11	1.04E+12
		Winter_2022	-3.23E+11	1.947E+11	.446	-1.12E+12	4.70E+11
Primary_10_per_kg	Spring_2021	Summer_2022	-1.52E+11*	31893611037	.030	-2.82E+11	-22405688240
		Winter_2022	5325000000.0	31893611037	.998	-1.25E+11	1.35E+11
		Summer_2023	3775000000.0	31893611037	.999	-1.26E+11	1.34E+11
	Summer_2022	Spring_2021	1.52E+11*	31893611037	.030	22405688240	2.82E+11
		Winter_2022	1.58E+11*	31893611037	.026	27730688240	2.87E+11
		Summer_2023	1.56E+11*	31893611037	.027	26180688240	2.86E+11
	Winter_2022	Spring_2021	-5325000000	31893611037	.998	-1.35E+11	1.25E+11
		Summer_2022	-1.58E+11*	31893611037	.026	-2.87E+11	-27730688240
		Summer_2023	-1550000000	31893611037	1.000	-1.31E+11	1.28E+11
	Summer_2023	Spring_2021	-3775000000	31893611037	.999	-1.34E+11	1.26E+11
		Summer_2022	-1.56E+11*	31893611037	.027	-2.86E+11	-26180688240
		Winter_2022	1550000000.0	31893611037	1.000	-1.28E+11	1.31E+11
Secondary_10_per_kg	Spring_2021	Summer_2022	94630000000	74279788132	.621	-2.08E+11	3.97E+11
		Winter_2022	93705000000	74279788132	.627	-2.09E+11	3.96E+11
		Summer_2023	-1.97E+11	74279788132	.171	-5.00E+11	1.05E+11
	Summer_2022	Spring_2021	-94630000000	74279788132	.621	-3.97E+11	2.08E+11
		Winter_2022	-925000000.00	74279788132	1.000	-3.03E+11	3.01E+11
		Summer_2023	-2.92E+11	74279788132	.056	-5.94E+11	10467353587
	Winter_2022	Spring_2021	-93705000000	74279788132	.627	-3.96E+11	2.09E+11
		Summer_2022	925000000.00	74279788132	1.000	-3.01E+11	3.03E+11
		Summer_2023	-2.91E+11	74279788132	.057	-5.93E+11	11392353587
	Summer_2023	Spring_2021	1.97E+11	74279788132	.171	-1.05E+11	5.00E+11
		Summer_2022	2.92E+11	74279788132	.056	-10467353587	5.94E+11
		Winter_2022	2.91E+11	74279788132	.057	-11392353587	5.93E+11
Digested_10_per_kg	Spring_2021	Summer_2022	-5.10E+10*	10630746681	.029	-94236243547	-7683756453
		Winter_2022	-1.36E+11*	10630746681	<.001	-1.79E+11	-92618756453
		Summer_2023	-6.65E+10*	10630746681	.011	-1.10E+11	-23228756453
	Summer_2022	Spring_2021	50960000000*	10630746681	.029	7683756452.9	94236243547
		Winter_2022	-8.49E+10*	10630746681	.005	-1.28E+11	-41658756453
		Summer_2023	-15545000000	10630746681	.530	-58821243547	27731243547
	Winter_2022	Spring_2021	1.36E+11*	10630746681	<.001	92618756453	1.79E+11
		Summer_2022	84935000000*	10630746681	.005	41658756453	1.28E+11
		Summer_2023	69390000000*	10630746681	.010	26113756453	1.13E+11
	Summer_2023	Spring_2021	66505000000*	10630746681	.011	23228756453	1.10E+11
		Summer_2022	15545000000	10630746681	.530	-27731243547	58821243547
		Winter_2022	-6.94E+10*	10630746681	.010	-1.13E+11	-26113756453
Dewatered_10_per_kg	Spring_2021	Summer_2022	-75030000000	24654087389	.120	-1.75E+11	25333250323
		Winter_2022	-29355000000	24654087389	.663	-1.30E+11	71008250323
		Summer_2023	-2285000000	24654087389	1.000	-1.03E+11	98078250323
	Summer_2022	Spring_2021	75030000000	24654087389	.120	-25333250323	1.75E+11
		Winter_2022	45675000000	24654087389	.371	-54688250323	1.46E+11
		Summer_2023	72745000000	24654087389	.130	-27618250323	1.73E+11
	Winter_2022	Spring_2021	29355000000	24654087389	.663	-71008250323	1.30E+11
		Summer_2022	-45675000000	24654087389	.371	-1.46E+11	54688250323
		Summer_2023	27070000000	24654087389	.710	-73293250323	1.27E+11
	Summer_2023	Spring_2021	2285000000.0	24654087389	1.000	-98078250323	1.03E+11
		Summer_2022	-72745000000	24654087389	.130	-1.73E+11	27618250323
		Winter_2022	-27070000000	24654087389	.710	-1.27E+11	73293250323

Based on observed means.
The error term is Mean Square(Error) = 607824025000000000000.000.

*. The mean difference is significant at the .05 level.

7 Statistical analysis result for microplastics size 10-25 µm in unit of particles per day

Table I-24. Descriptive Statistics of microplastics size 10-25 µm in unit of particles per day

	Seasons	Mean	Std. Deviation	N
	Seasons	Mean	Std. Deviation	N
Influent_10_per_day	Spring_2021	1.26E+16	2.888E+15	2
	Summer_2022	2.41E+15	1.753E+14	2
	Winter_2022	2.21E+16	1.278E+16	2
	Summer_2023	3.09E+15	5.287E+14	2
	Total	1.00E+16	9.910E+15	8
Primary_10_per_day	Spring_2021	1.48E+14	5.797E+13	2
	Summer_2022	7.69E+14	2.688E+14	2
	Winter_2022	1.18E+14	6.102E+12	2
	Summer_2023	8.40E+13	1.971E+13	2
	Total	2.80E+14	3.203E+14	8
Secondary_10_per_day	Spring_2021	5.71E+14	2.330E+14	2
	Summer_2022	4.13E+13	1.333E+13	2
	Winter_2022	4.52E+13	6.357E+12	2
	Summer_2023	1.49E+15	7.028E+14	2
	Total	5.36E+14	6.898E+14	8
Digested_10_per_day	Spring_2021	3.02E+13	1.901E+13	2
	Summer_2022	3.00E+14	8.269E+13	2
	Winter_2022	9.35E+14	6.589E+13	2
	Summer_2023	3.24E+14	4.813E+13	2
	Total	3.97E+14	3.570E+14	8
Dewatered_10_per_day	Spring_2021	2.12E+13	5.438E+12	2
	Summer_2022	4.20E+14	2.111E+14	2
	Winter_2022	1.70E+14	1.487E+14	2
	Summer_2023	2.30E+13	9.334E+11	2
	Total	1.59E+14	1.993E+14	8

Table I-23. Multivariate Tests[a] of microplastics size 10-25 µm in unit of particles per day

Effect		Value	F	Hypothesis df	Error df	Sig.	Partial Eta Squared
Intercept	Pillai's Trace	1.000	585.370[b]	4.000	1.000	.031	1.000
	Wilks' Lambda	.000	585.370[b]	4.000	1.000	.031	1.000
	Hotelling's Trace	2341.478	585.370[b]	4.000	1.000	.031	1.000
	Roy's Largest Root	2341.478	585.370[b]	4.000	1.000	.031	1.000
Seasons	Pillai's Trace	2.692	6.548	12.000	9.000	.004	.897
	Wilks' Lambda	.000	13.493	12.000	2.937	.029	.971
	Hotelling's Trace	.	.	12.000	.	.	.
	Roy's Largest Root	770.254	577.691[c]	4.000	3.000	<.001	.999

a. Design: Intercept + Seasons

b. Exact statistic

c. The statistic is an upper bound on F that yields a lower bound on the significance level.

Table I-25. Tests of Between-Subjects Effects of microplastics size 10-25 µm in unit of particles per day

Source	Dependent Variable	Type III Sum of Squares	df	Mean Square	F	Sig.	Partial Eta Squared
Corrected Model	Influent_10_per_day	5.155E+32[a]	3	1.718E+32	3.995	.107	.750
	Primary_10_per_day	6.422E+29[b]	3	2.141E+29	11.263	.020	.894
	Secondary_10_per_day	2.782E+30[c]	3	9.274E+29	6.763	.048	.835
	Digested_10_per_day	8.782E+29[d]	3	2.927E+29	84.502	<.001	.984
	Dewatered_10_per_day	2.113E+29[e]	3	7.044E+28	4.225	.099	.760
Intercept	Influent_10_per_day	8.050E+32	1	8.050E+32	18.718	.012	.824
	Primary_10_per_day	6.260E+29	1	6.260E+29	32.938	.005	.892
	Secondary_10_per_day	2.299E+30	1	2.299E+30	16.764	.015	.807
	Digested_10_per_day	1.263E+30	1	1.263E+30	364.481	<.001	.989
	Dewatered_10_per_day	2.013E+29	1	2.013E+29	12.072	.025	.751
Seasons	Influent_10_per_day	5.155E+32	3	1.718E+32	3.995	.107	.750
	Primary_10_per_day	6.422E+29	3	2.141E+29	11.263	.020	.894
	Secondary_10_per_day	2.782E+30	3	9.274E+29	6.763	.048	.835
	Digested_10_per_day	8.782E+29	3	2.927E+29	84.502	<.001	.984
	Dewatered_10_per_day	2.113E+29	3	7.044E+28	4.225	.099	.760
Error	Influent_10_per_day	1.720E+32	4	4.301E+31			
	Primary_10_per_day	7.602E+28	4	1.901E+28			
	Secondary_10_per_day	5.485E+29	4	1.371E+29			
	Digested_10_per_day	1.386E+28	4	3.464E+27			
	Dewatered_10_per_day	6.670E+28	4	1.667E+28			
Total	Influent_10_per_day	1.492E+33	8				
	Primary_10_per_day	1.344E+30	8				
	Secondary_10_per_day	5.629E+30	8				
	Digested_10_per_day	2.155E+30	8				
	Dewatered_10_per_day	4.793E+29	8				
Corrected Total	Influent_10_per_day	6.875E+32	7				
	Primary_10_per_day	7.182E+29	7				
	Secondary_10_per_day	3.331E+30	7				
	Digested_10_per_day	8.920E+29	7				
	Dewatered_10_per_day	2.780E+29	7				

a. R Squared = .750 (Adjusted R Squared = .562)
b. R Squared = .894 (Adjusted R Squared = .815)
c. R Squared = .835 (Adjusted R Squared = .712)
d. R Squared = .984 (Adjusted R Squared = .973)
e. R Squared = .760 (Adjusted R Squared = .580)

Table I-26. Multiple Comparisons (Turkey HSD) of microplastics size 10-25 µm in unit of particles per day

Dependent Variable	(I) Seasons	(J) Seasons	Mean Difference (I-J)	Std. Error	Sig.	95% Confidence Interval	
						Lower Bound	Upper Bound
Influent_10_per_day	Spring_2021	Summer_2022	1.02E+16	6.558E+15	.492	-1.65E+16	3.68E+16
		Winter_2022	-9.51E+15	6.558E+15	.536	-3.62E+16	1.72E+16
		Summer_2023	9.47E+15	6.558E+15	.539	-1.72E+16	3.62E+16
	Summer_2022	Spring_2021	-1.02E+16	6.558E+15	.492	-3.68E+16	1.65E+16
		Winter_2022	-1.97E+16	6.558E+15	.125	-4.64E+16	7.03E+15
		Summer_2023	-6.80E+14	6.558E+15	1.000	-2.74E+16	2.60E+16
	Winter_2022	Spring_2021	9.51E+15	6.558E+15	.536	-1.72E+16	3.62E+16
		Summer_2022	1.97E+16	6.558E+15	.125	-7.03E+15	4.64E+16
		Summer_2023	1.90E+16	6.558E+15	.137	-7.71E+15	4.57E+16
	Summer_2023	Spring_2021	-9.47E+15	6.558E+15	.539	-3.62E+16	1.72E+16
		Summer_2022	6.80E+14	6.558E+15	1.000	-2.60E+16	2.74E+16
		Winter_2022	-1.90E+16	6.558E+15	.137	-4.57E+16	7.71E+15
Primary_10_per_day	Spring_2021	Summer_2022	-6.21E+14*	1.379E+14	.036	-1.18E+15	-5.99E+13
		Winter_2022	2.96E+13	1.379E+14	.996	-5.32E+14	5.91E+14
		Summer_2023	6.37E+13	1.379E+14	.964	-4.97E+14	6.25E+14
	Summer_2022	Spring_2021	6.21E+14*	1.379E+14	.036	5.99E+13	1.18E+15
		Winter_2022	6.51E+14*	1.379E+14	.031	8.95E+13	1.21E+15
		Summer_2023	6.85E+14*	1.379E+14	.026	1.24E+14	1.25E+15
	Winter_2022	Spring_2021	-2.96E+13	1.379E+14	.996	-5.91E+14	5.32E+14
		Summer_2022	-6.51E+14*	1.379E+14	.031	-1.21E+15	-8.95E+13
		Summer_2023	3.42E+13	1.379E+14	.994	-5.27E+14	5.95E+14
	Summer_2023	Spring_2021	-6.37E+13	1.379E+14	.964	-6.25E+14	4.97E+14
		Summer_2022	-6.85E+14*	1.379E+14	.026	-1.25E+15	-1.24E+14
		Winter_2022	-3.42E+13	1.379E+14	.994	-5.95E+14	5.27E+14
Secondary_10_per_day	Spring_2021	Summer_2022	5.29E+14	3.703E+14	.546	-9.78E+14	2.04E+15
		Winter_2022	5.25E+14	3.703E+14	.551	-9.82E+14	2.03E+15
		Summer_2023	-9.16E+14	3.703E+14	.204	-2.42E+15	5.91E+14
	Summer_2022	Spring_2021	-5.29E+14	3.703E+14	.546	-2.04E+15	9.78E+14
		Winter_2022	-3.87E+12	3.703E+14	1.000	-1.51E+15	1.50E+15
		Summer_2023	-1.45E+15	3.703E+14	.057	-2.95E+15	6.18E+13
	Winter_2022	Spring_2021	-5.25E+14	3.703E+14	.551	-2.03E+15	9.82E+14
		Summer_2022	3.87E+12	3.703E+14	1.000	-1.50E+15	1.51E+15
		Summer_2023	-1.44E+15	3.703E+14	.058	-2.95E+15	6.57E+13
	Summer_2023	Spring_2021	9.16E+14	3.703E+14	.204	-5.91E+14	2.42E+15
		Summer_2022	1.45E+15	3.703E+14	.057	-6.18E+13	2.95E+15
		Winter_2022	1.44E+15	3.703E+14	.058	-6.57E+13	2.95E+15
Digested_10_per_day	Spring_2021	Summer_2022	-2.69E+14*	5.886E+13	.034	-5.09E+14	-2.99E+13
		Winter_2022	-9.05E+14*	5.886E+13	<.001	-1.14E+15	-6.65E+14
		Summer_2023	-2.94E+14*	5.886E+13	.025	-5.33E+14	-5.42E+13
	Summer_2022	Spring_2021	2.69E+14*	5.886E+13	.034	2.99E+13	5.09E+14
		Winter_2022	-6.36E+14*	5.886E+13	.001	-8.75E+14	-3.96E+14
		Summer_2023	-2.43E+13	5.886E+13	.973	-2.64E+14	2.15E+14
	Winter_2022	Spring_2021	9.05E+14*	5.886E+13	<.001	6.65E+14	1.14E+15
		Summer_2022	6.36E+14*	5.886E+13	.001	3.96E+14	8.75E+14
		Summer_2023	6.11E+14*	5.886E+13	.002	3.72E+14	8.51E+14
	Summer_2023	Spring_2021	2.94E+14*	5.886E+13	.025	5.42E+13	5.33E+14
		Summer_2022	2.43E+13	5.886E+13	.973	-2.15E+14	2.64E+14
		Winter_2022	-6.11E+14*	5.886E+13	.002	-8.51E+14	-3.72E+14
Dewatered_10_per_day	Spring_2021	Summer_2022	-3.99E+14	1.291E+14	.115	-9.24E+14	1.27E+14
		Winter_2022	-1.49E+14	1.291E+14	.681	-6.75E+14	3.77E+14
		Summer_2023	-1.80E+12	1.291E+14	1.000	-5.27E+14	5.24E+14
	Summer_2022	Spring_2021	3.99E+14	1.291E+14	.115	-1.27E+14	9.24E+14
		Winter_2022	2.50E+14	1.291E+14	.343	-2.76E+14	7.75E+14
		Summer_2023	3.97E+14	1.291E+14	.116	-1.29E+14	9.23E+14
	Winter_2022	Spring_2021	1.49E+14	1.291E+14	.681	-3.77E+14	6.75E+14
		Summer_2022	-2.50E+14	1.291E+14	.343	-7.75E+14	2.76E+14
		Summer_2023	1.47E+14	1.291E+14	.688	-3.78E+14	6.73E+14
	Summer_2023	Spring_2021	1.80E+12	1.291E+14	1.000	-5.24E+14	5.27E+14
		Summer_2022	-3.97E+14	1.291E+14	.116	-9.23E+14	1.29E+14
		Winter_2022	-1.47E+14	1.291E+14	.688	-6.73E+14	3.78E+14

Based on observed means.
The error term is Mean Square(Error) = 16674042737500000000000000000.000.

*. The mean difference is significant at the .05 level.

8 Statistical analysis result for microplastics size 0.2-10 µm in unit of particles per kg dry solid

Table I-27. Descriptive Statistics of microplastics size 0.2-10 µm in unit of particles per kg dry solid

	Seasons	Mean	Std. Deviation	N
Influent_0.2_per_kg	Spring_2021	3.84E+11	85574062659	2
	Summer_2022	86840000000	12331942264	2
	Winter_2022	6.67E+11	3.868E+11	2
	Summer_2023	3.49E+11	46068006794	2
	Total	3.72E+11	2.664E+11	8
Primary_.0.2_per_kg	Spring_2021	30635000000	9256027765.7	2
	Summer_2022	1.90E+11	58173674888	2
	Winter_2022	40320000000	6873077913.1	2
	Summer_2023	36070000000	11511698398	2
	Total	74187500000	74967592951	8
Secondary_0.2_per_kg	Spring_2021	1.10E+11	41351604564	2
	Summer_2022	10720000000	3917371567.8	2
	Winter_2022	15620000000	2644579361.6	2
	Summer_2023	3.26E+11	1.291E+11	2
	Total	1.16E+11	1.461E+11	8
Digested_0.2_per_kg	Spring_2021	7235000000.0	3288046532.5	2
	Summer_2022	58590000000	11087434329	2
	Winter_2022	1.47E+11	3118340905.0	2
	Summer_2023	71345000000	10472251429	2
	Total	70936250000	53607659351	8
Dewatered_0.2_per_kg	Spring_2021	17515000000	1619274528.9	2
	Summer_2022	95560000000	29755053352	2
	Winter_2022	45720000000	16602867222	2
	Summer_2023	6015000000.0	487903679.02	2
	Total	41202500000	39120117861	8

Table I-28. Multivariate Tests[a] of microplastics size 0.2-10 µm in unit of particles per kg dry solid

Effect		Value	F	Hypothesis df	Error df	Sig.	Squared
Intercept	Pillai's Trace	1.000	642.511[b]	4.000	1.000	.030	1.000
	Wilks' Lambda	.000	642.511[b]	4.000	1.000	.030	1.000
	Hotelling's Trace	2570.043	642.511[b]	4.000	1.000	.030	1.000
	Roy's Largest Root	2570.043	642.511[b]	4.000	1.000	.030	1.000
Seasons	Pillai's Trace	1.977	1.449	12.000	9.000	.293	.659
	Wilks' Lambda	.000	9.309	12.000	2.937	.048	.961
	Hotelling's Trace	.	.	12.000	.	.	.
	Roy's Largest Root	1062.877	797.158[c]	4.000	3.000	<.001	.999

a. Design: Intercept + Seasons

b. Exact statistic

c. The statistic is an upper bound on F that yields a lower bound on the significance level.

Table I-29. Tests of Between-Subjects Effects of microplastics size 0.2-10 µm in unit of particles per kg dry solid

Tests of Between-Subjects Effects

Source	Dependent Variable	Type III Sum of Squares	df	Mean Square	F	Sig.	Partial Eta Squared
Corrected Model	Influent_0.2_per_kg	1.745E+20[a]	3	5.815E+19	.892	.518	.401
	Primary_.0.2_per_kg	3.759E+20[b]	3	1.253E+20	5.848	.060	.814
	Secondary_0.2_per_kg	6.773E+20[c]	3	2.258E+20	4.641	.086	.777
	Digested_0.2_per_kg	3.447E+19[d]	3	1.149E+19	.718	.591	.350
	Dewatered_0.2_per_kg	3.074E+20[e]	3	1.025E+20	1.549	.333	.537
Intercept	Influent_0.2_per_kg	2.016E+21	1	2.016E+21	30.914	.005	.885
	Primary_.0.2_per_kg	5.680E+20	1	5.680E+20	26.509	.007	.869
	Secondary_0.2_per_kg	7.458E+20	1	7.458E+20	15.330	.017	.793
	Digested_0.2_per_kg	7.503E+19	1	7.503E+19	4.690	.096	.540
	Dewatered_0.2_per_kg	9.027E+20	1	9.027E+20	13.644	.021	.773
Seasons	Influent_0.2_per_kg	1.745E+20	3	5.815E+19	.892	.518	.401
	Primary_.0.2_per_kg	3.759E+20	3	1.253E+20	5.848	.060	.814
	Secondary_0.2_per_kg	6.773E+20	3	2.258E+20	4.641	.086	.777
	Digested_0.2_per_kg	3.447E+19	3	1.149E+19	.718	.591	.350
	Dewatered_0.2_per_kg	3.074E+20	3	1.025E+20	1.549	.333	.537
Error	Influent_0.2_per_kg	2.608E+20	4	6.521E+19			
	Primary_.0.2_per_kg	8.571E+19	4	2.143E+19			
	Secondary_0.2_per_kg	1.946E+20	4	4.865E+19			
	Digested_0.2_per_kg	6.400E+19	4	1.600E+19			
	Dewatered_0.2_per_kg	2.646E+20	4	6.616E+19			
Total	Influent_0.2_per_kg	2.451E+21	8				
	Primary_.0.2_per_kg	1.030E+21	8				
	Secondary_0.2_per_kg	1.618E+21	8				
	Digested_0.2_per_kg	1.735E+20	8				
	Dewatered_0.2_per_kg	1.475E+21	8				
Corrected Total	Influent_0.2_per_kg	4.353E+20	7				
	Primary_.0.2_per_kg	4.616E+20	7				
	Secondary_0.2_per_kg	8.719E+20	7				
	Digested_0.2_per_kg	9.847E+19	7				
	Dewatered_0.2_per_kg	5.721E+20	7				

a. R Squared = .401 (Adjusted R Squared = -.049)

b. R Squared = .814 (Adjusted R Squared = .675)

c. R Squared = .777 (Adjusted R Squared = .609)

d. R Squared = .350 (Adjusted R Squared = -.137)

e. R Squared = .537 (Adjusted R Squared = .190)

Table I-30. Multiple Comparisons (Turkey HSD) of microplastics size 0.2-10 µm in unit of particles per kg dry solid

Dependent Variable	(I) Seasons	(J) Seasons	Mean Difference (I-J)	Std. Error	Sig.	95% Confidence Interval	
						Lower Bound	Upper Bound
Influent_0.2_per_kg	Spring_2021	Summer_2022	5580000000.0	8075095200.7	.896	-27292553269	38452553269
		Winter_2022	-2545000000	8075095200.7	.988	-35417553269	30327553269
		Summer_2023	-7370000000	8075095200.7	.801	-40242553269	25502553269
	Summer_2022	Spring_2021	-5580000000	8075095200.7	.896	-38452553269	27292553269
		Winter_2022	-8125000000	8075095200.7	.756	-40997553269	24747553269
		Summer_2023	-12950000000	8075095200.7	.468	-45822553269	19922553269
	Winter_2022	Spring_2021	2545000000.0	8075095200.7	.988	-30327553269	35417553269
		Summer_2022	8125000000.0	8075095200.7	.756	-24747553269	40997553269
		Summer_2023	-4825000000	8075095200.7	.928	-37697553269	28047553269
	Summer_2023	Spring_2021	7370000000.0	8075095200.7	.801	-25502553269	40242553269
		Summer_2022	12950000000	8075095200.7	.468	-19922553269	45822553269
		Winter_2022	4825000000.0	8075095200.7	.928	-28047553269	37697553269
Primary_0.2_per_kg	Spring_2021	Summer_2022	-6850000000	4628986120.1	.522	-25693937939	11993937939
		Winter_2022	-15010000000	4628986120.1	.100	-33853937939	3833937939.3
		Summer_2023	2715000000.0	4628986120.1	.931	-16128937939	21558937939
	Summer_2022	Spring_2021	6850000000.0	4628986120.1	.522	-11993937939	25693937939
		Winter_2022	-8160000000	4628986120.1	.404	-27003937939	10683937939
		Summer_2023	9565000000.0	4628986120.1	.302	-9278937939	28408937939
	Winter_2022	Spring_2021	15010000000	4628986120.1	.100	-3833937939	33853937939
		Summer_2022	8160000000.0	4628986120.1	.404	-10683937939	27003937939
		Summer_2023	17725000000	4628986120.1	.061	-1118937939	36568937939
	Summer_2023	Spring_2021	-2715000000	4628986120.1	.931	-21558937939	16128937939
		Summer_2022	-9565000000	4628986120.1	.302	-28408937939	9278937939.3
		Winter_2022	-17725000000	4628986120.1	.061	-36568937939	1118937939.3
Secondary_0.2_per_kg	Spring_2021	Summer_2022	4900000000.0	6974603931.4	.891	-23492611303	33292611303
		Winter_2022	920000000.00	6974603931.4	.999	-27472611303	29312611303
		Summer_2023	-18880000000	6974603931.4	.163	-47272611303	9512611303.0
	Summer_2022	Spring_2021	-4900000000	6974603931.4	.891	-33292611303	23492611303
		Winter_2022	-3980000000	6974603931.4	.936	-32372611303	24412611303
		Summer_2023	-23780000000	6974603931.4	.086	-52172611303	4612611303.0
	Winter_2022	Spring_2021	-920000000.00	6974603931.4	.999	-29312611303	27472611303
		Summer_2022	3980000000.0	6974603931.4	.936	-24412611303	32372611303
		Summer_2023	-19800000000	6974603931.4	.144	-48192611303	8592611303.0
	Summer_2023	Spring_2021	18880000000	6974603931.4	.163	-9512611303	47272611303
		Summer_2022	23780000000	6974603931.4	.086	-4612611303	52172611303
		Winter_2022	19800000000	6974603931.4	.144	-8592611303	48192611303
Digested_0.2_per_kg	Spring_2021	Summer_2022	-390000000.00	3999893748.6	1.000	-16672993210	15892993210
		Winter_2022	-3440000000	3999893748.6	.825	-19722993210	12842993210
		Summer_2023	2400000000.0	3999893748.6	.927	-13882993210	18682993210
	Summer_2022	Spring_2021	390000000.00	3999893748.6	1.000	-15892993210	16672993210
		Winter_2022	-3050000000	3999893748.6	.868	-19332993210	13232993210
		Summer_2023	2790000000.0	3999893748.6	.893	-13492993210	19072993210
	Winter_2022	Spring_2021	3440000000.0	3999893748.6	.825	-12842993210	19722993210
		Summer_2022	3050000000.0	3999893748.6	.868	-13232993210	19332993210
		Summer_2023	5840000000.0	3999893748.6	.531	-10442993210	22122993210
	Summer_2023	Spring_2021	-2400000000	3999893748.6	.927	-18682993210	13882993210
		Summer_2022	-2790000000	3999893748.6	.893	-19072993210	13492993210
		Winter_2022	-5840000000	3999893748.6	.531	-22122993210	10442993210
Dewatered_0.2_per_kg	Spring_2021	Summer_2022	-3020000000	8133918182.5	.980	-36132013184	30092013184
		Winter_2022	1155000000.0	8133918182.5	.999	-31957013184	34267013184
		Summer_2023	13255000000	8133918182.5	.457	-19857013184	46367013184
	Summer_2022	Spring_2021	3020000000.0	8133918182.5	.980	-30092013184	36132013184
		Winter_2022	4175000000.0	8133918182.5	.952	-28937013184	37287013184
		Summer_2023	16275000000	8133918182.5	.322	-16837013184	49387013184
	Winter_2022	Spring_2021	-1155000000	8133918182.5	.999	-34267013184	31957013184
		Summer_2022	-4175000000	8133918182.5	.952	-37287013184	28937013184
		Summer_2023	12100000000	8133918182.5	.519	-21012013184	45212013184
	Summer_2023	Spring_2021	-13255000000	8133918182.5	.457	-46367013184	19857013184
		Summer_2022	-16275000000	8133918182.5	.322	-49387013184	16837013184
		Winter_2022	-12100000000	8133918182.5	.519	-45212013184	21012013184

Based on observed means.
The error term is Mean Square(Error) = 661606249999999900000.000.

Based on observed means.
The error term is Mean Square(Error) = 2909696249999999600000.000.

*. The mean difference is significant at the .05 level.

9 Statistical analysis result for microplastics size 0.2-10 µm in unit of particles per day

Table I-31. Descriptive Statistics of microplastics size 0.2-10 µm in unit of particles per day

	Seasons	Mean	Std. Deviation	N
Influent_0.2_per_day	Spring_2021	5.03E+14	2.163E+13	2
	Summer_2022	2.85E+14	2.069E+14	2
	Winter_2022	5.89E+14	3.700E+14	2
	Summer_2023	2.09E+14	9.329E+13	2
	Total	3.97E+14	2.331E+14	8
Primary_0.2_per_day	Spring_2021	1.99E+13	7.283E+12	2
	Summer_2022	4.50E+13	1.923E+13	2
	Winter_2022	1.02E+14	4.361E+13	2
	Summer_2023	3.34E+12	28284271247	2
	Total	4.25E+13	4.383E+13	8
Secondary_0.2_per_day	Spring_2021	3.51E+13	5.819E+12	2
	Summer_2022	6.69E+12	4.236E+12	2
	Winter_2022	2.44E+13	1.812E+13	2
	Summer_2023	1.18E+14	5.626E+13	2
	Total	4.61E+13	5.106E+13	8
Digested_0.2_per_day	Spring_2021	1.80E+13	2.885E+12	2
	Summer_2022	1.67E+13	2.280E+13	2
	Winter_2022	5.37E+13	2.711E+13	2
	Summer_2023	1.46E+12	2.828E+11	2
	Total	2.25E+13	2.449E+13	8
Dewatered_0.2_per_day	Spring_2021	7.07E+13	1.395E+13	2
	Summer_2022	8.76E+13	5.303E+13	2
	Winter_2022	6.28E+13	6.406E+13	2
	Summer_2023	7.70E+11	14142135624	2
	Total	5.55E+13	4.740E+13	8

Table I-32. Multivariate Testa of microplastics size 0.2-10 µm in unit of particles per day

Effect		Value	F	Hypothesis df	Error df	Sig.	Partial Eta Squared
Intercept	Pillai's Trace	1.000	2004.803[b]	4.000	1.000	.017	1.000
	Wilks' Lambda	.000	2004.803[b]	4.000	1.000	.017	1.000
	Hotelling's Trace	8019.214	2004.803[b]	4.000	1.000	.017	1.000
	Roy's Largest Root	8019.214	2004.803[b]	4.000	1.000	.017	1.000
Seasons	Pillai's Trace	2.052	1.623	12.000	9.000	.237	.684
	Wilks' Lambda	.000	11.028	12.000	2.937	.038	.966
	Hotelling's Trace	.	.	12.000	.	.	.
	Roy's Largest Root	4055.988	3041.991[c]	4.000	3.000	<.001	1.000

a. Design: Intercept + Seasons

b. Exact statistic

c. The statistic is an upper bound on F that yields a lower bound on the significance level.

Table I-33. Tests of Between-Subjects Effects of microplastics size 0.2-10 µm in unit of particles per day

Source	Dependent Variable	Type III Sum of Squares	df	Mean Square	F	Sig.	Partial Eta Squared
Corrected Model	Influent_0.2_per_day	1.916E+29[a]	3	6.386E+28	1.352	.377	.504
	Primary_0.2_per_day	1.112E+28[b]	3	3.707E+27	6.380	.053	.827
	Secondary_0.2_per_day	1.471E+28[c]	3	4.902E+27	5.531	.066	.806
	Digested_0.2_per_day	2.935E+27[d]	3	9.784E+26	3.099	.152	.699
	Dewatered_0.2_per_day	8.617E+27[e]	3	2.872E+27	1.616	.319	.548
Intercept	Influent_0.2_per_day	1.259E+30	1	1.259E+30	26.666	.007	.870
	Primary_0.2_per_day	1.445E+28	1	1.445E+28	24.871	.008	.861
	Secondary_0.2_per_day	1.700E+28	1	1.700E+28	19.186	.012	.827
	Digested_0.2_per_day	4.039E+27	1	4.039E+27	12.792	.023	.762
	Dewatered_0.2_per_day	2.461E+28	1	2.461E+28	13.845	.020	.776
Seasons	Influent_0.2_per_day	1.916E+29	3	6.386E+28	1.352	.377	.504
	Primary_0.2_per_day	1.112E+28	3	3.707E+27	6.380	.053	.827
	Secondary_0.2_per_day	1.471E+28	3	4.902E+27	5.531	.066	.806
	Digested_0.2_per_day	2.935E+27	3	9.784E+26	3.099	.152	.699
	Dewatered_0.2_per_day	8.617E+27	3	2.872E+27	1.616	.319	.548
Error	Influent_0.2_per_day	1.889E+29	4	4.721E+28			
	Primary_0.2_per_day	2.324E+27	4	5.811E+26			
	Secondary_0.2_per_day	3.545E+27	4	8.863E+26			
	Digested_0.2_per_day	1.263E+27	4	3.158E+26			
	Dewatered_0.2_per_day	7.111E+27	4	1.778E+27			
Total	Influent_0.2_per_day	1.639E+30	8				
	Primary_0.2_per_day	2.790E+28	8				
	Secondary_0.2_per_day	3.526E+28	8				
	Digested_0.2_per_day	8.238E+27	8				
	Dewatered_0.2_per_day	4.034E+28	8				
Corrected Total	Influent_0.2_per_day	3.804E+29	7				
	Primary_0.2_per_day	1.345E+28	7				
	Secondary_0.2_per_day	1.825E+28	7				
	Digested_0.2_per_day	4.198E+27	7				
	Dewatered_0.2_per_day	1.573E+28	7				

a. R Squared = .504 (Adjusted R Squared = .131)

b. R Squared = .827 (Adjusted R Squared = .698)

c. R Squared = .806 (Adjusted R Squared = .660)

d. R Squared = .699 (Adjusted R Squared = .474)

e. R Squared = .548 (Adjusted R Squared = .209)

Table I-34. Multiple Comparisons (Turkey HSD) of microplastics size 0.2-10 µm in unit of particles per day

Dependent Variable	(I) Seasons	(J) Seasons	Mean Difference (I-J)	Std. Error	Sig.	95% Confidence Interval	
						Lower Bound	Upper Bound
Influent_0.2_per_day	Spring_2021	Summer_2022	2.17E+14	2.173E+14	.758	-6.67E+14	1.10E+15
		Winter_2022	-8.66E+13	2.173E+14	.976	-9.71E+14	7.98E+14
		Summer_2023	2.93E+14	2.173E+14	.584	-5.91E+14	1.18E+15
	Summer_2022	Spring_2021	-2.17E+14	2.173E+14	.758	-1.10E+15	6.67E+14
		Winter_2022	-3.04E+14	2.173E+14	.560	-1.19E+15	5.81E+14
		Summer_2023	7.60E+13	2.173E+14	.983	-8.09E+14	9.61E+14
	Winter_2022	Spring_2021	8.66E+13	2.173E+14	.976	-7.98E+14	9.71E+14
		Summer_2022	3.04E+14	2.173E+14	.560	-5.81E+14	1.19E+15
		Summer_2023	3.80E+14	2.173E+14	.409	-5.05E+14	1.26E+15
	Summer_2023	Spring_2021	-2.93E+14	2.173E+14	.584	-1.18E+15	5.91E+14
		Summer_2022	-7.60E+13	2.173E+14	.983	-9.61E+14	8.09E+14
		Winter_2022	-3.80E+14	2.173E+14	.409	-1.26E+15	5.05E+14
Primary_0.2_per_day	Spring_2021	Summer_2022	-2.51E+13	2.411E+13	.738	-1.23E+14	7.30E+13
		Winter_2022	-8.18E+13	2.411E+13	.087	-1.80E+14	1.63E+13
		Summer_2023	1.66E+13	2.411E+13	.897	-8.16E+13	1.15E+14
	Summer_2022	Spring_2021	2.51E+13	2.411E+13	.738	-7.30E+13	1.23E+14
		Winter_2022	-5.68E+13	2.411E+13	.229	-1.55E+14	4.14E+13
		Summer_2023	4.17E+13	2.411E+13	.417	-5.65E+13	1.40E+14
	Winter_2022	Spring_2021	8.18E+13	2.411E+13	.087	-1.63E+13	1.80E+14
		Summer_2022	5.68E+13	2.411E+13	.229	-4.14E+13	1.55E+14
		Summer_2023	9.84E+13*	2.411E+13	.050	2.85E+11	1.97E+14
	Summer_2023	Spring_2021	-1.66E+13	2.411E+13	.897	-1.15E+14	8.16E+13
		Summer_2022	-4.17E+13	2.411E+13	.417	-1.40E+14	5.65E+13
		Winter_2022	-9.84E+13*	2.411E+13	.050	-1.97E+14	-2.85E+11
Secondary_0.2_per_day	Spring_2021	Summer_2022	2.84E+13	2.977E+13	.781	-9.28E+13	1.50E+14
		Winter_2022	1.07E+13	2.977E+13	.982	-1.10E+14	1.32E+14
		Summer_2023	-8.32E+13	2.977E+13	.151	-2.04E+14	3.80E+13
	Summer_2022	Spring_2021	-2.84E+13	2.977E+13	.781	-1.50E+14	9.28E+13
		Winter_2022	-1.77E+13	2.977E+13	.929	-1.39E+14	1.04E+14
		Summer_2023	-1.12E+14	2.977E+13	.065	-2.33E+14	9.62E+12
	Winter_2022	Spring_2021	-1.07E+13	2.977E+13	.982	-1.32E+14	1.10E+14
		Summer_2022	1.77E+13	2.977E+13	.929	-1.04E+14	1.39E+14
		Summer_2023	-9.39E+13	2.977E+13	.108	-2.15E+14	2.73E+13
	Summer_2023	Spring_2021	8.32E+13	2.977E+13	.151	-3.80E+13	2.04E+14
		Summer_2022	1.12E+14	2.977E+13	.065	-9.62E+12	2.33E+14
		Winter_2022	9.39E+13	2.977E+13	.108	-2.73E+13	2.15E+14
Digested_0.2_per_day	Spring_2021	Summer_2022	1.31E+12	1.777E+13	1.000	-7.10E+13	7.36E+13
		Winter_2022	-3.56E+13	1.777E+13	.320	-1.08E+14	3.67E+13
		Summer_2023	1.66E+13	1.777E+13	.791	-5.58E+13	8.89E+13
	Summer_2022	Spring_2021	-1.31E+12	1.777E+13	1.000	-7.36E+13	7.10E+13
		Winter_2022	-3.70E+13	1.777E+13	.298	-1.09E+14	3.54E+13
		Summer_2023	1.53E+13	1.777E+13	.826	-5.71E+13	8.76E+13
	Winter_2022	Spring_2021	3.56E+13	1.777E+13	.320	-3.67E+13	1.08E+14
		Summer_2022	3.70E+13	1.777E+13	.298	-3.54E+13	1.09E+14
		Summer_2023	5.22E+13	1.777E+13	.132	-2.01E+13	1.25E+14
	Summer_2023	Spring_2021	-1.66E+13	1.777E+13	.791	-8.89E+13	5.58E+13
		Summer_2022	-1.53E+13	1.777E+13	.826	-8.76E+13	5.71E+13
		Winter_2022	-5.22E+13	1.777E+13	.132	-1.25E+14	2.01E+13
Dewatered_0.2_per_day	Spring_2021	Summer_2022	-1.68E+13	4.216E+13	.976	-1.88E+14	1.55E+14
		Winter_2022	7.94E+12	4.216E+13	.997	-1.64E+14	1.80E+14
		Summer_2023	7.00E+13	4.216E+13	.444	-1.02E+14	2.42E+14
	Summer_2022	Spring_2021	1.68E+13	4.216E+13	.976	-1.55E+14	1.88E+14
		Winter_2022	2.48E+13	4.216E+13	.931	-1.47E+14	1.96E+14
		Summer_2023	8.68E+13	4.216E+13	.304	-8.49E+13	2.58E+14
	Winter_2022	Spring_2021	-7.94E+12	4.216E+13	.997	-1.80E+14	1.64E+14
		Summer_2022	-2.48E+13	4.216E+13	.931	-1.96E+14	1.47E+14
		Summer_2023	6.20E+13	4.216E+13	.526	-1.10E+14	2.34E+14
	Summer_2023	Spring_2021	-7.00E+13	4.216E+13	.444	-2.42E+14	1.02E+14
		Summer_2022	-8.68E+13	4.216E+13	.304	-2.58E+14	8.49E+13
		Winter_2022	-6.20E+13	4.216E+13	.526	-2.34E+14	1.10E+14

Based on observed means.
The error term is Mean Square(Error) = 17776416749999990000000000000.000.

*. The mean difference is significant at the .05 level.

APPENDIX J. CHAPTER 7- TREATMENT STUDY DATA AND STATISTICAL ANALYSIS

Table J. 35 Microplastics abundance (±SD) at each treatment stage

	Microplastics abundance					
	>25µm		10-25 µm		0.2-10 µm	
	$x10^6$ per kg dry solid	$x10^9$ per day	$x10^9$ per kg dry solid	$x10^{12}$ per day	$x10^9$ per kg dry solid	$x10^{12}$ per day
Influent	86 ± 17	3610 ± 689	742 ± 398	29497 ± 15412	30 ± 19	1130 ± 730
Primary Sludge	5 ± 2	30 ± 13	85 ± 29	564 ± 191	3 ± 2	23 ± 12
Secondary Sludge	6 ± 3	22 ± 11	132 ± 75	485 ± 278	4 ± 0.3	14 ± 1
Digested Sludge	2.7 ± 2	16 ± 10	63 ± 23	368 ± 137	8 ± 4	48 ± 21
Dewatered Sludge	2.9 ± 1	15 ± 5	9 ± 9.3	48 ± 47.9	6 ± 6.7	29 ± 34.5

1 Overall Treatments

1.1. Statistical analysis result for microplastics size above 25 µm in unit of particles per kg dry solid

Table J-36. Between-Subjects Factors of microplastics size above 25 µm in unit of particles per kg dry solid

		Value Label	N
Treatment	1	Influent	14
	2	Primary sedimentation	9
	3	Secondary sedimentation	3
	4	Digestion	3
	5	Dewatering	3

Table J-37. Descriptive Statistics of microplastics size above 25 µm in unit of particles per kg dry solid

Dependent Variable: Microplastics_25_per_kg

Treatment	Mean	Std. Deviation	N
Influent	86070000.00	42254275.705	14
Primary sedimentation	4526666.67	3530601.932	9
Secondary sedimentation	6006666.67	2913079.699	3
Digestion	2736666.67	1680039.682	3
Dewatering	2906666.67	928780.563	3
Total	40020937.50	49557414.885	32

Table I-38. Tests of Between-Subjects Effects of microplastics size above 25 µm in unit of particles per kg dry solid

Dependent Variable: Microplastics_25_per_kg

Source	Type III Sum of Squares	df	Mean Square	F	Sig.	Partial Eta Squared
Corrected Model	5.280E+16[a]	4	1.320E+16	15.273	<.001	.694
Intercept	8.841E+15	1	8.841E+15	10.229	.004	.275
Treatment	5.280E+16	4	1.320E+16	15.273	<.001	.694
Error	2.333E+16	27	8.642E+14			
Total	1.274E+17	32				
Corrected Total	7.613E+16	31				

a. R Squared = .694 (Adjusted R Squared = .648)

Table J-39. Multiple Comparisons of microplastics size above 25 µm in unit of particles per kg dry solid

Dependent Variable: Microplastics_25_per_kg

Tukey HSD

(I) Treatment	(J) Treatment	Mean Difference (I-J)	Std. Error	Sig.	95% Confidence Interval	
					Lower Bound	Upper Bound
Influent	Primary sedimentation	81543333.33*	12560204.033	<.001	44858969.53	118227697.14
	Secondary sedimentation	80063333.33*	18703283.823	.002	25436986.00	134689680.67
	Digestion	83333333.33*	18703283.823	.001	28706986.00	137959680.67
	Dewatering	83163333.33*	18703283.823	.001	28536986.00	137789680.67
Primary sedimentation	Influent	-81543333.33*	12560204.033	<.001	-118227697.14	-44858969.53
	Secondary sedimentation	-1480000.00	19598678.548	1.000	-58721510.73	55761510.73
	Digestion	1790000.00	19598678.548	1.000	-55451510.73	59031510.73
	Dewatering	1620000.00	19598678.548	1.000	-55621510.73	58861510.73
Secondary sedimentation	Influent	-80063333.33*	18703283.823	.002	-134689680.67	-25436986.00
	Primary sedimentation	1480000.00	19598678.548	1.000	-55761510.73	58721510.73
	Digestion	3270000.00	24003381.038	1.000	-66836246.70	73376246.70
	Dewatering	3100000.00	24003381.038	1.000	-67006246.70	73206246.70
Digestion	Influent	-83333333.33*	18703283.823	.001	-137959680.67	-28706986.00
	Primary sedimentation	-1790000.00	19598678.548	1.000	-59031510.73	55451510.73
	Secondary sedimentation	-3270000.00	24003381.038	1.000	-73376246.70	66836246.70
	Dewatering	-170000.00	24003381.038	1.000	-70276246.70	69936246.70
Dewatering	Influent	-83163333.33*	18703283.823	.001	-137789680.67	-28536986.00
	Primary sedimentation	-1620000.00	19598678.548	1.000	-58861510.73	55621510.73
	Secondary sedimentation	-3100000.00	24003381.038	1.000	-73206246.70	67006246.70
	Digestion	170000.00	24003381.038	1.000	-69936246.70	70276246.70

Based on observed means.

The error term is Mean Square(Error) = 864243451851851.500.

*. The mean difference is significant at the .05 level.

1.2. Statistical analysis result for microplastics size above 25 µm in unit of particles per day

Table J-40. Between-Subjects Factors of microplastics size above 25 µm in unit of particles per day

		Value Label	N
Treatment	1	Influent	14
	2	Primary sedimentation	9
	3	Secondary sedimentation	3
	4	Digestion	3
	5	Dewatering	3

Table J-41. Descriptive Statistics of microplastics size above 25 µm in unit of particles per day

Dependent Variable: Microplastics_25_per_day

Treatment	Mean	Std. Deviation	N
Influent	3.61E+12	1.893E+12	14
Primary sedimentation	30436666667	22991801256	9
Secondary sedimentation	22130000000	10722742187	3
Digestion	15983333333	9795225027.2	3
Dewatering	14903333333	4759215621.6	3
Total	1.59E+12	2.184E+12	32

Table J-42. Tests of Between-Subjects Effects of microplastics size above 25 µm in unit of particles per day

Dependent Variable: Microplastics_25_per_day

Source	Type III Sum of Squares	df	Mean Square	F	Sig.	Partial Eta Squared
Corrected Model	1.012E+26[a]	4	2.531E+25	14.667	<.001	.685
Intercept	1.153E+25	1	1.153E+25	6.683	.015	.198
Treatment	1.012E+26	4	2.531E+25	14.667	<.001	.685
Error	4.660E+25	27	1.726E+24			
Total	2.290E+26	32				
Corrected Total	1.478E+26	31				

a. R Squared = .685 (Adjusted R Squared = .638)

Table I-43. Multiple Comparisons of microplastics size above 25 µm in unit of particles per day

Dependent Variable: Microplastics_25_per_day

Tukey HSD

(I) Treatment	(J) Treatment	Mean Difference (I-J)	Std. Error	Sig.	95% Confidence Interval	
					Lower Bound	Upper Bound
Influent	Primary sedimentation	3.58E+12*	5.613E+11	<.001	1.94E+12	5.22E+12
	Secondary sedimentation	3.59E+12*	8.358E+11	.002	1.15E+12	6.03E+12
	Digestion	3.59E+12*	8.358E+11	.002	1.15E+12	6.03E+12
	Dewatering	3.59E+12*	8.358E+11	.002	1.15E+12	6.04E+12
Primary sedimentation	Influent	-3.58E+12*	5.613E+11	<.001	-5.22E+12	-1.94E+12
	Secondary sedimentation	8306666666.7	8.758E+11	1.000	-2.55E+12	2.57E+12
	Digestion	14453333333	8.758E+11	1.000	-2.54E+12	2.57E+12
	Dewatering	15533333333	8.758E+11	1.000	-2.54E+12	2.57E+12
Secondary sedimentation	Influent	-3.59E+12*	8.358E+11	.002	-6.03E+12	-1.15E+12
	Primary sedimentation	-8306666667	8.758E+11	1.000	-2.57E+12	2.55E+12
	Digestion	6146666666.7	1.073E+12	1.000	-3.13E+12	3.14E+12
	Dewatering	7226666666.7	1.073E+12	1.000	-3.13E+12	3.14E+12
Digestion	Influent	-3.59E+12*	8.358E+11	.002	-6.03E+12	-1.15E+12
	Primary sedimentation	-14453333333	8.758E+11	1.000	-2.57E+12	2.54E+12
	Secondary sedimentation	-6146666667	1.073E+12	1.000	-3.14E+12	3.13E+12
	Dewatering	1080000000.0	1.073E+12	1.000	-3.13E+12	3.13E+12
Dewatering	Influent	-3.59E+12*	8.358E+11	.002	-6.04E+12	-1.15E+12
	Primary sedimentation	-15533333333	8.758E+11	1.000	-2.57E+12	2.54E+12
	Secondary sedimentation	-7226666667	1.073E+12	1.000	-3.14E+12	3.13E+12
	Digestion	-1080000000	1.073E+12	1.000	-3.13E+12	3.13E+12

Based on observed means.

The error term is Mean Square(Error) = 1725779015527954000000000.000.

*. The mean difference is significant at the .05 level.

1.3. Statistical analysis result for microplastics size 10 - 25 µm in unit of particles per kg dry solid

Table J-44. Between-Subjects Factors of microplastics size 10 - 25 µm in unit of particles per kg dry solid

		Value Label	N
Treatment	1	Influent	20
	2	Primary sedimentation	9
	3	Secondary sedimentation	3
	4	Digestion	2
	5	Dewatering	2

Table J-45. Descriptive Statistics of microplastics size 10 - 25 µm in unit of particles per kg dry solid

Dependent Variable: Microplastics_10_per_kg

Treatment	Mean	Std. Deviation	N
Influent	7.53E+11	8.795E+11	20
Primary sedimentation	85114444444	1.080E+11	9
Secondary sedimentation	1.32E+11	75483439464	3
Digestion	63170000000	23461803000	2
Dewatering	9385000000.0	9340880579.5	2
Total	4.55E+11	7.335E+11	36

Table J-46. Tests of Between-Subjects Effects of microplastics size 10 - 25 µm in unit of particles per kg dry

Dependent Variable: Microplastics_10_per_kg

Source	Type III Sum of Squares	df	Mean Square	F	Sig.	Partial Eta Squared
Corrected Model	4.027E+24[a]	4	1.007E+24	2.109	.103	.214
Intercept	7.271E+23	1	7.271E+23	1.523	.226	.047
Treatment	4.027E+24	4	1.007E+24	2.109	.103	.214
Error	1.480E+25	31	4.775E+23			
Total	2.627E+25	36				
Corrected Total	1.883E+25	35				

a. R Squared = .214 (Adjusted R Squared = .112)

Table J-47. Multiple Comparisons of microplastics size 10 - 25 µm in unit of particles per kg dry solid

Dependent Variable: Microplastics_10_per_kg
Tukey HSD

(I) Treatment	(J) Treatment	Mean Difference (I-J)	Std. Error	Sig.	95% Confidence Interval	
					Lower Bound	Upper Bound
Influent	Primary sedimentation	6.68E+11	2.774E+11	.140	-1.35E+11	1.47E+12
	Secondary sedimentation	6.22E+11	4.278E+11	.599	-6.17E+11	1.86E+12
	Digestion	6.90E+11	5.124E+11	.665	-7.93E+11	2.17E+12
	Dewatering	7.44E+11	5.124E+11	.600	-7.40E+11	2.23E+12
Primary sedimentation	Influent	-6.68E+11	2.774E+11	.140	-1.47E+12	1.35E+11
	Secondary sedimentation	-46432222222	4.607E+11	1.000	-1.38E+12	1.29E+12
	Digestion	21944444444	5.402E+11	1.000	-1.54E+12	1.59E+12
	Dewatering	75729444444	5.402E+11	1.000	-1.49E+12	1.64E+12
Secondary sedimentation	Influent	-6.22E+11	4.278E+11	.599	-1.86E+12	6.17E+11
	Primary sedimentation	46432222222	4.607E+11	1.000	-1.29E+12	1.38E+12
	Digestion	68376666667	6.308E+11	1.000	-1.76E+12	1.89E+12
	Dewatering	1.22E+11	6.308E+11	1.000	-1.70E+12	1.95E+12
Digestion	Influent	-6.90E+11	5.124E+11	.665	-2.17E+12	7.93E+11
	Primary sedimentation	-21944444444	5.402E+11	1.000	-1.59E+12	1.54E+12
	Secondary sedimentation	-68376666667	6.308E+11	1.000	-1.89E+12	1.76E+12
	Dewatering	53785000000	6.910E+11	1.000	-1.95E+12	2.05E+12
Dewatering	Influent	-7.44E+11	5.124E+11	.600	-2.23E+12	7.40E+11
	Primary sedimentation	-75729444444	5.402E+11	1.000	-1.64E+12	1.49E+12
	Secondary sedimentation	-1.22E+11	6.308E+11	1.000	-1.95E+12	1.70E+12
	Digestion	-53785000000	6.910E+11	1.000	-2.05E+12	1.95E+12

Based on observed means.
The error term is Mean Square(Error) = 4774564177804480000000000.000.

1.4. Statistical analysis result for microplastics size 10 - 25 µm in unit of particles per day

Table J-48. Between-Subjects Factors of microplastics size 10 - 25 µm in unit of particles per day

		Value Label	N
Treatment	1	Influent	20
	2	Primary sedimentation	9
	3	Secondary sedimentation	3
	4	Digestion	2
	5	Dewatering	2

Table J-49. Descriptive Statistics of microplastics size 10 - 25 µm in unit of particles per day

Dependent Variable: Microplastics_10_per_day

Treatment	Mean	Std. Deviation	N
Influent	2.98E+16	3.140E+16	20
Primary sedimentation	5.64E+14	7.100E+14	9
Secondary sedimentation	4.85E+14	2.781E+14	3
Digestion	3.68E+14	1.368E+14	2
Dewatering	4.81E+13	4.789E+13	2
Total	1.68E+16	2.746E+16	36

Table J-50. Tests of Between-Subjects Effects of microplastics size 10 - 25 µm in unit of particles per day

Dependent Variable: Microplastics_10_per_day

Source	Type III Sum of Squares	df	Mean Square	F	Sig.	Partial Eta Squared
Corrected Model	7.650E+33[a]	4	1.913E+33	3.164	.027	.290
Intercept	6.540E+32	1	6.540E+32	1.082	.306	.034
Treatment	7.650E+33	4	1.913E+33	3.164	.027	.290
Error	1.874E+34	31	6.045E+32			
Total	3.650E+34	36				
Corrected Total	2.639E+34	35				

a. R Squared = .290 (Adjusted R Squared = .198)

Table J-51. Multiple Comparisons of microplastics size 10 - 25 µm in unit of particles per day

Dependent Variable: Microplastics_10_per_day

Tukey HSD

(I) Treatment	(J) Treatment	Mean Difference (I-J)	Std. Error	Sig.	95% Confidence Interval	
					Lower Bound	Upper Bound
Influent	Primary sedimentation	2.92E+16*	9.869E+15	.043	6.65E+14	5.78E+16
	Secondary sedimentation	2.93E+16	1.522E+16	.326	-1.48E+16	7.34E+16
	Digestion	2.94E+16	1.823E+16	.500	-2.34E+16	8.22E+16
	Dewatering	2.97E+16	1.823E+16	.489	-2.30E+16	8.25E+16
Primary sedimentation	Influent	-2.92E+16*	9.869E+15	.043	-5.78E+16	-6.65E+14
	Secondary sedimentation	7.98E+13	1.639E+16	1.000	-4.74E+16	4.75E+16
	Digestion	1.96E+14	1.922E+16	1.000	-5.54E+16	5.58E+16
	Dewatering	5.16E+14	1.922E+16	1.000	-5.51E+16	5.62E+16
Secondary sedimentation	Influent	-2.93E+16	1.522E+16	.326	-7.34E+16	1.48E+16
	Primary sedimentation	-7.98E+13	1.639E+16	1.000	-4.75E+16	4.74E+16
	Digestion	1.16E+14	2.244E+16	1.000	-6.49E+16	6.51E+16
	Dewatering	4.36E+14	2.244E+16	1.000	-6.45E+16	6.54E+16
Digestion	Influent	-2.94E+16	1.823E+16	.500	-8.22E+16	2.34E+16
	Primary sedimentation	-1.96E+14	1.922E+16	1.000	-5.58E+16	5.54E+16
	Secondary sedimentation	-1.16E+14	2.244E+16	1.000	-6.51E+16	6.49E+16
	Dewatering	3.20E+14	2.459E+16	1.000	-7.09E+16	7.15E+16
Dewatering	Influent	-2.97E+16	1.823E+16	.489	-8.25E+16	2.30E+16
	Primary sedimentation	-5.16E+14	1.922E+16	1.000	-5.62E+16	5.51E+16
	Secondary sedimentation	-4.36E+14	2.244E+16	1.000	-6.54E+16	6.45E+16
	Digestion	-3.20E+14	2.459E+16	1.000	-7.15E+16	7.09E+16

Based on observed means.

The error term is Mean Square(Error) = 604486515224934600000000000000000.000.

*. The mean difference is significant at the .05 level.

1.5. Statistical analysis result for microplastics size 0.2 - 10 µm in unit of particles per kg dry solid

Table J-52. Between-Subjects Factors of microplastics size 0.2 - 10 µm in unit of particles per kg dry solid

		Value Label	N
Treatment	1	Influent	20
	2	Primary sedimentation	9
	3	Secondary sedimentation	3
	4	Digestion	2
	5	Dewatering	2

Table J-53. Descriptive Statistics of microplastics size 0.2 - 10 µm in unit of particles per kg dry solid

Dependent Variable: Microplastics_0.2_per_kg

Treatment	Mean	Std. Deviation	N
Influent	29685500000	36760110314	20
Primary sedimentation	3357777777.8	2420334572.8	9
Secondary sedimentation	3723333333.3	330807093.84	3
Digestion	8180000000.0	3592102448.4	2
Dewatering	5585000000.0	6724585489.1	2
Total	18406388889	30022486064	36

Table J-54. Tests of Between-Subjects Effects of microplastics size 0.2 - 10 µm in unit of particles per kg dry solid

Dependent Variable: Microplastics_0.2_per_kg

Source	Type III Sum of Squares	df	Mean Square	F	Sig.	Partial Eta Squared
Corrected Model	5.767E+21[a]	4	1.442E+21	1.734	.168	.183
Intercept	1.709E+21	1	1.709E+21	2.055	.162	.062
Treatment	5.767E+21	4	1.442E+21	1.734	.168	.183
Error	2.578E+22	31	8.316E+20			
Total	4.374E+22	36				
Corrected Total	3.155E+22	35				

a. R Squared = .183 (Adjusted R Squared = .077)

Table J. 55. Multiple Comparisons of microplastics size 0.2 - 10 µm in unit of particles per kg dry solid

Dependent Variable: Microplastics_0.2_per_kg
Tukey HSD

(I) Treatment	(J) Treatment	Mean Difference (I-J)	Std. Error	Sig.	95% Confidence Interval	
					Lower Bound	Upper Bound
Influent	Primary sedimentation	26327722222	11575066116	.180	-7179934471	59835378915
	Secondary sedimentation	25962166667	17854554849	.599	-25723438258	77647771591
	Digestion	21505500000	21386616347	.851	-40404763939	83415763939
	Dewatering	24100500000	21386616347	.791	-37809763939	86010763939
Primary sedimentation	Influent	-26327722222	11575066116	.180	-59835378915	7179934470.7
	Secondary sedimentation	-365555555.56	19225138400	1.000	-56018744132	55287633021
	Digestion	-4822222222	22543473034	1.000	-70081370418	60436925974
	Dewatering	-2227222222	22543473034	1.000	-67486370418	63031925974
Secondary sedimentation	Influent	-25962166667	17854554849	.599	-77647771591	25723438258
	Primary sedimentation	365555555.56	19225138400	1.000	-55287633021	56018744132
	Digestion	-4456666667	26325104932	1.000	-80662933618	71749600285
	Dewatering	-1861666667	26325104932	1.000	-78067933618	74344600285
Digestion	Influent	-21505500000	21386616347	.851	-83415763939	40404763939
	Primary sedimentation	4822222222.2	22543473034	1.000	-60436925974	70081370418
	Secondary sedimentation	4456666666.7	26325104932	1.000	-71749600285	80662933618
	Dewatering	2595000000.0	28837707599	1.000	-80884782865	86074782865
Dewatering	Influent	-24100500000	21386616347	.791	-86010763939	37809763939
	Primary sedimentation	2227222222.2	22543473034	1.000	-63031925974	67486370418
	Secondary sedimentation	1861666666.7	26325104932	1.000	-74344600285	78067933618
	Digestion	-2595000000	28837707599	1.000	-86074782865	80884782865

Based on observed means.
The error term is Mean Square(Error) = 831613379587813800000.000.

1.6. Statistical analysis result for microplastics size 0.2 - 10 µm in unit of particles per day

Table J-56. Between-Subjects Factors of microplastics size 0.2 - 10 µm in unit of particles per day

		Value Label	N
Treatment	1	Influent	20
	2	Primary sedimentation	9
	3	Secondary sedimentation	3
	4	Digestion	2
	5	Dewatering	2

Table J-57. Descriptive Statistics of microplastics size 0.2 - 10 µm in unit of particles per day

Dependent Variable: Microplastics_0.2_per_day

Treatment	Mean	Std. Deviation	N
Influent	1.08E+15	1.327E+15	20
Primary sedimentation	2.27E+13	1.632E+13	9
Secondary sedimentation	1.37E+13	1.202E+12	3
Digestion	4.77E+13	2.094E+13	2
Dewatering	2.86E+13	3.449E+13	2
Total	6.13E+14	1.114E+15	36

Table J-58. Tests of Between-Subjects Effects of microplastics size 0.2 - 10 µm in unit of particles per day

Dependent Variable: Microplastics_0.2_per_day

Source	Type III Sum of Squares	df	Mean Square	F	Sig.	Partial Eta Squared
Corrected Model	9.970E+30[a]	4	2.492E+30	2.309	.080	.230
Intercept	9.582E+29	1	9.582E+29	.888	.353	.028
Treatment	9.970E+30	4	2.492E+30	2.309	.080	.230
Error	3.346E+31	31	1.080E+30			
Total	5.697E+31	36				
Corrected Total	4.343E+31	35				

a. R Squared = .230 (Adjusted R Squared = .130)

Table J-59. Multiple Comparisons of microplastics size 0.2 - 10 µm in unit of particles per day

Dependent Variable: Microplastics_0.2_per_day

Tukey HSD

(I) Treatment	(J) Treatment	Mean Difference (I-J)	Std. Error	Sig.	95% Confidence Interval	
					Lower Bound	Upper Bound
Influent	Primary sedimentation	1.06E+15	4.170E+14	.107	-1.46E+14	2.27E+15
	Secondary sedimentation	1.07E+15	6.433E+14	.470	-7.92E+14	2.93E+15
	Digestion	1.04E+15	7.705E+14	.666	-1.19E+15	3.27E+15
	Dewatering	1.06E+15	7.705E+14	.651	-1.18E+15	3.29E+15
Primary sedimentation	Influent	-1.06E+15	4.170E+14	.107	-2.27E+15	1.46E+14
	Secondary sedimentation	8.98E+12	6.927E+14	1.000	-2.00E+15	2.01E+15
	Digestion	-2.50E+13	8.122E+14	1.000	-2.38E+15	2.33E+15
	Dewatering	-5.96E+12	8.122E+14	1.000	-2.36E+15	2.35E+15
Secondary sedimentation	Influent	-1.07E+15	6.433E+14	.470	-2.93E+15	7.92E+14
	Primary sedimentation	-8.98E+12	6.927E+14	1.000	-2.01E+15	2.00E+15
	Digestion	-3.40E+13	9.485E+14	1.000	-2.78E+15	2.71E+15
	Dewatering	-1.49E+13	9.485E+14	1.000	-2.76E+15	2.73E+15
Digestion	Influent	-1.04E+15	7.705E+14	.666	-3.27E+15	1.19E+15
	Primary sedimentation	2.50E+13	8.122E+14	1.000	-2.33E+15	2.38E+15
	Secondary sedimentation	3.40E+13	9.485E+14	1.000	-2.71E+15	2.78E+15
	Dewatering	1.91E+13	1.039E+15	1.000	-2.99E+15	3.03E+15
Dewatering	Influent	-1.06E+15	7.705E+14	.651	-3.29E+15	1.18E+15
	Primary sedimentation	5.96E+12	8.122E+14	1.000	-2.35E+15	2.36E+15
	Secondary sedimentation	1.49E+13	9.485E+14	1.000	-2.73E+15	2.76E+15
	Digestion	-1.91E+13	1.039E+15	1.000	-3.03E+15	2.99E+15

Based on observed means.

The error term is Mean Square(Error) = 1079514034333082000000000000000.000.

2 Digestion Treatment

2.1. Statistical analysis result for microplastics size above 25 µm in unit of particles per kg dry solid – digestion treatment

Table J-60. Between-Subjects Factors of microplastics size above 25 µm in unit of particles per kg dry solid – digestion treatment

		Value Label	N
Time_day	0	0 day	3

Table J-61. Descriptive Statistics of microplastics size above 25 µm in unit of particles per kg dry solid – digestion treatment

Dependent Variable: Microplastics_25_per_kg

Time_day	Mean	Std. Deviation	N
0 day	1983333.33	1475477.324	3
11 days	3955000.00	883883.476	2
2 days	4580000.00	635531.274	3
32 days	2736666.67	1680039.682	3
39 days	2380000.00	1648848.083	3
4 days	7055000.00	1619274.529	2
Total	3566250.00	2019550.693	16

Dependent Variable: Microplastics_25_per_kg

Source	Type III Sum of Squares	df	Mean Square	F	Sig.	Partial Eta Squared
Corrected Model	4.153E+13[a]	5	8.306E+12	4.228	.025	.679
Intercept	2.206E+14	1	2.206E+14	112.301	<.001	.918
Time_day	4.153E+13	5	8.306E+12	4.228	.025	.679
Error	1.965E+13	10	1.965E+12			
Total	2.647E+14	16				
Corrected Total	6.118E+13	15				

Table J-62. Tests of Between-Subjects Effects of microplastics size above 25 µm in unit of particles per kg dry solid – digestion treatment

Table J-63. Multiple Comparisons of microplastics size above 25 µm in unit of particles per kg dry solid – digestion treatment

Dependent Variable: Microplastics_25_per_kg

Tukey HSD

(I) Time_day	(J) Time_day	Mean Difference (I-J)	Std. Error	Sig.	95% Confidence Interval	
					Lower Bound	Upper Bound
0 day	11 days	-1971666.67	1279571.326	.649	-6416026.89	2472693.56
	2 days	-2596666.67	1144483.387	.289	-6571823.30	1378489.96
	32 days	-753333.33	1144483.387	.983	-4728489.96	3221823.30
	39 days	-396666.67	1144483.387	.999	-4371823.30	3578489.96
	4 days	-5071666.67*	1279571.326	.024	-9516026.89	-627306.44
11 days	0 day	1971666.67	1279571.326	.649	-2472693.56	6416026.89
	2 days	-625000.00	1279571.326	.996	-5069360.22	3819360.22
	32 days	1218333.33	1279571.326	.923	-3226026.89	5662693.56
	39 days	1575000.00	1279571.326	.813	-2869360.22	6019360.22
	4 days	-3100000.00	1401700.158	.311	-7968552.70	1768552.70
2 days	0 day	2596666.67	1144483.387	.289	-1378489.96	6571823.30
	11 days	625000.00	1279571.326	.996	-3819360.22	5069360.22
	32 days	1843333.33	1144483.387	.610	-2131823.30	5818489.96
	39 days	2200000.00	1144483.387	.442	-1775156.63	6175156.63
	4 days	-2475000.00	1279571.326	.436	-6919360.22	1969360.22
32 days	0 day	753333.33	1144483.387	.983	-3221823.30	4728489.96
	11 days	-1218333.33	1279571.326	.923	-5662693.56	3226026.89
	2 days	-1843333.33	1144483.387	.610	-5818489.96	2131823.30
	39 days	356666.67	1144483.387	.999	-3618489.96	4331823.30
	4 days	-4318333.33	1279571.326	.058	-8762693.56	126026.89
39 days	0 day	396666.67	1144483.387	.999	-3578489.96	4371823.30
	11 days	-1575000.00	1279571.326	.813	-6019360.22	2869360.22
	2 days	-2200000.00	1144483.387	.442	-6175156.63	1775156.63
	32 days	-356666.67	1144483.387	.999	-4331823.30	3618489.96
	4 days	-4675000.00*	1279571.326	.038	-9119360.22	-230639.78
4 days	0 day	5071666.67*	1279571.326	.024	627306.44	9516026.89
	11 days	3100000.00	1401700.158	.311	-1768552.70	7968552.70
	2 days	2475000.00	1279571.326	.436	-1969360.22	6919360.22
	32 days	4318333.33	1279571.326	.058	-126026.89	8762693.56
	39 days	4675000.00*	1279571.326	.038	230639.78	9119360.22

Based on observed means.

The error term is Mean Square(Error) = 1964763333333.334.

*. The mean difference is significant at the .05 level.

2.2. Statistical analysis result for microplastics size above 25 µm in unit of particles per day – digestion treatment

Table J-64. Between-Subjects Factors of microplastics size above 25 µm in unit of particles per day – digestion treatment

		Value Label	N
Treatment	0	0 day	3
	11	11 days	2
	2	2 days	3
	32	32 days	3
	39	39 days	3
	4	4 days	2

Table J-65. Tests of Between-Subjects Effects of microplastics size above 25 µm in unit of particles per day – digestion treatment

Dependent Variable: Microplastic_25_per_day

Source	Type III Sum of Squares	df	Mean Square	F	Sig.	Partial Eta Squared
Corrected Model	2.150E+21[a]	5	4.300E+20	6.973	.005	.777
Intercept	9.585E+21	1	9.585E+21	155.415	<.001	.940
Treatment	2.150E+21	5	4.300E+20	6.973	.005	.777
Error	6.168E+20	10	6.168E+19			
Total	1.144E+22	16				
Corrected Total	2.767E+21	15				

a. R Squared = .777 (Adjusted R Squared = .666)

Table J-66. Descriptive Statistics of microplastics size above 25 µm in unit of particles per day – digestion treatment

Dependent Variable: Microplastic_25_per_day

Treatment	Mean	Std. Deviation	N
0 day	12860000000	9560465469.8	3
11 days	27370000000	6109402589.5	2
2 days	29680000000	4092969582.1	3
32 days	15983333333	9795225027.2	3
39 days	14903333333	4759215621.6	3
4 days	48755000000	11221784617	2
Total	23283125000	13581856387	16

Table J-67. Multiple Comparisons of microplastics size above 25 µm in unit of particles per day – digestion

Dependent Variable: Microplastic_25_per_day

Tukey HSD

(I) Treatment	(J) Treatment	Mean Difference (I-J)	Std. Error	Sig.	95% Confidence Interval	
					Lower Bound	Upper Bound
0 day	11 days	-14510000000	7169124675.4	.393	-39410661578	10390661578
	2 days	-16820000000	6412260045.3	.178	-39091828789	5451828789.0
	32 days	-3123333333	6412260045.3	.996	-25395162122	19148495456
	39 days	-2043333333	6412260045.3	.999	-24315162122	20228495456
	4 days	-3.59E+10*	7169124675.4	.005	-60795661578	-10994338422
11 days	0 day	14510000000	7169124675.4	.393	-10390661578	39410661578
	2 days	-2310000000	7169124675.4	.999	-27210661578	22590661578
	32 days	11386666667	7169124675.4	.623	-13513994911	36287328244
	39 days	12466666667	7169124675.4	.539	-12433994911	37367328244
	4 days	-21385000000	7853382604.5	.154	-48662308086	5892308085.8
2 days	0 day	16820000000	6412260045.3	.178	-5451828789	39091828789
	11 days	2310000000.0	7169124675.4	.999	-22590661578	27210661578
	32 days	13696666667	6412260045.3	.342	-8575162122	35968495456
	39 days	14776666667	6412260045.3	.276	-7495162122	37048495456
	4 days	-19075000000	7169124675.4	.168	-43975661578	5825661577.7
32 days	0 day	3123333333.3	6412260045.3	.996	-19148495456	25395162122
	11 days	-11386666667	7169124675.4	.623	-36287328244	13513994911
	2 days	-13696666667	6412260045.3	.342	-35968495456	8575162122.3
	39 days	1080000000.0	6412260045.3	1.000	-21191828789	23351828789
	4 days	-3.28E+10*	7169124675.4	.010	-57672328244	-7871005089
39 days	0 day	2043333333.3	6412260045.3	.999	-20228495456	24315162122
	11 days	-12466666667	7169124675.4	.539	-37367328244	12433994911
	2 days	-14776666667	6412260045.3	.276	-37048495456	7495162122.3
	32 days	-1080000000	6412260045.3	1.000	-23351828789	21191828789
	4 days	-3.39E+10*	7169124675.4	.008	-58752328244	-8951005089
4 days	0 day	35895000000*	7169124675.4	.005	10994338422	60795661578
	11 days	21385000000	7853382604.5	.154	-5892308086	48662308086
	2 days	19075000000	7169124675.4	.168	-5825661578	43975661578
	32 days	32771666667*	7169124675.4	.010	7871005089.0	57672328244
	39 days	33851666667*	7169124675.4	.008	8951005089.0	58752328244

Based on observed means.

The error term is Mean Square(Error) = 61675618333333330000.000.

*. The mean difference is significant at the .05 level.

2.3. Statistical analysis result for microplastics size 10-25 µm in unit of particles per kg dry solid – digestion treatment

Table J-68. Between-Subjects Factors of microplastics size 10-25 µm in unit of particles per kg dry solid – digestion treatment

		Value Label	N
Treatment	0	0 day	3
	11	11 days	3
	2	2 days	3
	32	32 days	2
	39	39 days	3
	4	4 days	3

Table J-69. Descriptive Statistics of microplastics size 10-25 µm in unit of particles per kg dry solid – digestion treatment

Dependent Variable: Microplastics_10_per_kg

Treatment	Mean	Std. Deviation	N
0 day	30446666667	8028077810.6	3
11 days	30623333333	7312826630.9	3
2 days	18306666667	7563890092.6	3
32 days	63170000000	23461803000	2
39 days	60010000000	31417262771	3
4 days	97010000000	26089712532	3
Total	49148823529	32392069995	17

Table J-70. Tests of Between-Subjects Effects of microplastics size 10-25 µm in unit of particles per kg dry solid – digestion treatment

Dependent Variable: Microplastics_10_per_kg

Source	Type III Sum of Squares	df	Mean Square	F	Sig.	Partial Eta Squared
Corrected Model	1.255E+22[a]	5	2.510E+21	6.519	.005	.748
Intercept	4.142E+22	1	4.142E+22	107.551	<.001	.907
Treatment	1.255E+22	5	2.510E+21	6.519	.005	.748
Error	4.236E+21	11	3.851E+20			
Total	5.785E+22	17				
Corrected Total	1.679E+22	16				

a. R Squared = .748 (Adjusted R Squared = .633)

Table J-71. Multiple Comparisons of microplastics size 10-25 µm in unit of particles per kg dry solid – digestion treatment

Dependent Variable: Microplastics_10_per_kg

Tukey HSD

(I) Treatment	(J) Treatment	Mean Difference (I-J)	Std. Error	Sig.	95% Confidence Interval	
					Lower Bound	Upper Bound
0 day	11 days	-176666666.67	16023034555	1.000	-54820925876	54467592543
	2 days	12140000000	16023034555	.969	-42504259210	66784259210
	32 days	-32723333333	17914297236	.488	-93817472420	28370805753
	39 days	-29563333333	16023034555	.478	-84207592543	25080925876
	4 days	-6.66E+10*	16023034555	.015	-1.21E+11	-11919074124
11 days	0 day	176666666.67	16023034555	1.000	-54467592543	54820925876
	2 days	12316666667	16023034555	.967	-42327592543	66960925876
	32 days	-32546666667	17914297236	.494	-93640805753	28547472420
	39 days	-29386666667	16023034555	.484	-84030925876	25257592543
	4 days	-6.64E+10*	16023034555	.015	-1.21E+11	-11742407457
2 days	0 day	-12140000000	16023034555	.969	-66784259210	42504259210
	11 days	-12316666667	16023034555	.967	-66960925876	42327592543
	32 days	-44863333333	17914297236	.203	-1.06E+11	16230805753
	39 days	-41703333333	16023034555	.176	-96347592543	12940925876
	4 days	-7.87E+10*	16023034555	.005	-1.33E+11	-24059074124
32 days	0 day	32723333333	17914297236	.488	-28370805753	93817472420
	11 days	32546666667	17914297236	.494	-28547472420	93640805753
	2 days	44863333333	17914297236	.203	-16230805753	1.06E+11
	39 days	3160000000.0	17914297236	1.000	-57934139086	64254139086
	4 days	-33840000000	17914297236	.455	-94934139086	27254139086
39 days	0 day	29563333333	16023034555	.478	-25080925876	84207592543
	11 days	29386666667	16023034555	.484	-25257592543	84030925876
	2 days	41703333333	16023034555	.176	-12940925876	96347592543
	32 days	-3160000000	17914297236	1.000	-64254139086	57934139086
	4 days	-37000000000	16023034555	.267	-91644259210	17644259210
4 days	0 day	66563333333*	16023034555	.015	11919074124	1.21E+11
	11 days	66386666667*	16023034555	.015	11742407457	1.21E+11
	2 days	78703333333*	16023034555	.005	24059074124	1.33E+11
	32 days	33840000000	17914297236	.455	-27254139086	94934139086
	39 days	37000000000	16023034555	.267	-17644259210	91644259210

Based on observed means.

The error term is Mean Square(Error) = 385106454545454500000.000.

*. The mean difference is significant at the .05 level.

2.4. Statistical analysis result for microplastics size 10-25 µm in unit of particles per day – digestion treatment

Table J-72. Between-Subjects Factors of microplastics size 10-25 µm in unit of particles per day – digestion treatment

		Value Label	N
Treatment	0	0 day	3
	11	11 days	3
	2	2 days	3
	32	32 days	2
	39	39 days	3
	4	4 days	3

Table J-73. Descriptive Statistics of microplastics size 10-25 µm in unit of particles per day – digestion treatment

Dependent Variable: Microplastics_10_per_kg

Treatment	Mean	Std. Deviation	N
0 day	2.31E+14	7.662E+13	3
11 days	2.12E+14	5.055E+13	3
2 days	1.19E+14	4.902E+13	3
32 days	3.68E+14	1.368E+14	2
39 days	3.50E+14	1.832E+14	3
4 days	4.43E+14	4.230E+14	3
Total	2.82E+14	2.053E+14	17

Table J-74. Tests of Between-Subjects Effects of microplastics size 10-25 µm in unit of particles per day – digestion treatment

Dependent Variable: Microplastics_10_per_kg

Source	Type III Sum of Squares	df	Mean Square	F	Sig.	Partial Eta Squared
Corrected Model	2.091E+29[a]	5	4.183E+28	.989	.467	.310
Intercept	1.369E+30	1	1.369E+30	32.349	<.001	.746
Treatment	2.091E+29	5	4.183E+28	.989	.467	.310
Error	4.654E+29	11	4.231E+28			
Total	2.029E+30	17				
Corrected Total	6.745E+29	16				

a. R Squared = .310 (Adjusted R Squared = -.004)

Table J-75. Multiple Comparisons of microplastics size 10-25 µm in unit of particles per day – digestion treatment

Dependent Variable: Microplastics_10_per_kg

Tukey HSD

(I) Treatment	(J) Treatment	Mean Difference (I-J)	Std. Error	Sig.	95% Confidence Interval	
					Lower Bound	Upper Bound
0 day	11 days	1.90E+13	1.680E+14	1.000	-5.54E+14	5.92E+14
	2 days	1.12E+14	1.680E+14	.982	-4.61E+14	6.85E+14
	32 days	-1.38E+14	1.878E+14	.973	-7.78E+14	5.03E+14
	39 days	-1.19E+14	1.680E+14	.977	-6.92E+14	4.53E+14
	4 days	-2.12E+14	1.680E+14	.798	-7.85E+14	3.61E+14
11 days	0 day	-1.90E+13	1.680E+14	1.000	-5.92E+14	5.54E+14
	2 days	9.30E+13	1.680E+14	.992	-4.80E+14	6.66E+14
	32 days	-1.57E+14	1.878E+14	.954	-7.97E+14	4.84E+14
	39 days	-1.38E+14	1.680E+14	.957	-7.11E+14	4.34E+14
	4 days	-2.31E+14	1.680E+14	.740	-8.04E+14	3.42E+14
2 days	0 day	-1.12E+14	1.680E+14	.982	-6.85E+14	4.61E+14
	11 days	-9.30E+13	1.680E+14	.992	-6.66E+14	4.80E+14
	32 days	-2.50E+14	1.878E+14	.764	-8.90E+14	3.91E+14
	39 days	-2.31E+14	1.680E+14	.739	-8.04E+14	3.41E+14
	4 days	-3.24E+14	1.680E+14	.434	-8.97E+14	2.49E+14
32 days	0 day	1.38E+14	1.878E+14	.973	-5.03E+14	7.78E+14
	11 days	1.57E+14	1.878E+14	.954	-4.84E+14	7.97E+14
	2 days	2.50E+14	1.878E+14	.764	-3.91E+14	8.90E+14
	39 days	1.85E+13	1.878E+14	1.000	-6.22E+14	6.59E+14
	4 days	-7.43E+13	1.878E+14	.998	-7.15E+14	5.66E+14
39 days	0 day	1.19E+14	1.680E+14	.977	-4.53E+14	6.92E+14
	11 days	1.38E+14	1.680E+14	.957	-4.34E+14	7.11E+14
	2 days	2.31E+14	1.680E+14	.739	-3.41E+14	8.04E+14
	32 days	-1.85E+13	1.878E+14	1.000	-6.59E+14	6.22E+14
	4 days	-9.28E+13	1.680E+14	.992	-6.66E+14	4.80E+14
4 days	0 day	2.12E+14	1.680E+14	.798	-3.61E+14	7.85E+14
	11 days	2.31E+14	1.680E+14	.740	-3.42E+14	8.04E+14
	2 days	3.24E+14	1.680E+14	.434	-2.49E+14	8.97E+14
	32 days	7.43E+13	1.878E+14	.998	-5.66E+14	7.15E+14
	39 days	9.28E+13	1.680E+14	.992	-4.80E+14	6.66E+14

Based on observed means.

The error term is Mean Square(Error) = 42310874253090900000000000000.000.

2.5. Statistical analysis result for microplastics size 0.2-10 µm in unit of particles per kg dry solid – digestion treatment

Table J-76. Between-Subjects Factors of microplastics size 0.2-10 µm in unit of particles per kg dry solid – digestion treatment

		Value Label	N
Treatment	0	0 day	3
	11	11 days	3
	2	2 days	3
	32	32 days	2
	39	39 days	3
	4	4 days	3

Table J-77. Descriptive Statistics of microplastics size 0.2-10 µm in unit of particles per kg dry solid – digestion treatment

Dependent Variable: Microplastics_0.2um_per_kg

Treatment	Mean	Std. Deviation	N
0 day	620000000.00	516430053.35	3
11 days	5796666666.7	2584421276.3	3
2 days	4676666666.7	2985537360.9	3
32 days	8180000000.0	3592102448.4	2
39 days	1433333333.3	584494083.23	3
4 days	3323333333.3	580201114.56	3
Total	3759411764.7	3024969980.4	17

Table J-78. Tests of Between-Subjects Effects of microplastics size 0.2-10 µm in unit of particles per kg dry solid – digestion treatment

Dependent Variable: Microplastics_0.2um_per_kg

Source	Type III Sum of Squares	df	Mean Square	F	Sig.	Partial Eta Squared
Corrected Model	1.004E+20[a]	5	2.009E+19	4.805	.014	.686
Intercept	2.665E+20	1	2.665E+20	63.761	<.001	.853
Treatment	1.004E+20	5	2.009E+19	4.805	.014	.686
Error	4.598E+19	11	4.180E+18			
Total	3.867E+20	17				
Corrected Total	1.464E+20	16				

a. R Squared = .686 (Adjusted R Squared = .543)

Table J-79. Multiple Comparisons of microplastics size 0.2-10 µm in unit of particles per kg dry solid – digestion treatment

Dependent Variable: Microplastics_0.2um_per_kg

	(I) Treatment	(J) Treatment	Mean Difference (I-J)	Std. Error	Sig.	95% Confidence Interval Lower Bound	95% Confidence Interval Upper Bound
Tukey HSD	0 day	11 days	-5176666667	1669303368.9	.082	-10869586174	516252840.77
		2 days	-4056666667	1669303368.9	.226	-9749586174	1636252840.8
		32 days	-7560000000*	1866337903.9	.018	-13924877505	-1195122495
		39 days	-813333333.33	1669303368.9	.996	-6506252841	4879586174.1
		4 days	-2703333333	1669303368.9	.604	-8396252841	2989586174.1
	11 days	0 day	5176666666.7	1669303368.9	.082	-516252840.77	10869586174
		2 days	1120000000.0	1669303368.9	.982	-4572919507	6812919507.4
		32 days	-2383333333	1866337903.9	.791	-8748210838	3981544171.2
		39 days	4363333333.3	1669303368.9	.173	-1329586174	10056252841
		4 days	2473333333.3	1669303368.9	.682	-3219586174	8166252840.8
	2 days	0 day	4056666666.7	1669303368.9	.226	-1636252841	9749586174.1
		11 days	-1120000000	1669303368.9	.982	-6812919507	4572919507.4
		32 days	-3503333333	1866337903.9	.462	-9868210838	2861544171.2
		39 days	3243333333.3	1669303368.9	.428	-2449586174	8936252840.8
		4 days	1353333333.3	1669303368.9	.959	-4339586174	7046252840.8
	32 days	0 day	7560000000*	1866337903.9	.018	1195122495.5	13924877505
		11 days	2383333333.3	1866337903.9	.791	-3981544171	8748210837.9
		2 days	3503333333.3	1866337903.9	.462	-2861544171	9868210837.9
		39 days	6746666667*	1866337903.9	.036	381789162.14	13111544171
		4 days	4856666666.7	1866337903.9	.176	-1508210838	11221544171
	39 days	0 day	813333333.33	1669303368.9	.996	-4879586174	6506252840.8
		11 days	-4363333333	1669303368.9	.173	-10056252841	1329586174.1
		2 days	-3243333333	1669303368.9	.428	-8936252841	2449586174.1
		32 days	-6746666667*	1866337903.9	.036	-13111544171	-381789162.14
		4 days	-1890000000	1669303368.9	.858	-7582919507	3802919507.4
	4 days	0 day	2703333333.3	1669303368.9	.604	-2989586174	8396252840.8
		11 days	-2473333333	1669303368.9	.682	-8166252841	3219586174.1
		2 days	-1353333333	1669303368.9	.959	-7046252841	4339586174.1
		32 days	-4856666667	1866337903.9	.176	-11221544171	1508210837.9
		39 days	1890000000.0	1669303368.9	.858	-3802919507	7582919507.4

Based on observed means.
The error term is Mean Square(Error) = 4179860606060606500.000.

*. The mean difference is significant at the .05 level.

2.6. Statistical analysis result for microplastics size 0.2-10 µm in unit of particles per day – digestion treatment

Table J-80. Between-Subjects Factors of microplastics size 0.2-10 µm in unit of particles per day – digestion treatment

		Value Label	N
Treatment	0	0 day	3
	11	11 days	3
	2	2 days	3
	32	32 days	2
	39	39 days	3
	4	4 days	3

Table J-81. Descriptive Statistics of microplastics size 0.2-10 µm in unit of particles per day – digestion treatment

Dependent Variable: Microplastics_0.2um_per_day

Treatment	Mean	Std. Deviation	N
0 day	4.03E+12	3.347E+12	3
11 days	4.01E+13	1.788E+13	3
2 days	3.03E+13	1.936E+13	3
32 days	4.77E+13	2.094E+13	2
39 days	8.37E+12	3.409E+12	3
4 days	2.30E+13	4.026E+12	3
Total	2.43E+13	1.913E+13	17

Table J-82. Tests of Between-Subjects Effects of microplastics size 0.2-10 µm in unit of particles per day – digestion treatment

Dependent Variable: Microplastics_0.2um_per_day

Source	Type III Sum of Squares	df	Mean Square	F	Sig.	Partial Eta Squared
Corrected Model	3.950E+27[a]	5	7.900E+26	4.560	.017	.675
Intercept	1.087E+28	1	1.087E+28	62.736	<.001	.851
Treatment	3.950E+27	5	7.900E+26	4.560	.017	.675
Error	1.906E+27	11	1.733E+26			
Total	1.587E+28	17				
Corrected Total	5.856E+27	16				

a. R Squared = .675 (Adjusted R Squared = .527)

Table J-83. Multiple Comparisons of microplastics size 0.2-10 µm in unit of particles per day – digestion treatment

Dependent Variable: Microplastics_0.2um_per_day

	(I) Treatment	(J) Treatment	Mean Difference (I-J)	Std. Error	Sig.	95% Confidence Interval Lower Bound	95% Confidence Interval Upper Bound
Tukey HSD	0 day	11 days	-3.60E+13	1.075E+13	.055	-7.27E+13	6.12E+11
		2 days	-2.63E+13	1.075E+13	.222	-6.29E+13	1.04E+13
		32 days	-4.37E+13*	1.202E+13	.035	-8.47E+13	-2.72E+12
		39 days	-4.34E+12	1.075E+13	.998	-4.10E+13	3.23E+13
		4 days	-1.90E+13	1.075E+13	.522	-5.56E+13	1.77E+13
	11 days	0 day	3.60E+13	1.075E+13	.055	-6.12E+11	7.27E+13
		2 days	9.78E+12	1.075E+13	.936	-2.69E+13	4.64E+13
		32 days	-7.65E+12	1.202E+13	.985	-4.86E+13	3.33E+13
		39 days	3.17E+13	1.075E+13	.104	-4.95E+12	6.83E+13
		4 days	1.71E+13	1.075E+13	.621	-1.96E+13	5.37E+13
	2 days	0 day	2.63E+13	1.075E+13	.222	-1.04E+13	6.29E+13
		11 days	-9.78E+12	1.075E+13	.936	-4.64E+13	2.69E+13
		32 days	-1.74E+13	1.202E+13	.699	-5.84E+13	2.35E+13
		39 days	2.19E+13	1.075E+13	.381	-1.47E+13	5.86E+13
		4 days	7.30E+12	1.075E+13	.981	-2.93E+13	4.40E+13
	32 days	0 day	4.37E+13*	1.202E+13	.035	2.72E+12	8.47E+13
		11 days	7.65E+12	1.202E+13	.985	-3.33E+13	4.86E+13
		2 days	1.74E+13	1.202E+13	.699	-2.35E+13	5.84E+13
		39 days	3.94E+13	1.202E+13	.062	-1.63E+12	8.03E+13
		4 days	2.47E+13	1.202E+13	.372	-1.62E+13	6.57E+13
	39 days	0 day	4.34E+12	1.075E+13	.998	-3.23E+13	4.10E+13
		11 days	-3.17E+13	1.075E+13	.104	-6.83E+13	4.95E+12
		2 days	-2.19E+13	1.075E+13	.381	-5.86E+13	1.47E+13
		32 days	-3.94E+13	1.202E+13	.062	-8.03E+13	1.63E+12
		4 days	-1.46E+13	1.075E+13	.748	-5.13E+13	2.20E+13
	4 days	0 day	1.90E+13	1.075E+13	.522	-1.77E+13	5.56E+13
		11 days	-1.71E+13	1.075E+13	.621	-5.37E+13	1.96E+13
		2 days	-7.30E+12	1.075E+13	.981	-4.40E+13	2.93E+13
		32 days	-2.47E+13	1.202E+13	.372	-6.57E+13	1.62E+13
		39 days	1.46E+13	1.075E+13	.748	-2.20E+13	5.13E+13

Based on observed means.
The error term is Mean Square(Error) = 1732520363636364000000000000.000.

*. The mean difference is significant at the .05 level.

APPENDIX K. FLOW CYTOMETRY AND RAMAN MICROSPECTROSCOPY SIMULTANEOUS TECHNIQUE DEVELOPMENT

1 Background

While FTIR Microspectroscopy proves incapable of detecting microplastics smaller than 20 µm, Raman microspectroscopy excels in this regard. [2, 3] Nevertheless, the quantification of plastic particles using Raman microspectroscopy still relies on manual counting, a laborious process that becomes particularly time-consuming when dealing with samples containing a high number of plastic particles. Conversely, Flow Cytometry offers the ability to count particles within the ranges of 0.2-150 µm[4], but it lacks the capability to identify specific plastic types. A synergistic integration of both Raman microspectroscopy and Flow Cytometry emerges as a comprehensive solution, encompassing both the quantification and identification of microplastics below 20 µm.

This innovative concept has been substantiated by Schwaferts et.al.,[1] who introduces a pioneering online coupling technique integrating Raman Microscopy and Field-Flow-Fractionation Enabled by Optical Tweezers, as depicted in Figure K-119. The setup demonstrates proficiency in identifying various materials, encompassing both polymers and inorganic particles, within the size range of 200 nm to 50 µm. Motivated by this precedent, our research endeavors to develop a similar technique tailored for microplastics analysis, with a specific focus on smaller particles that elude detection by FTIR microspectroscopy.

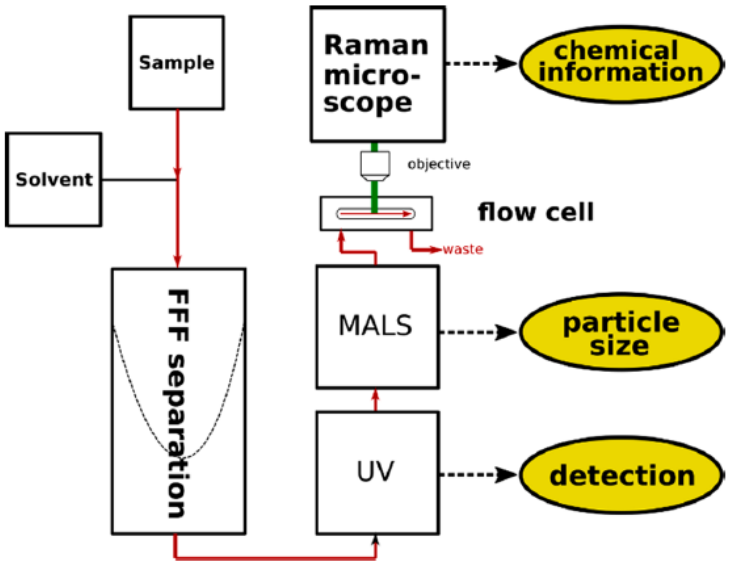

Figure K-119. Schematic of Online Coupling of Raman Microscopy and Field-Flow Fractionation Enabled by Optical Tweezers[1]

2 Set-up

The primary instruments employed in this study were the Flow Cytometer and Raman microspectroscopy, integrated through a flow cell to facilitate concurrent analysis of microplastics, as illustrated in Figure K-120.

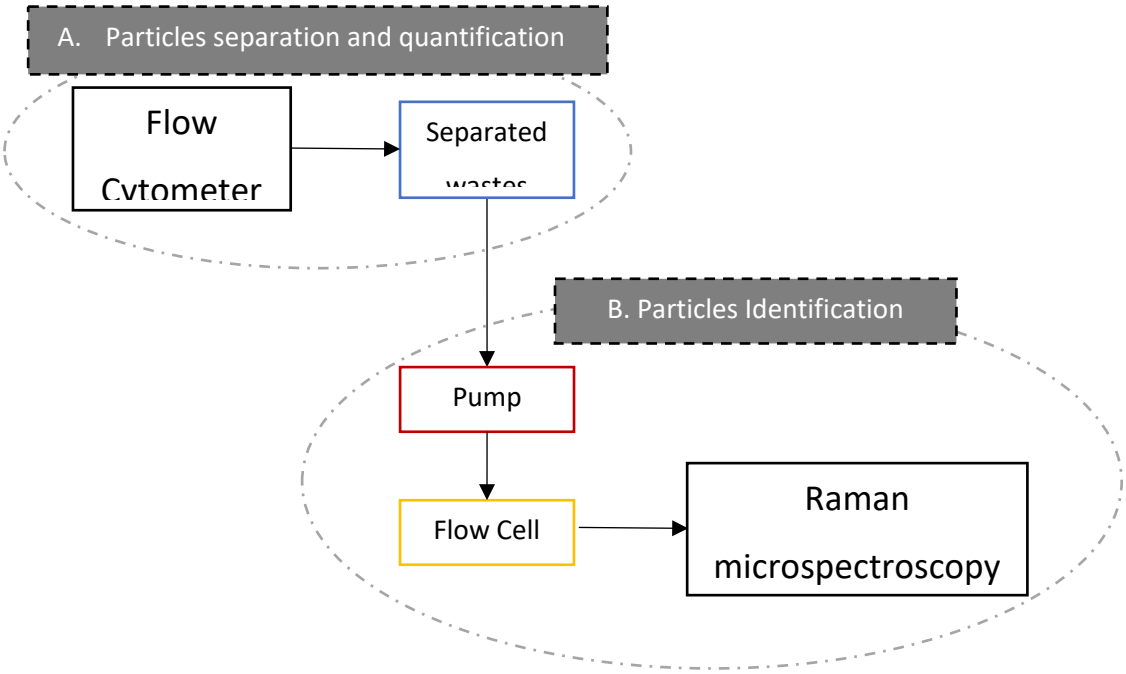

Figure K-120. Schematic of Flow-Raman simultaneous techniques for microplastics analysis

Due to temporal constraints, our focus was limited to Part B of the comprehensive setup. We initiated the examination by testing a peristaltic pump (Ismatec series ISM 597D) to propel the particle suspension into the Raman instrument. Initial tests involved ultra-purified water, followed by ethanol, and suspension of polystyrene microspheres. The flow cell utilized in these experiments is a glass cell, boasting four channels with a length of 58.5 mm and a depth of 37 µm (refer to Figure K-121).

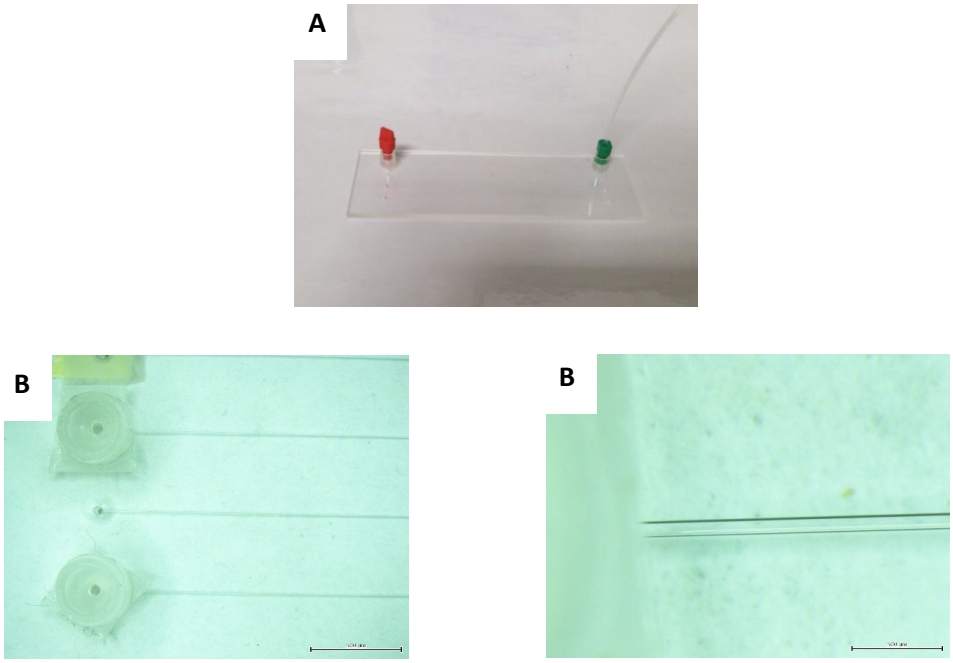

Figure K-121. A) a glass flow cell with four channels; (B) Flow cell's channels under stereomicroscope; (C) a channel under stereomicroscope

3 Test results

The configuration of Part B, dedicated to particle identification, is showcased in Figure K-122. Subsequently, the flow cell was positioned beneath the Raman microscope, as illustrated in Figure K-123.

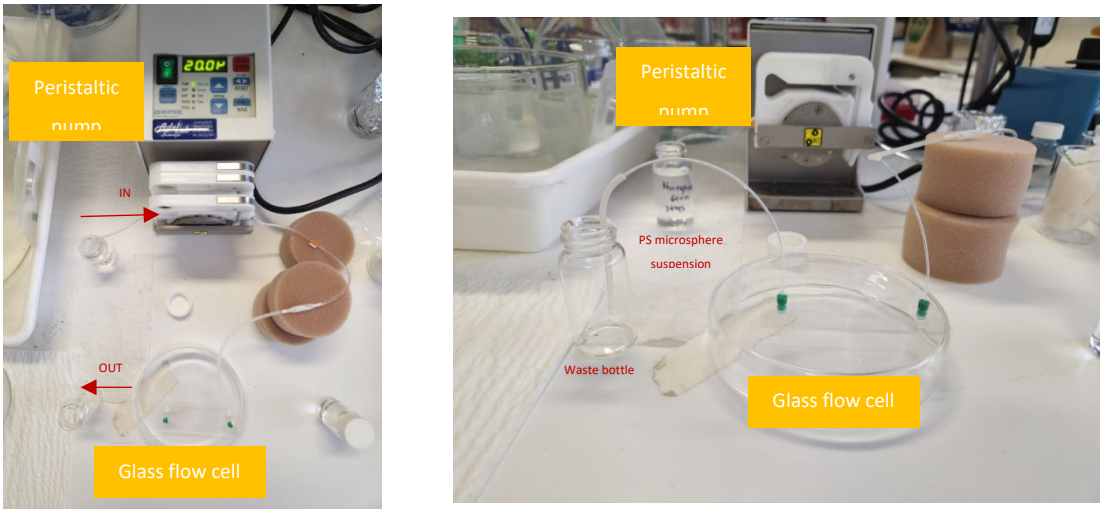

Figure K-122. Setup of peristaltic pump connected to a glass flow cell

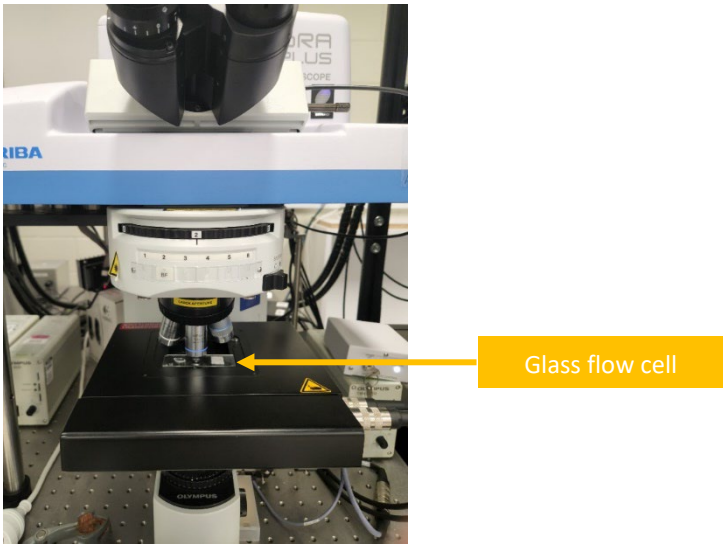

Figure K-123. A glass flow cell under Raman microspectroscopy objective

Ultra Purified Water and Ethanol

The initial trials involved testing the setup with 0.22 µm ultra-purified water and ethanol to validate the functionality of the pump-flow cell connection. Subsequent examination under the Raman microscope (Figure K-124) confirmed the successful identification of the channel depth and the flow of ethanol (Figure K-125). Flow rates were established at 20 µl and 10 µl per second for water and ethanol, respectively.

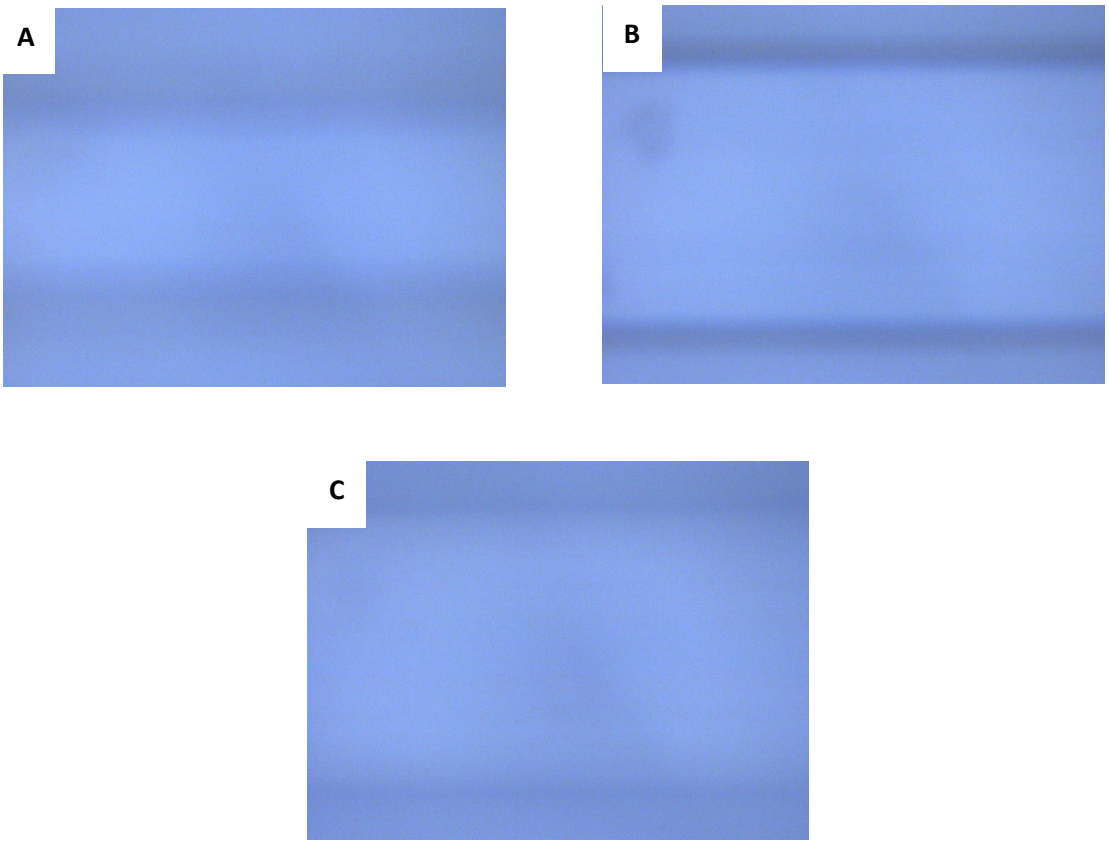

Figure K-124. Channel images under Raman microscope at (A) Z scan channel 0 nm; (B) Z scan channel -45 nm; and (C) Z scan channel -90 nm

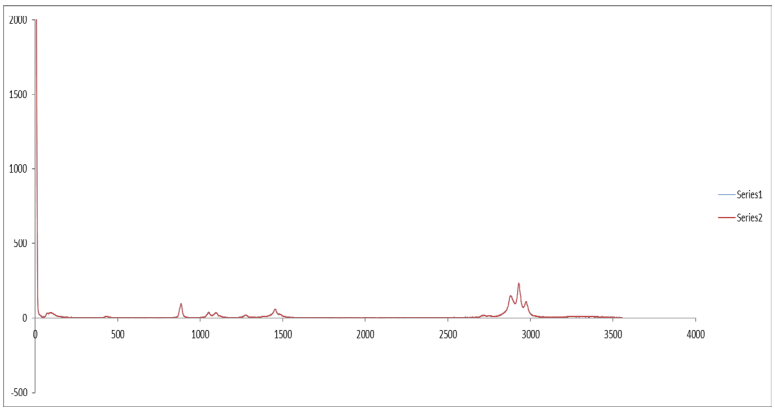

Figure K-125. Raman spectra of ethanol flowing through the glass flow cell

Polystyrene

Encouraged by the success with ethanol, we proceeded to test polystyrene microspheres (d=60nm) in suspension. While some trials resulted in successful particle flow through the channel, most attempts led to particle entrapment and channel blockage, as depicted in Figure K-126.

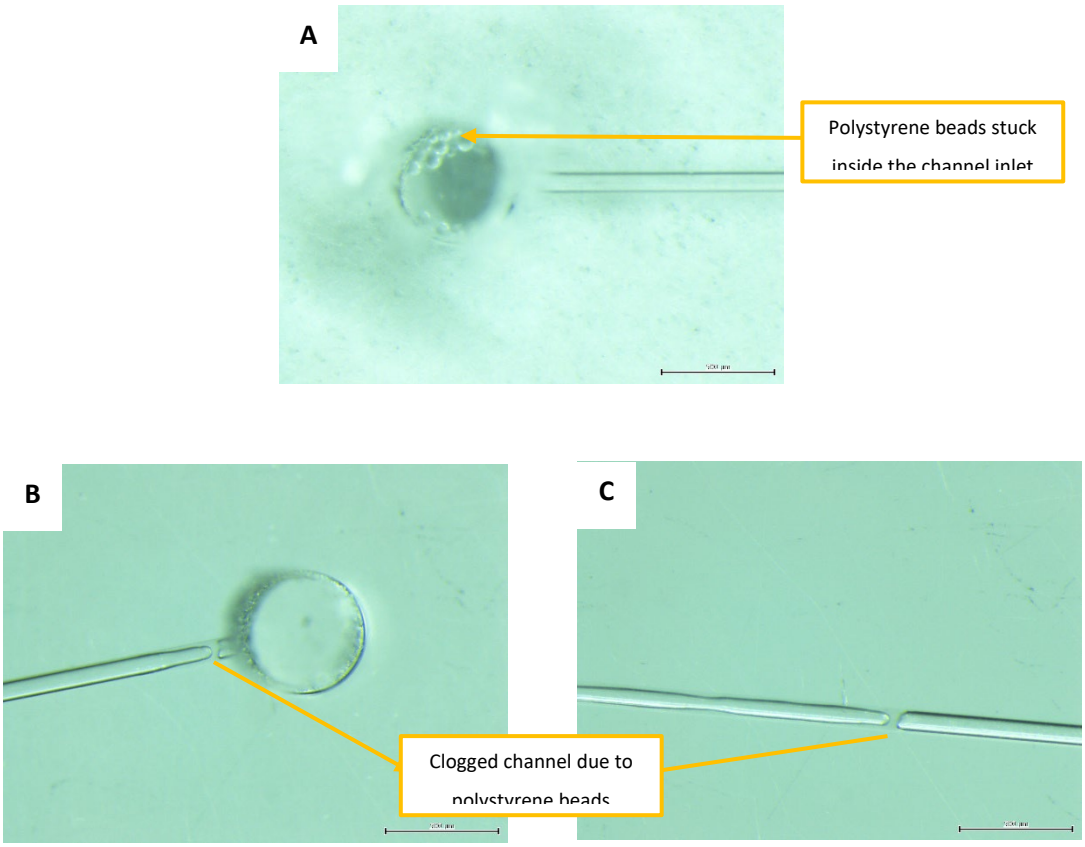

Figure K-126. Glass flow cell channel (A) with styrene beads inside the channel inlet; (B) and (C) clogged channel

4 Evaluations and further development

Subsequent to the trials with polystyrene beads, the decision was made to explore larger channel sizes. Consequently, various flow cells were procured each differing in channel depth and material composition, including:

1. Glass flow cell – chamber

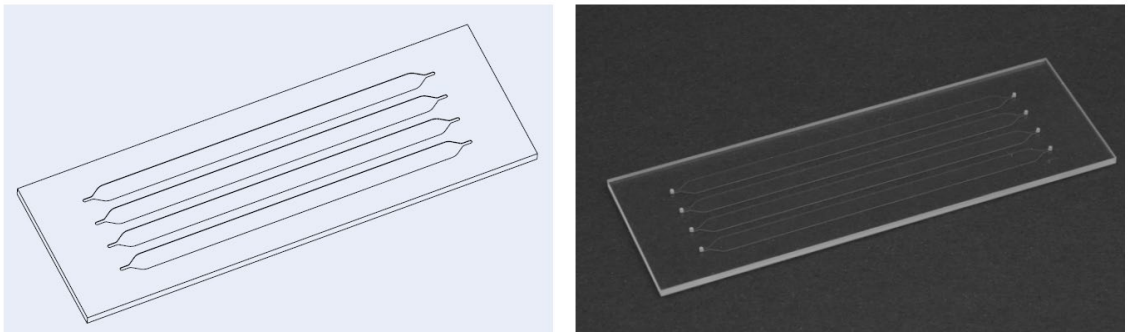

Figure K-127. (left) Schematic drawing of chamber glass chip; (right) Chamber glass chip. Courtesy "Microfluidic ChipShop GmbH"

Channel dimension: Length 5.85 cm; Width 3100 µm; Depth 96 µm

2. Zeonor/COP (cyclo-olefin polymer)

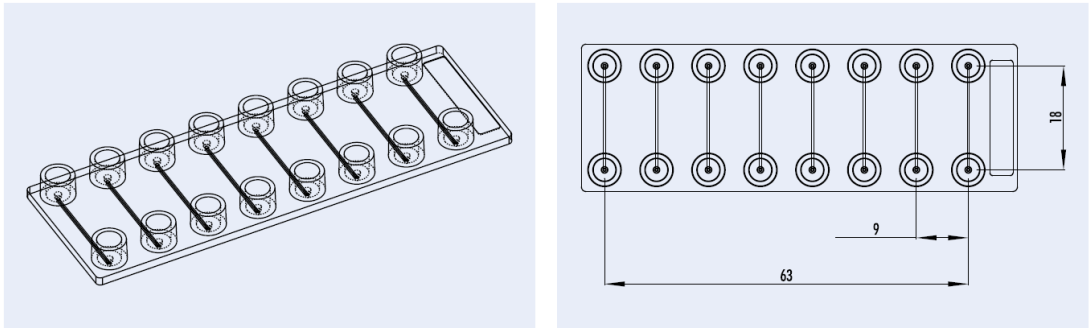

Figure K-128. (left) Schematic drawing of the eight-channel Luer chip family with crosswise orientation; (right) Details of the eight-channel Luer chip family. Courtesy "Microfluidic ChipShop GmbH".

Channel dimension: Length 1.8cm; Width 2910µm; Depth 100µm

3. Topas/COC (cyclo-olefin copolymer)

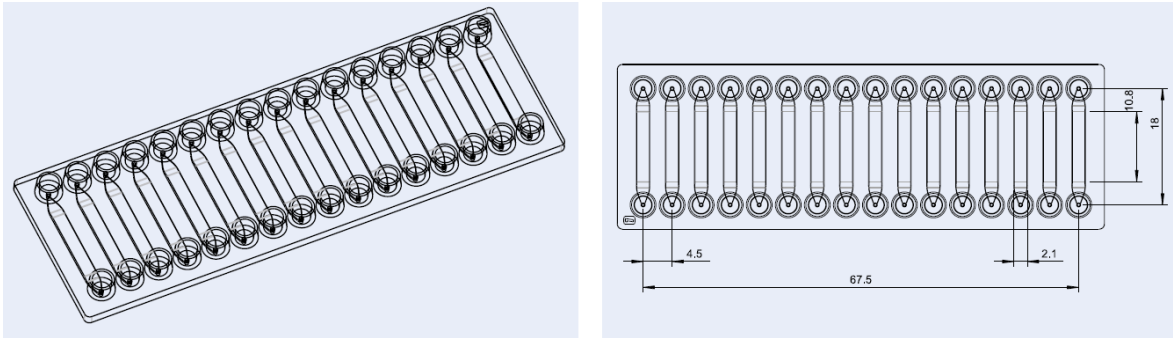

Figure K-129. (left) Schematic drawing of 16-channel chip Fluidic 561 with Mini Luer interfaces; (right) Channel chip Fluidic 561 with a total channel volume of 10 µl and a channel depth of 350 µm.

Channel dimension: Length 1.8cm; Width 2100µm; Depth 350µm

While these alternatives present larger channels, mitigating the likelihood of particle entrapment, time constraints hindered further development in this study. Addressing challenges, such as determining an optimal flow rate for microplastics suspension, and the segregation of waste from the flow cytometer representing different plastic types, remains imperative for future investigations.

References

1. Schwaferts, C.; Sogne, V.; Welz, R.; Meier, F.; Klein, T.; Niessner, R.; Elsner, M.; Ivleva, N. P., Nanoplastic Analysis by Online Coupling of Raman Microscopy and Field-Flow Fractionation Enabled by Optical Tweezers. *Analytical Chemistry* **2020,** *92* (8), 5813-5820.
2. Okoffo, E. D.; O'Brien, S.; O'Brien, J. W.; Tscharke, B. J.; Thomas, K. V., Wastewater treatment plants as a source of plastics in the environment: a review of occurrence, methods for identification, quantification and fate. *Environmental Science: Water Research & Technology* **2019,** *5* (11), 1908-1931.
3. Bayo, J.; Olmos, S.; López-Castellanos, J., Removal of Microplastics from Wastewater. *Handbook of Microplastics in the Environment* **2020**, 1-20.
4. Bio-Rad Laboratories, I., *Flow Cytometry Basics Guide-Practical Advice to Get you Started in Flow*.

APPENDIX L. STANDARD OPERATING PROCEDURE: SEMI-AUTOMATED MAPPING TECHNIQUE OF FTIR MICROSPECTROSCOPY FOR MICROPLASTICS ANALYSIS

	1. Fill the chamber (as pictured) with Liquid Nitrogen.
	2. Turn on the instrument at the left side of machine.
	3. Turn on the lights and adjust as necessary.
	4. Turn on the PC and the microscope stage controller underneath the screen.
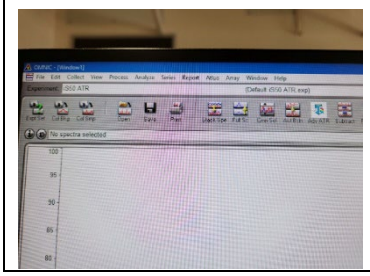	5. Open “OMNIC” software 6. Select Experiment: PK_MICROSCOPE_MICRO_MAP

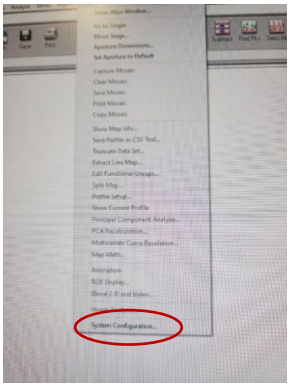

7. Open ‘Atlus – System Configuration - Initalization Z-axis (make sure the stage and condenser position as per below images), and wait untill the process is completed.

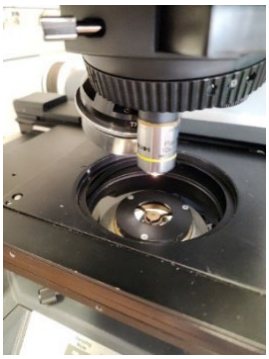

Red button to adjust the condenser position

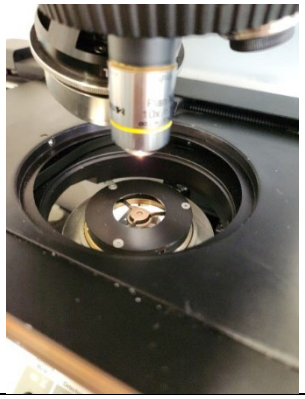	8. Do the “X-Y stage initialization”, but make sure the stage position is not too close to the condensor (as pictured). Select “OK” once the process is completed.
	Final position of the stage
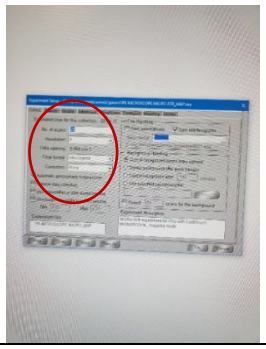	9. Select “Collect” and check the experiment set-up as below setting: No. of scans: 25 Resolution: 8cm-1
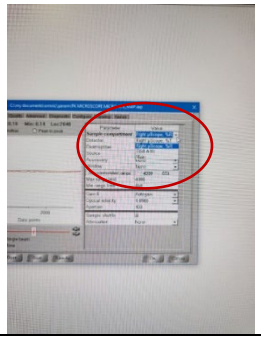	10. Under “Bench”, setting in Reflectance mode (%R)
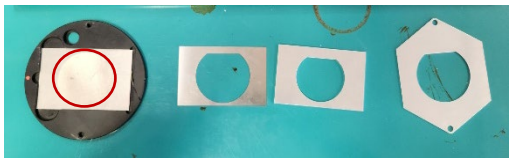	11. Assemble the mesh holder (located in the container under the bench) with the sample mesh on it.

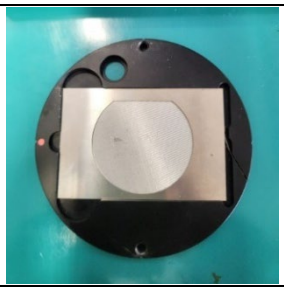	12. Final look of the assembled mesh.
	13. Put the last part of the mesh holder i.e., the “diamond shape” metal, and fit the screw parts at the top and bottom section of the metal.
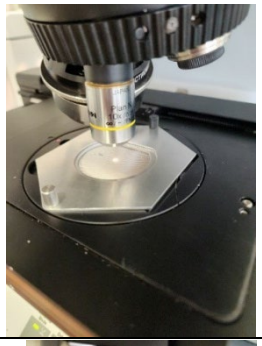	14. Put the mesh holder unto the microscope stage, and set the focus (using the focus adjustment knob as below image) with 10X objective lens. 
	15. Change into 15x lens, and open the OMNIC Atlus Window (“Show Atlus Window”). Adjust the focus as neccesary.
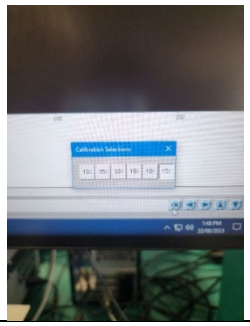	16. Open “Atlus” window, and ensure the calibration on the system is same as the lens magnification i.e., 15x (bottom right side of the window, symbol xX)

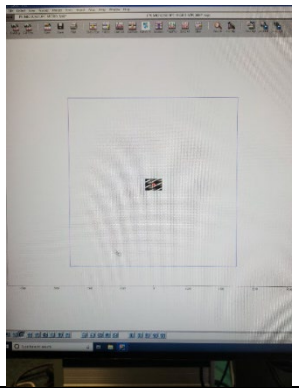	17. Draw a “5x5” mm box (□) using the tools on the bottom left on the software. 18. Move the “blue box” into the red cross (X) as center of the box.
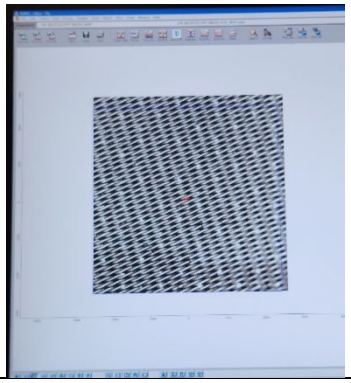	19. Go to “Atlus – Capture Mosaic”, once finished, save the mosaic. 20. Go to “Collect – Experiment Set up – Mapping”, and select “Default” to delete the mapping scale, and select “OK”.
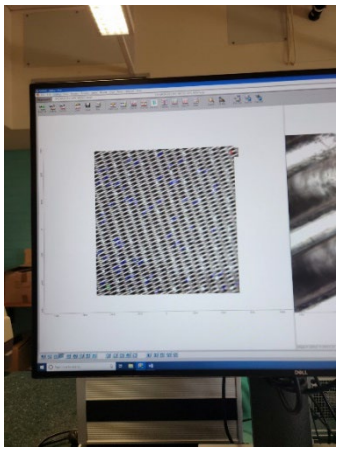	21. Move the stage into the bottom left of the mesh (using the stage mover tool at the bottom left of the software), The symbol has a “B” and arrows. 22. Choose where on the stainless-steel mesh clean/no particle detected, and point as a “Background or B” on the right hand window. 23. Start pin-pointing the particles (sample) on the map by scanning through the mosaic using the stage mover/joystick (Figure below) from the bottom to the top 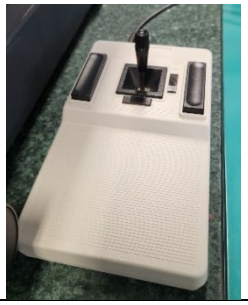
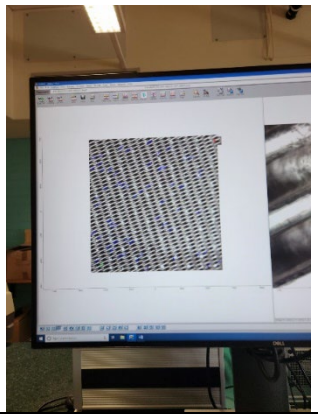	24. Focus on the image. Once the “pinpointing” process is finished (DO NOT move the stage or point!), select “Collect Map” form the “Collect” tool at the top left of the software but focus on the image before collection.

25. Let the instrument automatically collect the spectra of each pointed-particles (around 8 particles per minute)

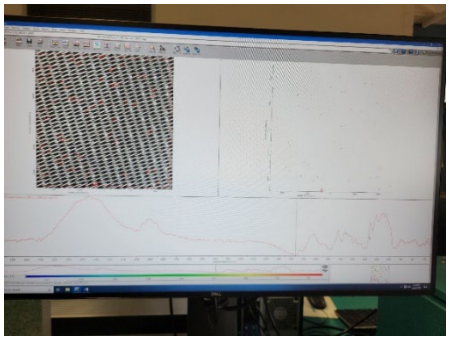

26. Once finished, select “Split map” from the “Atlus” section, and split the map into .SPA format. Choose “Select Path” to save the data.

27. Select the “Image Analysis” from the Atlus section, and record the area of the mapped mesh (under “Feature Sizing – Total Image Area”)

28. Do the spectra identification using “OMNIC Specta” software and summarize the data in an excel file (template/form – at the end of this file). Open spectrum to do this.

29. Extrapolate the number of confirmed microplastics/fibers on the “5x5” mapped area into the tested sample using the following formula:

$$Number\ of \frac{MPs}{Fs}\ in\ a\ tested\ sample = \frac{total\ mesh\ area}{small\ mapped\ area} x\ number\ of\ confirmed\ microplastics\ in\ small\ mapped\ area$$

30. Shut down procedures:
a. Take the sample off from the microscope stage
b. Move the stage/lens position into the original one (Select “Go to Origin” from “Atlus” tool
c. Keep the mesh holder on the provided container
d. Turn off the intrument’s lights (yellow knobs)
e. Turn off the instrument
f. Cover the Microsope
g. Close the “OMNIC” software
h. Turn off the stage controller, and shut down the PC.

Template form “Spectra identification”

Sample Name						
Point #	**Instrument Library**		**Microplastics**			**Possible sources**
	Chemical Composition	**%match /HQI**	**(Yes/No)**		**Type**	
1			Yes	1		

2						
3						
4						
5						
etc…						